ABSTRACT

Title of Dissertation:	DEVELOPMENT AND EVALUATION OF SPATIALLY-EXPLICIT POPULATION MODELS FOR ESTIMATING THE ABUNDANCE OF CHESAPEAKE BAY FISHES
	Samara Nehemiah, Doctor of Philosophy, 2024
Dissertation directed by:	Professor Michael J. Wilberg, Marine Estuarine and Environmental Science

Although fish populations typically experience spatially varying abundance and fishing mortality, stock assessments that inform management decisions commonly model a population that is assumed to be well-mixed with homogenous mortality rates. When assumptions about population mixing are not met, these models can result in biased estimates. Spatial population estimates are particularly beneficial to the Chesapeake Bay because this region faces unique challenges as a result of climate change and fishing pressure. However, use of spatial population models for fisheries management relies on models that can provide more accurate estimates of biological parameters than non-spatial models. Objectives for this research were to 1) develop and implement a multi-stock, spatially-explicit population model for Striped Bass (*Morone saxatilis*) to estimate abundance and fishing mortality in the Chesapeake Bay and along the Atlantic coast; 2) assess the performance of spatially-explicit models compared to spatially-implicit models (i.e., fleets-as-areas) to estimate abundance, determine how improved data

quality (e.g., stock composition) affects model performance, and determine the effect of aging error on model accuracy; and 3) determine how spatial model performance is affected by potential changes in population dynamics resulting from climate change (e.g., time-varying natural mortality). The population model was a two-stock model with two sub-annual time-steps and two regions with stock and age-specific occupancy probabilities representing movement into and out of the Chesapeake Bay. Fishing mortality was estimated to be higher in the Ocean than the Chesapeake Bay, and abundance increased during 1982-2004 for both stocks before declining slightly until 2017. Simulations were conducted to test the ability of models to estimate abundance and fishing mortality under alternative scenarios of data availability and quality. Spatially-explicit estimates were approximately unbiased when they closely matched the assumptions of the data generating model. Models that ignored potential aging bias in datasets resulted in highly biased estimates of abundance and fishing mortality. Although the performance of all models degraded under most climate change scenarios, spatially-explicit models produced the most accurate model estimates compared to fleets-as-areas models. This research highlights the potential benefits of implementing spatially-explicit population models for Striped Bass and ecologically valuable fish species in the Chesapeake Bay.

DEVELOPMENT AND EVALUATION OF SPATIALLY-EXPLICIT POPULATION MODELS FOR ESTIMATING THE ABUNDANCE OF CHESAPEAKE BAY FISHES

by

Samara Nehemiah

Dissertation submitted to the Faculty of the Graduate School of the
University of Maryland, College Park, in partial fulfillment
of the requirements for the degree of
Doctor of Philosophy
2024

Advisory Committee:
Professor Dr. Michael J. Wilberg, Chair
Professor Dr. David H. Secor
Associate Research Professor Dr. Geneviève Nesslage
Professor Dr. Robert J. Latour
Dr. Amy M. Schueller

Dedication

This dissertation is dedicated to my grandmother, Rosie Soto, who never failed to express how proud she was of me. You are missed. Love you, cutie.

Acknowledgements

There are so many people in my life that I would like to thank for helping me throughout this wonderful journey. First, I would like to extend the greatest of thanks to my advisor, Mike Wilberg, for being a great teacher, mentor, and motivator during these last 4+ years. I never could have imagined where this experience could have led me when I started in a pandemic, but I very much appreciate you for guiding me through it all. This journey has been made much more delightful because of your mentorship and I can't thank you enough for believing in me and all of my big ideas.

I'd also like to thank my committee members, each of whom made this experience so much brighter. Thank you to Dave Secor for your contagious curiosity and positivity. Thank you to Rob Latour for your never-ending expertise, and always being willing to drive to CBL for any milestone. Thank you to Amy Schueller, my NOAA mentor, for your professional mentorship, confidence, and being a great example for me to strive towards. A big thank you to Genny Nesslage for your friendship and endless support of all that I wished to do; I couldn't have navigated through this all without you. I'd also like to thank Jorge Holzer, for serving as my Deans' representative.

There are so many people in my ever-growing community to acknowledge for their support and guidance. First to my CBL community of past and present: thank you my lab mates, Sam Schiano, Lael Collins, Maya Drzewicki, Kaitlynn Wade, and Ray Mroch, for always cheering me on. Thank you to Katie Lankowicz, Nina Santos, Matt Stefanak, Nick Coleman, Kohma Arai, and many, many others for your friendships and collaboration. To Tom Miller, Stacy Hutchinson, Sarah Brzezinski,

Lora Harris, and Jerry Frank for your support and collaboration planning our workshop, D.E.I. efforts, and many outreach events. To my extended research community: a huge thank you to Adena Schonfeld for your Striped Bass collaboration and friendship. Thank you to Katie Drew and Gary Nelson for your expertise on all things related to Striped Bass stock assessment and for helping me request data. To my Southern Maryland Community and especially, Michael Kent: thank you for being a wonderful friend and always looking for ways to connect CBL to Southern Maryland. To my UF Community: thank you to Mike Allen, my MS advisor, and the rest of the NCBS lab including Scott Alford, Emily Colson, and many others, for your constant support and check-ins. To my NOAA Community that I've been fortunate to grow and connect with these last few years: thank you to all of the current and former Population and Ecosystem Dynamics fellows, Janelle Morano, Matt Damiano, Emily Liljestrand, and many others, for your friendship and guidance. Thank you to Dan Goethel and Jim Thorson for being great mentors and colleagues. I'd especially like to thank LaTreese Denson for your incredible mentorship, friendship, and making this field a little less intimidating.

The work described throughout this dissertation could not have been completed without my funding sources, of which I am lucky to have many: The NOAA Chesapeake Bay office (grant number NA19OAR4320074), the NMFS-Sea Grant Population and Ecosystem Dynamics fellowship (grant number NA21OAR4170244), the Marine Fisheries Section of the American Fisheries Society Travel Award, the MEES Debbie Morrin-Nordlund Memorial Graduate Travel Award, the UMD Jacob K. Goldhaber Travel Award, the CBL Graduate Education

Committee Travel Award, the American Fisheries Society Equal Opportunity Section Travel Award, the UMD Clint Waters Award sponsored by the Mid-Shore Fishing Club, the American Fisheries Society Skinner Travel Award, and the 2024 American Fisheries Society J. Frances Allen Scholarship.

Finally, and most importantly, I want to especially thank all of my friends and family, who have not a clue of what I have been studying for the last 4+ years, but have supported me nonetheless. To my mom, Gloria, for making this ride so much more enjoyable and showering me with so much love. To my dad, Renaldo, for always encouraging me to pursue all of my dreams. To my sister, Ariel (the first Dr. Nehemiah), for being my biggest cheerleader, role model, and always finding time to watch anime with me when I needed a break. To my friends Olivia, Erika, Kristen, and many others that are too many to name, thank you for your love and encouragement. And last but not least, I'd like to thank my amazing partner, Nate, for your forever support and for championing me through all of the ups and downs.

Table of Contents

List of Tables

model for striped bass. The base model the multi-stock, spatially-explicit population model for striped bass described. All sensitivity models were the same as the base model with the exception of the specific aspects that were modified. Model 2 and 4 did not apply an aging error matrix (Table S2.1) to catch-at-age for the fishery or surveys. Model 3 and 4 assumed selectivity for the Chesapeake Bay followed a logistic function. Model 5 explored how priors of occupancy probabilities impacted model output. Model 6 evaluated assumptions of natural morality by assuming spatially- and time-varying mortality in the Chesapeake Bay (Table S2.3).

Chapter 3

Table 3.1. Symbols and descriptions of variables for data-generating and estimation models. Values are for the Chesapeake Bay stock (CB) and Atlantic coast stock (AC), when applicable.

Table 3.2. Equations for the operating model that assumes two stocks, two region, and two 6-month time-steps for striped bass dynamics.

Table 3.3. Standard deviations (σ) and effective sample sizes (ESS) for generating each dataset. Effective sample size is weighted proportionally to the relative abundance of each stock in a region at a given time-step so that the total ESS sums to 100 in each region. Values are assumed the same for each time-step and/or region if only a single value is presented.

Table 3.4. Description of the five estimation models for striped bass. Fleets-as-area models are denoted as 'FAA' models and spatially-explicit models are denoted as 'SE' models. Regions specify the number of spatial areas assumed in each model, Stocks refers to the number of stocks assumed in each model, Fleets refers to the number of fishery fleets assumed for each model, and Time-Step refers to either annual (12-months) or two sub-annual time-steps (6-months).

Table 3.5. Equations for the fleets-as-areas (FAA) estimation models that assumes one stocks, two fleets, and 12-month time-steps for striped bass dynamics.

Table 3.6. Negative log likelihood components for the two-stock spatially-explicit striped bass models. Additive constants have been removed from the negative log likelihood functions. Parameter definitions are in Table 3.1.

Table 3.7. Datasets used in the likelihood functions (Table 3.6) for each estimation model. Descriptions of the estimation models and their names are found in Table 3.4. Datasets and their assumptions are described for the fishery, fishery-independent surveys, age-1 surveys, young-of-the-year (YOY) surveys, and movement.

Table 3.8. Median relative error (MRE) and root mean squared relative error (RMSRE) for estimated values for five estimation models. The values are presented for the terminal year estimated total annual abundance (N), spawning stock biomass (SSB), fishing mortality for age-8 (F-8), and the fishing mortality that yields 40% spawning potential ration (F40% SPR). Models are described in Table 3.4.

Supplemental Table S3.1. Spawning stock biomass weight-at-age for 30 years used to calculate spawning stock biomass. Values used are the same as those assumed for the benchmark assessment from years 1988-2017 (Northeast Fisheries Science Center 2019).

Supplemental Table S3.2 Aging-error matrices used applied to the fisheries-independent and dependent data sources for striped bass ages 1-15+. Striped bass used for to develop this matrix were collected from Massachusetts, Rhode Island, and New Jersey that were aged with both scales and otoliths. Otolith (true) ages are along the columns and scale ages are along the rows.

Chapter 4

Table 4.1. Symbols and descriptions of variables for data-generating and estimation models. Values are for the Chesapeake Bay stock (CB) and Atlantic coast stock (AC), when applicable. When variables differ for a 6-month time-step, they are denoted with the number 1 (January-June) or 2 (July-December).

Table 4.2. Equations for the operating model that assumes two stocks, two regions, and six 2-month time-steps for striped bass dynamics. Normally distributed errors are denoted with N(mean, error) and multinomial errors are denoted by Multi(Mean, effective sample size).

Table 4.3. Instantaneous natural mortality rates (yr^{-1}) for striped bass in the Chesapeake Bay (CB) and Ocean (Oc) region from the Brownie mark-recapture model described in Schonfeld (2023). Age-1 estimates of natural mortality are from the benchmark assessment for striped bass (Northeast Fisheries Science Center 2019). Natural mortality for ages 12-15+ were the same as natural mortality for age 11.

Table 4.4. Average log recruitment (log R) for the Chesapeake Bay region for each year used in the OM-R scenario.

Table 4.5. A) Description and assumptions of each operating model (OM) scenario for Striped Bass; B) Description of the fleets-as-areas (FAA) and spatially-explicit (SE) estimations models for striped bass.

Table 4.6. Standard deviations (σ) and effective sample sizes (ESS) used to generate each data set for a 6-month period. When multiple values are provided, it represents approximately the weighted ESS for the Base scenario for each region and time-step.

Table 4.7. Negative log-likelihood components for the estimation models for striped bass. Equations are written for the two-stock, spatially-explicit models but were similar for the fleets-as-areas model. Additive constants have been removed from the negative log-likelihood functions. Parameter definitions are in Table 4.1.

Table 4.8. Total number of model convergence for each estimation model under the five operating model scenarios.

Table 4.9. Median relative error (MRE) for estimated values for three estimation models and five operating model scenarios. The values are presented for total annual abundance (N), spawning stock biomass (SSB), and the fishing mortality for age-8 (F). Operating models and estimation models are described in Table 4.5.

Table 4.10. Root mean squared relative error (RMSRE) for estimated values for three estimation models and five operating model scenarios. The values are presented for total annual abundance (N), spawning stock biomass (SSB), and the fishing mortality for age-8 (F). Operating models and estimation models are described in Table 4.5.

List of Figures

Chapter 2

Figure 2.8. Estimated weighted average instantaneous fishing mortality (F) rates for each 6-month period ($6mo^{-1}$) for striped bass (7-15+) in the Chesapeake Bay region (orange) and the Ocean region (blue) during January-June (left) and July-December (right). F is weighted based on abundance of each age class in a given region during each time-step. The dashed lines represent the maximum likelihood estimates of $F6mo^{-1}$ and the shaded regions represent approximate 95% confidence intervals.

Figure 2.9. Estimated stock specific annual fishing mortality (Fyr^{-1}) for striped bass (7-15+) for the Chesapeake Bay stock (orange) and Atlantic coast stock (blue) during 1982-2017. The solid lines represent the maximum likelihood estimates of (Fyr^{-1}) and the shaded regions represent approximate 95% confidence intervals.

Figure 2.10. Estimated occupancy probability for striped bass (1-15+) in the Ocean region during January-June (left) and July-December). The solid-colored lines correspond to estimates of occupancy for the Atlantic coast stock (blue) and the Chesapeake Bay stock (orange) and the error bars correspond to approximately 95% confidence intervals. The black dashed lines correspond to the informative priors derived from conventional tagging data from Schonfeld (2023) and the and the gray shaded regions correspond to approximately 95% confidence intervals. The black solid lines correspond to the informative priors derived from acoustic tagging data from Secor et al. 2020 and the gray shaded area is approximately the 95% confidence intervals.

Figure 2.11. Estimated survey selectivity of striped bass for each fishery-independent survey in the Ocean (blue) and Chesapeake Bay (orange) regions during each time-step. The solid lines are selectivity for the January-June time-step and dashed lines are for selectivity estimated for the July-December time-step. The selectivity functions represent the Chesapeake Bay Multispecies Monitoring and Assessment Program (ChesMMAP), the Connecticut Long Island Sound Survey (CTLIST), Delaware 30 Foot Trawl Survey (DE30), Delaware Spawning Stock Electrofishing Survey (DESSN), Maryland Spawning Stock Survey (MDSSN), New Jersey Bottom Trawl Survey (NJBT), and New York Ocean Haul Seine Survey (NYOHS).

Supplemental Figure S2.1. Comparison of age classifications for striped bass aged with scales and otolith. Striped bass were collected from Rhode Island, Massachusetts, and New Jersey. The solid line represents when scale ages would equal the otolith ages. The dashed black line represents the linear regression through the observed age comparisons. The lower and upper hinge of the box represents the 25th and 75th percentiles. The middle line represents the median. The whiskers extend to the minimum and maximum values.

Supplemental Figure S2.2. Components of the total likelihood objective function for the spatially-explicit population model. The penalty names correspond to the negative log likelihood component that contributes to the total negative log likelihood (nll_tot). For the L_index component, the total contributions are separated for each targeted age class and survey. Surveys include the Chesapeake Bay Multispecies Monitoring and Assessment Program (ChesMMAP), the Connecticut Long Island Sound Survey (CTLIST), Delaware 30 Foot Trawl Survey (DE30), Delaware Spawning Stock Electrofishing Survey (DESSN), Maryland Spawning Stock Survey

(MDSSN), New Jersey Bottom Trawl Survey (NJBT), New York Ocean Haul Seine Survey (NYOHS), Maryland Yearling Survey (MD1), the New York Yearling Survey (NY1), the Atlantic Coast YOY surveys (which include the New York YOY survey and New Jersey YOY survey), and the Chesapeake Bay YOY aggregate survey.

Supplemental Figure S2.3. Estimates of striped bass (1-15+) total catch over time in the Chesapeake Bay (top) and Ocean region (bottom) during January-June (left) and July-December (right). The solid black lines correspond to the best estimates of total catch and the red circles represent the observed total catch for reach region.

Supplemental Figure S2.4. One-step ahead residual plots for the estimated age composition for the Chesapeake Bay fleet in January-June. The top left plot shows positive (blue) and negative (red) one-step ahead residuals for each age-class and year, and the size of the circle represents the relative size of the residual. The top right plot shows the autocorrelation function for each age (green), year (purple) and cohort (orange). The bottom left plot shows the quantile plots of residuals for each age (colored circles), where the black line represents normally distributed errors. The bottom right plot represents the dispersion of residuals through time.

Supplemental Figure S2.5. One-step ahead residual plots for the estimated age composition for the Chesapeake Bay fleet in July-December. The top left plot shows positive (blue) and negative (red) one-step ahead residuals for each age-class and year, and the size of the circle represents the relative size of the residual. The top right plot shows the autocorrelation function for each age (green), year (purple) and cohort (orange). The bottom left plot shows the quantile plots of residuals for each age (colored circles), where the black line represents normally distributed errors. The bottom right plot represents the dispersion of residuals through time.

Supplemental Figure S2.6. One-step ahead residual plots for the estimated age composition for the Ocean fleet in January-June. The top left plot shows positive (blue) and negative (red) one-step ahead residuals for each age-class and year, and the size of the circle represents the relative size of the residual. The top right plot shows the autocorrelation function for each age (green), year (purple) and cohort (orange). The bottom left plot shows the quantile plots of residuals for each age (colored circles), where the black line represents normally distributed errors. The bottom right plot represents the dispersion of residuals through time.

Supplemental Figure S2.7. One-step ahead residual plots for the estimated age composition for the Ocean fleet in July-December. The top left plot shows positive (blue) and negative (red) one-step ahead residuals for each age-class and year, and the size of the circle represents the relative size of the residual. The top right plot shows the autocorrelation function for each age (green), year (purple) and cohort (orange). The bottom left plot shows the quantile plots of residuals for each age (colored circles), where the black line represents normally distributed errors. The bottom right plot represents the dispersion of residuals through time.

Supplemental Figure S2.8. Estimated residuals for the fishery-independent surveys. The black solid line are the logged residuals that subtract the predicted trend from the observed trend divided by the standard deviation ($\frac{obs-est}{sd}$). The red dotted line

indicates when the residual would be zero. The months correspond to time-step the survey was conducted in. Residuals are presented for the Chesapeake Bay Multispecies Monitoring and Assessment Program (ChesMMAP), the Connecticut Long Island Sound Survey (CTLIST), Delaware 30 Foot Trawl Survey (DE30), Delaware Spawning Stock Electrofishing Survey (DESSN), Maryland Spawning Stock Survey (MDSSN), New Jersey Bottom Trawl Survey (NJBT), and New York Ocean Haul Seine Survey (NYOHS).

Supplemental Figure S2.9. One-step ahead residual plots for the Chesapeake Bay Multispecies Monitoring and Assessment Program (ChesMMAP) survey's estimated age-composition in January-June. The top left plot shows positive (blue) and negative (red) one-step ahead residuals for each age-class and year, and the size of the circle represents the relative size of the residual. The top right plot shows the autocorrelation function for each age (green), year (purple) and cohort (orange). The bottom left plot shows the quantile plots of residuals for each age (colored circles), where the black line represents normally distributed errors. The bottom right plot represents the dispersion of residuals through time.

Supplemental Figure S2.10. One-step ahead residual plots for the Chesapeake Bay Multispecies Monitoring and Assessment Program (ChesMMAP) survey's estimated age-composition in July-December. The top left plot shows positive (blue) and negative (red) one-step ahead residuals for each age-class and year, and the size of the circle represents the relative size of the residual. The top right plot shows the autocorrelation function for each age (green), year (purple) and cohort (orange). The bottom left plot shows the quantile plots of residuals for each age (colored circles), where the black line represents normally distributed errors. The bottom right plot represents the dispersion of residuals through time.

Supplemental Figure S2.11. One-step ahead residual plots for the Connecticut Long Island Sound Survey's (CTLIST) estimated age-composition in January-June. The top left plot shows positive (blue) and negative (red) one-step ahead residuals for each age-class and year, and the size of the circle represents the relative size of the residual. The top right plot shows the autocorrelation function for each age (green), year (purple) and cohort (orange). The bottom left plot shows the quantile plots of residuals for each age (colored circles), where the black line represents normally distributed errors. The bottom right plot represents the dispersion of residuals through time.

Supplemental Figure S2.12. One-step ahead residual plots for the Connecticut Long Island Sound Survey's (CTLIST) estimated age-composition in July-December. The top left plot shows positive (blue) and negative (red) one-step ahead residuals for each age-class and year, and the size of the circle represents the relative size of the residual. The top right plot shows the autocorrelation function for each age (green), year (purple) and cohort (orange). The bottom left plot shows the quantile plots of residuals for each age (colored circles), where the black line represents normally distributed errors. The bottom right plot represents the dispersion of residuals through time.

Supplemental Figure S2.13. One-step ahead residual plots for the Delaware 30 Foot Trawl Survey's (DE30) estimated age-composition in July-December. The top left plot shows positive (blue) and negative (red) one-step ahead residuals for each age-class and year, and the size of the circle represents the relative size of the residual. The top right plot shows the autocorrelation function for each age (green), year (purple) and cohort (orange). The bottom left plot shows the quantile plots of residuals for each age (colored circles), where the black line represents normally distributed errors. The bottom right plot represents the dispersion of residuals through time.

Supplemental Figure S2.14. One-step ahead residual plots for the Delaware Spawning Stock Survey's (DESSN) estimated age-composition in January-June. The top left plot shows positive (blue) and negative (red) one-step ahead residuals for each age-class and year, and the size of the circle represents the relative size of the residual. The top right plot shows the autocorrelation function for each age (green), year (purple) and cohort (orange). The bottom left plot shows the quantile plots of residuals for each age (colored circles), where the black line represents normally distributed errors. The bottom right plot represents the dispersion of residuals through time.

Supplemental Figure S2.15. One-step ahead residual plots for the Maryland Spawning Stock Survey's (MDSSN) estimated age-composition in January-June. The top left plot shows positive (blue) and negative (red) one-step ahead residuals for each age-class and year, and the size of the circle represents the relative size of the residual. The top right plot shows the autocorrelation function for each age (green), year (purple) and cohort (orange). The bottom left plot shows the quantile plots of residuals for each age (colored circles), where the black line represents normally distributed errors. The bottom right plot represents the dispersion of residuals through time.

Supplemental Figure S2.16. One-step ahead residual plots for the New Jersey Bottom Trawl (NJBT) survey's estimated age-composition in January-June. The top left plot shows positive (blue) and negative (red) one-step ahead residuals for each age-class and year, and the size of the circle represents the relative size of the residual. The top right plot shows the autocorrelation function for each age (green), year (purple) and cohort (orange). The bottom left plot shows the quantile plots of residuals for each age (colored circles), where the black line represents normally distributed errors. The bottom right plot represents the dispersion of residuals through time.

Supplemental Figure S2.17. One-step ahead residual plots for the New York Ocean Haul Seine (NYOHS) survey's estimated age-composition in January-June. The top left plot shows positive (blue) and negative (red) one-step ahead residuals for each age-class and year, and the size of the circle represents the relative size of the residual. The top right plot shows the autocorrelation function for each age (green), year (purple) and cohort (orange). The bottom left plot shows the quantile plots of residuals for each age (colored circles), where the black line represents normally

distributed errors. The bottom right plot represents the dispersion of residuals through time.

Supplemental Figure S2.18. Estimated log standardized residuals of the index of abundance for the fishery-independent Age-1 surveys for striped bass. The black solid line are the logged residuals that subtract the predicted trend from the observed trend divided by the standard deviation ($\frac{obs-est}{sd}$). The red dotted line indicates when the residual would be equal to zero. Estimates are provided for the Maryland Yearling Survey (MD1) and the New York Yearling Survey (NY1).

Supplemental Figure S2.19. Estimated log standardized residuals of the index of abundance for the fishery independent young-of-the-year surveys for striped bass. The black solid line are the logged residuals that subtract the predicted trend from the observed trend divided by the standard deviation ($\frac{obs-est}{sd}$). The red dotted line indicates when the residual would be equal to zero. Estimates are provided for the Chesapeake Bay YOY Index (CBYOY), the New Jersey YOY Survey (NJYOY), and the New York YOY Survey (NYYOY). The CBYOY is an aggregate index of YOY abundance for the Chesapeake Bay, with data from the Virginia YOY survey conducted by the Virginia Institute of Marine Science and the Maryland YOY survey conducted by the Maryland Department of Natural Resources.

Supplemental Figure S2.20. Estimated striped bass spawning stock biomass (SSB) for the base model and five sensitivity runs of the spatially-explicit multi-stock model (see Table S2.4 for definitions of runs).

Supplemental Figure S2.21. Mean estimates of abundance for striped bass (7-15+) for each stock, region, and 6-month time-step estimated from sensitivity runs. The top two rows correspond to estimates in the Chesapeake Bay region for both stock in both time-steps, and the bottom two rows correspond to estimates in the Ocean region for both stock in both time-steps (see Table S2.4 for definition of runs).

Supplemental Figure S2.22. Estimated weighted average of instantaneous fishing mortality (F) for each 6-month time-step ($6mo^{-1}$) for striped bass (7-15+) from sensitivity runs. The top row is estimates in the Chesapeake Bay region and the bottom row is estimates from the Ocean region (see Table S2.4 for definition of runs).

Chapter 3

Figure 3.1. A) Boxplots of the distribution of relative errors of total abundance over stocks and regions (N), annual fishing mortality at age-8 (F-8), and fishing mortality that achieves a 40% spawning potential ratio (SPR) for the entire population (F40). B) Boxplots of the distribution of relative errors of stock-specific abundance for the Chesapeake Bay stock (N CB) and Atlantic coast stock (N AC), fishing mortality that produces 40% SPR for the Chesapeake Bay stock (F40 CB), and fishing mortality that produces 40% SPR for the Atlantic coast stock (F40 AC). Estimation models are described in Table 3.4. For both figures, the dashed red line represents when relative error is equal to 0. The lower and upper hinge of the box represents the 25th and 75th

percentiles. The middle line represents the median. The whiskers extend to the minimum and maximum values of relative error.

Figure 3.2. Relative error of total abundance (over stocks and regions) for each year and estimation model. Models are described in Table 3.4. The dashed red line represents when relative error is equal to 0. Boxplot definitions are found in Figure 3.1.

Figure 3.3. Relative error of total spawning stock biomass (SSB) (over stocks and regions) for each year and estimation model. Models are described in Table 3.4. The dashed red line represents when relative error is equal to 0. Boxplot definitions are found in Figure 3.1.

Figure 3.4. Relative error of total fishing mortality for age 8 (F-8) (over stocks and regions) for each year and estimation model. Models are described in Table 3.4. The dashed red line represents when relative error is equal to 0. Boxplot definitions are found in Figure 3.1.

Figure 3.5. Relative error of fishing mortality for each age (over stocks and regions), shown for each year and estimation model. Models are described in Table 3.4. The dashed red line represents when relative error is equal to 0. Boxplot definitions are found in Figure 3.1.

Chapter 4

Figure 4.1. Natural mortality for each region of each 2-month time-step and year used in the OM-M scenario. Each panel represents a different decade of the operating model.

Figure 4.2. Occupancy probabilities of the Chesapeake Bay stock in the Ocean region over-time, including average occupancy and the percent remaining for each time-step, for each 2-month time-step used in the OM-P scenario.

Figure 4.3. Boxplots of the distribution of relative errors of annual abundance over stocks and regions (N), spawning stock biomass in January 1 (SSB), and fishing mortality at age 8 in the terminal year of all operating model simulations for three estimation models. The estimation models are a fleets-as-areas model (FAA), the multi-stock spatially-explicit model (SE), and the multi-stock spatially-explicit model with additional stock composition data (SE-S). The dashed red line represents when relative error is equal to 0. The box represents the 25th and 75th percentiles. The middle line represents the median. The whiskers extend to the minimum and maximum relative error for each metric.

Figure 4.4. Relative error of Striped Bass abundance (1-15+) for all model years for each operating model and estimation model scenario. Estimates for RE of abundance are provided for the base model (OM-B, top row), natural mortality (OM-M, second row), time-varying movement (OM-P, 3rd row), time-varying average recruitment

(OM-R, 4th row), and the mortality, movement and recruitment model (OM-MPR, last row) for the fleets-as-areas model (FAA), spatially-explicit model without stock data (SE), and the spatially-explicit model with additional stock data in the last 10 years (SE-S). Boxplot definitions are the same as Figure 4.3.

Figure 4.5. Relative error for each year of Striped Bass spawning stock biomass (SSB) for each operating model and estimation model scenario. Estimates for RE of abundance are provided for the base model (OM-B, top row), natural mortality (OM-M, second row), time-varying movement (OM-P, 3rd row), time-varying average recruitment (OM-R, 4th row), and the mortality, movement and recruitment model (OM-MPR, last row) for the fleets-as-areas model (FAA), spatially-explicit model without stock data (SE), and the spatially-explicit model with additional stock data in the last 10 years (SE-S). Boxplot definitions are the same as Figure 4.3.

Figure 4.6. Relative error of fishing mortality for age-8 for each year, operating model, and estimation model. Estimates for RE of abundance are provided for the base model (OM-B, top row), natural mortality (OM-M, second row), time-varying movement (OM-P, 3rd row), time-varying average recruitment (OM-R, 4th row), and the mortality, movement and recruitment model (OM-MPR, last row) for the fleets-as-areas model (FAA), spatially-explicit model without stock data (SE), and the spatially-explicit model with additional stock data in the last 10 years (SE-S). Boxplot definitions are the same as Figure 4.3.

Figure S4.1. Stock specific estimates of relative error in the terminal year of all operating model simulations and the spatially-explicit estimation model without additional stock composition data (SE) and the spatially-explicit model with additional stock composition data (SE-S). Error is provided for the terminal RE for stock specific abundance when applicable for the Chesapeake Bay (N CB) and Atlantic Coast (N AC). Boxplot definitions are the same as Figure 4.3.

Figure S4.2. Occupancy probabilities-at-age for the Chesapeake Bay stock in the Ocean region over-time, including average occupancy and the percent remaining for each time-step, for each 2-month time-step used in the OM-P 50% scenario.

Figure S4.3. Relative error in the terminal year for the estimation models under the OM-P model that assumes changes of 50% migration each decade. Relative error is provided for total annual abundance (N), spawning stock biomass (SSB), and fishing mortality at age 8 (F). Boxplot definitions are the same as Figure 4.3.

Chapter 1: Introduction

Stock assessment models make assumptions to simplify biological and fishery complexity. For example, stock assessments usually represent a population that is assumed to be well-mixed and closed (i.e., no net immigration or emigration) with homogenous fishing mortality across the stock's range (Cadrin 2020; Goethel et al. 2023). However, most fish populations experience spatially varying fishing mortality or other biological processes, which can violate the assumptions made by many stock assessment models. When the spatial scale of assessment models does not match the spatial scale of biological characteristics, estimation of biomass and fishing mortality have the potential to under- or overestimate parameters or increase bias of estimates of spawning stock biomass and fishing mortality (Guan et al. 2013; Bosley et al. 2022). When spatial complexity exists in life history and fishery characteristics, spatially-explicit population models can reduce bias of abundance estimates, while spatially-implicit (e.g., fleets-as-areas) approaches may result in bias in estimates of mortality over time (Punt et al. 2015; Bosley et al. 2022). Additionally, not accounting for or mis-specifying spatial complexity of both fishing pressure and population dynamics has the potential to increase bias in estimates of fishing mortality and biomass (Guan et al. 2013).

Although studies have demonstrated the benefits of incorporating spatial structure into stock assessments, the use of spatial assessments has been limited. Simulation studies have demonstrated that stock assessment models that match the spatial dynamics of a population can improve model estimates for management

purposes (Goethel and Berger 2016; Punt 2019a; Goethel et al. 2023). Use of spatial models has been restricted due to computational capabilities and a lack of available data (e.g., tagging data) at the appropriate spatial scales (Goethel et al. 2011). For highly mobile stocks, spatially-explicit stock assessments require information on fish movements, which can sometimes be lacking (Cadrin and Secor 2009; Guan et al. 2013; Goethel et al. 2015a; Vincent et al. 2016; Punt 2019a). Incorporation of spatial structure into stock assessments has increased in recent years (Cadrin and Secor 2009; Guan et al. 2013; Goethel et al. 2015a; Punt 2019b), and various models have been developed for use in management (Carruthers et al. 2011; Taylor et al. 2011; Robinson et al. 2013; Punt et al. 2014). While increased spatial complexity in population models can likely improve information to support management decisions, there remain few examples of spatially-explicit models used for management purposes (Goethel et al. 2023).

The Chesapeake Bay is the largest estuary in the United States, and it supports important recreational and commercial fisheries. Many species in the Chesapeake Bay have life history strategies that include migration into and out of the Chesapeake Bay at different life stages. Disregarding spatial structure in stock assessments of Chesapeake Bay fishes could hinder effective management and may increase the potential for overexploitation (Cope and Punt 2011; Ying et al. 2011; Guan et al. 2013). The Chesapeake Bay has experienced increased hypoxia (Hagy et al. 2004; Du et al. 2018), varying nutrient loads due to land use practices (Goetz et al. 2004), declines in ecological engineers such as Eastern Oyster (*Crassostrea virginica*) (Wilberg et al. 2011), and the spread of invasive species like Blue Catfish (*Ictalurus*

furcatus) (Schloesser et al. 2011), in the last several decades. Habitat quality in the Chesapeake Bay is expected to worsen over time with climate change (Du et al. 2018). Chesapeake Bay species have also exhibited distribution shifts. For example, Black Sea Bass (*Centropristis striata*) and Summer Flounder (*Paralichthys dentatus*) have undergone northward range shifts as a result of climate change and warming waters (Pinsky and Fogarty 2012; Kleisner et al. 2017; Slesinger et al. 2019), while numerous other species are expected to see range shifts in the future. If population models cannot account for shifts in distribution or productivity, abundance estimates may be biased. Management decisions like catch limits that are based on these estimates may lead to over or underutilized resources (Wayte 2013).

Striped Bass (*Morone saxatilis*) supports an important recreational and commercial fishery on the Atlantic coast and in the Chesapeake Bay (Hartman and Margraf 2003). The Chesapeake Bay serves as important habitat for Striped Bass, as about 50-90% of the Atlantic coastal population is sourced from the Chesapeake Bay spawning stock annually (Hartman and Margraf 2003; Kneebone et al. 2014; Hasegawa et al. 2022). Striped Bass that inhabit the Atlantic coast between New York to North Carolina embark on seasonal migrations that vary by sex, size, and age (Secor et al. 2020). However, a proportion of fish in the Chesapeake Bay remain resident annually and do not enter the migratory, coastal population (Secor et al. 2020). The Striped Bass population has fluctuated in abundance over time due to overexploitation, recruitment patterns, and disease (Hartman and Margraf 2003; Northeast Fisheries Science Center 2019). Stock assessments of Striped Bass assume a homogenous population that is assessed as one coast-wide unit stock from Maine to

North Carolina. However, fishery regulations are implemented at the state level and fishing effort varies among each state along the Atlantic coast. This could potentially provide incorrect recommendations for Striped Bass management because the stock assessment informs management with a model that has different spatial resolution and assumptions than that which management decisions are implemented.

The overall goal of this dissertation was to develop and evaluate new methods for spatially-explicit population models that can be applied to ecologically and economically significant Chesapeake Bay fishes. Striped Bass are one of many species for which the population estimates used for management purposes do not match the spatial resolution and temporal scales of management (Northeast Fisheries Science Center 2019) and were used as a test species to develop and apply spatial stock assessment methods. Although incorporating spatial structure into population models has many potential benefits for management (Goethel and Berger 2016), the reliability of spatial assessment models must first be validated before use in management (Goethel et al. 2015b). Simulation models are a valuable way for testing new approaches of spatial stock assessment because they allow for estimated parameters to be compared to known values (Cadrin and Dickey-Collas 2015). Simulation studies are frequently used to evaluate assessment models including spatiotemporal models (Cao et al. 2019), models that incorporate spatial structure (Goethel et al. 2015b), and models with mis-specified natural mortality (Deroba and Schueller 2013). Striped Bass served as an excellent pilot species for this analysis because there is abundant data at various spatial resolutions. Data available for Striped Bass include tagging data in the Chesapeake Bay and surrounding regions

under the US Fish and Wildlife Service's tagging program (Schonfeld 2023). The goals for Chapter 2 were to develop and implement a new multi-stock, spatially-explicit population model for Striped Bass to estimate abundance and fishing mortality rates in the Chesapeake Bay and coastal Atlantic Ocean. The goal for Chapter 3 was to evaluate new statistical methods for population estimation by conducting a simulation analysis for Striped Bass as a model species to assess the data requirements needed for reliably estimating population abundance, fishing mortality, and fishing mortality reference points. Finally, the goal for Chapter 4 was to understand the ability of the models to estimate abundance, mortality, or reference points under various scenarios that assumed climate induced population changes for Striped Bass.

1.1 References

Bosley, K. M., A. M. Schueller, D. R. Goethel, D. H. Hanselman, K. H. Fenske, A. M. Berger, J. J. Deroba, and B. J. Langseth. 2022. Finding the perfect mismatch: Evaluating misspecification of population structure within spatially explicit integrated population models. Fish and Fisheries 23(2):294–315.

Cadrin, S. X. 2020. Defining spatial structure for fishery stock assessment. Fisheries Research 221(105397):1–12.

Cadrin, S. X., and M. Dickey-Collas. 2015. Stock assessment methods for sustainable fisheries. ICES Journal of Marine Science 72(1):1–6.

Cadrin, S. X., and D. H. Secor. 2009. Accounting for spatial population structure in stock assessment: Past, present, and future. The Future of Fisheries Science in North America:405–426.

Cao, J., J. T. Thorson, A. E. Punt, and C. Szuwalski. 2019. A novel spatiotemporal stock assessment framework to better address fine-scale species distributions: Development and simulation testing. Fish and Fisheries 21(2):350–367.

Carruthers, T. R., M. K. McAllister, and N. G. Taylor. 2011. Spatial surplus production modeling of Atlantic tunas and billfish. Ecological Applications 21(7):2734–2755.

Cope, J. M., and A. E. Punt. 2011. Reconciling stock assessment and management scales under conditions of spatially varying catch histories. Fisheries Research 107(1–3):22–38.

Deroba, J. J., and A. M. Schueller. 2013. Performance of stock assessments with misspecified age- and time-varying natural mortality. Fisheries Research 146:27–40.

Du, J., J. Shen, K. Park, Y. P. Wang, and X. Yu. 2018. Worsened physical condition due to climate change contributes to the increasing hypoxia in Chesapeake Bay. Science of the Total Environment 630:707–717.

Goethel, D. R., and A. M. Berger. 2016. Accounting for spatial complexities in the calculation of biological reference points: Effects of misdiagnosing population structure for stock status indicators. Canadian Journal of Fisheries and Aquatic Sciences 74(11):1878–1894.

Goethel, D. R., A. M. Berger, and S. X. Cadrin. 2023. Spatial awareness: Good practices and pragmatic recommendations for developing spatially structured stock assessments. Fisheries Research 264(106703).

Goethel, D. R., C. M. Legault, and S. X. Cadrin. 2015a. Demonstration of a spatially explicit, tag-integrated stock assessment model with application to three interconnected stocks of yellowtail flounder off of New England. ICES Journal of Marine Science 72(1):164–177.

Goethel, D. R., C. M. Legault, and S. X. Cadrin. 2015b. Testing the performance of a spatially explicit tag-integrated stock assessment model of yellowtail flounder (*Limanda ferruginea*) through simulation analysis. Canadian Journal of Fisheries and Aquatic Sciences 72(4):582–601.

Goethel, D. R., T. J. Quinn, and S. X. Cadrin. 2011. Incorporating spatial structure in stock assessment: Movement modeling in marine fish population dynamics. Reviews in Fisheries Science 19(2):119–136.

Goetz, S. J., C. A. Jantz, S. D. Prince, A. J. Smith, D. Varlyguin, and R. K. Wright. 2004. Integrated analysis of ecosystem interactions with land use change: The Chesapeake bay watershed. Geophysical Monograph Series 153:263–275.

Guan, W., J. Cao, Y. Chen, and M. Cieri. 2013. Impacts of population and fishery spatial structures on fishery stock assessment. Canadian Journal of Fisheries and Aquatic Sciences 70(8):1178–1189.

Hagy, J. D., W. R. Boynton, C. W. Keefe, and K. V. Wood. 2004. Hypoxia in Chesapeake Bay, 1950-2001: Long-term change in relation to nutrient loading and river flow. Estuaries 27(4):634–658.

Hartman, K. J., and F. J. Margraf. 2003. US Atlantic coast striped bass: Issues with a recovered population. Fisheries Management and Ecology 10(5):309–312.

Hasegawa, E. H., J. Waldman, and I. Wirgin. 2022. Stock composition of Atlantic coastal migratory striped bass using microsatellite DNA analysis. Fisheries Research 254(106384):1–10.

Kleisner, K. M., M. J. Fogarty, S. McGee, J. A. Hare, S. Moret, C. T. Perretti, and V. S. Saba. 2017. Marine species distribution shifts on the U.S. Northeast Continental Shelf under continued ocean warming. Progress in Oceanography 153:24–36.

Kneebone, J., W. S. Hoffman, M. J. Dean, D. A. Fox, and M. P. Armstrong. 2014. Movement patterns and stock composition of adult striped bass tagged in

Massachusetts coastal waters. Transactions of the American Fisheries Society 143(5):1115–1129.

Northeast Fisheries Science Center. 2019. 66th Northeast Regional Stock Assessment Workshop (66th SAW) Assessment Report. Northeast Fisheries Science Center Reference Document (19–08):457–1170.

Pinsky, M. L., and M. Fogarty. 2012. Lagged social-ecological responses to climate and range shifts in fisheries. Climatic Change 115(3–4):883–891.

Punt, A. E. 2019a. Spatial stock assessment methods: A viewpoint on current issues and assumptions. Fisheries Research 213:132–143.

Punt, A. E. 2019b. Modelling recruitment in a spatial context: A review of current approaches, simulation evaluation of options, and suggestions for best practices. Fisheries Research 217:140–155.

Punt, A. E., M. Haddon, and G. N. Tuck. 2015. Which assessment configurations perform best in the face of spatial heterogeneity in fishing mortality, growth and recruitment? A case study based on pink ling in Australia. Fisheries Research 168:85–99.

Punt, A. E., T. Hakamada, T. Bando, and T. Kitakdao. 2014. Assessment of Antarctic minke whales using statistical catch-at- age analysis (SCAA). Journal of Cetacean Research Management (2013):93–116.

Robinson, J. M., M. J. Wilberg, J. V. Adams, and M. L. Jones. 2013. A spatial age-structured model for describing sea lamprey (*Petromyzon marinus*) population dynamics. Canadian Journal of Fisheries and Aquatic Sciences 70(12):1709–1722.

Schloesser, R. W., M. C. Fabrizio, R. J. Latour, G. C. Garman, B. Greenlee, M. Groves, and J. Gartland. 2011. Ecological Role of Blue Catfish in Chesapeake Bay Communities and Implications for Management. Page VIMS Books and Book Chapters.

Schonfeld, A. J. 2023. Climate Impacts on Spatiotemporal Habitat Usage of Mid-Atlantic Fishes. William & Mary Ph.D. Dissertation.

Secor, D. H., M. H. P. O'Brien, B. I. Gahagan, J. Carter Watterson, and D. A. Fox. 2020. Differential migration in Chesapeake Bay striped bass. PLoS ONE 15(5):1–19.

Slesinger, E., A. Andres, R. Young, B. Seibel, V. Saba, B. Phelan, J. Rosendale, D. Wieczorek, and G. Saba. 2019. The effect of ocean warming on black sea bass (*Centropristis striata*) aerobic scope and hypoxia tolerance. PLoS ONE 14(6):1–22.

Taylor, N. G., M. K. McAllister, G. L. Lawson, T. Carruthers, and B. A. Block. 2011. Atlantic bluefin tuna: A novel multistock spatial model for assessing population biomass. PLoS ONE 6(12).

Vincent, M. T., T. O. Brenden, and J. R. Bence. 2016. Simulation testing the robustness of a multiregion, tag-integrated assessment model that exhibits natal homing and estimates natural mortality and reporting rate. Canadian Journal of Fisheries and Aquatic Sciences 74(11):1930–1949.

Wayte, S. E. 2013. Management implications of including a climate-induced recruitment shift in the stock assessment for jackass morwong (Nemadactylus macropterus) in south-eastern Australia. Fisheries Research 142:47–55.

Wilberg, M. J., M. E. Livings, J. S. Barkman, B. T. Morris, and J. M. Robinson. 2011. Overfishing, disease, habitat loss, and potential extirpation of oysters in upper Chesapeake Bay. Marine Ecology Progress Series 436:131–144.

Ying, Y., Y. Chen, L. Lin, and T. Gao. 2011. Risks of ignoring fish population spatial structure in fisheries management. Canadian Journal of Fisheries and Aquatic Sciences 68(12):2101–2120.

Chapter 2: A multi-stock spatial population model to estimate abundance of striped bass in the Chesapeake Bay and Atlantic coast

2.1 Abstract

Many fisheries stock assessments assume a single, well-mixed population and spatially homogeneous fishing mortality. Violations of these assumptions can result in biased estimates of abundance and fishing mortality. Currently, striped bass (*Morone saxatilis*) is assessed as a single stock from Maine to North Carolina, although the population is known to be composed of several biologically distinct stocks and management measures vary spatially. Our objective was to develop a multi-stock, spatially-explicit statistical catch-at-age model to estimate abundance and mortality rates of striped bass in the Chesapeake Bay and along the Atlantic coast. The population model was a two-stock model with two sub-annual time-steps and two spatial regions. Striped bass from each stock had age-specific occupancy probabilities to represent movement into and out of the Bay that were different for each time-step. Estimated abundance increased until 2004 and then declined slightly through 2017. Estimated spawning stock biomass for the Chesapeake Bay stock increased substantially during 1987-2005, but has remained fairly constant through 2017. Fishing mortality was estimated to be higher in the Ocean than the Chesapeake Bay.

2.2 Introduction

Estimates from stock assessment models are often used to inform fishery management decisions that are implemented at different spatial units from the

assessment (Cadrin 2020; Goethel et al. 2023). However, most fish populations likely experience spatially varying fishing mortality as a result of spatially varying management implementations (Berger et al. 2016a; Cadrin 2020), as well as other spatially varying biological processes, which can violate the assumptions made by many stock assessment models (Cadrin and Secor 2009). Stock assessments usually assume a single, well-mixed, and closed population with homogeneous fishing mortality across the stock's range (Cadrin 2020; Goethel et al. 2023). Ideally, population models with spatial structure for ecologically and economically important fish species should estimate biological parameters at the same spatial scale as management decisions are made. Incorporating spatial structure into stock assessments adds realism into models for species that do not exhibit homogenous distribution across space and can increase accuracy of estimates (Cadrin and Secor 2009; Berger et al. 2012; Punt 2019a).

When the spatial scale of assessment models does not match the spatial scale of biological characteristics, estimates of biomass and fishing mortality can be substantially biased (Guan et al. 2013; Bosley et al. 2022; Goethel et al. 2023). For example, models that assumed a homogenous unit stock for populations with spatial heterogeneity in fishing effort have the potential to overestimate fishing mortality (Guan et al. 2013). Furthermore, simulation studies have demonstrated that stock assessment models that match the spatial dynamics of a population can improve model estimates for management purposes (Goethel and Berger 2016; Punt 2019a; Goethel et al. 2023). Ignoring spatial and stock structure is thought to be a contributing factor in the collapse of Atlantic cod (*Gadus morhua*) (Hutchinson

2008). Therefore, modeling species at a spatial resolution that matches their stock structure, movement patterns, and mortality rates has the potential to improve accuracy of stock assessment estimates (Cope and Punt 2011; Cao et al. 2019; Punt 2019a).

The use of spatial stock assessment models has been limited (Berger et al. 2016a), but incorporation of spatial structure into stock assessments has increased in recent years (Cadrin and Secor 2009; Guan et al. 2013; Goethel et al. 2015a), and various models have been developed for use in management (Carruthers et al. 2011; Taylor et al. 2011; Robinson et al. 2013). Use of spatial stock assessment models has been restricted due to a long tradition of single area stock assessment models, increased computational requirements for spatial models, and a lack of available data at the appropriate spatial scales (Goethel et al. 2011). Many stocks with spatially-varying biological and fishery dynamics have been assessed as separate stocks with no net immigration or emigration to incorporate a degree of stock structure and spatial heterogeneity (Northeast Fisheries Science Center 2017a, 2017b; ICCAT 2022). Modeling a population in this manner, however, does not allow for mixing among spatial units which can cause bias in assessment estimates for migratory species (Morse et al. 2020). For highly mobile stocks, spatially-explicit stock assessments that incorporate stock mixing rely on additional information to inform fish movements (Cadrin and Secor 2009; Guan et al. 2013).

Striped bass (*Morone saxatilis*) supports an important recreational and commercial fishery on the U.S. Atlantic coast and in the Chesapeake Bay (Hartman and Margraf 2003). The multi-stock complex that inhabits the Atlantic coast between

New York to North Carolina embarks on seasonal migrations that vary by sex, size, and age (Secor et al. 2020). Striped bass are anadromous and exhibit natal homing by returning to their natal rivers in the winter and early spring to spawn (Dorazio et al. 1994; Northeast Fisheries Science Center 2019; Rothermel et al. 2020). The spawning season for all stocks occurs between March and June (Northeast Fisheries Science Center 2019); however, striped bass may enter the Chesapeake Bay as early as December (Secor et al. 2020). This migratory stock complex is composed of four major spawning stocks, including the Hudson River stock, Delaware Bay stock, Chesapeake Bay stock, and Roanoke River stock (Northeast Fisheries Science Center 2019). However, other smaller spawning areas along the Atlantic coast have been identified (Grothues et al. 2009). The Roanoke River spawning stock and other stocks farther south are not managed with the rest of the Atlantic coast stocks as little mixing is thought to occur between these stocks and the more northerly coastal stocks based on tagging data (Northeast Fisheries Science Center 2019). Striped bass abundance has fluctuated over time due to changing fishing mortality rates, recruitment, and disease (Hartman and Margraf 2003; Northeast Fisheries Science Center 2019). The Chesapeake Bay serves as important habitat for striped bass. About 50-90% of the Atlantic multi-stock complex is produced by the Chesapeake Bay spawning stock annually, informed by genetic studies (Hartman and Margraf 2003; Kneebone et al. 2014; Hasegawa et al. 2022). However, a proportion of fish in the Chesapeake Bay do not enter the migratory, coastal multi-stock complex (Secor et al. 2020).

Stock assessments of striped bass assume a single population that is assessed as one coast-wide unit stock from Maine to North Carolina. However, fishery

regulations are implemented at the state level, and fishing effort and regulations vary among states along the Atlantic coast, which likely leads to spatial differences in fishing mortality rates. Our objective was to develop and implement a new multi-stock, spatially-explicit population model for striped bass to estimate abundance and fishing mortality rates for both the Chesapeake Bay and coastal Atlantic Ocean. In this dissertation, the word 'stock' will be used to refer to distinct spawning units of striped bass. We developed a population model that considers population dynamics across two regions and two subannual time-steps to allow for stock-specific recruitment, movement, mortality and abundance.

2.3 Methods

A multi-stock, spatially-explicit statistical catch-at-age model (Fournier and Archibald 1982; Quinn et al. 1990) was developed for striped bass. The model tracked ages 1-15+, where age 15+ was an aggregate age group representing fish that are age-15 and older. The model included two stocks to represent some of the population complexity of the striped bass multi-stock complex: one for the Chesapeake Bay and another for the rest of the Atlantic coast stocks (hereafter referred to as the Atlantic coast stock). The Atlantic coast stock included the Hudson River and Delaware Bay stocks as well as spawning stocks in other smaller systems. The model had two regions that represented the Chesapeake Bay and the "Ocean" (Figure 2.1). The border of the Chesapeake Bay region extended north from Cape Charles and Cape Henry, Virginia to the head of the Bay in Maryland (Northeast Fisheries Science Center 2019). The Ocean region was defined as the area outside of the Chesapeake Bay from Maine to Virginia (including the estuaries), and coastal

North Carolina (Northeast Fisheries Science Center 2019). The model included two sub-annual time-steps, January-June and July-December, to allow it to represent striped bass migratory behavior and seasonal fishery dynamics. Spatially disaggregated data were available for the period 1982-2017. The assessment model was developed in AD Model Builder (Fournier et al. 2012).

2.3.1 Data

We used available fishery-independent and fishery-dependent data from Maine to North Carolina in the model. The federally-managed portion of the U.S. Exclusive Economic Zone (greater than 4.3 km offshore) is closed to fishing for striped bass (Northeast Fisheries Science Center 2019). Catch-at-age was assumed to represent all the individuals killed by fishing, both retained and estimated mortality from discards and releases, and was summarized by region for each time-step. Stock composition data (i.e., fraction of the catch from each stock) were not routinely collected for the catch. Catches for each region and time-step were composed of the commercial harvest obtained from state agencies, recreational harvest from the U.S. National Oceanic and Atmospheric Administration National Marine Fisheries Service's Marine Recreational Information Program (MRIP), and of the number of fish from each fishery that were assumed to have died from post-release mortality. The proportion of discards that was assumed to die was dependent on the gear as described in the benchmark assessment (e.g., 9% for hook-and-line; Northeast Fisheries Science Center 2019). Catches were aggregated across recreational and commercial fleets to simplify data inputs as has been done in previous striped bass stock assessments (Northeast Fisheries Science Center 2019) because disaggregated

catch-at-age data were not available from all sources to be able to consider alternative approaches. Catches from the Chesapeake Bay fleet included those from commercial and recreational fisheries within the Chesapeake Bay from Maryland, Virginia, and the Potomac River. The Ocean fleet included catches reported by Maine, New Hampshire, New York, New Jersey, Delaware, coastal Maryland, coastal Virginia, and coastal North Carolina. Catch proportions-at-age were calculated by applying age-length keys to catch-at-length frequencies from each fishery and state and summarizing them over states within a region for each time step (Northeast Fisheries Science Center 2019). When samples of fish from a fishery and time-step were insufficient to develop age-length keys, biologists from that state used data from other gears, fisheries, or state samples to inform their age-length keys (Northeast Fisheries Science Center 2019). With the exception of Virginia, who aged fish using otoliths, all states used scale ages to estimate the age-composition of their fishery catch (Northeast Fisheries Science Center 2019).

Multiple fishery-independent surveys regularly catch striped bass and were used to develop indices of abundance (Table 2.1), and details for the survey methods and index standardization can be found in Northeast Fisheries Science Center (2019). Seven surveys were used that sampled striped bass age-1 and older. Bottom trawl surveys included the Connecticut Long Island Sound Trawl Survey (CTLIST), New York Ocean Haul Seine Survey (NYOHS), New Jersey Bottom Trawl Survey (NJBT), Delaware 30 Foot Trawl Survey (DE30), and the Chesapeake Bay Multispecies Monitoring and Assessment Program (ChesMMAP). The Delaware Spawning Stock Electrofishing Survey (DESSN) used electrofishing to sample fish,

and the Maryland Spawning Stock Survey (MDSSN) used drift gillnets. For a majority of the surveys, an index of abundance was estimated by the agency that conducted each survey, and most indices were calculated as geometric means (Northeast Fisheries Science Center 2019). However, methods for standardizations varied among agencies. For the ChesMMAP survey, an index of abundance was calculated as the geometric mean catch-per-unit-effort separately for each model time-step. The CTLIST survey included two indices of abundance, one for each time-step, that were calculated by the Connecticut Department of Energy and Environmental Protection. A revised MDSSN index of abundance from the one used in Northeast Fisheries Science Center (2019) was calculated as the annual geometric mean during 1995-2017. A 1995 starting year was selected due to changes in the survey design prior to 1995. Each index of abundance was assumed to represent the abundance trend for that region and sub-annual time-step in which the survey was conducted. For the two spawning stock surveys, the indices of abundance were assumed to represent trends in the respective Chesapeake Bay or Atlantic coast spawning stocks, respectively.

Beach seine surveys provided fishery-independent data for age-0 and age-1 striped bass. Two age-1 surveys were used, the New York Yearling Survey (NY1) and Maryland Yearling Survey (MD1). Finally, three young-of-year (YOY) surveys were used as data inputs including the New York YOY Survey (NYYOY), New Jersey YOY Survey (NJYOY), and the Chesapeake Bay YOY Index (CBYOY). The CBYOY is an aggregate index of YOY abundance for the Chesapeake Bay, which includes data from the Virginia YOY survey conducted by the Virginia Institute of

Marine Science and the Maryland YOY survey conducted by the Maryland Department of Natural Resources. The Virginia YOY and Maryland YOY surveys were combined to generate an aggregate index of abundance using the Conn method (Conn 2010; Northeast Fisheries Science Center 2019). Although the NY1 survey occurs during May-August, the index was assumed to represent age-1 striped bass at the beginning of the second time-step.

Proportions-at-age for each index were also developed for each survey and time-step for surveys with multiple age classes. Age ranges for the multi-age surveys were 1-15+, 2-15+, or 2-13+ (Table 2.1). For most surveys, the agency provided proportions-at-age for the survey indices. For the ChesMMAP survey, proportions-at-age were calculated using cruise-specific age-length keys informed by otolith-aged fish. For the CTLIST survey, proportions-at-age for the survey during time-step two were calculated using age-length keys from New York from 1997 to 2017. Proportions-at-age calculated for the DE30 survey were also informed by otolith ages. Proportions-at-age calculated for NYOHS, CTLIST, NJBT, DESSN, and MDSSN were informed by scale ages.

Age-specific natural mortality, sex proportions-at-age, and female maturity-at-age were assumed constant over time and regions, and were the same as the current benchmark stock assessment model (Northeast Fisheries Science Center 2019). Age-specific natural mortality rates were derived from tagging data (Northeast Fisheries Science Center 2019). The proportion female at age was calculated using fish with known sex and age determined by otolith aging (Jiang et al. 2007; Northeast Fisheries Science Center 2019). Female maturity-at-age was estimated from a binomial

generalized linear model using striped bass sampled in the Chesapeake Bay and Atlantic coast during March-December between 2014 and 2016 (Northeast Fisheries Science Center 2019).

Many studies have documented the bias and uncertainty of aging striped bass using scales. Aging error can cause bias in estimates of abundance and fishing mortality in age-structured stock assessment models (Bertignac et al. 2007; Liao et al. 2013; Tyszko and Pritt 2017). For striped bass, using scales to inform age is imprecise relative to otolith ages and has strong negative bias for age classes above 9 (Secor et al. 1995; Liao et al. 2013). To correct for the extensive use of scales to age striped bass (Figure S2.1), aging error matrices were developed to describe the bias and precision of scale ages relative to otolith ages. The aging error matrix was developed from fish from Massachusetts, Rhode Island, and New Jersey that were aged with both scales and otoliths. The aging error matrix was calculated as the proportions of scale ages for fish with a given otolith age, assuming that the otolith age was the true age. Three aging error matrixes were calculated to correspond to the age composition of each survey (e.g., 1-15+, 2-15+, and 2-13+; Table S2.1). The aging error matrix was applied to the fishery proportions-at-age and survey proportions of age (for surveys that aged fish using scales) to convert between true ages in the model and the expected age distribution under scale age reading. Explicitly incorporating aging errors helps to adjust correct for potential bias in model estimates for striped bass when age composition is based on scale aged fish (Liao et al. 2013).

2.3.2 Model Description

Abundance in the first year and first time-step was estimated to be in equilibrium

$$Nt_{s,\mathrm{y=1,ts=1},a} = Nt_{s,\mathrm{y=1,ts=1},a-1} \times e^{-M_{a-1}+Feq_{s,a-1}} \quad (2.1)$$

where Nt was the abundance of stock *s* summed over the two spatial regions, M was the instantaneous natural mortality, Feq was the estimated equilibrium instantaneous fishing mortality in the first year, y was the year index, a was the age index, and ts was the time-step index. Feq was calculated as

$$Feq_{s,a} = afsel_a \times afeq_s, \quad (2.2)$$

where $afsel$ was the fishery selectivity-at-age for both stocks in equilibrium and $afeq$ was the fully selected fishing intensity in equilibrium. Recruitment (R), or abundance at age-1 was estimated as normal on the log-scale for each year for each stock,

$$Nt_{s,y=1,ts=1,a=1} = e^{(R_{s,y})}. \quad (2.3)$$

The model assumed that movement occurs before mortality, and total abundance for each stock was apportioned to each region based on the occupancy probabilities. Abundance-at-age for each stock was calculated as the sum over regions of the product of total stock abundance and estimated survival in each region in the previous time-step,

$$Nt_{s,y,ts,a} = \sum_r N_{s,r,y,ts-1,a} \times e^{-Z_{r,ts-1,a}}, \quad (2.4)$$

Where r was the region index, Z was the instantaneous total mortality rate and N was the abundance of stock s in a region. Regional abundance-at-age for each stock at the

beginning of the time step, N, was calculated as the product of the total stock abundance and the proportion of the stock at age in each region during a given time-step,

$$N_{s,r,y,ts,a} = Nt_{s,y,ts,a} \times occ_{s,r,ts,a}, \tag{2.5}$$

where occ was the proportion of the stock within a region. For the plus group, abundance for each stock was calculated as the stock-specific sum of the individuals that survived from the previous age, time-step, and region, added to the stock specific abundances that survived from the plus group in the previous time-step for a given region,

$$Nt_{s,y,ts,A} = \sum_r N_{s,r,y,ts-1,A-1} \times e^{-Z_{r,ts-1,A-1}} + \sum_r N_{s,r,y,ts-1,A} \times e^{-Z_{r,ts-1,A}}, \tag{2.6}$$

where A was age 15+. Spawning stock biomass (SSB) for each stock was estimated as the product of abundance-at-age, the weight-at-age during the spawning season ($w_{y,a}$), the proportion female-at-age (sex), and the proportion of mature females-at-age (mat),

$$SSB_{s,y} = \sum_{a,r} N_{s,r,y,ts=1,a} \times w_{y,a} \times sex_a \times mat_a. \tag{2.7}$$

The instantaneous total mortality rate for a given time-step, age, and region was calculated as the sum of the instantaneous natural mortality (M) and fishing mortality rates (F),

$$Z_{r,y,ts,a} = M_a + F_{r,y,ts,a}. \quad (2.8)$$

The instantaneous fishing mortality rate-at-age was calculated as the product of the fully selected fishing mortality (or fishing intensity) for each region (f) and the age-specific fishery selectivity,

$$F_{r,y,ts,a} = fsel_{r,t,ts,a} \times f_{r,y,ts}, \quad (2.9)$$

where t was the index for the fishery selectivity time-block. Fully selected fishing mortality is estimated as normal on the log-scale. Fishery selectivity varied over time with four selectivity time-blocks to account for changes in fishing regulations and practices. The first time-block was 1982-1989 to represent regulations prior to and during a moratorium that were implemented in the Chesapeake Bay and Delaware Bay. The second time-block was during 1990-1994 to represent the rebuilding management period after the Chesapeake Bay fishery was reopened. The third time-block was during 1995-2014 to represented when the stock was considered recovered and regulations were liberalized. The final time-block was 2015-2017, which represented a period with reductions in daily bag limits for striped bass. Fishery selectivity was estimated using a logistic function for the Ocean region to account for changes in availability due to migration,

$$fsel = \frac{1}{1+e^{-p_1 \times (a-p_2)}}, \quad (2.10)$$

where p_1 described the rate of increase, and p_2 was the age at 50% selectivity. A double logistic function was used for the Chesapeake Bay region,

$$fsel = \frac{1}{1+e^{-p_1\times(a-p_2)}} \times \frac{1}{1+e^{-p_3\times(p_4-a)}}, \quad (2.11)$$

where $p_1$was the slope of the ascending limb, p_2 was the age at 50% selectivity for the ascending limb, $p_3$was the descending slope, and p_4 was the age at 50% selectivity for the descending limb. Selectivity functions differ for each region because regulations vary by region and striped bass are assumed to have different vulnerability to the fishery depending on the region. Our assumptions for selectivity were similar to those made in the current assessment used to inform management (Northeast Fisheries Science Center 2019). For example, a double logistic function was used for selectivity of the fishery in the Chesapeake Bay because older ages of striped bass tend to only be in the Chesapeake for a portion of each six-month time step (Secor et al. 2020). Parameters for fishery selectivity varied between subannual time-steps and fishery time-blocks for a region. Stock specific average fishing mortality for ages 7+, $Fstock$, was calculated as the F experienced by each stock by multiplying by the occupancy probability and then taking the weighted average for that F given total abundance of each stock,

$$Fstock_{s,y} = \sum_{ts=1}^{2}(occ_{s,,\mathrm{ts},r,a} \times F_{r,ts,y,a}) \times \frac{Nt_{s,ts,y,a}}{\sum_{a=7}^{a=A} Nt_{s,ts,y,a}}. \quad (2.12)$$

$Fstock$ was calculated for ages 7-15+ to reflect the ages that were mostly fully selected in the fishery, though this varied by time-block and area.

Catch-at-age (CAA) for a region and time-step was estimated using the Baranov catch equation (Ricker 1975),

$$CAA_{r,y,ts,a} = \frac{F_{r,y,ts}}{Z_{r,y,ts}} \times (1 - e^{-Z_{r,y,ts}}) \times N_{s,r,y,ts}, \quad (2.13)$$

and catch-at-age, corrected for aging error ($CAAerr$), was calculated by multiplying CAA by the aging error matrix ($ageerr$),

$$CAAerr_{r,y,ts,a} = \sum_{a} ageerr_{a,i} \times CAA_{r,y,ts,a}, \quad (2.14)$$

where i is the scale age and a the otolith age. Total catch (C) was estimated by summing the catch-at-age with aging error over ages and stocks within a region,

$$C_{y,ts,r} = \sum_a CAAerr_{r,y,ts,a}. \quad (2.15)$$

Proportions-at-age (PAA) for each region and time-step were calculated by dividing the catch-at-age by the total catch,

$$PAA_{y,ts,r,a} = \frac{CAAerr_{r,y,ts,a}}{C_{y,ts,r}}. \quad (2.16)$$

Estimated indices of abundance (I) for the fishery-independent surveys were the product of abundance at age for each time-step and region, survey catchability (q), and survey selectivity for each age ($ssel$),

$$I_{v,y} = q_v \times \sum_{s,a} N_{s,r,y,ts,a} \times ssel_{v,a}, \quad (2.17)$$

for each survey v. The index of abundance was then summed over ages to get a total index for each survey for a time-step. For each index of abundance, the region is defined as either the Chesapeake Bay or Ocean depending on where the survey is conducted (e.g., region is the Ocean for the NJBT). Survey selectivity and catchability were assumed to be constant over years for each survey. For surveys that sampled during both time-steps in a year, selectivity was estimated separately for each time step. Indices of abundance for spawning stock surveys were estimated

using the abundance-at-age for their respective stock and region of spawning (e.g., the Chesapeake Bay stock for the MDSSN),

$$I_{s,v,y} = q_v \times \sum_a N_{s,r,y,ts=1,a} \times ssel_{v,a}. \quad (2.18)$$

Logistic functions were used to estimate selectivity for the spawning stock surveys and ChesMMAP (Eq. 2.10) because these surveys were designed to monitor mature striped bass. Double logistic functions with four parameters were used to estimate selectivity for the remaining fishery-independent surveys (Eq. 2.11) because older fish may have decreased availability or catchability to these surveys based on the timing, location, or gear. Predicted proportions-at-age in each survey were calculated by dividing the estimated index-at-age during a time-step by the sum of the estimated index-at-age over ages during a time-step (Eq. 2.16). For the ChesMMAP and DE30, which used otoliths to inform age-composition, an aging error matrix was not applied to calculate the estimated index-at-age. For the other surveys that used scales to inform age-composition, an aging error matrix was applied to the index-at-age calculations (Eq. 2.14, Table S2.1).

Parameters were estimated by minimizing the sum of the negative log likelihood functions representing each data source and penalties on several parameters. Likelihood components of the objective function and their respective equations can be found in Table 2.3. Log-normal observation errors were assumed for total catch ($-ln(L_{catch})$) and indices of abundance ($-ln(L_{Index})$) (Eq. 2.3.1). Similarly, occupancy probabilities were assumed to be normally distributed on the log-scale (Eq. 2.3.1). “Robust multinomial” (Fournier et al. 1990) error distributions were assumed for the age composition of the catch and the survey indices

($-ln(L_{PAA})$, Eq. 2.3.2). Binomial error distributions were assumed for the stock composition to inform the proportion of the catch for the coastal fishery from each stock for ages 4-15+ in 2010 during July-December, based on stock composition estimated by Kneebone et al. (2014) ($-ln(L_{prop})$, Eq. 2.3.3). The proportion for the Atlantic Coast stock was summed across Delaware and Hudson stocks. Recruitment was assumed to be normally distributed on the log scale with an assumed standard deviation of 1.0 ($-ln(L_{recruitment})$, Eq. 2.3.4). A log-normal penalty was applied to Feq with a standard deviation of 0.5 to restrict equilibrium fishing mortality from being too high to generate initial age compositions ($-ln(Feq)$, Eq. 2.3.5). We applied a weak smoothing penalty to the change in fishing mortality from one year to the next for each time-step and region ($-ln(L_{Fdev})$, Eq. 2.3.6). Log-scale standard deviations (CV) for the surveys and effective sample size (ESS) for the surveys and fishery catches were determined by iterative re-weighting (McAllister and Ianelli 1997; Francis 2011). If iterative reweighting produced an estimate <0.2, the CV was set to equal 0.2. The CVs were held constant across years for each survey. The ESS minimum was set to 15, where if the reweighting process yielded estimates <15, the ESS was set to 15. For the Chesapeake Bay fishery, ESS was allowed to differ between two time-blocks, 1982-1989 and 1990-2017, to account for poor model fits during 1982-1989, potentially as a result of low sample sizes during the Chesapeake Bay moratorium.

Informative priors were used to inform the occupancy probabilities ($-ln(L_{occ})$, Eq. 2.3.7), based on conventional and acoustic tagging data for striped bass. Conventional tagging estimates of occupancy probabilities were from a spatial

Brownie mark-recapture model (Schonfeld 2023). The spatial Brownie model incorporated conventional tag and recapture data to track striped bass from three producer regions (Chesapeake Bay, Delaware Bay, and the Hudson River) and recaptures in two recovery regions (Chesapeake Bay and Ocean), which matched the spatial regions and intra-annual time steps of the our spatially-explicit model. Age-specific occupancy probabilities from the Delaware Bay and Hudson River producer regions were averaged to generate one set of occupancy probabilities for the Atlantic coast stock. This approach implicitly assumes that the Delaware and Hudson River stocks are approximately the same size. Standard deviations used in Eq. 2.3.7 for each stock were estimated in the Brownie mark-recapture model. Acoustic tagging data (Secor et al. 2020) were also used to create informative priors for the occupancy probabilities. Striped bass were tagged in 2014 and 2016 during the spawning season in the Potomac River and were assumed to represent the Chesapeake Bay stock. Fish that were not tagged during the spawning season in the Chesapeake Bay were excluded from analyses. In total, 78 striped bass were used for these calculations. Acoustic transmissions for each unique fish were gathered from receivers from Maine to North Carolina. Each transmission was assigned to be in either the Chesapeake Bay or Ocean region based on the location of the receiver. Means for the occupancy probability priors were then calculated as the average proportion of unique months in which a fish was observed in a region out of the total number of months a fish was observed in either region during each time-step. Mean occupancy probabilities were calculated for each age that had at least one observation. For ages with more than one

individual, standard deviations for each age were calculated as the square root of the squared deviations from the average divided by the total number of observations.

Additional penalties were included in the model to constrain selectivity parameters ($-ln(L_{sel})$, Eq. 2.3.8) to reduce correlation among estimated parameters and allow for model convergence. Many selectivity parameters for the Chesapeake Bay fishery in 1982-1989 were constrained as this timeframe had difficulty estimating selectivity for this fishery. Specifically, the ascending slope parameter in July-December was constrained with a mean of 3 and standard deviation of 0.5. The slope of the descending limb for January-June and July-December assumed a mean of 1 and standard deviation of 0.25. Additionally, several of the descending limbs of double logistic selectivity functions were poorly estimated when they were not constrained and penalties were added to prevent the point of inflection of the descending limb from being less than the point of inflection for the ascending limb (Eq. 2.3.9). These penalties on selectivity were added for the Chesapeake Bay fishery and CTLIST survey and were conditioned on the descending inflection point being less than the ascending inflection point. Penalties on selectivity were normally distributed with a standard deviation of approximately 0.7. Parameters were estimated by minimizing the objective function (nll_{tot}), that is the sum of the negative log likelihood components, penalties, and priors,

$$\begin{aligned} nll_{tot} = &-ln(L_{Catch}) - ln(L_{Index}) - ln(L_{CatchPAA}) - \\ &ln\left(L_{SurveyPAA}\right) - ln\left(L_{prop}\right) - ln(L_{recruitment}) - ln(Feq) - \\ &ln(L_{Fdevs}) - ln(L_{occ}) - ln(L_{sel}) - ln\,(p_4). \end{aligned} \quad (2.19)$$

Model fits of estimated parameters were evaluated using the standardized residuals for fishery-independent indices of abundance,

$$Res_y = \frac{\log(I_y) - \log(\widehat{I_y})}{\sigma_y}, \quad (2.20)$$

where Res is the standardized residual, I is the observed index, $\hat{I}$ is the estimated index, and σ is the log-scale standard deviation of the index. Residuals for the age-compositions of the fishery and the surveys were evaluated using the one-step ahead approach in R (Thygesen et al. 2017; Trijoulet et al. 2023) and the compResidual package (Trijoulet and Nielsen 2022). One-step ahead residuals use the Laplace approach (Tierney and Kadane 1986) and can be used on data that has an assumed multinomial distribution, such as age compositions (Trijoulet et al. 2023).

2.3.3 Sensitivity Runs

Additional spatially-explicit models with alternative assumptions of aging error, selectivity, movement, age composition, and natural mortality were considered to understand the effects of specific decisions on model estimates (Table S2.4). The previously described model will be referred to as the 'base' model. All sensitivity models were the same as the base model with the exception of the specific aspects that were modified. Model 2 assumed no aging error and, therefore, did not utilize any aging error matrices. Model 3 assumed that fishery selectivity in the Chesapeake Bay region followed a logistic selectivity function (Eq. 2.11) rather than a double logistic selectivity function. Model 4 assumed no aging error and also assumed logistic fishery selectivity in the Chesapeake Bay region. Model 5 assumed a 50% reduction of occupancy probabilities for the Chesapeake Bay stock for ages 4-15+ in the Ocean region during January-June, to evaluate the impacts of movement assumptions on SSB estimates. Model 6 evaluated assumptions of natural morality by

assuming spatially- and time-varying mortality in the Chesapeake Bay based on results of a Brownie mark-recapture model developed for striped bass (Schonfeld 2023). The mark-recapture model estimated age-specific natural mortality rates for ages 2-11+, which were constant during three periods: 1990-1999, 2000-2009, and 2010-2019 (Schonfeld 2023). For Model 6, natural mortality between 1982-1999 was set equal to the 1990-1999 Schonfeld (2023) estimates, natural mortality between 2000-2010 was set equal to the 2000-2009 estimates from Schonfeld (2023), and from 2010-2017, natural mortality was set equal to the 2010-2020 estimates from Schonfeld (2023) (Table S2.3). Natural mortality for age-1 for all years was set equal to the natural mortality for age 1 in the benchmark assessment (Northeast Fisheries Science Center 2019) and natural mortality for ages 12-15+ were set equal to age-11 for each year. Model 6 also required additional penalties in the objective function for parameters estimating fishery selectivity across multiple time-blocks (Eq. 2.3.8) for the descending inflection point in 1982-1989 during January-June and July-December. Additionally, penalties on the descending limb of the NYOHS were added (Eq. 2.3.9).

2.4 Results

The model fit the data inputs (i.e., fishery-independent indices of abundance and total catch) relatively well according to the diagnostics (Figures S2.2-S2.19). Final estimates of ESS and CV for all surveys and fleets that were used in the spatially-explicit models are in Table S2.2. The model fit many of the fishery-independent data sources well but had more difficulty estimating indices of

abundance and proportions-at-age for DE30, NJBT, and the CTLST in July-December.

Estimated recruitment of the Chesapeake Bay stock was about 68% higher, on average, than the Atlantic coast stock and had an increasing trend over time in both regions (Figure 2.2). Recruitment of the Atlantic coast stock increased through the mid-1990s, with peaks in 1994, 1997, 2002, 2004, 2012, and 2016. After 2005, estimated average recruitment of the Atlantic coast stock was slightly lower than during 1993-2005. For the Chesapeake Bay stock, recruitment increased until 1994, and fluctuated around a relatively constant mean during 1995-2017, though years of high recruitment were observed in 2004 and 2012 (Figure 2.2). Additionally, estimates of recruitment for each stock were positively correlated (Pearson correlation coefficient r=0.79) with large recruitment events in both stocks in 1994 and 2004. Estimated total abundance for both stocks was lowest in 1982, which was followed by an increase until the mid-1990s (Figure 2.3). Peak estimated total abundance of over 755 million was in 2012. The Chesapeake Bay stock was more abundant than the Atlantic coast stock during 1982-2017, though abundance was similar in 1982. Abundance of the Chesapeake Bay stock age-7 and older increased until 2004 (Figure 2.4). The Chesapeake Bay stock age-7 and older declined approximately 14% since 2005, particularly in the Chesapeake Bay region (Figure 2.4). Abundance of the Atlantic coast stock age-7 and older increased until 2010, although abundance was relatively stable during 2003-2010. Between 2010 and 2017, Atlantic coast stock abundance declined by about 35% (Figure 2.4). The Chesapeake Bay stock age-7 and older were more abundant in the Ocean region in July-December after 1990 and were

the dominant contributor to the Ocean region for the remainder of the time-series (Figure 2.4).

Estimated SSB of the Chesapeake Bay stock increased from less than 2,200 MT in 1982 to over 293,900 MT 2016 (Figure 2.5). For the Atlantic coast stock, estimated SSB was relatively stable around 37,000 MT during 1982-1986 (Figure 2.5). Atlantic coast SSB increased to approximately 108,336 MT by 2008, followed by a slight decline to under 97,000 MT in 2017 (Figure 2.5).

Estimated fishery selectivity in the Ocean suggests that fish were fully selected to the fishery at younger ages during the 1982-1989 time-block during in January-June compared to the later time-blocks (Figure 2.6). Striped bass in the Ocean region were fully selected at younger ages in 2015-2017 during July-December relative to earlier time-blocks (Figure 2.6). However, overall selectivity in the Ocean region was not estimated to have changed substantially over time in both time-steps (Figure 2.6). In the Chesapeake Bay during January-June, selectivity changed over time from a dome-shaped selectivity pattern during the moratorium during 1982-1989 and the post-moratorium block from 1990-1994, followed by logistic shaped during the recovery 1995-2014 and recent selectivity time-block during 2015-2017 time-block (Figure 2.7). During the 1990-1994 selectivity block, the selectivity estimates suggested that ages 4-8 were fully selected to the fishery, but ages 11 and older had lower selectivity. In the Chesapeake Bay region, during the July-December time-step in 1982-1989, selectivity was estimated to increase with age, and striped bass reached full selectivity at age 15+ (Figure 2.7). During the July-

December time-step in the Chesapeake Bay, selectivity was dome-shape during 1990-2017 with peak selectivity between ages 4 and 7.

Estimated average fishing mortality rates for ages 7+ were always higher in the Ocean region than the Chesapeake Bay region (Figure 2.8). During January-June, fishing mortality in the Chesapeake Bay region declined from 0.001 per six-month period ($6mo^{-1}$) in 1982 to 0.0009 $6mo^{-1}$ in 1987 and increased to a high of approximately 0.024 $6mo^{-1}$ in 2016. In the Ocean region in January-June, fishing mortality declined from 0.030 $6mo^{-1}$ in 1982 to less than 0.003 $6mo^{-1}$ in 1987, increased to a high of 0.05 $6mo^{-1}$ in 2006, and was followed by a decline to 0.031 $6mo^{-1}$ in 2017. During the July-December time-step in the Chesapeake Bay region, fishing mortality decreased from less than 0.027 $6mo^{-1}$ in 1982 to 0.001 $6mo^{-1}$ in 1987. In 1993, fishing mortality in the Chesapeake Bay region increased and reached a high of 0.027 $6mo^{-1}$ in 2003, after which it declined to 0.014 $6mo^{-1}$ in 2017. In the Ocean region during July-December, fishing mortality decreased from 0.034 $6mo^{-1}$ in 1982 to 0.020 $6mo^{-1}$ in 1987, increased to 0.066 $6mo^{-1}$ in 1995 and remained relatively constant until 2017 with a slight decrease to 0.048 $6mo^{-1}$ in 2016.

Estimates of stock-specific average fishing mortality rates for ages 7+ suggested that the Atlantic coast stock experienced a consistently higher level of fishing mortality than the Chesapeake Bay stock during 1982-2017 (Figure 2.9). Fishing mortality for the Atlantic coast stock increased from less than 0.022 yr^{-1} in 1987 to approximately 0.115 yr^{-1} in 2013, followed by declines in fishing mortality to 0.088 yr^{-1} in 2017. For the Chesapeake Bay stock, fishing mortality was estimated to have been less than 0.01 yr^{-1} in 1987, during the moratorium, followed by increases to

0.061 yr^{-1} by 2013. In 2014-2017, the fishing mortality experienced by the Chesapeake Bay stock declined to 0.045 yr^{-1} in 2017 (Figure 2.9).

Estimated occupancy probabilities closely followed the informative prior from the conventional tagging data (Schonfeld 2023) but differed from the acoustic tagging data (Secor et al. 2020). The estimated occupancy probabilities for the Atlantic coast stock of all ages indicated that they largely remained in the Ocean region through the entire year, with age-3 having the lowest probability of being in the Ocean at over 80% occurrence in January-June and in July-December (Figure 2.10). Striped bass from the Chesapeake Bay stock were estimated to mostly reside in the Chesapeake Bay during January-June for ages 2-8. During July-December, the occupancy probability of the Chesapeake Bay stock in the Ocean region increased with age and reached its highest probability of 83% occurrence at age-11, though fish age 2-3 had a slightly higher occupancy than age-4. Estimates of occupancy probabilities for the Chesapeake Bay stock were higher than the acoustic tagging data for all ages in January-June. In July-December, estimates of occupancy were lower than the acoustic tagging data for age 6 and ages 12-15+, as the acoustic data suggests fish 13-15+ never enter the Chesapeake Bay (Figure 2.10).

Survey selectivity was estimated for each of the seven fishery-independent surveys across the two subannual time-steps (Figure 2.11). Selectivity for the ChesMMAP survey was similar for both time-steps, with 50% selectivity occurring around age-7. Selectivity for the CTLIST had a strong domed pattern across the two time-steps, with age-4 being fully selected in both time-steps, which was also similar to the DE30 survey. Estimated selectivity for ages older than 10 in the CTLIST and

NYOHS was low. Selectivity for the NJBT estimated ages 3-6 were fully selected, followed by gradually decreasing selectivity with age. The MDSSN and DESSN had similar selectivity patterns, with the first age for full selection at approximately age-4 for both surveys.

2.4.1 Sensitivity Runs

The model estimates were highly sensitive to assumptions about aging error and time-varying natural mortality but were relatively insensitive to assumptions about the occupancy probabilities and shape of the fishery selectivity functions (Figure S2.20). Estimates of SSB from the model that assumed logistic selectivity (Model 3) were similar to the base model for both stocks. The model that assumed reduced occupancy probabilities (Model 5), followed similar estimates of SSB to the base model, but SSB was much lower during 1982-1995 for the Atlantic coast stock, and higher for the Chesapeake Bay stock. The two models that assumed no aging error (Model 2 and 4) had similar trends in SSB over time for both stocks, but estimated SSB was about 54% lower than the base model, on average. Striped bass SSB for both stocks from the model that assumed time-varying natural mortality (Model 6) had different trends in SSB over time and different terminal year SSB than the base model. For Model 6, SSB was estimated to be 102% higher for the Atlantic coast stock than the base model in 2008, and SSB declined 61% from 2008-2017 for the Chesapeake Bay stock. Age-specific differences in abundance between the base model and sensitivity models were largely similar to the patterns for SSB (Figure S2.21).

Estimates for average fishing mortality of striped bass over ages 7-15+ from models with alternative assumptions showed similar trends over time to the base model in both regions and time-steps (Figure S2.22). Models that did not include correction for aging error had the highest estimates of fishing mortality in the Ocean region. The model that assumed logistic selectivity in the Chesapeake Bay region had similar estimates of fishing mortality as the base model, except in the Chesapeake Bay during July-December when estimates were higher. The model that assumed time-varying natural mortality had the lowest estimates of fishing mortality for most of the time-series in the Ocean region, but had the highest estimates of fishing mortality in the Chesapeake Bay for both time-steps.

2.5 Discussion

We developed and implemented a multi-stock, spatially-explicit population model to estimate abundance, recruitment, fishing mortality, and movement across two regions for striped bass. Although others have developed multi-stock, spatially-explicit models (e.g., Taylor et al. 2011; Punt et al. 2014; Goethel et al. 2015a; Little et al. 2016), there are still relatively few in the literature (Punt 2019b). Our model was similar to previous ones that estimated recruitment independently for each stock with lognormal deviations (e.g., Goethel et al. 2015a) rather than a stock-recruit function (e.g., Taylor et al. 2011; Little et al. 2016). However, it differed from many finfish models in that it did not directly integrate tagging data, and its estimation of movement was based on the probability of occurrence rather than the probability of movement (e.g., Taylor et al. 2011; Goethel et al. 2015b, 2015a). Additionally, our multi-stock model reflects behavior of natal homing for striped bass. The

development of multi-stock, spatially-explicit models have likely been scarce due to data limitations, since these models are complex. For species that experience natal homing, tagging data are required to inform movement (Berger et al. 2016; Vincent et al. 2016). Additionally, the multi-stock, spatially-explicit model required quantified stock composition information through the use of informative priors in the likelihood function, as we found this model had difficulty converging or providing reliable estimates of abundance for two stocks without stock information and information on movement.

In the 1980s, low commercial catch and poor recruitment trends suggested that striped bass had reached a historic low (ASMFC 1985; Richards and Deuel 1987; Richards and Rago 1999; Secor 2000). As a result, Maryland and Delaware implemented a fishing moratorium during 1985-1989, and Virginia implemented a moratorium for 1989. Effects of the moratorium in the Chesapeake Bay are apparent in our model estimates, as fishing mortality declined after 1982 and remained near zero in the Chesapeake Bay from 1985-1989. Abundance and SSB were also estimated to increase in the late 1980s after being severely depleted in the early 1980s. Furthermore, our model estimated an increasing contribution to the Ocean region during July-December from the Chesapeake Bay stock during the 1980s (<3% of total abundance (ages 7-15+) in 1982) to approximately 38% in 1989. Previous studies suggest that the collapse of the striped bass multi-stock complex in the 1980s was driven by declines to the Chesapeake Bay stock (Northeast Fisheries Science Center 2019). This is supported by our model estimates, as the Chesapeake Bay stock was the most depleted in 1982-1989, though both stocks had low abundance.

Our model differed from the current assessment in assumptions of striped bass biology, fishery characteristics, and quality of aging data, and estimates differed substantially between the models. The current assessment used to inform management of striped bass is a spatially-implicit fleets-as-areas (FAA) model that assumes a single region and a single stock (Northeast Fisheries Science Center 2019). The FAA model estimated increasing abundance from 1982-2004, followed by declines from 2005-2017 (Northeast Fisheries Science Center 2019). The spatially-explicit model estimated similar trends in abundance, although abundance does not decline to as low of a level during 2005-2017 as the FAA model. The FAA model estimated fishing mortality that was increasing for the Chesapeake Bay fleet from 1990-2016. For the Atlantic coast fleet, the FAA model estimated fishing mortality increasing from 1987-2013, followed by declines from 2014-2017. The spatially-explicit model estimated similar trends of fishing mortality to the FAA model, particularly in January-June, though the scale of estimates was lower. The FAA model estimated female SSB increased during 1986-2003, but declined during 2003-2017 (Northeast Fisheries Science Center 2019). In contrast, our model estimated increasing SSB for the entirety of the time-series, especially for the Chesapeake Bay stock, which was largely driven by an accumulation of fish in the plus group and is likely a result of our assumptions about aging error. These differences in the trend of SSB over time are important because current management relies of estimates of SSB relative to the SSB in 1995 for determining stock status (Northeast Fisheries Science Center 2019). Because of the differences in the trends over time, the two models

differ in their estimates of terminal SSB relative to the 1995 level (Northeast Fisheries Science Center 2019).

Including aging error in the model had a substantial effect on estimated SSB and fishing mortality rates. The model with aging-error estimated higher abundance and SSB compared to models that did not consider aging error with combined SSB estimated at approximately 170,000 MT for Models 2 and 4 in 2010 compared to over 375,000 MT in the base model. Estimated SSB for Model 2 and 4 were more similar to, but still higher than, those from the benchmark assessment model than our base model, which likely indicates that much of the difference in population scale may be due to assumptions about aging error. Aging error matrices are often incorporated in the stock assessment models in order to correct for potential biases in age composition data (Punt et al. 2008; Candy et al. 2012; Liao et al. 2013; Hulson and Williams 2024). Reeves (2003) found that ignoring aging bias in catch data resulted in biased estimates of SSB and fishing mortality which forecasted a higher value of total allowable catch than is sustainable. Hulson and Williams (2024) found that incorporating aging error matrices into statistical catch-at-age models can reduce estimates of input sample size, which influences the uncertainty in age composition estimates. Estimates from statistical catch-at-age models for striped bass that use scale-based age composition data will underestimate abundance or spawning stock biomass and overestimate fishing mortality when compared to models that use otolith corrected age composition (Liao et al. 2013). Estimates based on scale-age composition data could provide incorrect reference points for management of striped bass.

Stock assessments that model fisheries with spatial heterogeneity as a single area often provide biased estimates of SSB (Punt et al. 2015), and, therefore, a spatially-explicit model is likely necessary for striped bass. Our results suggest striped bass in the Ocean region experienced higher fishing mortality than the Chesapeake Bay region, and the Atlantic coast stock has experienced a higher fishing mortality over time compared to the Chesapeake Bay stock. Most stock assessment models assume natural mortality-at-age is constant over time, as our base model does, though this assumption is unrealistic for most stocks (Maunder et al. 2023). We evaluated the effect of using a natural mortality that varies by regions and over time (Model 6) from a Brownie mark recapture model (Schonfeld 2023). The Brownie model found that natural mortality differed between the Ocean and Chesapeake Bay regions, and that natural mortality was generally increasing in the Chesapeake Bay during 1990-2020, which has been supported by other studies (Groner et al., 2018; Secor et al., 2020). The sensitivity model that allowed natural mortality to change over time estimated abundance with a substantial decline in abundance at the end of the time series. Although natural mortality is likely changing over time for striped bass and has an impact on model results, further research is needed to validate these estimates and trends. Thus, assumptions of natural mortality for striped bass should be re-evaluated.

The spatially-explicit model assumed logistic fishery selectivity in the Ocean and double logistic selectivity in the Chesapeake Bay. Additionally, we assumed selectivity changed over time in four selectivity time-blocks. Fishing regulations have changed frequently between 1982-2017 as the Atlantic States Marine Fisheries

Commission has mandated changes to recover the striped bass population following its collapse, and states have been given some level of flexibility to implement regulations. The estimated selectivity in the Ocean regions suggests that striped bass were fully selected at younger ages during 1982-1989 than in later years, particularly in January-June. Our results are consistent with the minimum size limits implemented during the time period, which was the smallest allowed in the model time series. In 1982, Striped bass had a minimum size limit of 14 inches in the producer regions (e.g., Chesapeake Bay, Delaware Bay, Hudson River) and a minimum size limit of 24 inches along the Atlantic coast for the recreational fishery (ASMFC 1981; Richards and Deuel 1987). Between 1985-1989, regulations were changed many times, including a moratorium in Maryland and Delaware in 1985, and gradual increases in minimum size limit to 33 inches for fisheries outside the Chesapeake Bay by 1988 (ASMFC 1985; Richards and Deuel 1987). Selectivity estimates for the Chesapeake Bay region during 1982-1989 in July-December differed from the later years, and these differences in shape may be due to low sample sizes of catch during the moratorium. Additionally, fishing regulations changed substantially within this time-block, as regulations were more restrictive during 1985-1989, than 1982-1984. However, models with an additional time block in the 1980s would not converge on unique parameter estimates. Therefore, we assumed constant selectivity during 1982-1989. However, selectivity parameters were difficult to estimate in the Chesapeake Bay during July-December, resulting in different selectivity patterns than other regions and time-blocks. Following the moratorium, the Chesapeake Bay fishery reopened in 1990 with a minimum size limit of 18 inches, while the Ocean region had

a 28-inch minimum size limit (ASMFC 1989). In 1995, the Atlantic States Marine Fisheries Commission declared the stock recovered and a minimum size limit of 20 inches and 28 inches were set for producer regions and the coast, respectively (ASMFC 1995). Estimates of fishery selectivity in 1990-1994 and 1995-2014 appear to follow the minimum size limits that were in place during that time.

Numerous studies have estimated the composition of striped bass spawning stocks in the migratory complex (Fabrizio 1987; Wirgin et al. 1993; Kneebone et al. 2014; Hasegawa et al. 2022). Estimates of stock composition from these studies are influenced by the size of striped bass sampled, the location of sampling, the timing of sampling, and the methods of stock determination (Table 2.4). Our spatially-explicit model makes different assumptions about stock structure than some of the cited literature (Kneebone et al. 2014; Hasegawa et al. 2022), as we assume the Chesapeake Bay stock is demographically different from the Roanoke River, Delaware Bay, and Hudson River stocks, with no net emigration between stocks. Yet, estimates of stock composition in the Ocean region from our model were similar to previous studies, with an average of 61% of abundance from the Chesapeake Bay stock (ages 7-15+) between 1995-2017 during July-December. However, our estimates of stock composition in the Ocean during July-December in 1982 for fish ages 2-4 (<5%) are significantly lower than Fabrizio (1987), likely because our model estimated very low abundance of the Chesapeake Bay stock in the Ocean in 1982. During 1990-2017, the Chesapeake Bay 7+ stock made up between 50-67% of the Ocean region in July-December.

We modeled the movement of striped bass differently than most other spatial fish stock assessments (Goethel et al. 2011, 2015a, 2023; Punt et al. 2014; Berger et al. 2016; Goethel and Berger 2016; Punt 2019a; Cadrin 2020) but similar to cetacean assessments (Punt 2017). Many spatial stock assessments assume no movement between regions, especially for sessile invertebrates (e.g., Mace et al. 2021; Hernández-Padilla et al. 2024). Assuming no movement is not appropriate for striped bass due to their complex seasonal migration patterns (Dorazio et al. 1994; Grothues et al. 2009; Kneebone et al. 2014; Secor et al. 2020; Hasegawa et al. 2022). Further, spatially-explicit stock assessment models that include movement often use the box-transfer method (Goethel et al. 2011), in which a portion of a stock moves from each region to other regions at the beginning of a time-step. Our spatially-explicit model differed from the box-transfer method, as we estimate the occupancy probability of each stock in a region during a time step, rather than a movement rate. Conventional tagging data for each striped bass stock was necessary in order to estimate occupancy probabilities. Occupancy probabilities, or the proportion of each stock in a given area, has been used to model whale migrations in cetacean stock assessments (Punt et al. 2014; Punt 2017). This approach was appropriate for striped bass because striped bass have consistent seasonal movement patterns and the spatial, temporal, and population dynamics assumptions matched those of the Schonfeld (2023) tagging study that was used to inform occupancy probabilities. Movement probabilities for each stock could not be estimated from conventional tagging data because tagged striped bass were only assigned to stock based on their proximity to spawning locations at the time of spawning. If individual tagged fish were assigned to a spawning stock using genetics

approach, for example, then estimates could be developed to support a box-transfer method. Spatially-explicit models that assume a single stock or annual time-step may be able to better incorporate the box transfer methods because tagging data are available at the appropriate temporal and biological resolution.

Many spatially-explicit assessment models also rely on tagging data, which have the potential to improve model estimates of fishing mortality and SSB (Goethel et al. 2011, 2015b, 2015a). Movement in our spatially-explicit model relied on occupancy probabilities for each stock and age that were informed by tag-derived probabilities estimated in Schonfeld (2023). The mark re-capture model in Schonfeld (2023) had a similar model structure as the spatially-explicit model, with two subannual time-steps, two-spatial regions, and three stocks, allowing for relative agreement between estimates from the two models. However, ages assigned to the striped bass in the tagging studies were from scale ages. Although we did not develop a true tag integrated statistical catch-at-age model, incorporating informative priors from a mark recapture model with matching model structure is similar to a tag integrated model. However, it is important to note that our approach differs from a fully tag integrated model. Therefore, the informative priors provided reliable information to estimate movement rates. However, our model does not include the tag mortality – the live release of striped bass but the removal of conventional tag – in estimates of fishing and total instantaneous mortality, as is done in Schonfeld (2023). Though estimates of fishing mortality were generally higher in Schonfeld (2023) than our model, trends for both regions and time-steps are similar. Therefore, incorporating tag mortality may not be necessary for striped bass.

Our estimated occupancy probabilities closely followed priors from the conventional tagging data (Schonfeld 2023) but deviated from priors developed from acoustic telemetry data (Secor et al. 2020). The model could not fit both because the informative priors disagreed in that the conventional tagging data suggested higher occurrence of striped bass from the Chesapeake Bay stock in the Ocean region than the acoustic telemetry priors during January-June for all ages for which data were available. In July-December, the conventional tagging data suggested higher occurrence of striped bass in the Ocean region for age-4 and ages 7-11, while the acoustic tagging data suggested higher probability of occurrence of the Chesapeake Bay stock in the Ocean region for ages greater than 11. Disagreement between these data sources could be attributed to differences in what the estimates represent; the conventional tagging estimates represented the probability of capture for each region, and the acoustic estimates represented the proportion of time striped bass spent in each region during a given time-step. Additionally, these priors were informed by different years, ages, and number of observations of data, where the conventional data included many observations for each age, but some ages in the acoustic data were only informed by one or two fish. Additionally, the acoustic data only included striped bass tagged in the Potomac River, which may have migration behavior that differ from other Chesapeake Bay striped bass. Notably, the informative priors from the conventional tagging data provided most of the information about stock composition in the model. In fact, the spatially-explicit model was unable to estimate a unique set of best parameters without the occupancy priors. Thus, estimates of stock abundance and movement were heavily reliant on these priors. Additionally, our

model included movement as a pulse at the beginning of each six-month interval. In reality, striped bass do not move at fixed 6-month interval and their movement can vary throughout the year (Dorazio et al. 1994; Northeast Fisheries Science Center 2019; Rothermel et al. 2020). In addition to the lack of stock-composition data, many of the data sources that describe age-composition (e.g., survey catch-at-age) are derived from scales, which have been shown to be biased. We recommend sampling efforts for the fishery and fishery-independent surveys prioritize collecting data to use in a spatially-explicit stock assessment that will better inform movement and abundance estimates for striped bass. Specifically, we recommend that stock composition of fishery catch and/or fishery-independent surveys be regularly assessed and age data be informed by otoliths.

When spatial complexity exists in life history and fishery characteristics, spatially-explicit population models can improve accuracy of abundance estimates compared to spatially-implicit (e.g., fleets-as-areas) approaches (Bosley et al. 2022). If spatial dynamics are ignored, overexploitation becomes more likely (Goethel and Berger 2016) and the ability of a population to recover from collapse may be diminished (Bosley et al. 2022; Goethel et al. 2023). Estimates from our spatially-explicit model for striped bass differed substantially from the current model used for management and would potentially change estimates of stock status should this model be considered for management. However, adjusting assumptions in the spatially-explicit model for selectivity, aging error, and natural mortality can significantly alter estimates. Particularly, time-varying natural mortality had the greatest impact on the trend of model estimates over time. However, aging error had the greatest impact on

the scale of estimates especially fishing mortality. Thus, we recommend that age composition of fishery catch and fishery-independent surveys be informed by otoliths and that stock composition begin to be regularly monitored. While otolith-based ages have been considered and begun to be implemented, it has not yet been adopted throughout the whole area and across all data sources. This multi-stock, spatially-explicit model more closely resembles striped bass population dynamics and migration patterns along the Atlantic coast than the FAA model currently used for management. The striped bass fishery varies spatially, as regulations are implemented differently at each state level. Additionally, the FAA model does not account for striped bass migratory behavior that leads to individuals being vulnerable to the fishery at different months of the year. Spatial differences in fishing mortality estimated in the multi-stock, spatially-explicit model highlight the need to utilize spatially-explicit stock assessment models for assessment and management striped bass.

2.6 Acknowledgements

I would like to thank my collaborators on this chapter, R. Latour, A. Schonfeld, K. Drew, G. Nelson, D. Secor, and M. J. Wilberg. We thank NOAA and Sea Grant for funding this research. We thank the many state agencies for providing data for this project including the Maine Department of Marine Resources, Rhode Island Department of Environmental Management, Massachusetts Division of Marine Fisheries, Connecticut Department of Energy and Environmental Protection, New York State Department of Environmental Conservation, New Jersey Division of Fish and Wildlife, Delaware Department of Natural Resources and Environmental Control,

Maryland Department of Natural Resources, Potomac River Fisheries Commission, Virginia Institute of Marine Science, Virginia Department of Marine Resources, and North Carolina Department of Environmental Quality. We thank G. Nesslage and A. Schueller for suggested improvements to the model. We thank. L. Collins for providing assistance in statistical analyses of data sources and M. O'Brien for providing telemetry data.

2.7 Funding Statement

This research was supported by Sea Grant and the National Marine Fisheries Service Population and Ecosystem Dynamics Fellowship (grant number NA21OAR4170244) and the NOAA Chesapeake Bay Office (grant number NA19OAR4320074).

2.8 Supplemental Material – Model Diagnostics

The age compositions for the fisheries were the largest contributors to the total likelihood function followed by the age compositions for the CTLIST and ChesMMAP surveys (Figure S2.2). Estimated total catch matched the observed catch for all regions and time-steps well (Figure S2.3). One-step ahead residuals for the fishery age-composition showed some patterning in residuals for specific cohorts over-time in the Chesapeake Bay fleet during January-June, as well as strong residuals for age 3 in 1982-1987 (Figure S2.4). However, other years and ages fit the data substantially better (Figure S2.4). Additionally, the Chesapeake Bay fleet from July-December had a noticeable residual pattern in 1982-1990, particularly for ages 2-4 (Figure S2.5). For the Ocean fleet one-step ahead residuals suggest a pattern in residuals during 1982-1985 for ages 3-5 in January-June and ages 5-9 in July-December. Additionally, for the Ocean in both time-steps, one-step ahead residuals indicated some age-specific patterns, where age classes tended to be over or underestimated across most model years, but the magnitude of the residuals was relatively small (Figures S2.6, S2.7).

Residual plots for the fishery-independent surveys suggest that the estimated indices of abundance fit the observed data reasonably well (Figure S2.8). Some autocorrelation of the residuals was evident for ChesMMAP, the CTLIST survey, and the NYOHS (Figure S2.8). However, the remaining indices had less autocorrelation in the residuals. For the age compositions, the data sets that used otoliths to age fish had less residual patterning than those that used scales. One-step ahead residuals for the ChesMMAP survey suggested a relatively good fit to age composition data in

January-June (Figure S2.9) but less so for July-December (Figure S2.10). One-step ahead residuals for the CTLIST survey showed reasonably good fits for most age classes in January-June (Figure S2.11). The CTLIST survey fit well in July-December, although there was one extreme outlier in 2011 for age-1 (Figure S2.12). The model fitted age compositions for the DE30 survey well, though there were strong cohort trends in 2014-2017, and age-1 was not well fit to the data during 2010 – 2017 (Figure S2.13). One-step ahead residuals for the DESSN suggested some auto-correlation among age-classes (e.g., ages 5-8) (Figure S2.14). MDSSN residuals for the age-compositions indicated a relatively poor fit for age 5 (Figure S2.15). Age composition residuals for the NJBT had the largest deviations for ages-2 and 3, with better fits for ages 4-15+ (Figure S2.16). One-step ahead residuals for the NYOHS showed somewhat increased residuals for age-3, though this survey overall was a relatively good fit to the data (Figure S2.16).

Residual plots for the age-1 (Figure S2.18) and YOY surveys (Figure S2.19) indicated little patterning of residuals over time, although the NJYOY survey had three large negative residuals at the beginning of the time series.

2.9 Tables

Table 2.1. Fishery-independent data sources used as inputs for the striped bass spatially-explicit population model. The location describes the state and location in which the survey is conducted. The age describes which age classes the survey targets. Years describes the sampling timeframe. Time-step refers to which sub-annual time-step the survey is conducted in (1=January-June, 2=July-December). Region corresponds to the regions of the spatially-explicit model (Ocean =Ocean region, CB=Chesapeake Bay region).

Survey Name	Location	Age	Gear	Years	Time-Step	Region
Connecticut Long Island Sound Trawl Survey (CTLIST)	Connecticut: Long Island Sound	1-15+	Bottom Trawl	1984-Present	1,2	Ocean
New York Ocean Haul Seine Survey (NYOHS)	New York: East of Long Island	2-13+	Ocean Haul Seine	1987-2006	2	Ocean
New Jersey Bottom Trawl Survey (NJBT)	New Jersey: Delaware Bay through New York Harbor	2-15+	Bottom Trawl	1989-Present	1	Ocean
Delaware Spawning Stock Electrofishing Survey (DESSN)	Delaware: Delaware River	2-13+	Electrofishing	1996-Present	1	Ocean
Delaware 30 Foot Trawl Survey (DE30)	Delaware: Delaware Bay	1-15+	9m (30') Bottom Trawl	1990-Present	2	Ocean
Maryland Spawning Stock Survey (MDSSN)	Maryland: Chesapeake Bay	2-15+	Multi-panel Drift Gillnet	1985-Present	1	CB
Chesapeake Bay Multispecies Monitoring and Assessment Program (ChesMMAP)	Virginia: Chesapeake Bay	1-15+	Trawl	2002-Present	1,2	CB
New York Yearling Survey (NY1)	New York: Western Long Island	1	Beach Seine	1980-Present	1,2	Ocean
Maryland Yearling Survey (MD1)	Maryland: Chesapeake Bay	1	Beach Seine	1954-Present	2	CB

New York YOY Survey (NYYOY)	New York: Western Long Island	YOY	Beach Seine	1979-Present	2	Ocean
New Jersey YOY Survey (NJYOY)	New Jersey, Delaware River	YOY	Beach Seine	1980-Present	2	Ocean
Chesapeake Bay YOY Index (CBYOY)	Maryland and Virginia: Chesapeake Bay	YOY	Beach Seine	1980-Present	2	CB
Maryland YOY Survey (MDYOY)	Maryland portion of Chesapeake Bay	YOY	Beach Seine	1954-Present	2	CB
Virginia YOY Survey (VAYOY)	Virginia portion of Chesapeake Bay	YOY	Beach Seine	1980-Present	2	CB

Table 2.2. Assumptions of 6-month natural mortality, sex proportions-at-age, and female maturity-at-age used in the spatially-explicit model. Estimates were similar to those used in the benchmark stock assessment for striped bass (Northeast Fisheries Science Center 2019)

Parameter	**1**	**2**	**3**	**4**	**5**	**6**	**7**	**8**	**9**	**10**	**11**	**12**	**13**	**14**	**15+**
Natural Mortality	0.565	0.34	0.225	0.165	0.125	0.095	0.075	0.075	0.075	0.075	0.075	0.075	0.075	0.075	0.075
Sex Proportions-at-age	0.530	0.56	0.560	0.520	0.570	0.650	0.730	0.810	0.880	0.920	0.950	0.970	1.000	1.000	1.000
Female Maturity-at-age	0.000	0.00	0.000	0.090	0.320	0.450	0.840	0.890	1.000	1.000	1.000	1.000	1.000	1.000	1.000

Table 2.3. Likelihood components for the two stock spatially-explicit striped bass model described in Chapter 2.

Num.	Equation	Description
2.3.1	$-ln(L_{Catch/Index}) = \sum_{y} \frac{\left(ln(X) - ln(\hat{X})\right)^2}{2\sigma^2}$	Log-normal negative log-likelihood
2.3.2	$-ln(L_{Catch/SurveyPAA}) = \sum - ln\left(e^{\frac{0.5\times(-PAA-\widehat{PAA})^2}{\sigma^2}+0.01}\right)$	Multinomial negative log-likelihood
2.3.3	$-ln(L_{prop}) = -ESS \times \left(prop_{s_{=1},r} \times ln\left(0.1 + \frac{\sum_{a=4:lage} CAA_{s_{=1},r}}{\sum_{s,a=4:lage} CAA_r}\right) + (1 - prop_{s_{=1},r}) \times ln\left(0.1 + \frac{\sum_{a=4:lage} CAA_{s_{=2},r}}{\sum_{s,a=4:lage} CAA_r}\right)\right)$	Binomial negative log-likelihood for stock composition
2.3.4	$-ln(L_{recruitment}) = \sum_{y} \left(ln(Rdev_{s=ac})\right) + \left(ln(Rdev_{s=cb})\right)$	Log-normal negative log-likelihood for recruitment deviations with mean of 0 and standard deviation of 1
2.3.5	$-ln(L_{Feq}) = \frac{1}{2}\frac{\left(Feq_{r,ts} - 0.3\right)^2}{0.1^2}$	Log normal negative log-likelihood for equilibrium fishing mortality with a standard deviation of 0.1
2.3.6	$-ln(L_{Fdev}) = \frac{\left(F_{dev_{r,y,ts}} - F_{dev_{r,y-1,ts}}\right)^2}{0.5^2}$	Log normal negative log-likelihood for F deviations with standard deviation of 0.5
2.3.7	$-ln(L_{occ}) = \sum_{s,r,a} \frac{0.5\left(prop_{s,r,ts,a} - \widehat{prop}_{s,r,ts,a}\right)^2}{\sigma^2{}_{s,r,ts,a}}$	Log-normal informative priors of occupancy probability
2.3.8	$-ln(L_{sel}) = \frac{\left(\widehat{p4}_{r,a} - X\right)^2}{\sigma^2}$	Log-normal penalty on selectivity parameters where X is the mean and σ is the standard deviation
2.3.9	$-ln(p_4) = \begin{cases} 0, & if\ \ p_{4_{ts}} \geq p_{2_{ts}} \\ 10 \times (p_{4_{ts}} - p_{2_{ts}})^2, & if\ \ p_{4_{ts}} < p_{2_{ts}} \end{cases}$	Conditional log normal penalty on descending point of inflection for double logistic function

Table 2.4. Comparison of stock composition for striped bass in the Ocean from this study to estimates from previous studies. Aggregation of stocks compositions vary for each study. Estimates from this study include the percent of Chesapeake Bay striped bass (7-15+) in Ocean during July-December.

Study	Location	Year(s)	Month(s)	Stock	Estimates	This Study
Fabrizio 1987	Rhode Island	1982	November	Chesapeake Bay	54%	2.9%
Wirgin et al. 1993	Hudson River, New York	1989	Fall	Chesapeake Bay	27%	37.9%
Kneebone et al. 2014	Massachusetts	2008-2010	June-October	Chesapeake Bay/Roanoke River	55-67%	55.3-59.5%
Hasegawa et al. 2022	Montauk, New York	2019	June-October	Chesapeake Bay/Delaware Bay	78%	63.1% *(2017)*

Supplemental Table S2.1. Aging-error matrices used applied to the fisheries-independent and dependent data sources. Striped bass used for to develop this matrix were collected from Massachusetts, Rhode Island, and New Jersey that were aged with both scales and otoliths. A) Aging error matrix for ages 1 to 15+; B) Aging error matrix for ages 2 to 15+; C) Aging error matrix for age 2 to 13+.

A)

Scale Age \ Otolith Age	1	2	3	4	5	6	7	8	9	10	11	12	13	14	15+
1	0.667	0.051	0	0	0	0	0	0	0	0	0	0	0	0	0
2	0.333	0.949	0.481	0	0	0	0	0	0	0	0	0	0	0	0
3	0	0	0.444	0.047	0	0	0	0	0	0	0	0	0	0	0
4	0	0	0.074	0.748	0.096	0.014	0.003	0	0	0	0	0	0	0	0
5	0	0	0	0.168	0.426	0.15	0.036	0	0	0	0	0	0	0	0
6	0	0	0	0.037	0.415	0.652	0.27	0.046	0.009	0	0	0	0	0	0
7	0	0	0	0	0.043	0.171	0.593	0.282	0.101	0.047	0.041	0	0	0.009	0.005
8	0	0	0	0	0.011	0.014	0.075	0.541	0.332	0.215	0.091	0.066	0.014	0.009	0.005
9	0	0	0	0	0.011	0	0.022	0.12	0.447	0.366	0.231	0.077	0.041	0.009	0.01
10	0	0	0	0	0	0	0	0.012	0.097	0.331	0.248	0.165	0.068	0.094	0.01
11	0	0	0	0	0	0	0	0	0.014	0.041	0.331	0.319	0.205	0.142	0.062
12	0	0	0	0	0	0	0	0	0	0	0.05	0.352	0.37	0.179	0.12
13	0	0	0	0	0	0	0	0	0	0	0.008	0.022	0.247	0.34	0.193
14	0	0	0	0	0	0	0	0	0	0	0	0	0.055	0.179	0.245
15+	0	0	0	0	0	0	0	0	0	0	0	0	0	0.038	0.349

B)

Scale Age \ Otolith Age	2	3	4	5	6	7	8	9	10	11	12	13	14	15+
2	1	0.481	0	0	0	0	0	0	0	0	0	0	0	0
3	0	0.444	0.047	0	0	0	0	0	0	0	0	0	0	0
4	0	0.074	0.748	0.096	0.014	0.003	0	0	0	0	0	0	0	0
5	0	0	0.168	0.426	0.15	0.036	0	0	0	0	0	0	0	0
6	0	0	0.037	0.415	0.652	0.27	0.046	0.009	0	0	0	0	0	0
7	0	0	0	0.043	0.171	0.593	0.282	0.101	0.047	0.041	0	0	0.009	0.005
8	0	0	0	0.011	0.014	0.075	0.541	0.332	0.215	0.091	0.066	0.014	0.009	0.005
9	0	0	0	0.011	0	0.022	0.12	0.447	0.366	0.231	0.077	0.041	0.009	0.01

10	0	0	0	0	0	0	0.012	0.097	0.331	0.248	0.165	0.068	0.094	0.01
11	0	0	0	0	0	0	0	0.014	0.041	0.331	0.319	0.205	0.142	0.062
12	0	0	0	0	0	0	0	0	0	0.05	0.352	0.37	0.179	0.12
13	0	0	0	0	0	0	0	0	0	0.008	0.022	0.247	0.34	0.193
14	0	0	0	0	0	0	0	0	0	0	0	0.055	0.179	0.245
15+	0	0	0	0	0	0	0	0	0	0	0	0	0.038	0.349

C)

Scale Age \ Otolith Age	2	3	4	5	6	7	8	9	10	11	12	13+
2	1	0.481	0	0	0	0	0	0	0	0	0	0
3	0	0.444	0.047	0	0	0	0	0	0	0	0	0
4	0	0.074	0.748	0.096	0.014	0.003	0	0	0	0	0	0
5	0	0	0.168	0.426	0.15	0.036	0	0	0	0	0	0
6	0	0	0.037	0.415	0.652	0.27	0.046	0.009	0	0	0	0
7	0	0	0	0.043	0.171	0.593	0.282	0.101	0.047	0.041	0	0.005
8	0	0	0	0.011	0.014	0.075	0.541	0.332	0.215	0.091	0.066	0.008
9	0	0	0	0.011	0	0.022	0.12	0.447	0.366	0.231	0.077	0.016
10	0	0	0	0	0	0	0.012	0.097	0.331	0.248	0.165	0.046
11	0	0	0	0	0	0	0	0.014	0.041	0.331	0.319	0.113
12	0	0	0	0	0	0	0	0	0	0.05	0.352	0.186
13+	0	0	0	0	0	0	0	0	0	0.008	0.022	0.625

Supplemental Table S2.2. Final effective sample size (ESS) and log-scale standard deviation (σ) for each fishery fleet and fishery-independent survey used in the spatially-explicit model. Surveys include the Chesapeake Bay Multispecies Monitoring and Assessment Program (ChesMMAP), the Connecticut Long Island Sound Survey (CTLIST), Delaware 30 Foot Trawl Survey (DE30), Delaware Spawning Stock Electrofishing Survey (DESSN), Maryland Spawning Stock Survey (MDSSN), New Jersey Bottom Trawl Survey (NJBT), and New York Ocean Haul Seine Survey (NYOHS).

Survey/Fishery	**Time-step**	σ	**ESS**
Ocean Fleet	1	0.2	25
Ocean Fleet	2	0.2	25
Chesapeake Bay Fleet 1982-1989	1	0.2	15
Chesapeake Bay Fleet 1982-1989	2	0.2	15
Chesapeake Bay Fleet 1990-2017	1	0.2	25
Chesapeake Bay Fleet 1990-2017	2	0.2	25
ChesMMAP	1	0.41	15
ChesMMAP	2	0.43	15
DE30	2	0.77	15
CTLIST	1	0.51	15
CTLIST	2	0.75	15
MDSSN	1	0.30	32
NJBT	2	0.76	15
DESSN	1	0.40	27
NYOHS	1	0.46	16
NY1	2	0.54	-
MD1	2	0.66	-

Survey/Fishery	Time-step	σ	ESS
NYYOY	2	0.50	-
NJYOY	2	0.50	-
CBYOY	2	0.52	-

Supplemental Table S2.3. 6-month natural mortality used for each region in sensitivity run to evaluate time-varying natural mortality estimated from Schonfeld (2023). Natural mortality was assumed to be the same for each 6-month time-step.

Region	Years	1	2	3	4	5	6	7	8	9	10	11	12	13	14	15+
Ocean	1982-1999	0.565	0.265	0.142	0.166	0.084	0.072	0.056	0.078	0.022	0.033	0.061	0.061	0.061	0.061	0.061
Ocean	2000-2009	0.565	0.375	0.140	0.179	0.102	0.112	0.070	0.071	0.021	0.066	0.051	0.051	0.051	0.051	0.051
Ocean	2010-2017	0.565	0.489	0.112	0.234	0.103	0.175	0.057	0.078	0.047	0.081	0.059	0.059	0.059	0.059	0.059
Chesapeake Bay	1982-1999	0.565	0.276	0.148	0.145	0.126	0.098	0.138	0.058	0.166	0.121	0.040	0.040	0.040	0.040	0.040
Chesapeake Bay	2000-2009	0.833	0.833	0.208	0.180	0.229	0.211	0.168	0.203	0.226	0.219	0.035	0.035	0.035	0.035	0.035
Chesapeake Bay	2010-2017	0.715	0.715	0.324	0.191	0.289	0.138	0.319	0.288	0.351	0.307	0.131	0.131	0.131	0.131	0.131

Supplemental Table S2.4. Assumptions of movement, natural mortality, selectivity, and aging error for the models used in sensitivity analyses for a spatial, multi-stock model for striped bass. The base model the multi-stock, spatially-explicit population model for striped bass described. All sensitivity models were the same as the base model with the exception of the specific aspects that were modified. Model 2 and 4 did not apply an aging error matrix (Table S2.1) to catch-at-age for the fishery or surveys. Model 3 and 4 assumed selectivity for the Chesapeake Bay (CB) followed a logistic function. Model 5 explored how priors of occupancy probabilities impacted model output. Model 6 evaluated assumptions of natural morality by assuming spatially- and time-varying mortality in the Chesapeake Bay (Table S2.3).

Model No.	Model Name	Error in Age Composition	Chesapeake Bay Selectivity	Occupancy Probabilities	Natural Mortality
1	Base	Yes	Double Logistic	Base	Constant
2	Without Aging Error	No	Double Logistic	Base	Constant
3	Logistic	Yes	Logistic	Base	Constant
4	Logistic Without Aging Error	No	Logistic	Base	Constant
5	Occupancy 50%	Yes	Double Logistic	CB Reduced Jan-Jun	Constant
6	Time Varying M	Yes	Double Logistic	Base	Vary across Time and Space

2.10 Figures

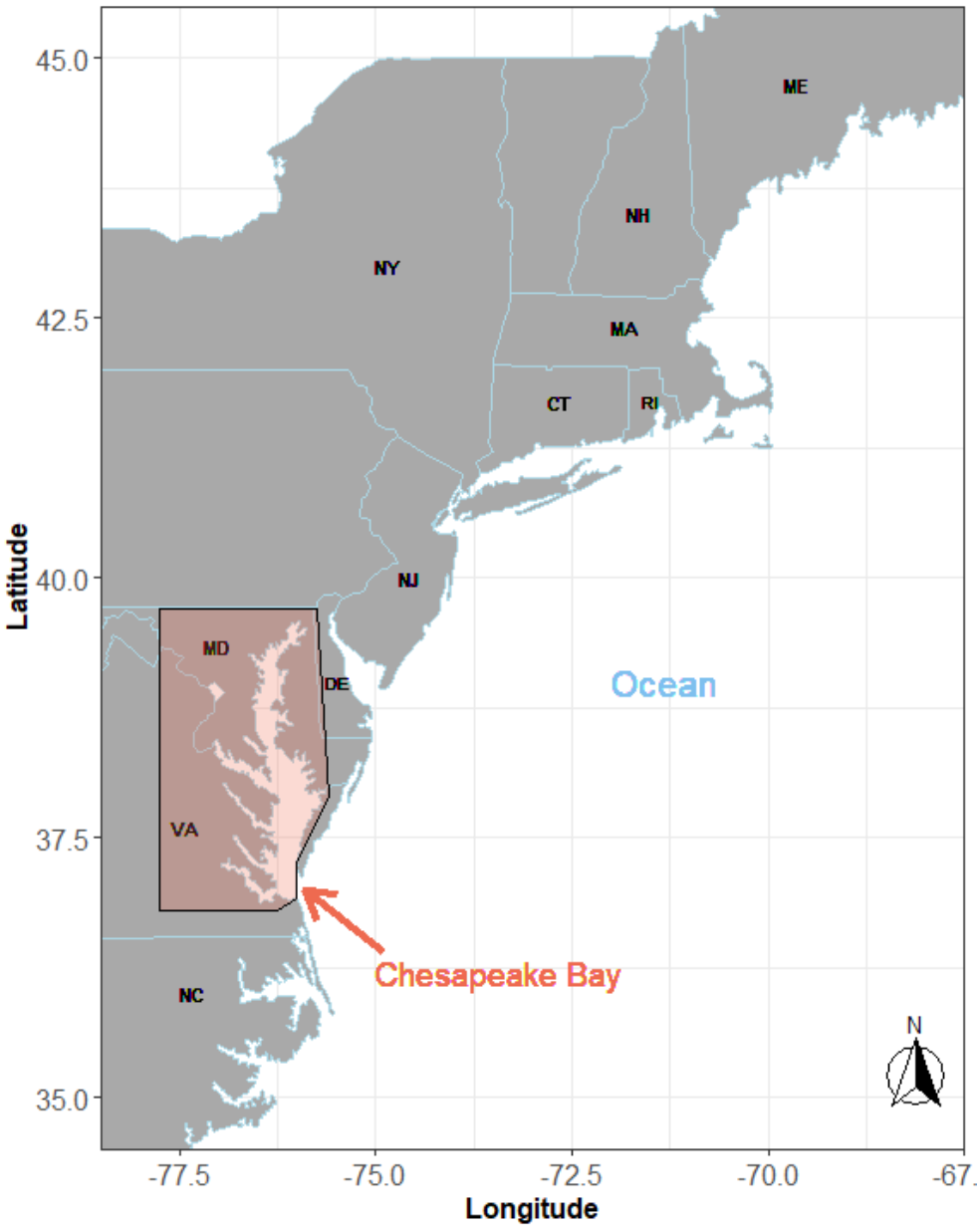

Figure 2.1. Study region of spatially-explicit population model. The red box represents the Chesapeake Bay region. The portions outside of the red box, represent

the Ocean region, excluding “inland” North Carolina, waters inside of Albemarle sound and the Roanoke River.

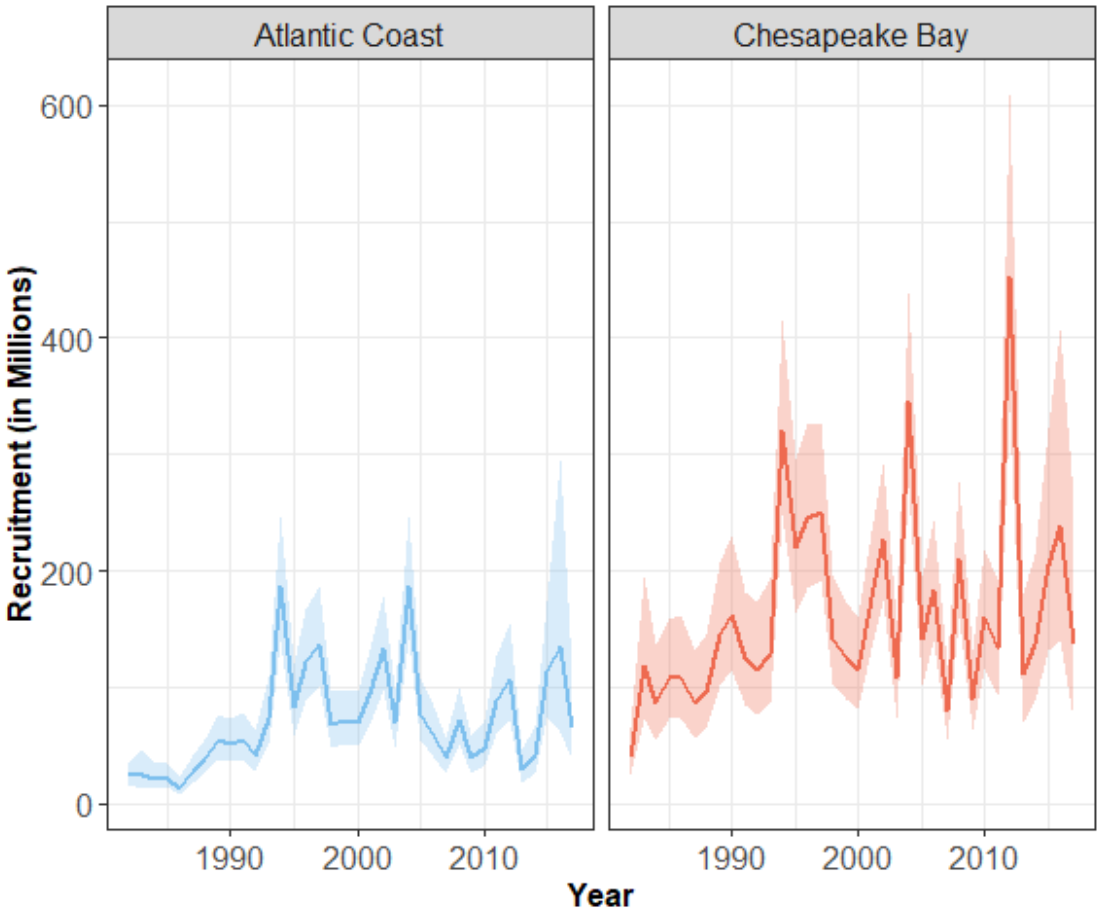

Figure 2.2. Estimated recruitment (age-1) for the Atlantic coast (blue) and Chesapeake Bay (red) striped bass stocks. The solid lines represent the maximum likelihood estimates of recruitment and the shaded regions represent approximate 95% confidence intervals.

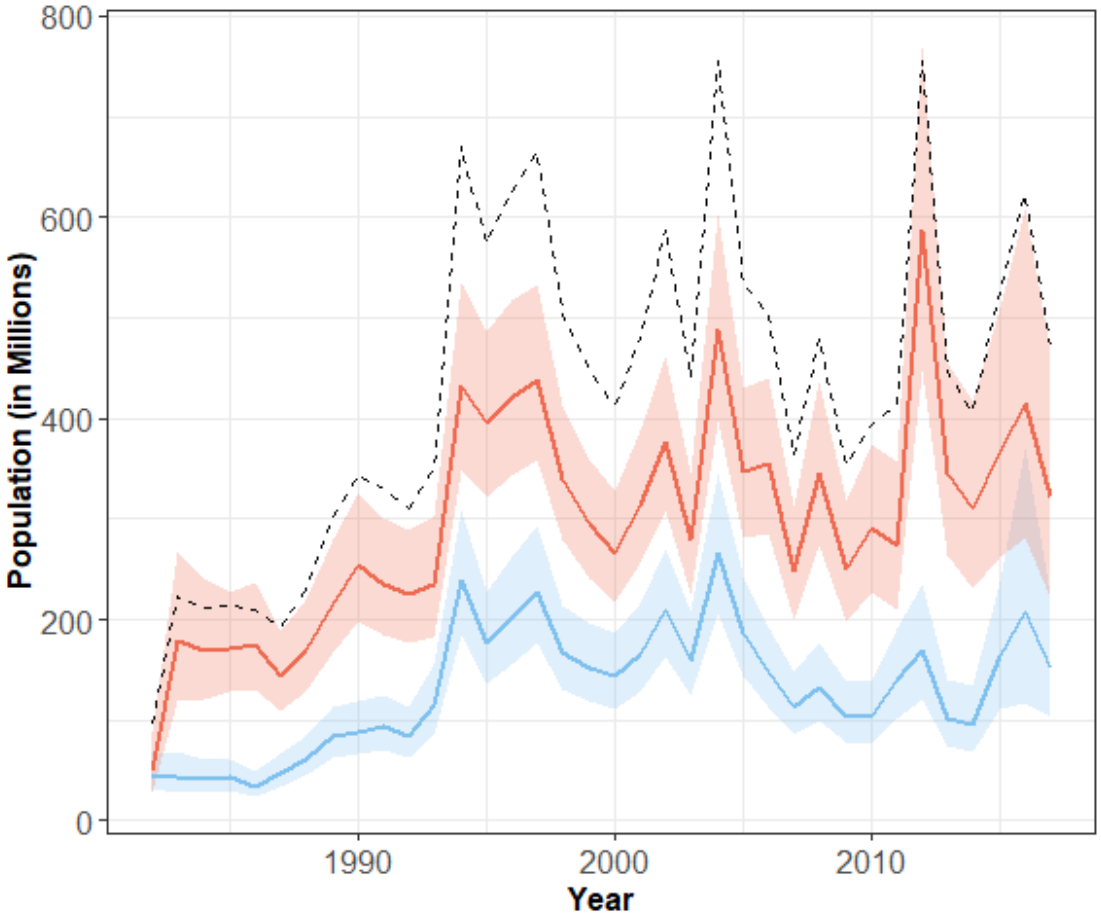

Figure 2.3. Estimated abundance (Ages 1-15+) of striped bass from the Atlantic coast (blue) and Chesapeake Bay (red) stocks. The dashed black line represents the estimated abundance of both stocks combined. The solid lines represent the best estimates for each stock, and the shaded region represents approximate 95% confidence intervals.

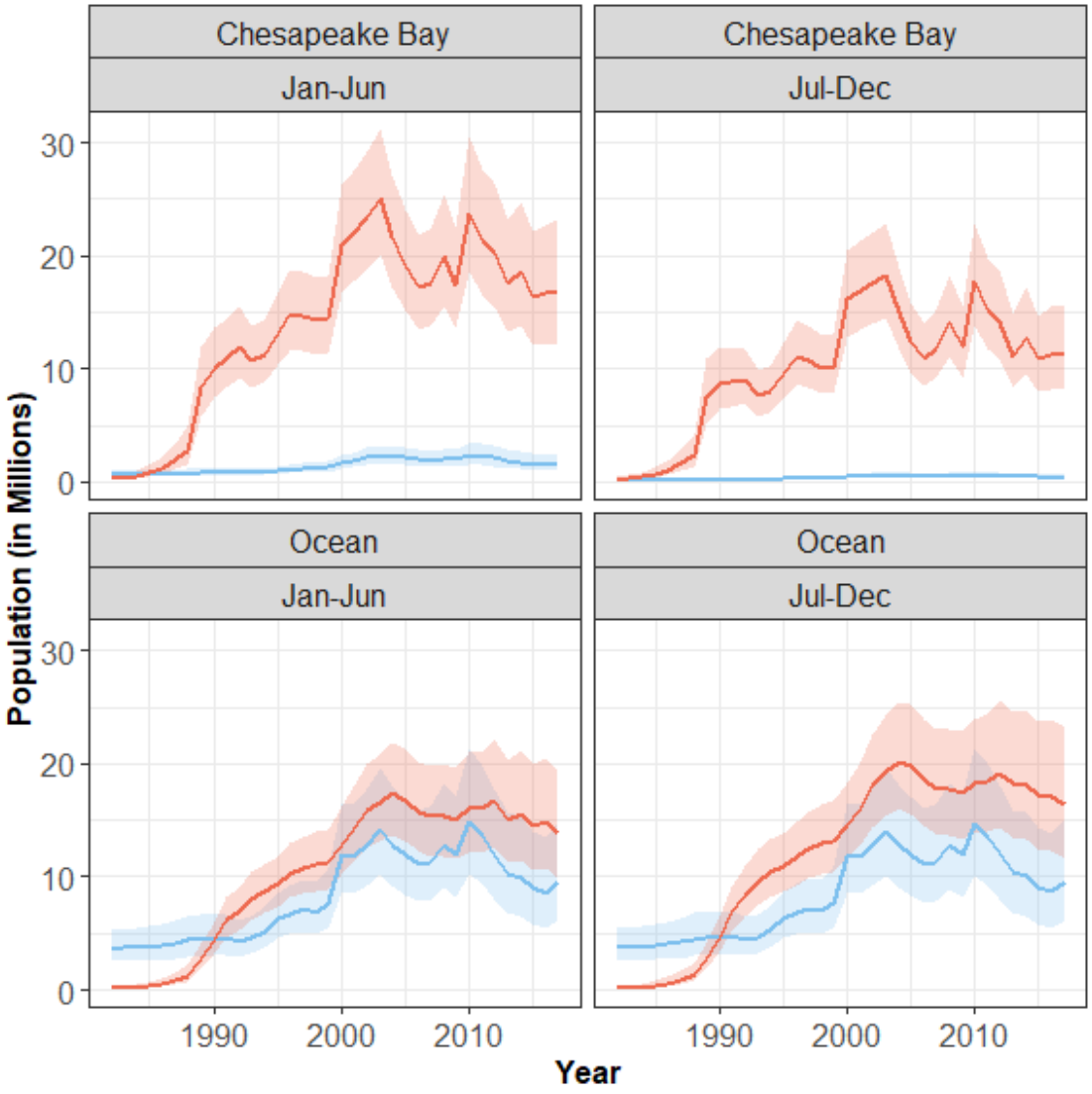

Figure S2.4. Estimates of abundance in numbers for striped bass (7-15+) in the Chesapeake Bay (top) and Ocean region (bottom) in January-June (left) and July-December (right). The solid-colored lines represent estimates of abundance from the spatially-explicit model where orange represents estimates for the Chesapeake Bay stock and blue represents estimates for the Atlantic Coast stock. The colored shaded regions correspond to approximately 95% confidence intervals.

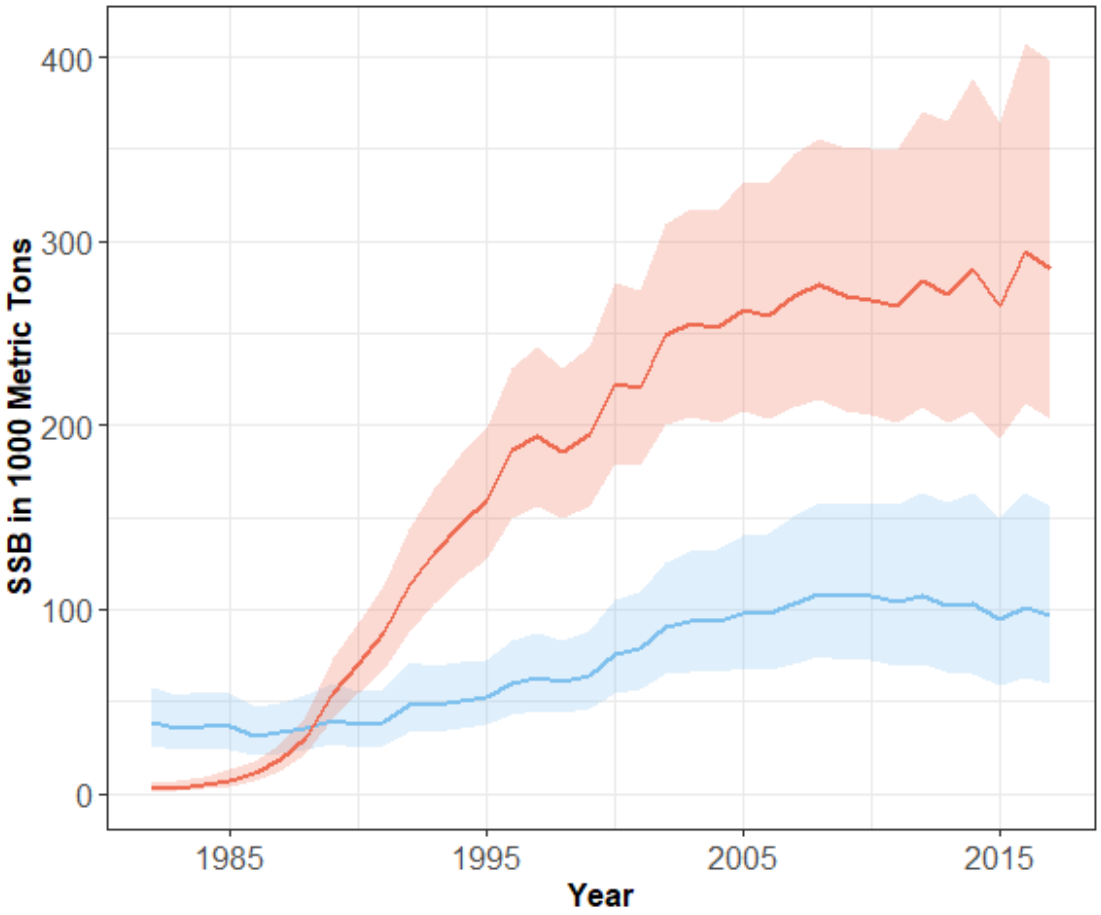

Figure 2.5. Total spawning stock biomass for striped bass for in January-June for the Atlantic coast stock (blue) and Chesapeake Bay stock (orange). The solid line represents the best estimates for each stock and the shaded regions represents approximate 95% confidence intervals.

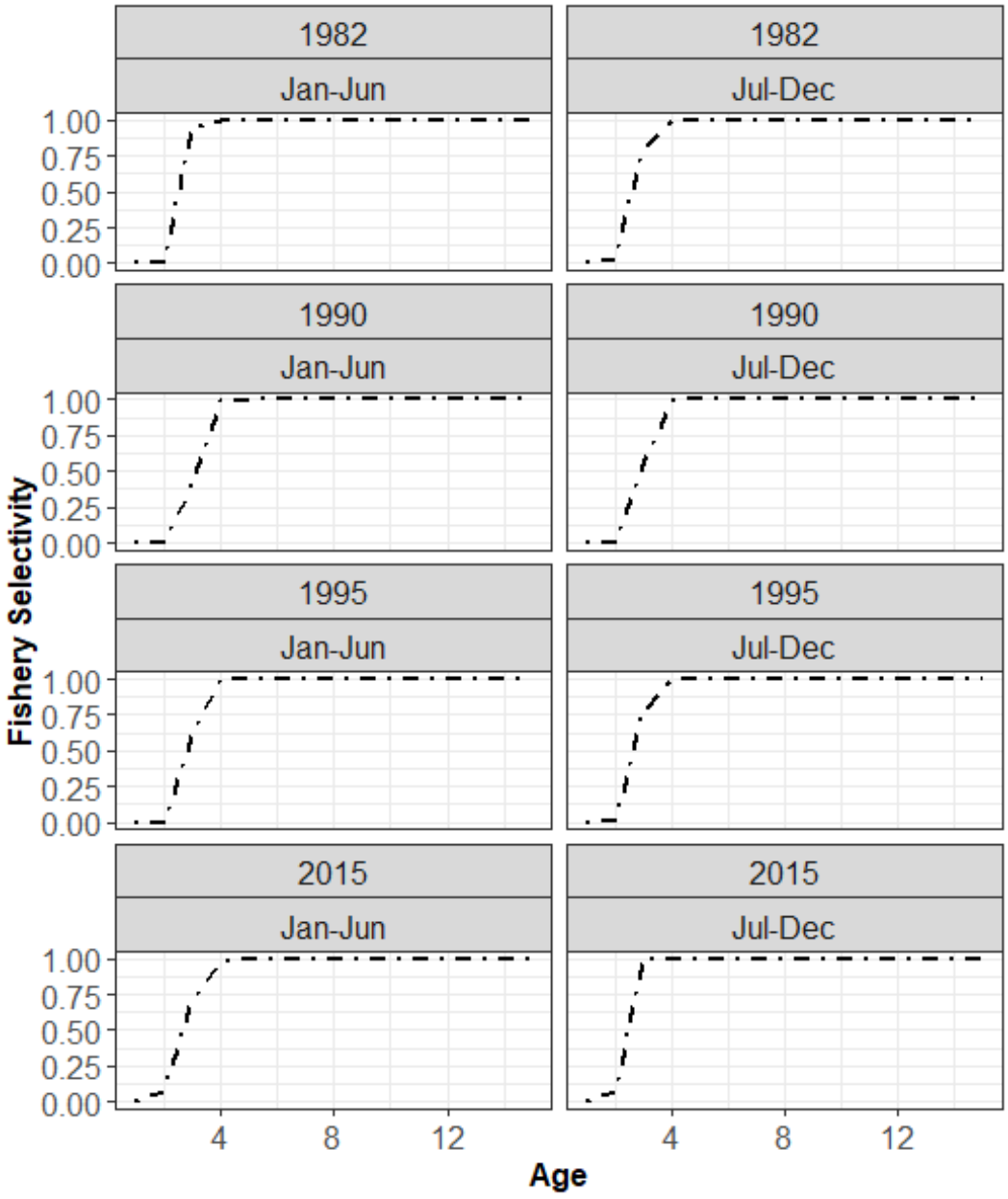

Figure 2.6. Estimated fishery selectivity for striped bass (1-15+) over time for the Ocean fleet. The columns indicate the time-step during the year where the first column is selectivity from January through June and the second column is fishery selectivity from June through December. The rows correspond to the fishery time-block through time, where the first row is the Moratorium from 1982-1989, the

second row is the Post-Moratorium block from 1990-1994, the third row is the Recovery block from 1995-2014, and the fourth row is the Recent Block from 2015-2017.

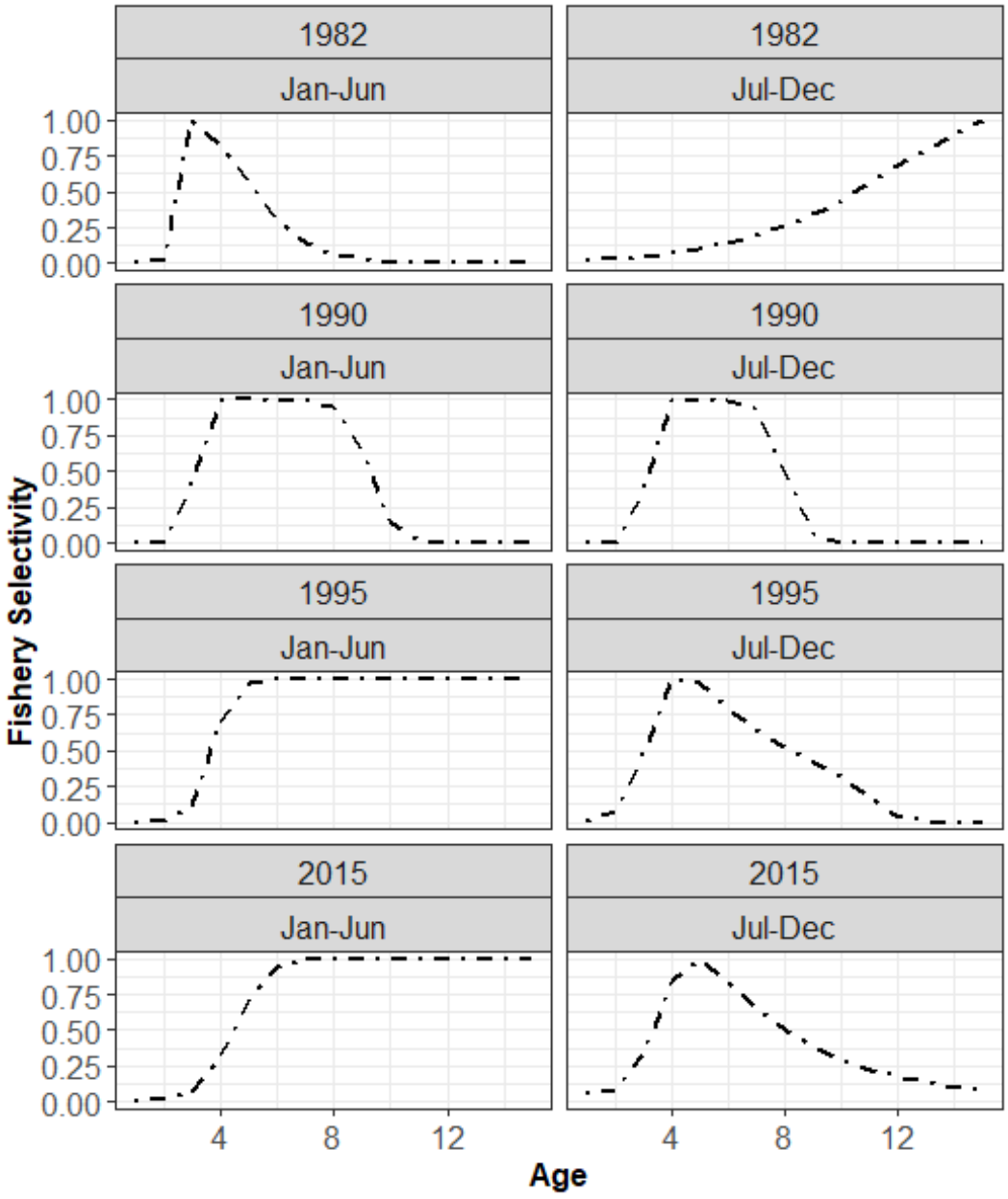

Figure 2.7. Estimated fishery selectivity for striped bass (1-15+) over time for the Chesapeake Bay fleet. The columns indicate the time-step during the year where the first column is selectivity from January through June and the second column is fishery selectivity from June through December. The rows correspond to the fishery time-block through time, where the first row is the Moratorium from 1982-1989, the

second row is the Post-Moratorium block from 1990-1994, the third row is the Recovery block from 1995-2014, and the fourth row is the Recent Block from 2015-2017.

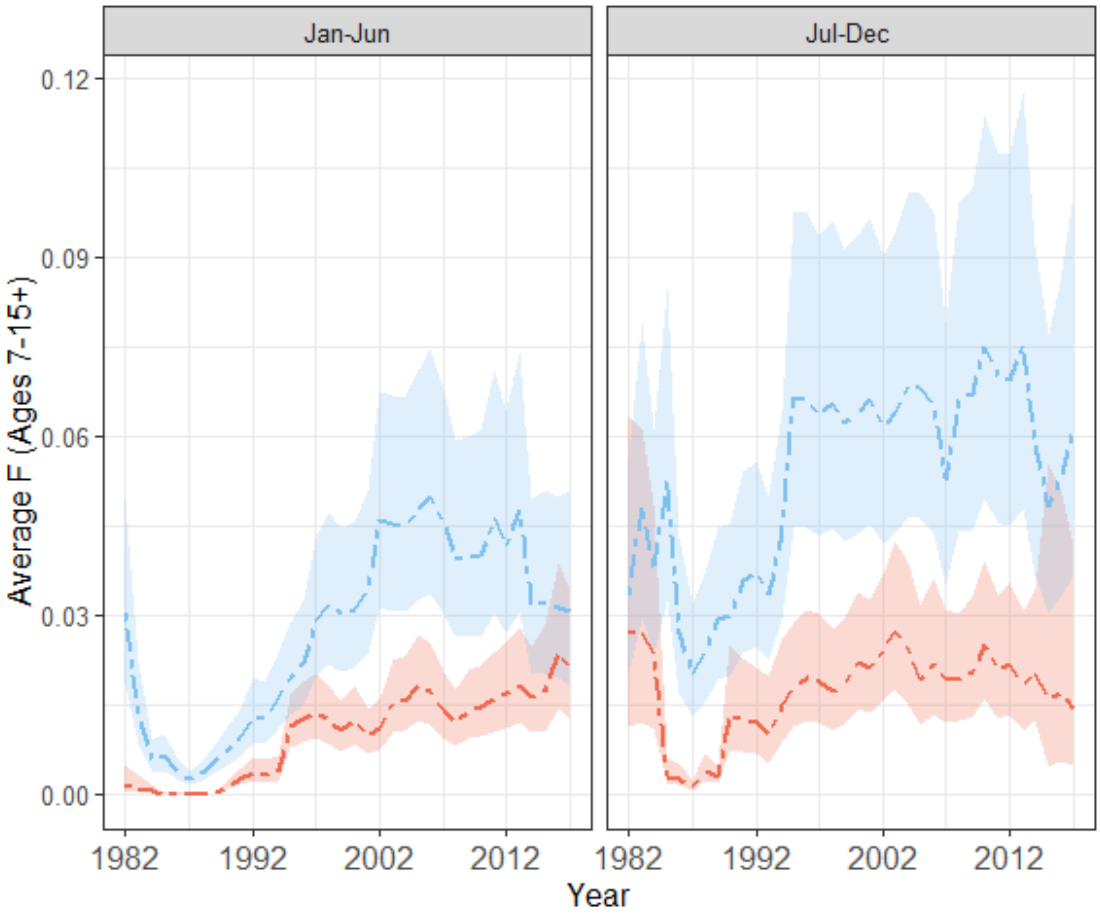

Figure 2.8. Estimated weighted average instantaneous fishing mortality (F) rates for each 6-month period ($6mo^{-1}$) for striped bass (7-15+) in the Chesapeake Bay region (orange) and the Ocean region (blue) during January-June (left) and July-December (right). F is weighted based on abundance of each age class in a given region during each time-step. The dashed lines represent the maximum likelihood estimates of $F6mo^{-1}$ and the shaded regions represent approximate 95% confidence intervals.

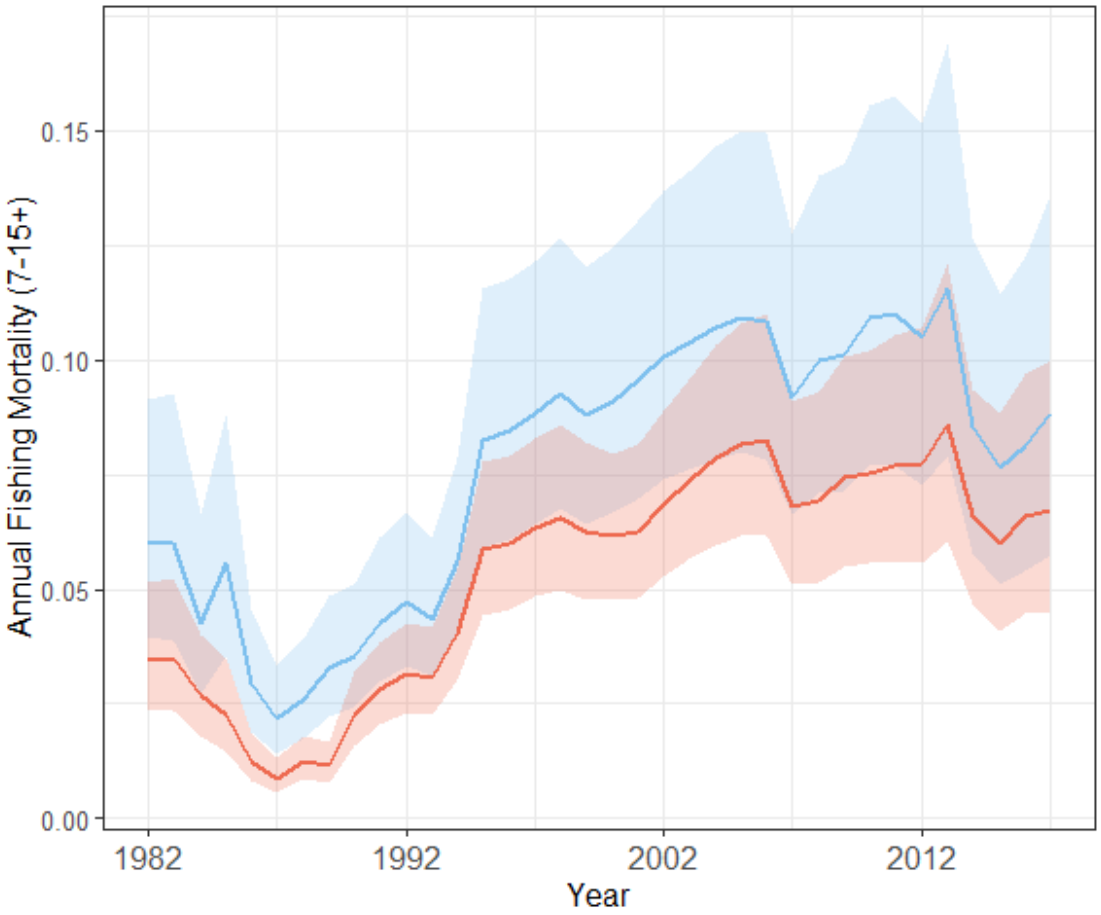

Figure 2.9. Estimated stock specific annual fishing mortality (Fyr^{-1}) for striped bass (7-15+) for the Chesapeake Bay stock (orange) and Atlantic coast stock (blue) during 1982-2017. The solid lines represent the maximum likelihood estimates of (Fyr^{-1}) and the shaded regions represent approximate 95% confidence intervals.

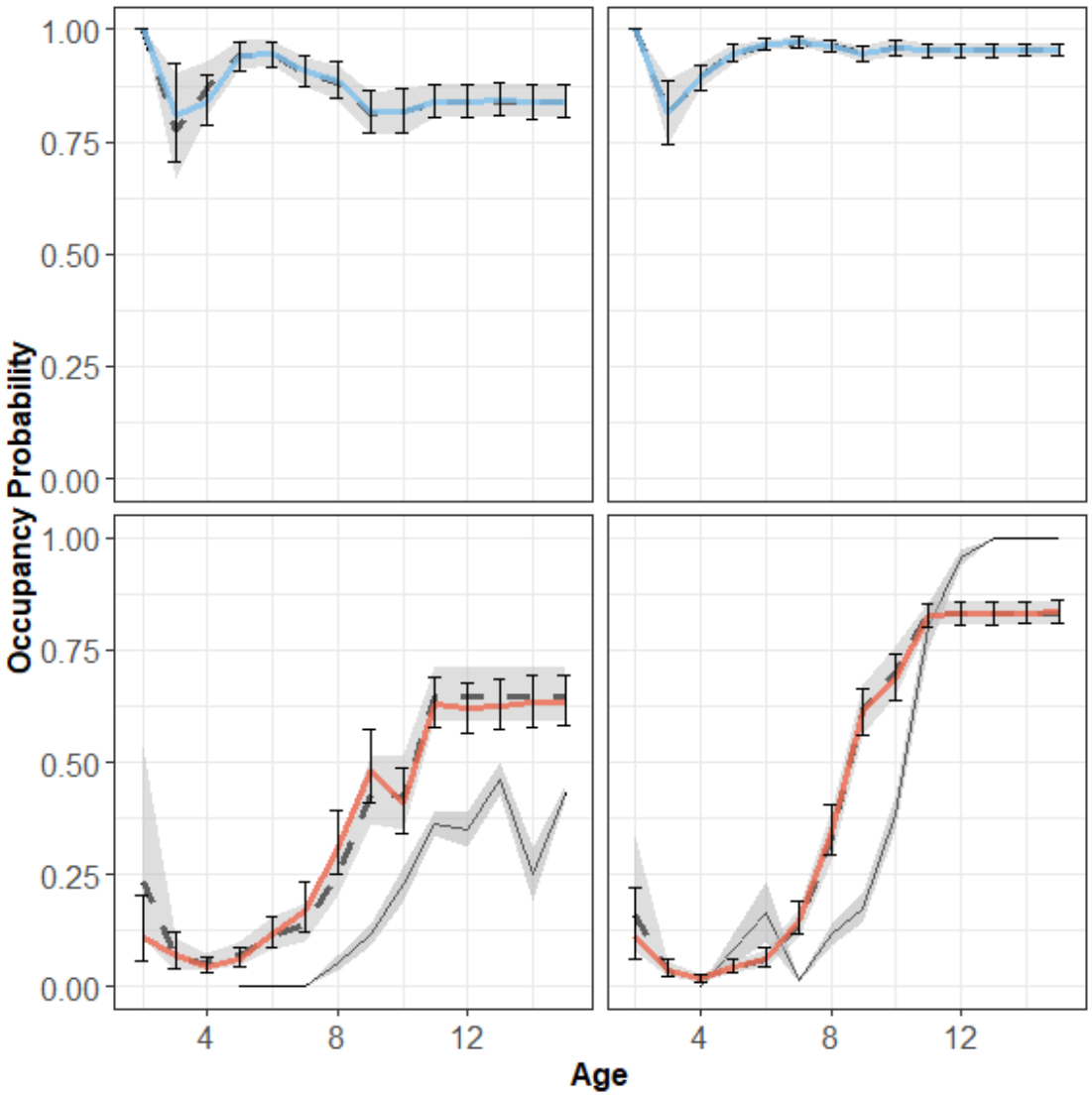

Figure 2.10. Estimated occupancy probability for striped bass (1-15+) in the Ocean region during January-June (left) and July-December). The solid-colored lines correspond to estimates of occupancy for the Atlantic coast stock (blue) and the Chesapeake Bay stock (orange) and the error bars correspond to approximately 95% confidence intervals. The black dashed lines correspond to the informative priors derived from conventional tagging data from Schonfeld (2023) and the and the gray shaded regions correspond to approximately 95% confidence intervals. The black

solid lines correspond to the informative priors derived from acoustic tagging data from Secor et al. 2020 and the gray shaded area is approximately the 95% confidence intervals.

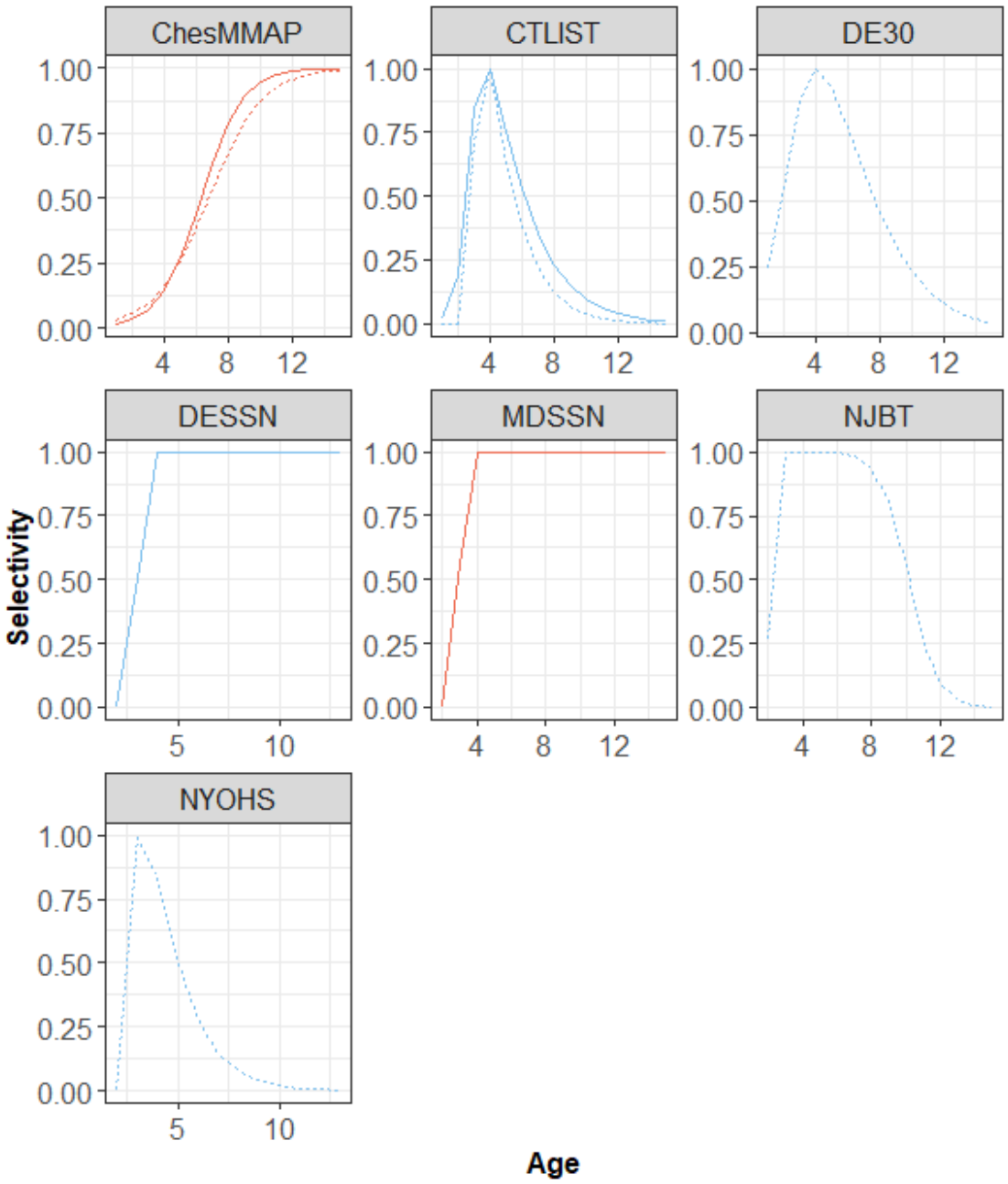

Figure 2.11. Estimated survey selectivity of striped bass for each fishery-independent survey in the Ocean (blue) and Chesapeake Bay (orange) regions during each time-step. The solid lines are selectivity for the January-June time-step and dashed lines are for selectivity estimated for the July-December time-step. The selectivity functions represent the Chesapeake Bay Multispecies Monitoring and Assessment

Program (ChesMMAP), the Connecticut Long Island Sound Survey (CTLIST), Delaware 30 Foot Trawl Survey (DE30), Delaware Spawning Stock Electrofishing Survey (DESSN), Maryland Spawning Stock Survey (MDSSN), New Jersey Bottom Trawl Survey (NJBT), and New York Ocean Haul Seine Survey (NYOHS).

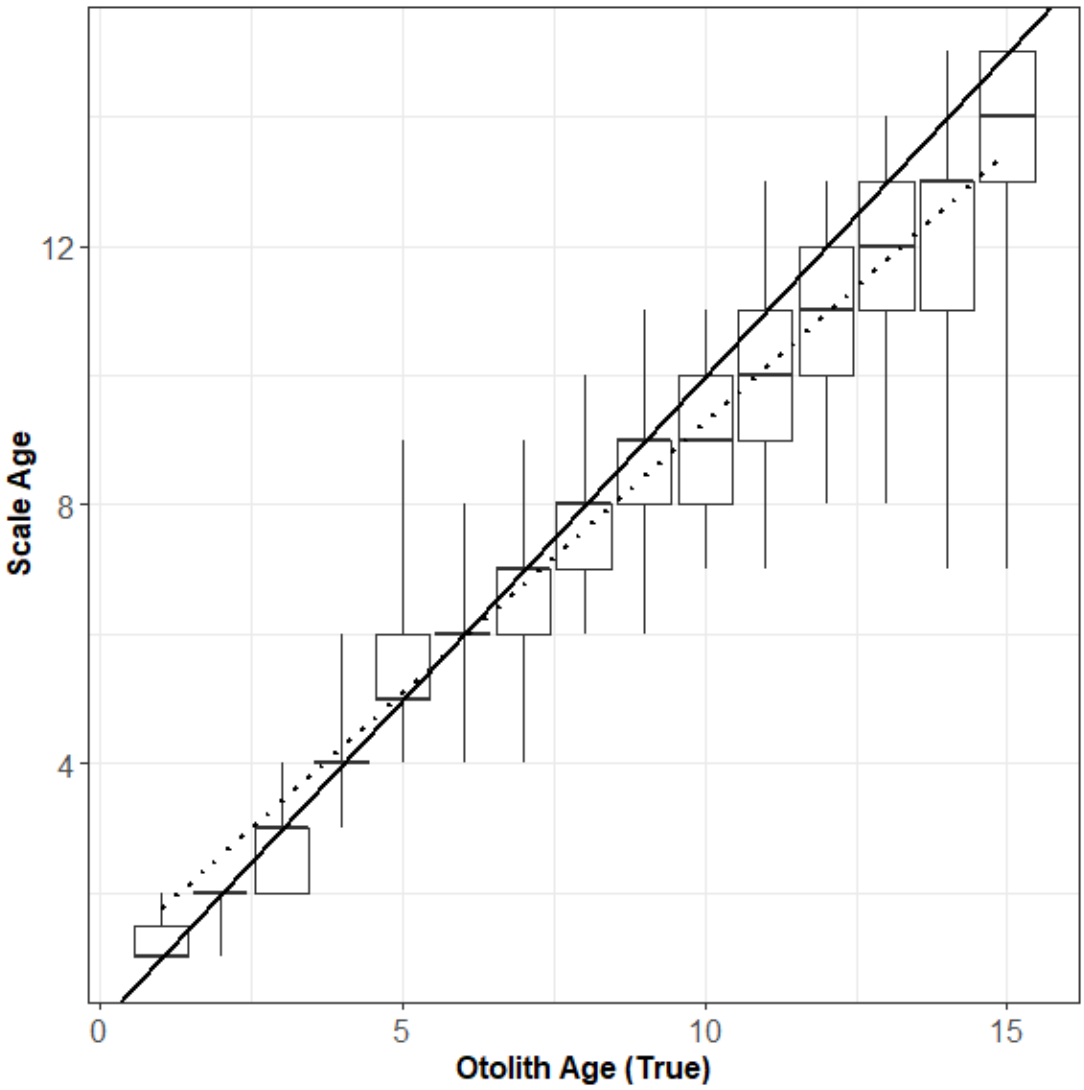

Figure S2.1. Comparison of age classification for striped bass aged with scales and otolith. Striped bass were collected from Rhode Island, Massachusetts, and New Jersey. The solid line represents when scale ages would equal the otolith ages. The dashed black line represents the linear regression through the observed age comparisons. The lower and upper hinge of the box represents the 25th and 75th percentiles. The middle line represents the median. The whiskers extend to the minimum and maximum values.

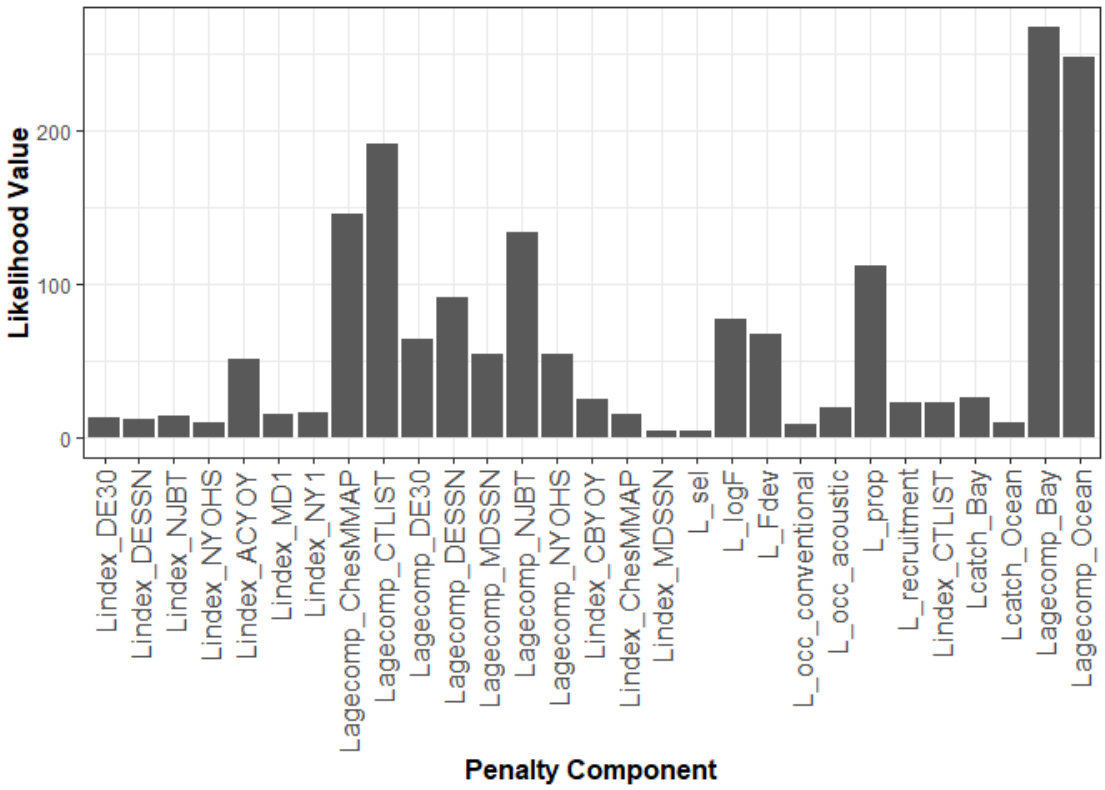

Supplemental Figure S2.2. Components of the total likelihood objective function for the spatially-explicit population model. The penalty names correspond to the negative log likelihood component that contributes to the total negative log likelihood (nll_tot). For the L_index component, the total contributions are separated for each targeted age class and survey. Surveys include the Chesapeake Bay Multispecies Monitoring and Assessment Program (ChesMMAP), the Connecticut Long Island Sound Survey (CTLIST), Delaware 30 Foot Trawl Survey (DE30), Delaware Spawning Stock Electrofishing Survey (DESSN), Maryland Spawning Stock Survey (MDSSN), New Jersey Bottom Trawl Survey (NJBT), New York Ocean Haul Seine Survey (NYOHS), Maryland Yearling Survey (MD1), the New York Yearling Survey (NY1), the Atlantic Coast YOY surveys (which include the New York YOY survey and New Jersey YOY survey), and the Chesapeake Bay YOY aggregate survey.

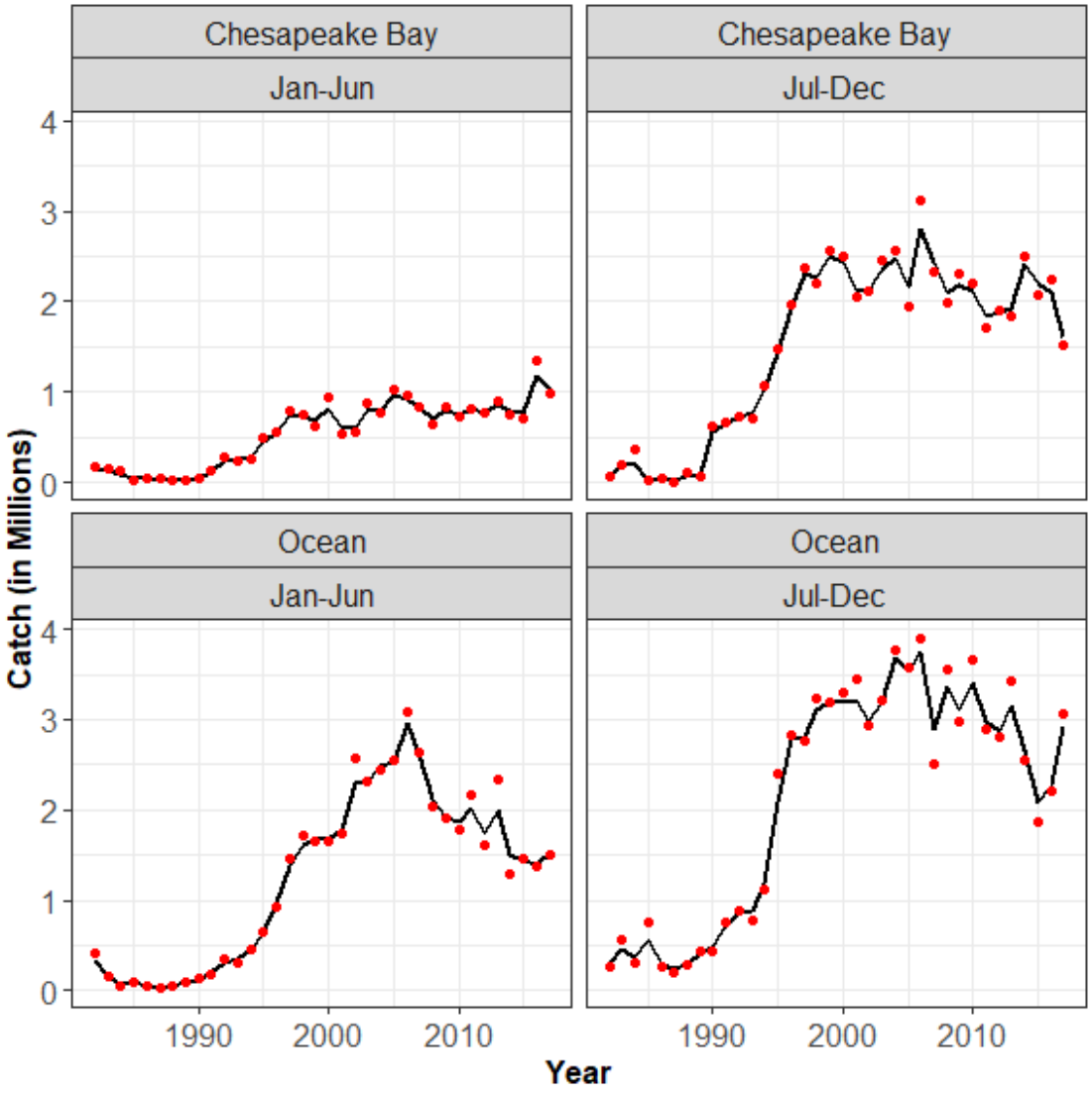

Supplemental Figure S2.3. Estimates of striped bass (1-15+) total catch over time in the Chesapeake Bay (top) and Ocean region (bottom) during January-June (left) and July-December (right). The solid black lines correspond to the best estimates of total catch and the red circles represent the observed total catch for reach region.

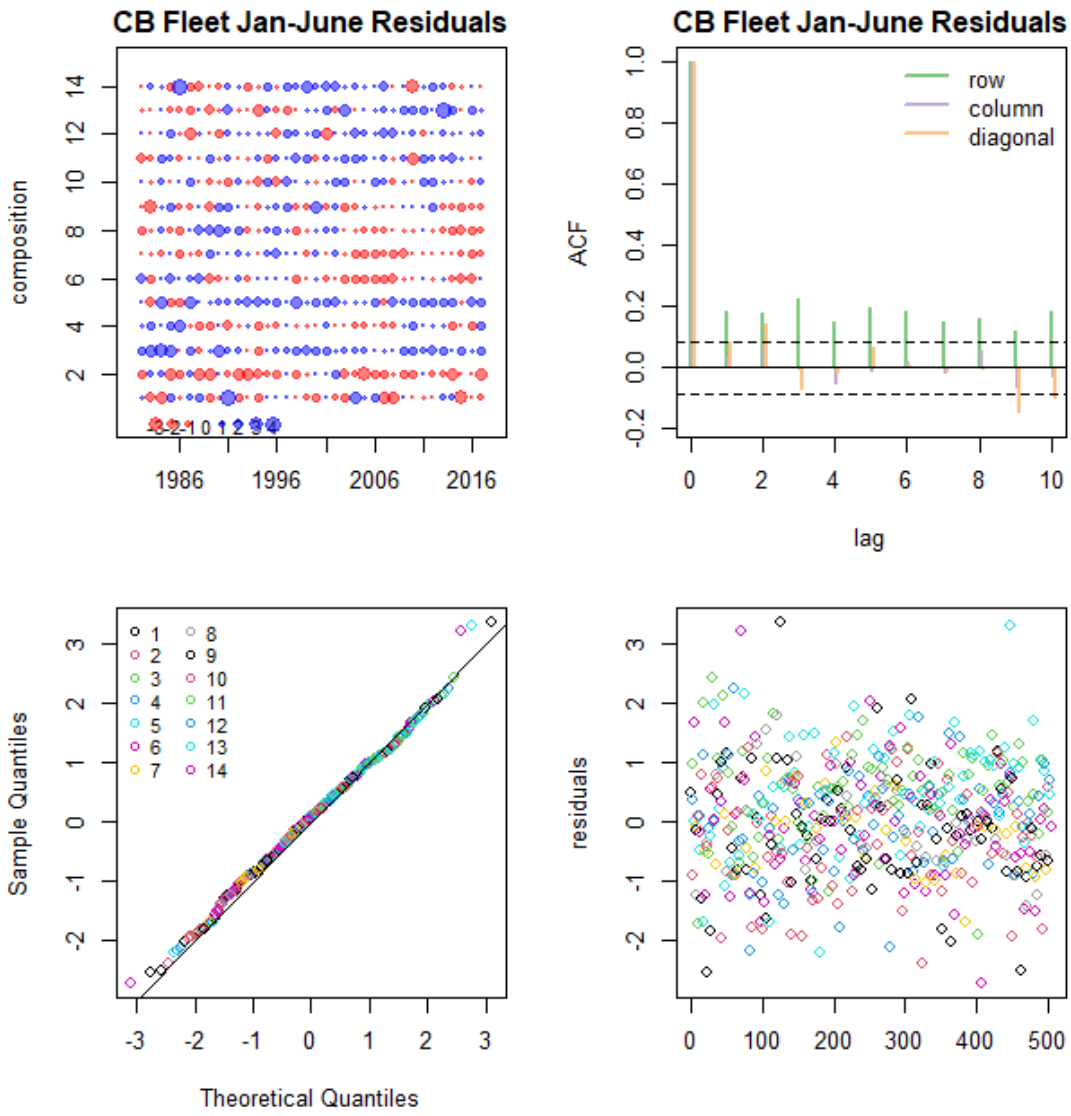

Supplemental Figure S2.4. One-step ahead residual plots for the estimated age composition for the Chesapeake Bay fleet in January-June. The top left plot shows positive (blue) and negative (red) one-step ahead residuals for each age-class and year, and the size of the circle represents the relative size of the residual. The top right plot shows the autocorrelation function for each age (green), year (purple) and cohort (orange). The bottom left plot shows the quantile plots of residuals for each age

(colored circles), where the black line represents normally distributed errors. The bottom right plot represents the dispersion of residuals through time.

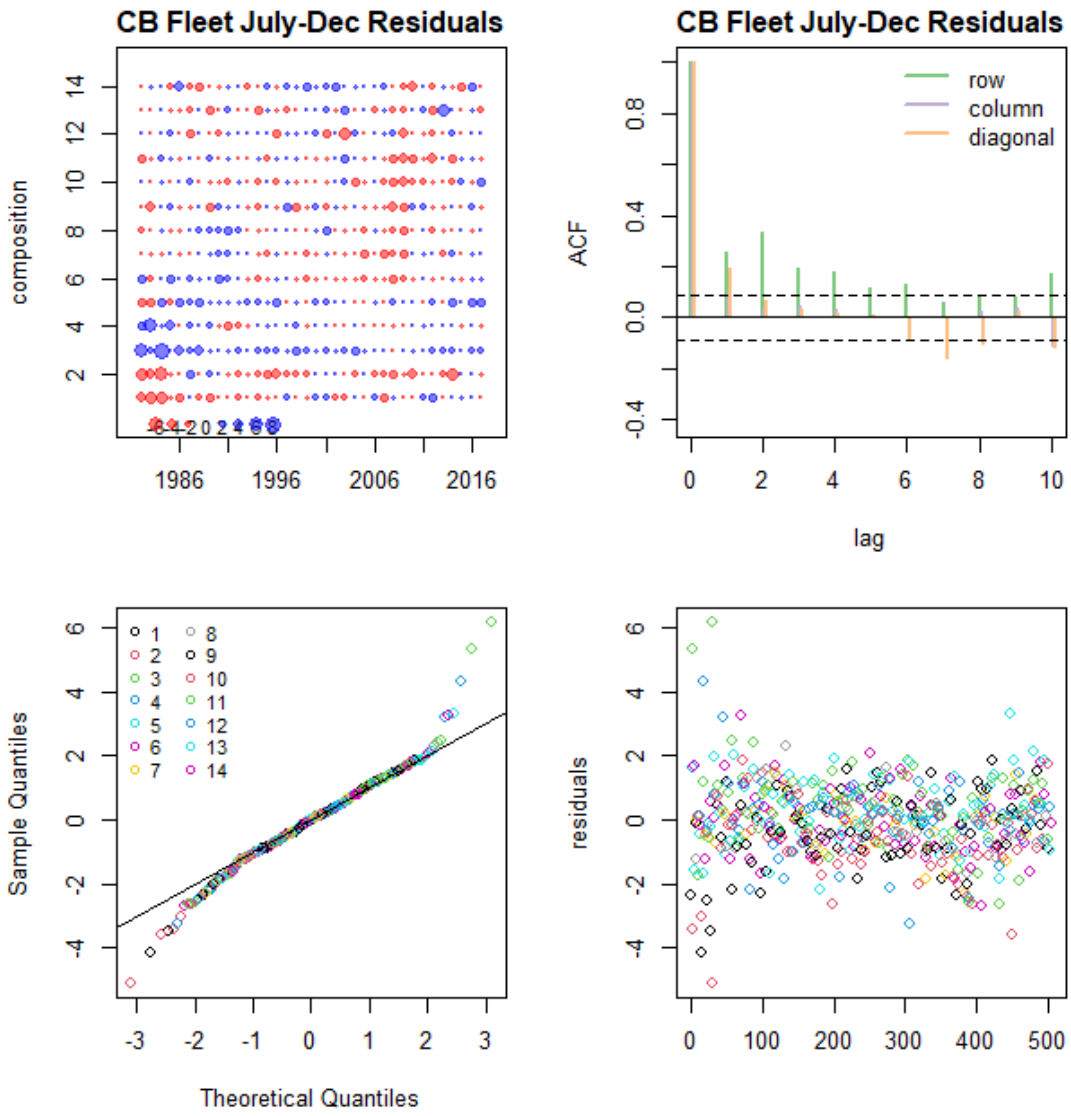

Supplemental Figure S2.5. One-step ahead residual plots for the estimated age composition for the Chesapeake Bay fleet in July-December. The top left plot shows positive (blue) and negative (red) one-step ahead residuals for each age-class and year, and the size of the circle represents the relative size of the residual. The top right plot shows the autocorrelation function for each age (green), year (purple) and cohort (orange). The bottom left plot shows the quantile plots of residuals for each age

(colored circles), where the black line represents normally distributed errors. The bottom right plot represents the dispersion of residuals through time.

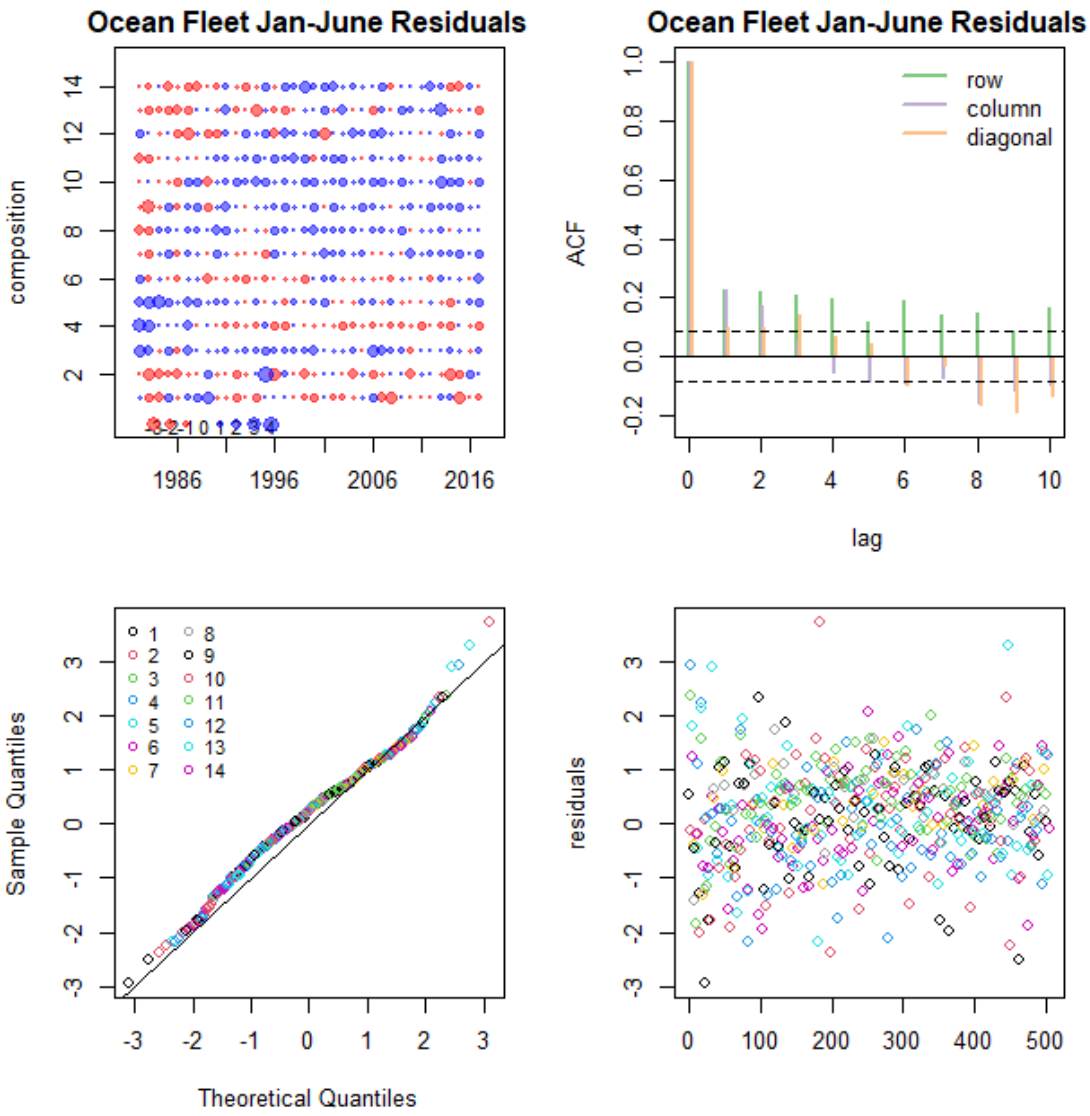

Supplemental Figure S2.6. One-step ahead residual plots for the estimated age composition for the Ocean fleet in January-June. The top left plot shows positive (blue) and negative (red) one-step ahead residuals for each age-class and year, and the size of the circle represents the relative size of the residual. The top right plot shows the autocorrelation function for each age (green), year (purple) and cohort (orange). The bottom left plot shows the quantile plots of residuals for each age (colored

circles), where the black line represents normally distributed errors. The bottom right plot represents the dispersion of residuals through time.

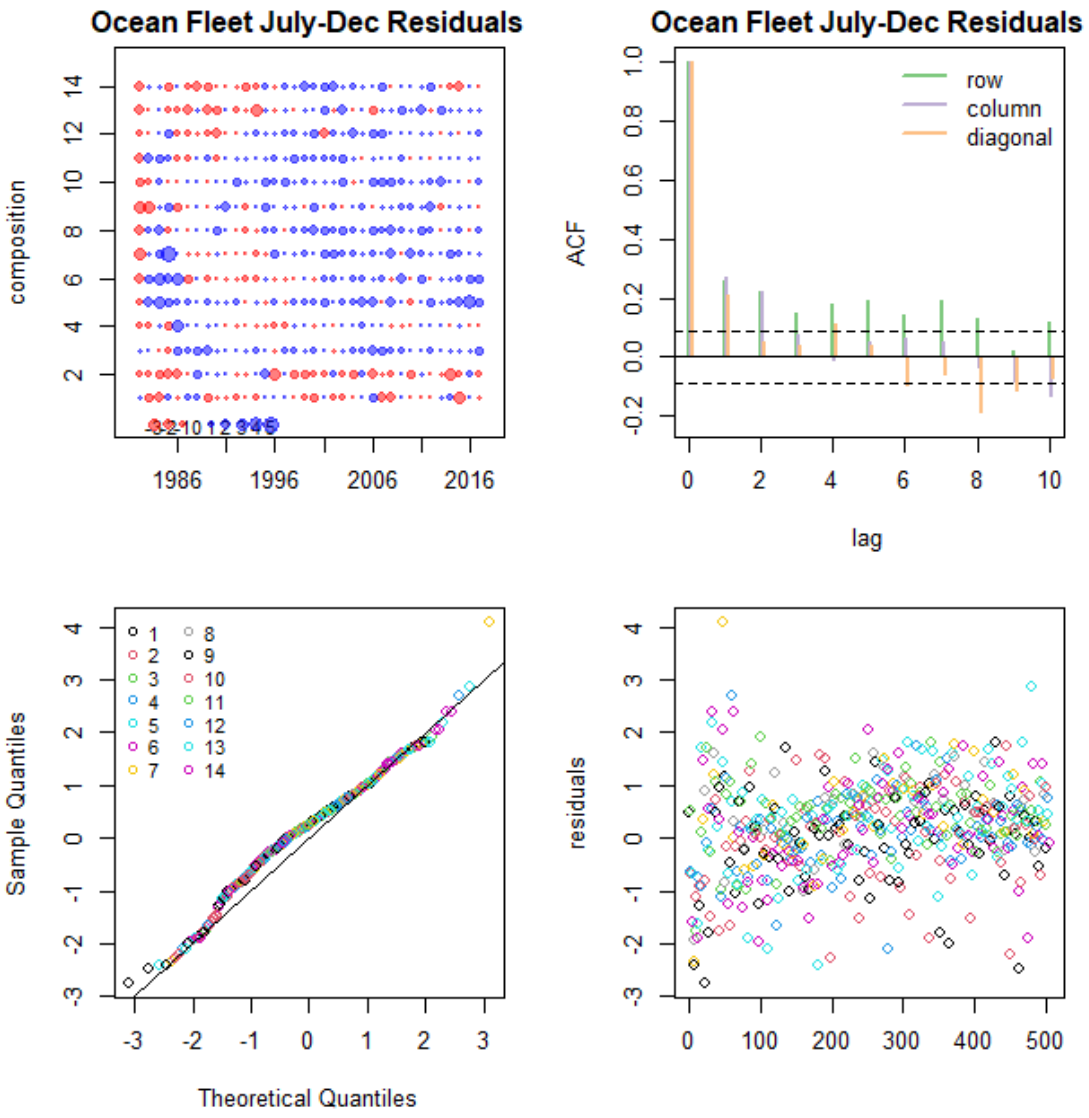

Supplemental Figure S2.7. One-step ahead residual plots for the estimated age composition for the Ocean fleet in July-December. The top left plot shows positive (blue) and negative (red) one-step ahead residuals for each age-class and year, and the size of the circle represents the relative size of the residual. The top right plot shows the autocorrelation function for each age (green), year (purple) and cohort (orange). The bottom left plot shows the quantile plots of residuals for each age (colored

circles), where the black line represents normally distributed errors. The bottom right plot represents the dispersion of residuals through time.

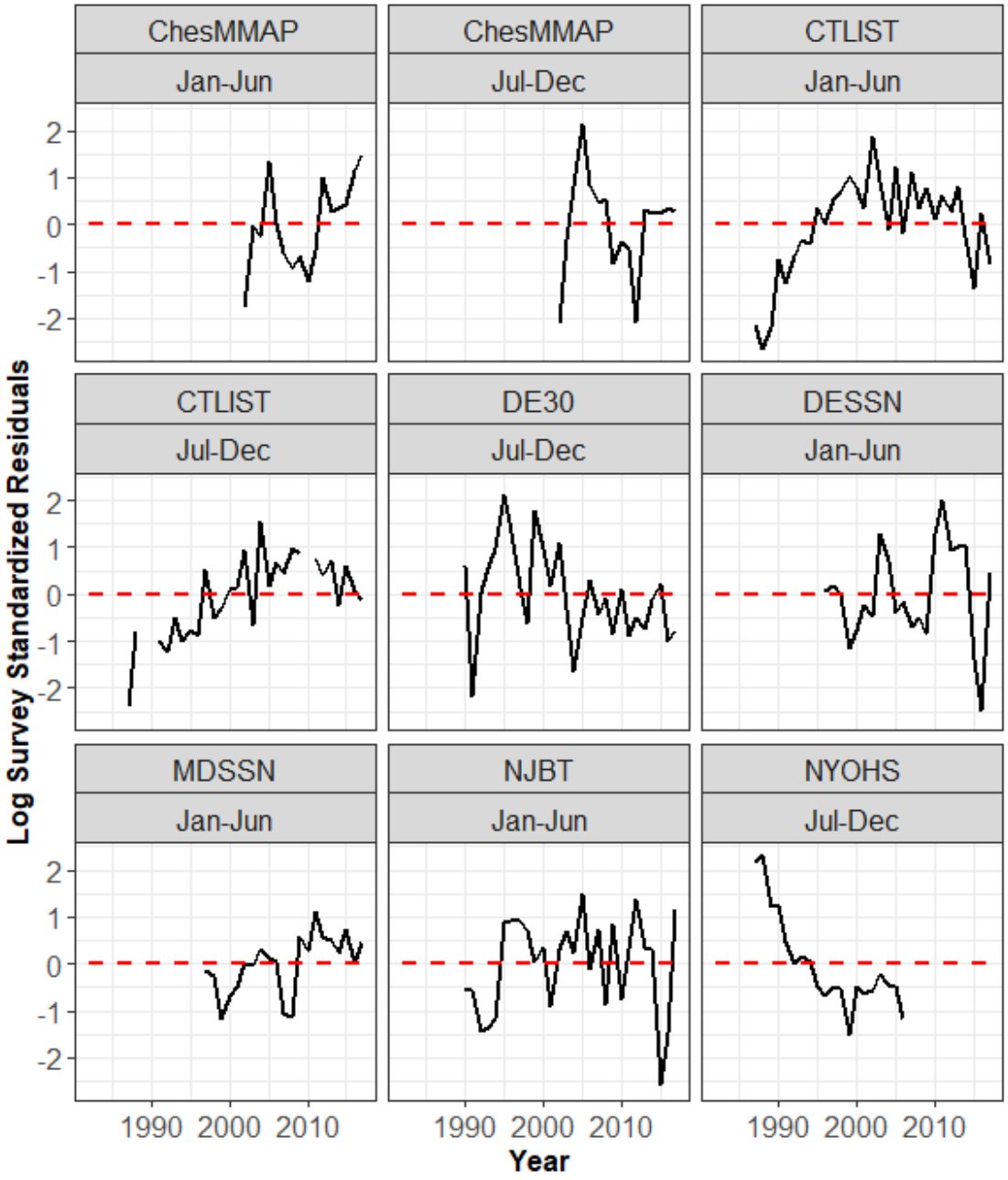

Supplemental Figure S2.8. Estimated residuals for the fishery-independent surveys. The black solid line are the logged residuals that subtract the predicted trend from the observed trend divided by the standard deviation ($\frac{obs-est}{sd}$). The red dotted line indicates when the residual would be zero. The months correspond to time-step the

survey was conducted in. Residuals are presented for the Chesapeake Bay Multispecies Monitoring and Assessment Program (ChesMMAP), the Connecticut Long Island Sound Survey (CTLIST), Delaware 30 Foot Trawl Survey (DE30), Delaware Spawning Stock Electrofishing Survey (DESSN), Maryland Spawning Stock Survey (MDSSN), New Jersey Bottom Trawl Survey (NJBT), and New York Ocean Haul Seine Survey (NYOHS).

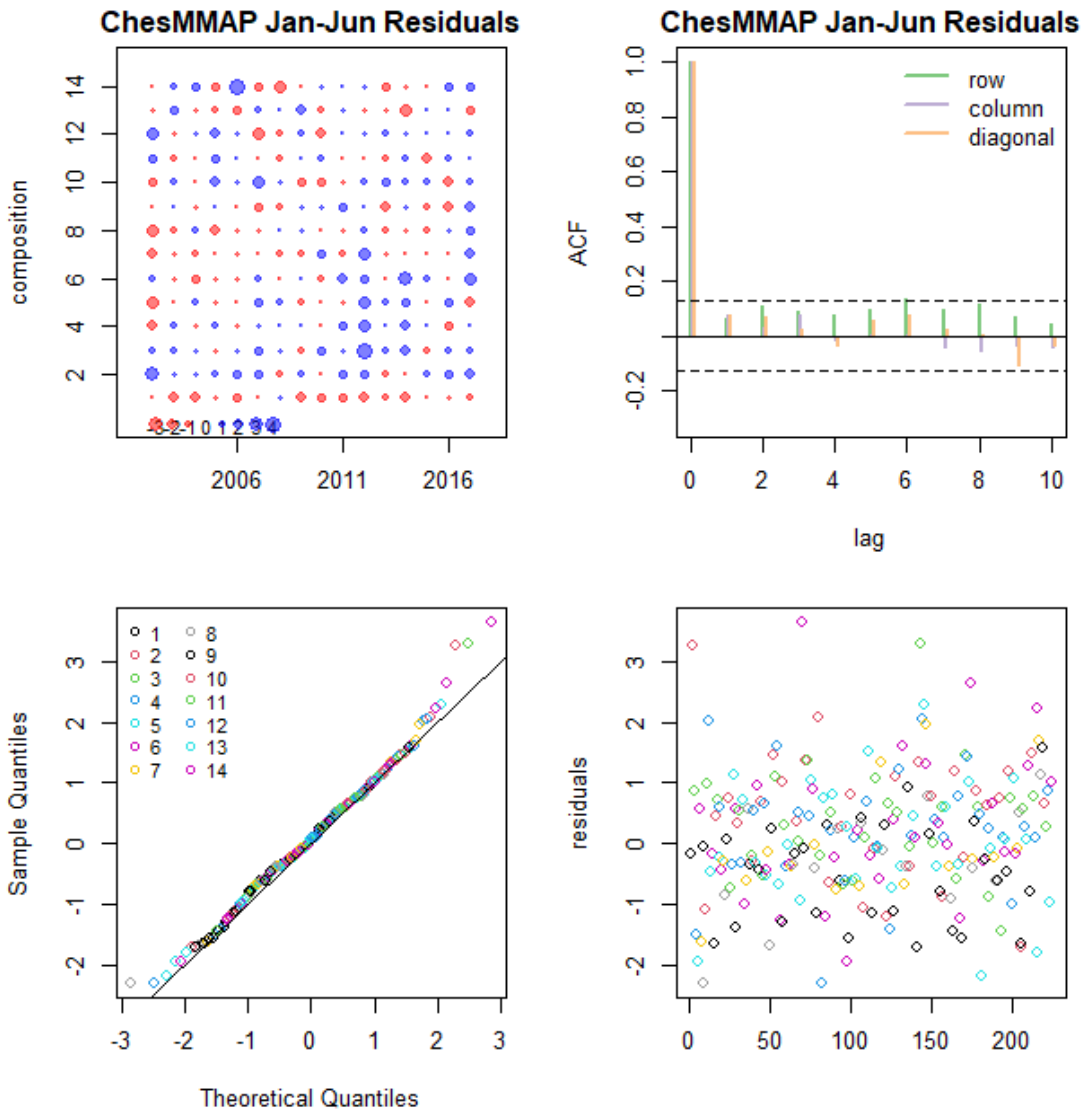

Supplemental Figure S2.9. One-step ahead residual plots for the Chesapeake Bay Multispecies Monitoring and Assessment Program (ChesMMAP) survey's estimated age-composition in January-June. The top left plot shows positive (blue) and negative (red) one-step ahead residuals for each age-class and year, and the size of the circle represents the relative size of the residual. The top right plot shows the autocorrelation function for each age (green), year (purple) and cohort (orange). The bottom left plot shows the quantile plots of residuals for each age (colored circles),

where the black line represents normally distributed errors. The bottom right plot represents the dispersion of residuals through time.

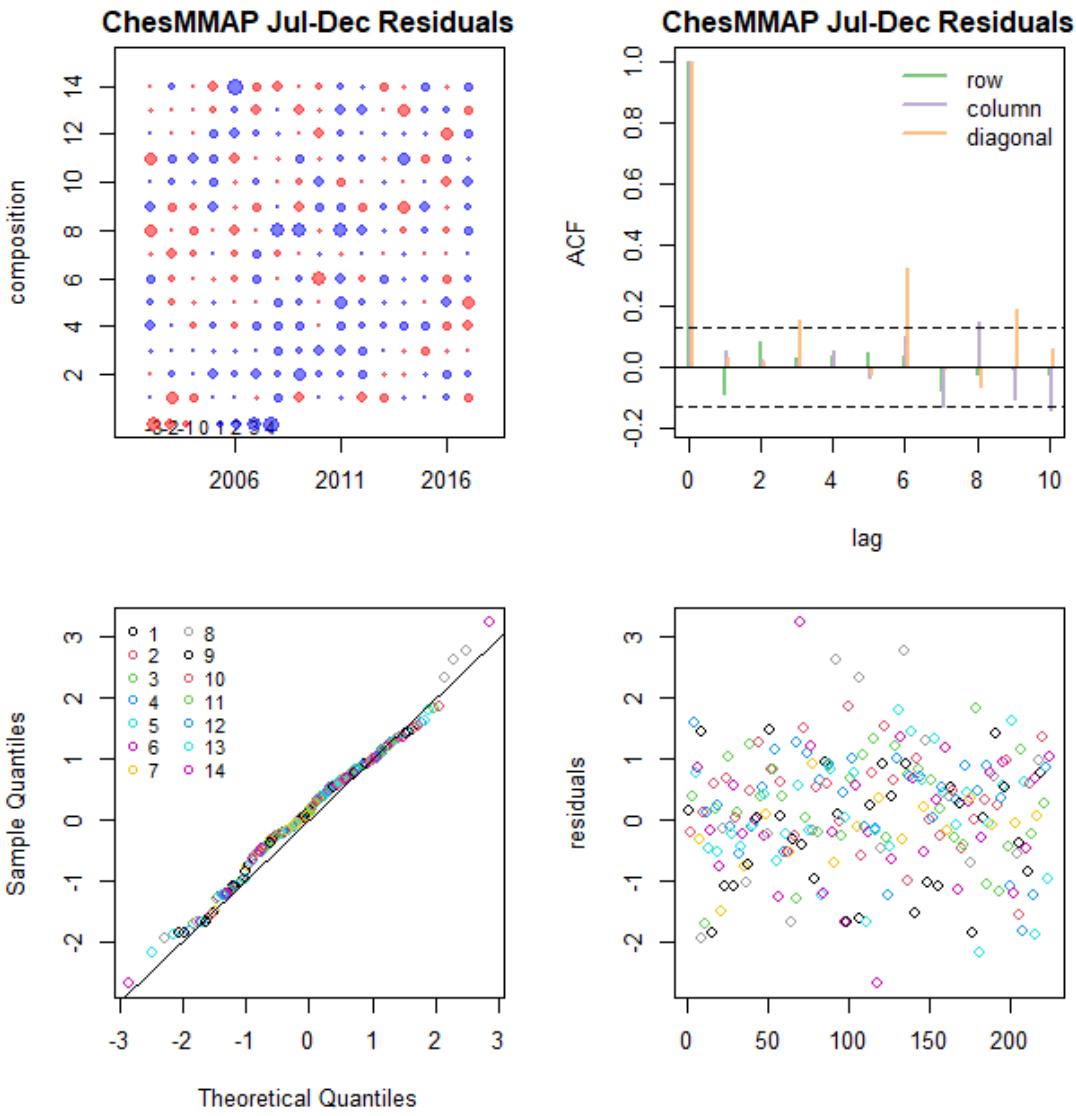

Supplemental Figure S2.10. One-step ahead residual plots for the Chesapeake Bay Multispecies Monitoring and Assessment Program (ChesMMAP) survey's estimated age-composition in July-December. The top left plot shows positive (blue) and negative (red) one-step ahead residuals for each age-class and year, and the size of the circle represents the relative size of the residual. The top right plot shows the autocorrelation function for each age (green), year (purple) and cohort (orange). The bottom left plot shows the quantile plots of residuals for each age (colored circles),

where the black line represents normally distributed errors. The bottom right plot represents the dispersion of residuals through time.

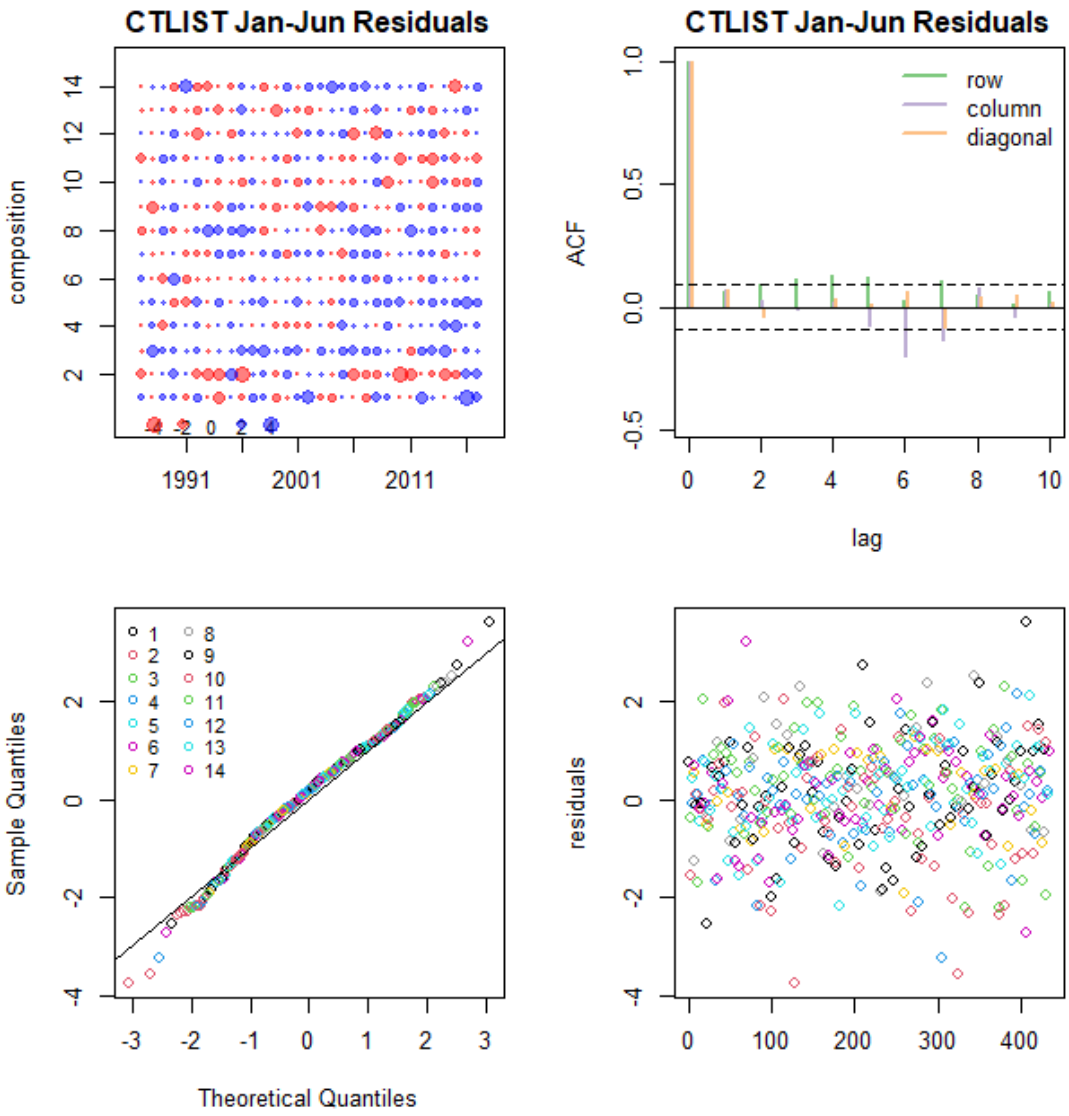

Supplemental Figure S2.11. One-step ahead residual plots for the Connecticut Long Island Sound Survey's (CTLIST) estimated age-composition in January-June. The top left plot shows positive (blue) and negative (red) one-step ahead residuals for each age-class and year, and the size of the circle represents the relative size of the residual. The top right plot shows the autocorrelation function for each age (green), year (purple) and cohort (orange). The bottom left plot shows the quantile plots of residuals for each age (colored circles), where the black line represents normally

distributed errors. The bottom right plot represents the dispersion of residuals through time.

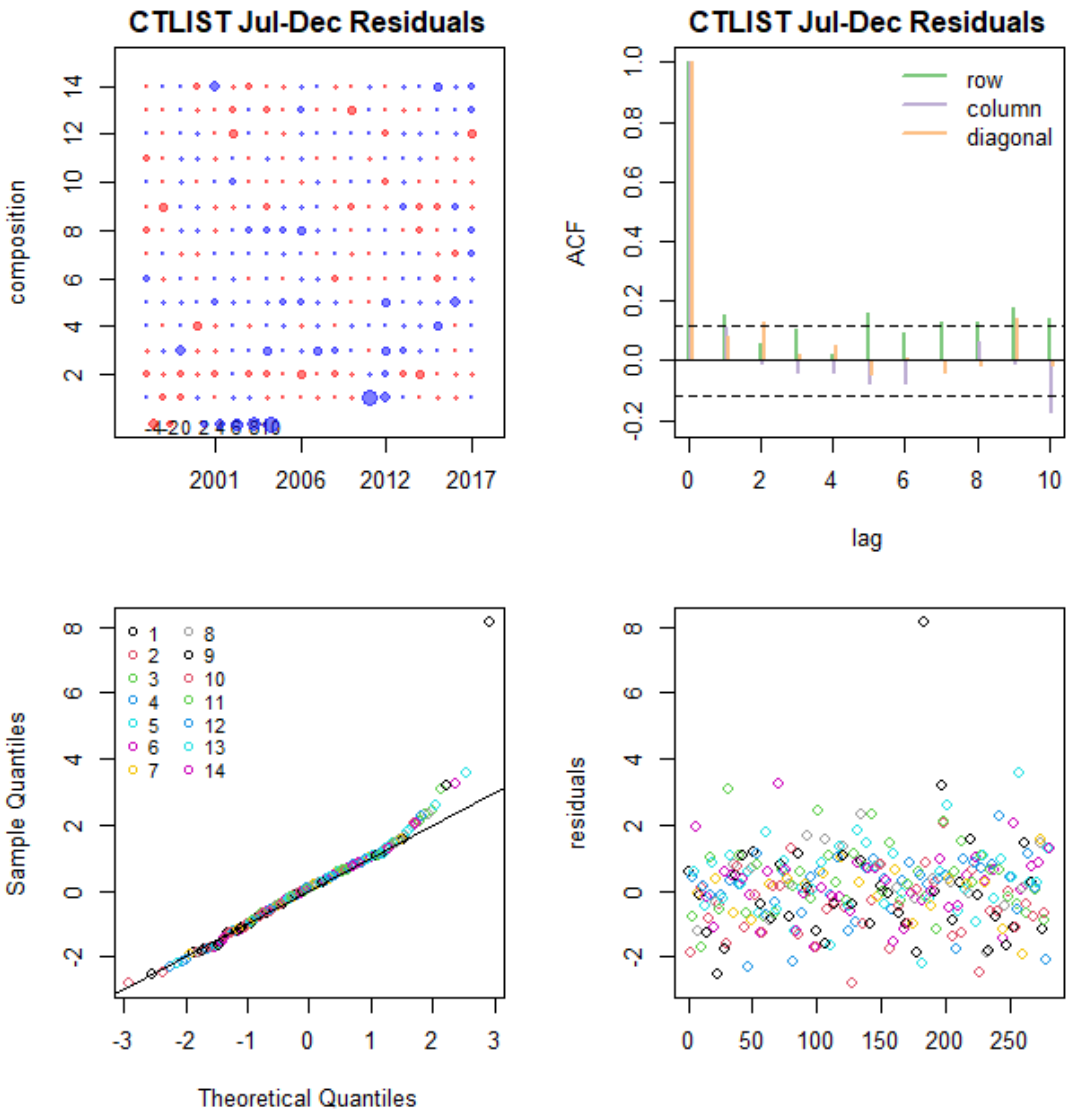

Supplemental Figure S2.12. One-step ahead residual plots for the Connecticut Long Island Sound Survey's (CTLIST) estimated age-composition in July-December. The top left plot shows positive (blue) and negative (red) one-step ahead residuals for each age-class and year, and the size of the circle represents the relative size of the residual. The top right plot shows the autocorrelation function for each age (green), year (purple) and cohort (orange). The bottom left plot shows the quantile plots of residuals for each age (colored circles), where the black line represents normally

distributed errors. The bottom right plot represents the dispersion of residuals through time.

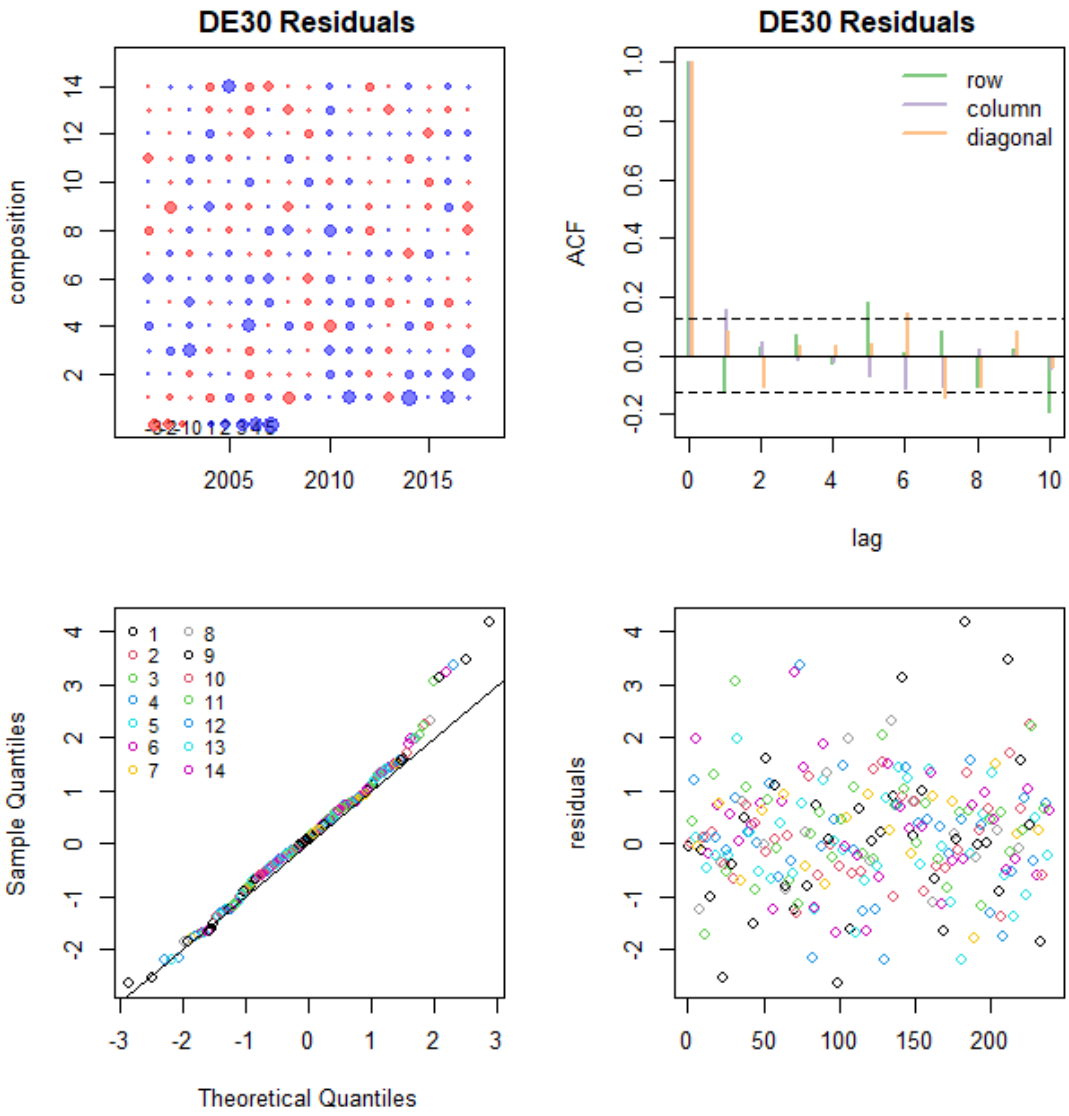

Supplemental Figure S2.13. One-step ahead residual plots for the Delaware 30 Foot Trawl Survey's (DE30) estimated age-composition in July-December. The top left plot shows positive (blue) and negative (red) one-step ahead residuals for each age-class and year, and the size of the circle represents the relative size of the residual. The top right plot shows the autocorrelation function for each age (green), year (purple) and cohort (orange). The bottom left plot shows the quantile plots of residuals for each age (colored circles), where the black line represents normally

distributed errors. The bottom right plot represents the dispersion of residuals through time.

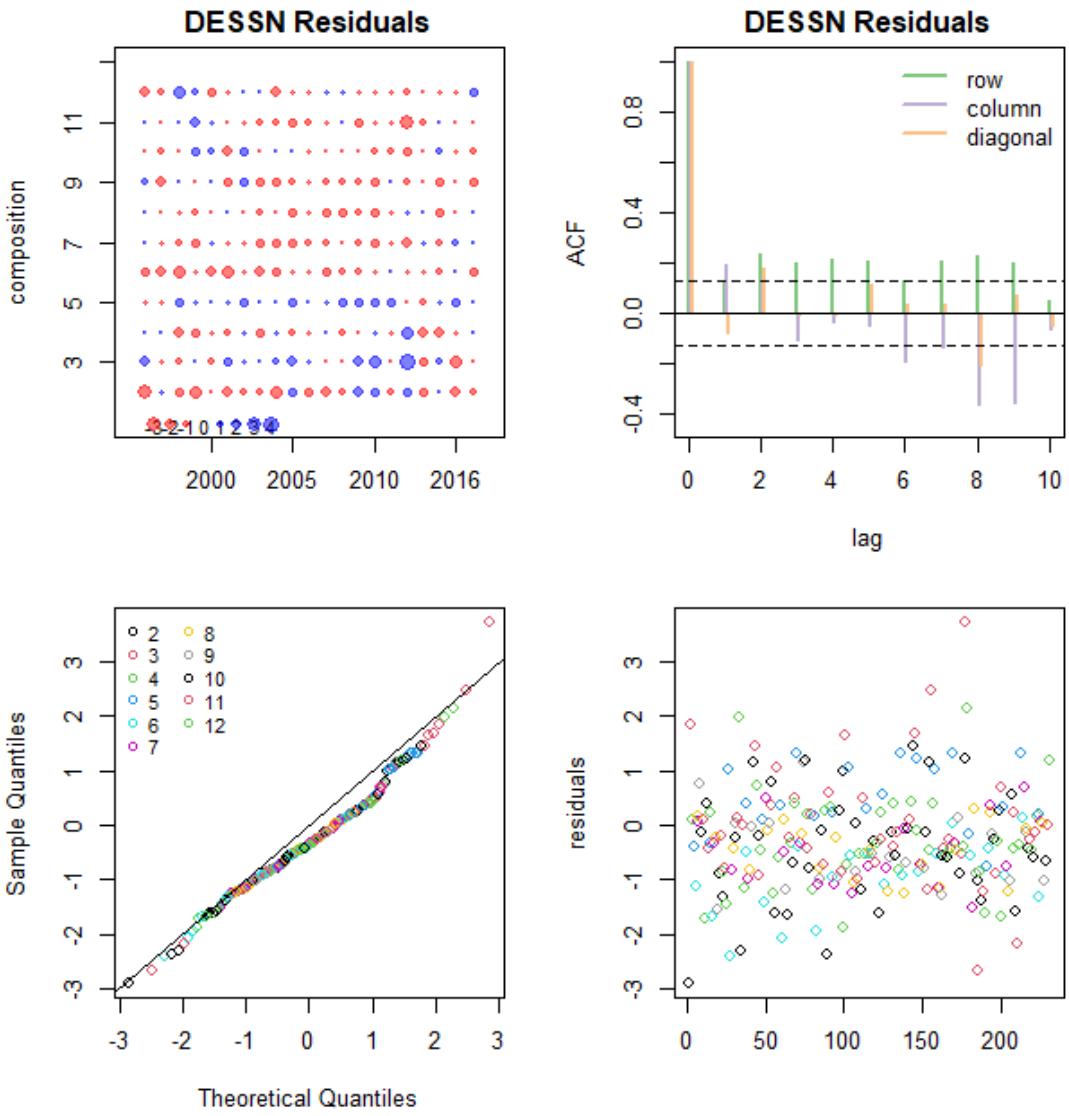

Supplemental Figure S2.14. One-step ahead residual plots for the Delaware Spawning Stock Survey's (DESSN) estimated age-composition in January-June. The top left plot shows positive (blue) and negative (red) one-step ahead residuals for each age-class and year, and the size of the circle represents the relative size of the residual. The top right plot shows the autocorrelation function for each age (green), year (purple) and cohort (orange). The bottom left plot shows the quantile plots of residuals for each age (colored circles), where the black line represents normally

distributed errors. The bottom right plot represents the dispersion of residuals through time.

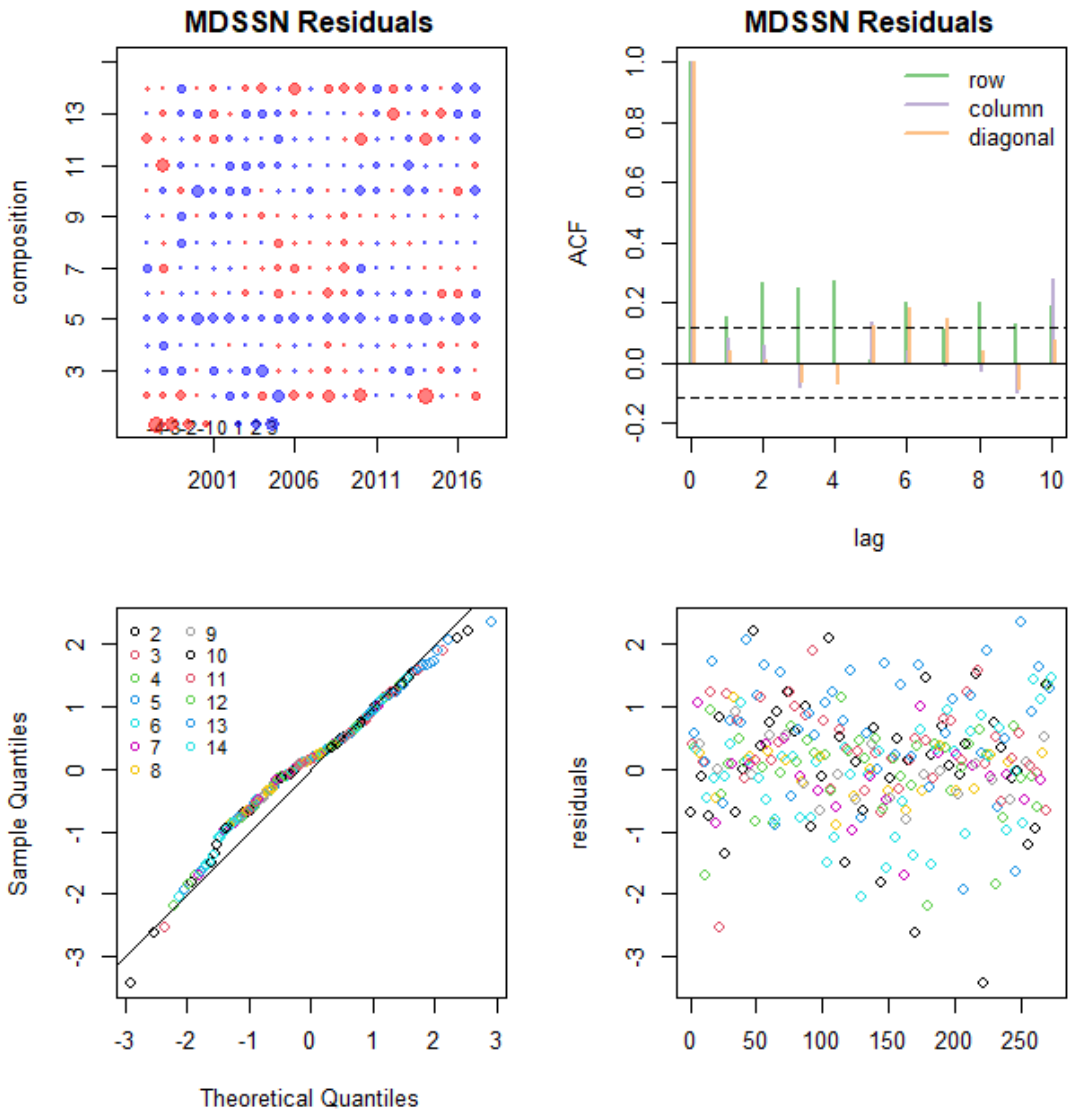

Supplemental Figure S2.15. One-step ahead residual plots for the Maryland Spawning Stock Survey's (MDSSN) estimated age-composition in January-June. The top left plot shows positive (blue) and negative (red) one-step ahead residuals for each age-class and year, and the size of the circle represents the relative size of the residual. The top right plot shows the autocorrelation function for each age (green), year (purple) and cohort (orange). The bottom left plot shows the quantile plots of residuals for each age (colored circles), where the black line represents normally

distributed errors. The bottom right plot represents the dispersion of residuals through time.

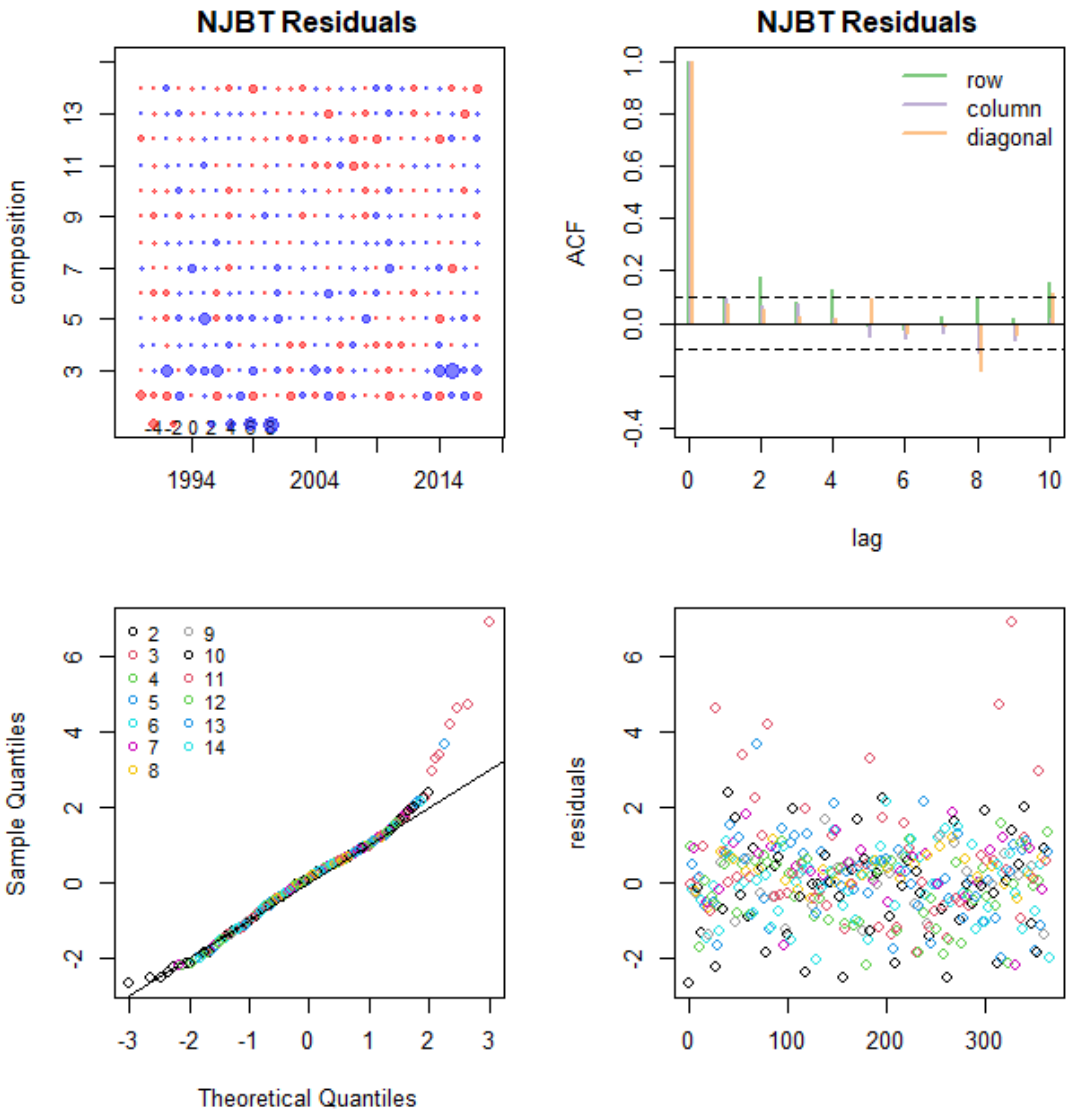

Supplemental Figure S2.16. One-step ahead residual plots for the New Jersey Bottom Trawl (NJBT) survey's estimated age-composition in January-June. The top left plot shows positive (blue) and negative (red) one-step ahead residuals for each age-class and year, and the size of the circle represents the relative size of the residual. The top right plot shows the autocorrelation function for each age (green), year (purple) and cohort (orange). The bottom left plot shows the quantile plots of residuals for each age (colored circles), where the black line represents normally

distributed errors. The bottom right plot represents the dispersion of residuals through time.

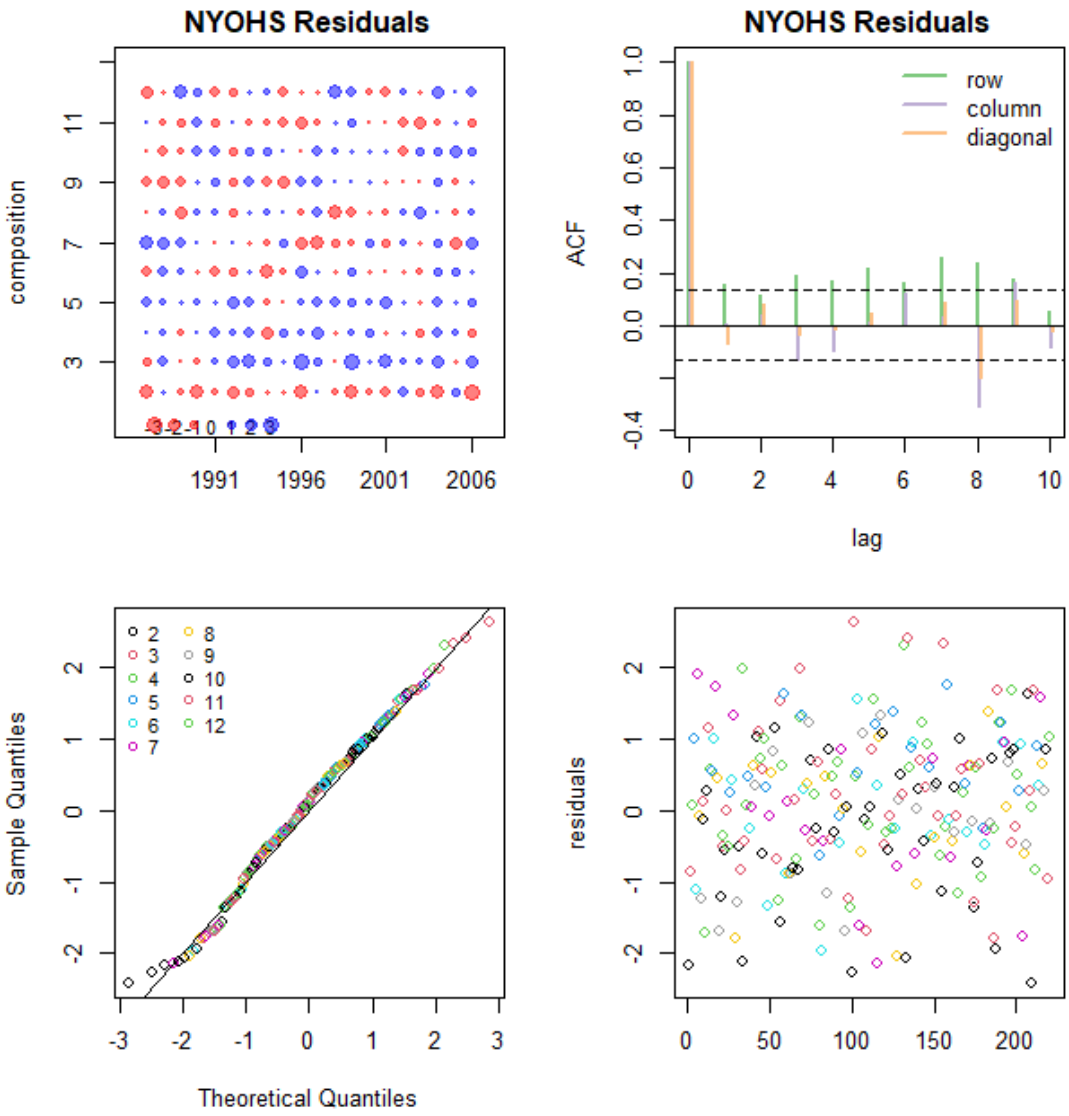

Supplemental Figure S2.17. One-step ahead residual plots for the New York Ocean Haul Seine (NYOHS) survey's estimated age-composition in January-June. The top left plot shows positive (blue) and negative (red) one-step ahead residuals for each age-class and year, and the size of the circle represents the relative size of the residual. The top right plot shows the autocorrelation function for each age (green), year (purple) and cohort (orange). The bottom left plot shows the quantile plots of residuals for each age (colored circles), where the black line represents normally

distributed errors. The bottom right plot represents the dispersion of residuals through time.

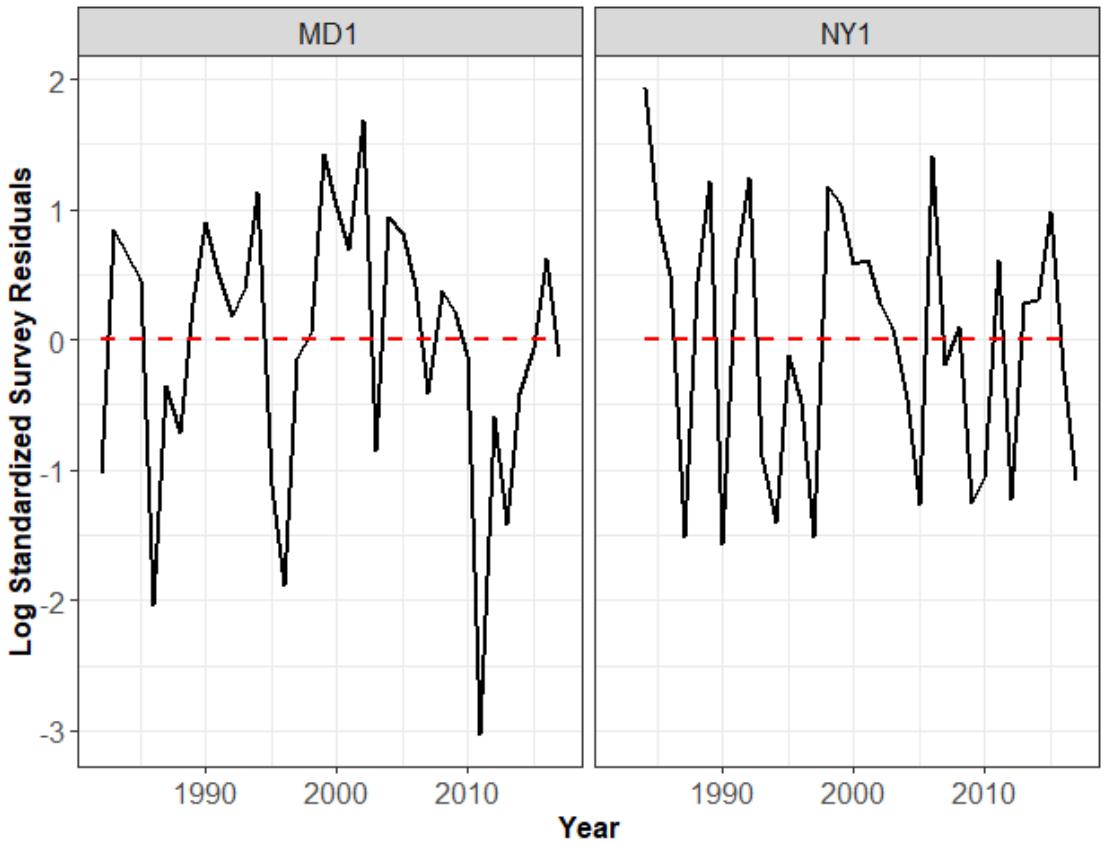

Supplemental Figure S2.18. Estimated log standardized residuals of the index of abundance for the fishery-independent Age-1 surveys for striped bass. The black solid line are the logged residuals that subtract the predicted trend from the observed trend divided by the standard deviation ($\frac{obs-est}{sd}$). The red dotted line indicates when the residual would be equal to zero. Estimates are provided for the Maryland Yearling Survey (MD1) and the New York Yearling Survey (NY1).

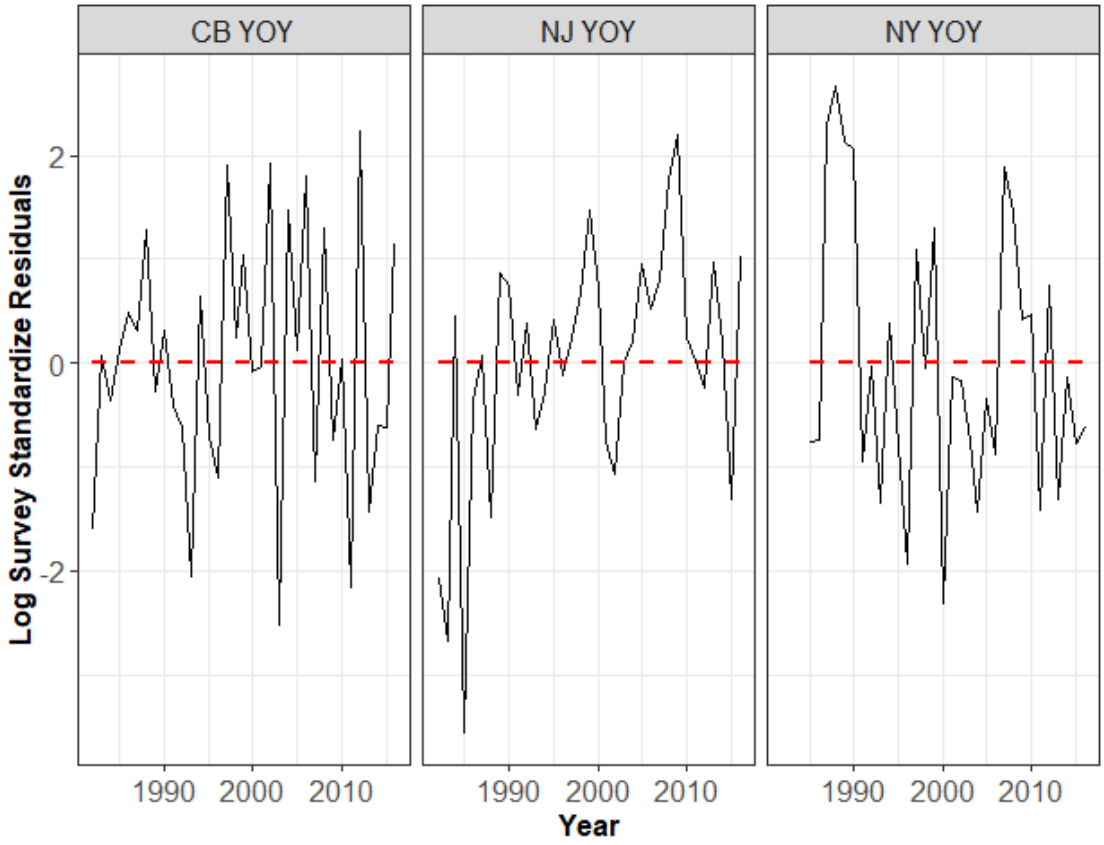

Supplemental Figure S2.19. Estimated log standardized residuals of the index of abundance for the fishery independent young-of-the-year surveys for striped bass. The black solid line are the logged residuals that subtract the predicted trend from the observed trend divided by the standard deviation ($\frac{obs-est}{sd}$). The red dotted line indicates when the residual would be equal to zero. Estimates are provided for the Chesapeake Bay YOY Index (CBYOY), the New Jersey YOY Survey (NJYOY), and the New York YOY Survey (NYYOY). The CBYOY is an aggregate index of YOY abundance for the Chesapeake Bay, with data from the Virginia YOY survey conducted by the Virginia Institute of Marine Science and the Maryland YOY survey conducted by the Maryland Department of Natural Resources.

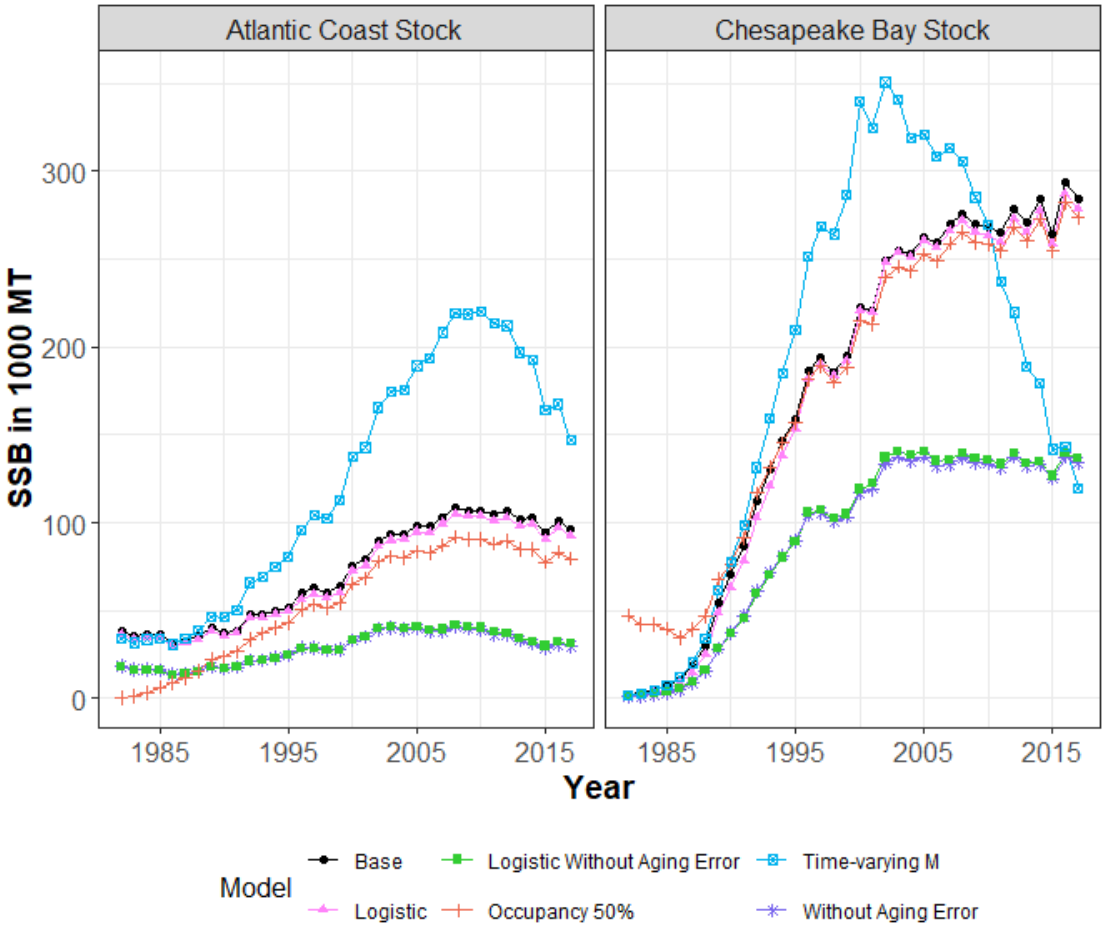

Supplemental Figure S2.20. Estimated striped bass spawning stock biomass (SSB) for the base model and five sensitivity runs of the spatially-explicit multi-stock model (see Table S2.4 for definitions of runs).

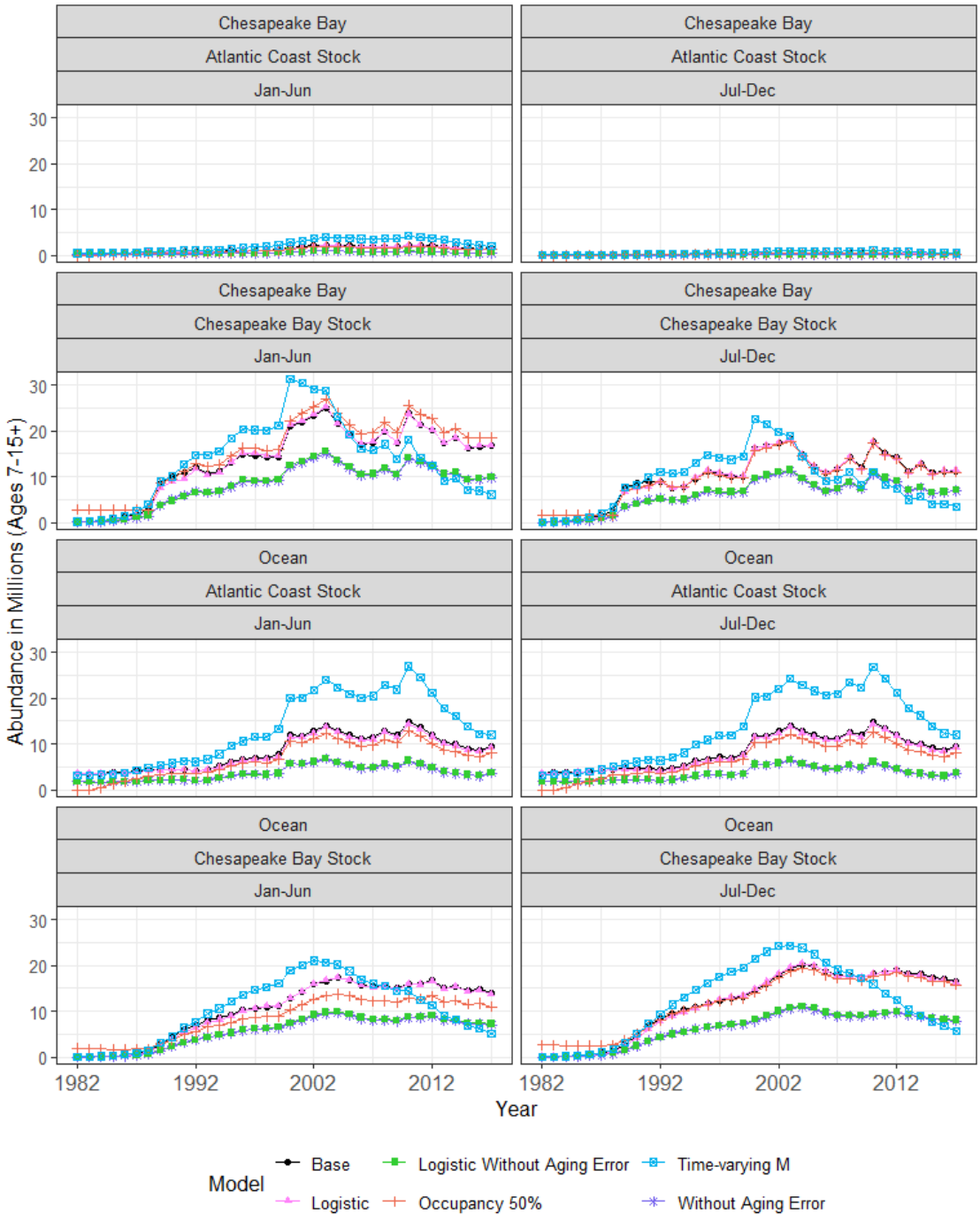

Supplemental Figure S2.21. Mean estimates of abundance for striped bass (7-15+) for each stock, region, and 6-month time-step estimated from sensitivity runs. The top two rows correspond to estimates in the Chesapeake Bay region for both stock in both

time-steps, and the bottom two rows correspond to estimates in the Ocean region for both stock in both time-steps (see Table S4.4 for definition of runs).

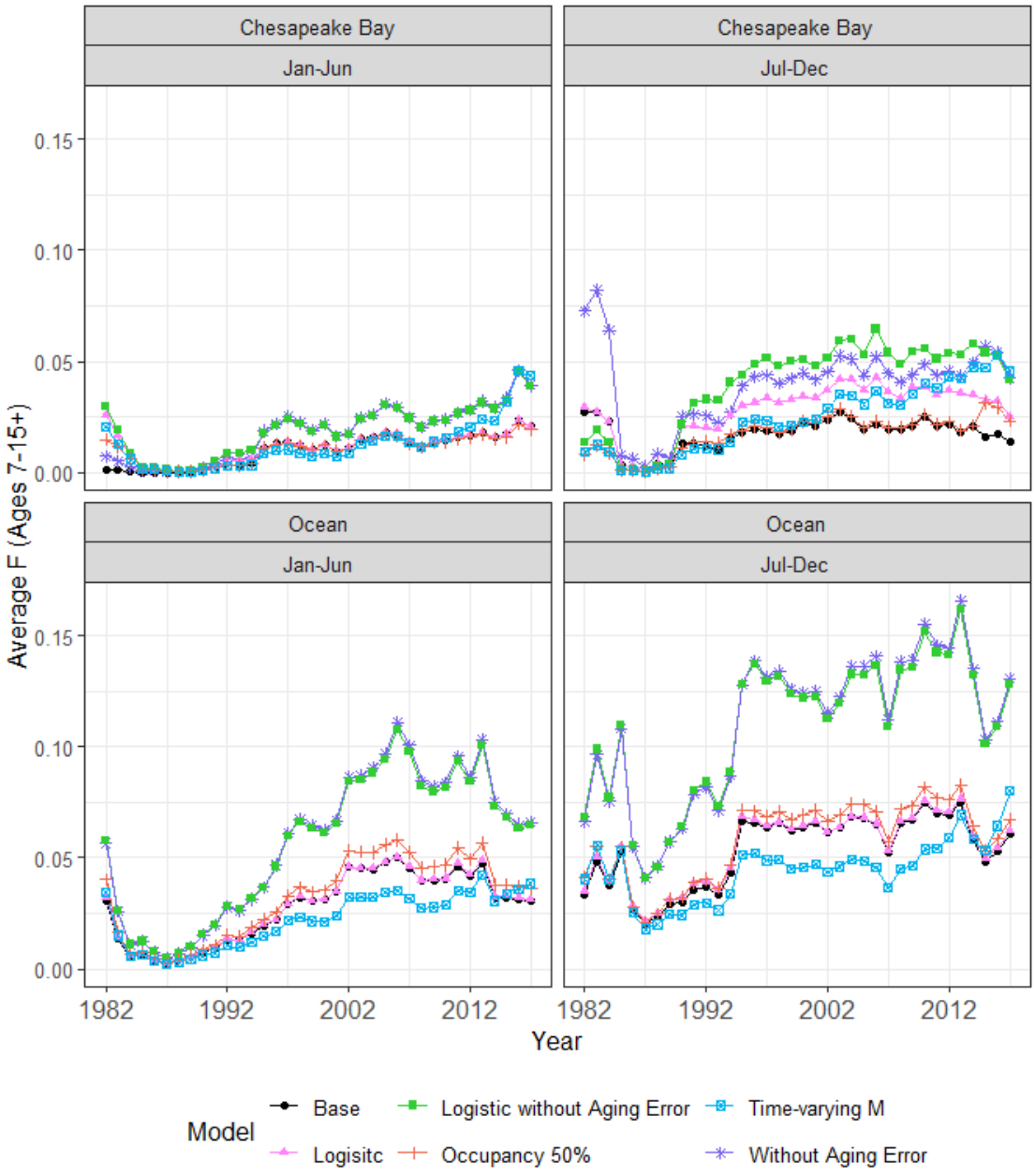

Supplemental Figure S2.22. Estimated weighted average of instantaneous fishing mortality (F) for each 6-month time-step ($6mo^{-1}$) for striped bass (7-15+) from sensitivity runs. The top row is estimates in the Chesapeake Bay region and the bottom row is estimates from the Ocean region (see Table S4.4 for definition of runs).

2.11 References

ASMFC (Atlantic States Marine Fisheries Commission). 1985. Amendment 3 to the Interstate Fishery Management Atlantic Striped Bass.

ASMFC (Atlantic States Marine Fisheries Commission). 1989. Supplement to the Striped Bass FMP-Amendment #4.

ASMFC (Atlantic States Marine Fisheries Commission). 1995. Amendment #5 to the Interstate Fishery Management Plan for Striped Bass.

ASMFC (Atlantic States Marine Fisheries Commission). 1981. Interstate Fisheries Management Plan for the Striped Bass of the Atlantic Coast from Maine to North Carolina. Prepared by Versar, Inc., Columbia, Maryland. April.

Berger, A.M., Goethel, D.R., Lynch, P.D., Quinn, T., Mormede, S., McKenzie, J., and Dunn, A. 2016. Space oddity: The mission for spatial integration. Canadian Journal of Fisheries and Aquatic Sciences **74**(11): 1698–1716. doi:10.1139/cjfas-2017-0150.

Berger, A.M., Jones, M.L., Zhao, Y., and Bence, J.R. 2012. Accounting for spatial population structure at scales relevant to life history improves stock assessment: The case for Lake Erie walleye *Sander vitreus*. Fish Res **115–116**: 44–59. doi:10.1016/j.fishres.2011.11.006.

Bertignac, M., Ne De Pontual, H., and Bertignac, M. 2007. Consequences of bias in age estimation on assessment of the northern stock of European hake (*Merluccius merluccius*) and on management advice. International Council for the Exploration of the Sea: 981–988.

Bosley, K.M., Schueller, A.M., Goethel, D.R., Hanselman, D.H., Fenske, K.H., Berger, A.M., Deroba, J.J., and Langseth, B.J. 2022. Finding the perfect mismatch: Evaluating misspecification of population structure within spatially explicit integrated population models. Fish and Fisheries **23**(2): 294–315. doi:10.1111/faf.12616.

Cadrin, S.X. 2020. Defining spatial structure for fishery stock assessment. Fish Res **221**(105397): 1–12. doi:10.1016/j.fishres.2019.105397.

Cadrin, S.X., and Secor, D.H. 2009. Accounting for spatial population structure in stock assessment: Past, present, and future. The Future of Fisheries Science in North America: 405–426. doi:10.1007/978-1-4020-9210-7_22.

Candy, S.G., Nowara, G.B., Welsford, D.C., and McKinlay, J.P. 2012. Estimating an ageing error matrix for Patagonian toothfish (Dissostichus eleginoides) otoliths using between-reader integer errors, readability scores, and continuation ratio models. Fish Res **115–116**: 14–23. doi:10.1016/j.fishres.2011.11.005.

Cao, J., Thorson, J.T., Punt, A.E., and Szuwalski, C. 2019. A novel spatiotemporal stock assessment framework to better address fine-scale species distributions: Development and simulation testing. Fish and Fisheries **21**(2): 350–367. doi:10.1111/faf.12433.

Carruthers, T.R., McAllister, M.K., and Taylor, N.G. 2011. Spatial surplus production modeling of Atlantic tunas and billfish. Ecological Applications **21**(7): 2734–2755. doi:10.1890/10-2026.1.

Conn, P.B. 2010. Hierarchical analysis of multiple noisy abundance indices. Canadian Journal of Fisheries and Aquatic Sciences **67**(1): 108–120. doi:10.1139/F09-175.

Cope, J.M., and Punt, A.E. 2011. Reconciling stock assessment and management scales under conditions of spatially varying catch histories. Fish Res **107**(1–3): 22–38. doi:10.1016/j.fishres.2010.10.002.

Dorazio, R.M., Hattala, K.A., McCollough, C.B., and Skjeveland, J.E. 1994. Tag Recovery Estimates of Migration of Striped Bass from Spawning Areas of the Chesapeake Bay. Trans Am Fish Soc **123**(6): 950–963.

Fabrizio, M.C. 1987. Contribution of Chesapeake Bay and Hudson River Stocks of Striped Bass to Rhode Island Coastal Waters as Estimated by Isoelectric Focusing of Eye Lens Proteins. Trans Am Fish Soc **116**(4): 588–593. doi:10.1577/1548-8659(1987)116<588:cocbah>2.0.co;2.

Fournier, D., and Archibald, C.P. 1982. A general theory for analyzing catch at age data. Canadian Journal of Fisheries and Aquatic Sciences **39**(8): 1195–1207.

Fournier, D.A., Sibert, J.R., Majkowski, J., and Harnpton, J. 1990. MULTIFAN a Likeihood-Based Method for Estimating Growth Parameters and Age Composition from Multiple Length Frequency Data Sets Illustrated using Data for Southern Bluefin Tuna (*Thunnus maccoyii*). Canadian Journal of Fisheries and Aquatic Sciences **47**: 301–317.

Fournier, D.A., Skaug, H.J., Ancheta, J., Ianelli, J., Magnusson, A., Maunder, M.N., Nielsen, A., and Sibert, J. 2012. AD Model Builder: Using automatic differentiation for statistical inference of highly parameterized complex

nonlinear models. Optim Methods Softw **27**: 233–249. doi:10.1080/10556788.2011.597854.

Francis, R.I.C.C. 2011. Data weighting in statistical fisheries stock assessment models. Canadian Journal of Fisheries and Aquatic Sciences **68**(6): 1124–1138. doi:10.1139/f2011-025.

Goethel, D.R., and Berger, A.M. 2016. Accounting for spatial complexities in the calculation of biological reference points: Effects of misdiagnosing population structure for stock status indicators. Canadian Journal of Fisheries and Aquatic Sciences **74**(11): 1878–1894. doi:10.1139/cjfas-2016-0290.

Goethel, D.R., Berger, A.M., and Cadrin, S.X. 2023. Spatial awareness: Good practices and pragmatic recommendations for developing spatially structured stock assessments. Fish Res **264**(106703). doi:10.1016/j.fishres.2023.106703.

Goethel, D.R., Legault, C.M., and Cadrin, S.X. 2015a. Demonstration of a spatially explicit, tag-integrated stock assessment model with application to three interconnected stocks of yellowtail flounder off of New England. ICES Journal of Marine Science **72**(1): 164–177. doi:10.4135/9781412953924.n678.

Goethel, D.R., Legault, C.M., and Cadrin, S.X. 2015b. Testing the performance of a spatially explicit tag-integrated stock assessment model of yellowtail flounder (*Limanda ferruginea*) through simulation analysis. Canadian Journal of Fisheries and Aquatic Sciences **72**(4): 582–601. doi:10.1139/cjfas-2014-0244.

Goethel, D.R., Quinn, T.J., and Cadrin, S.X. 2011. Incorporating spatial structure in stock assessment: Movement modeling in marine fish population dynamics.

Reviews in Fisheries Science **19**(2): 119–136. doi:10.1080/10641262.2011.557451.

Grothues, T.M., Able, K.W., Carter, J., and Arienti, T.W. 2009. Migration patterns of striped bass through nonnatal estuaries of the U.S. Atlantic coast. American Fisheries Society Symposium **69**: 135–150.

Guan, W., Cao, J., Chen, Y., and Cieri, M. 2013. Impacts of population and fishery spatial structures on fishery stock assessment. Canadian Journal of Fisheries and Aquatic Sciences **70**(8): 1178–1189. doi:10.1139/cjfas-2012-0364.

Hartman, K.J., and Margraf, F.J. 2003. US Atlantic coast striped bass: Issues with a recovered population. Fish Manag Ecol **10**(5): 309–312. doi:10.1046/j.1365-2400.2003.00361.x.

Hasegawa, E.H., Waldman, J., and Wirgin, I. 2022. Stock composition of Atlantic coastal migratory striped bass using microsatellite DNA analysis. Fish Res **254**(106384): 1–10. doi:10.1016/j.fishres.2022.106384.

Hernández-Padilla, J.C., Luquin-Covarrubias, M.A., Morales-Bojórquez, E., Salas, S., Navarro-González, J.A., Rábago-Quiroz, C.H., and Capetillo-Piñar, N. 2024. Stock assessment and fishing management of green abalone (*Haliotis fulgens*) along the West Coast of Baja California Sur, Mexico. Ocean Coast Manag **253**. Elsevier Ltd. doi:10.1016/j.ocecoaman.2024.107134.

Hulson, P.J.F., and Williams, B.C. 2024. Inclusion of ageing error and growth variability using a bootstrap estimation of age composition and conditional age-at-length input sample size for fisheries stock assessment models. Fish Res **270**. Elsevier B.V. doi:10.1016/j.fishres.2023.106894.

Hutchinson, W.F. 2008. The dangers of ignoring stock complexity in fishery management: the case of the North Sea cod. Biol Lett **4**: 693–695. doi:10.1890/03-5066.

ICCAT (International Commission for the Conservation of Atlantic Tunas). 2022. Report of the 2022 ICCAT Eastern Atlantic and Mediterranean Bluefin Tuna Stock Assessment Meeting. Madrid.

Jiang, H., Pollock, K.H., Brownie, C., Hoenig, J.M., Latour, R.J., Wells, B.K., and Hightower, J.E. 2007. Tag Return Models Allowing for Harvest and Catch and Release: Evidence of Environmental and Management Impacts on Striped Bass Fishing and Natural Mortality Rates. N Am J Fish Manag **27**(2): 387–396. doi:10.1577/m06-089.1.

Kneebone, J., Hoffman, W.S., Dean, M.J., Fox, D.A., and Armstrong, M.P. 2014. Movement patterns and stock composition of adult striped bass tagged in Massachusetts coastal waters. Trans Am Fish Soc **143**(5): 1115–1129. doi:10.1080/00028487.2014.889752.

Liao, H., Sharov, A.F., and Nelson, G.A. 2013. Quantifying the effects of aging bias in Atlantic striped bass stock assessment. Trans Am Fish Soc **142**: 193–207. doi:10.1080/00028487.2012.705255.

Little, L.R., Punt, A.E., Tuck, G.N., and Mapstone, B.D. 2016. Exploring the effect of sampling, protogyny, and larval advection on stock estimates subject to no-take closures in a spatially complex coral reef line fishery on the Great Barrier Reef, Australia. Canadian Journal of Fisheries and Aquatic Sciences **74**(11): 1950–1959. Canadian Science Publishing. doi:10.1139/cjfas-2016-0349.

Mace, M.M., Doering, K.L., Wilberg, M.J., Larimer, A., Marenghi, F., Sharov, A., and Tarnowski, M. 2021. Spatial population dynamics of eastern oyster in the Chesapeake Bay, Maryland. Fish Res **237**. Elsevier B.V. doi:10.1016/j.fishres.2020.105854.

Maunder, M.N., Hamel, O.S., Lee, H.H., Piner, K.R., Cope, J.M., Punt, A.E., Ianelli, J.N., Castillo-Jordán, C., Kapur, M.S., and Methot, R.D. 2023. A review of estimation methods for natural mortality and their performance in the context of fishery stock assessment. Fish Res **257**. Elsevier B.V. doi:10.1016/j.fishres.2022.106489.

McAllister, M.K., and Ianelli, J.N. 1997. Bayesian stock assessment using catch-age data and the sampling - Importance resampling algorithm. Canadian Journal of Fisheries and Aquatic Sciences **54**(2): 284–300. doi:10.1139/cjfas-54-2-284.

Morse, M.R., Kerr, L.A., Galuardi, B., and Cadrin, S.X. 2020. Performance of stock assessments for mixed-population fisheries: The illustrative case of Atlantic bluefin tuna. ICES Journal of Marine Science **77**(6): 2043–2055. doi:10.1093/ICESJMS/FSAA082.

Northeast Fisheries Science Center. 2017a. 62nd Northeast Regional Stock Assessment Workshop (62nd SAW) Assessment Report.

Northeast Fisheries Science Center. 2017b. 63rd Northeast Regional Stock Assessment Workshop. doi:10.7289/V5/RD-NEFSC-17-09.

Northeast Fisheries Science Center. 2019. 66th Northeast Regional Stock Assessment Workshop (66th SAW) Assessment Report. Northeast Fisheries Science Center Reference Document (19–08): 457–1170.

Punt, A.E. 2017. Review of contemporary cetacean stock assessment models. Journal of Cetacean Research Management **17**: 35–56.

Punt, A.E. 2019a. Spatial stock assessment methods: A viewpoint on current issues and assumptions. Fish Res **213**: 132–143. doi:10.1016/j.fishres.2019.01.014.

Punt, A.E. 2019b. Modelling recruitment in a spatial context: A review of current approaches, simulation evaluation of options, and suggestions for best practices. Fish Res **217**: 140–155. Elsevier B.V. doi:10.1016/j.fishres.2017.08.021.

Punt, A.E., Haddon, M., and Tuck, G.N. 2015. Which assessment configurations perform best in the face of spatial heterogeneity in fishing mortality, growth and recruitment? A case study based on pink ling in Australia. Fish Res **168**: 85–99. Elsevier. doi:10.1016/j.fishres.2015.04.002.

Punt, A.E., Hakamada, T., Bando, T., and Kitakdao, T. 2014. Assessment of Antarctic minke whales using statistical catch-at- age analysis (SCAA). Journal of Cetacean Research Management (2013): 93–116.

Punt, A.E., Smith, D.C., KrusicGolub, K., and Robertson, S. 2008. Quantifying age-reading error for use in fisheries stock assessments, with application to species in Australia's southern and eastern scalefish and shark fishery. Canadian Journal of Fisheries and Aquatic Sciences **65**(9): 1991–2005. doi:10.1139/F08-111.

Quinn, T.J., Deriso, R.B., and Neal, P.R. 1990. Migratory catch-age analysis. Canadian Journal of Fisheries and Aquatic Science **47**: 2315–2327.

Reeves, S.A. 2003. A simulation study of the implications of age-reading errors for stock assessment and management advice. ICES Journal of Marine Science **60**(2): 314–328. Academic Press. doi:10.1016/S1054-3139(03)00011-0.

Richards, R.A., and Deuel, D.G. 1987. Atlantic striped bass: stock status and the recreational fishery. Marine Fisheries Review **49**(2): 58–66.

Richards, R.A., and Rago, P.J. 1999. A case history of effective fishery management: Chesapeake Bay Striped Bass. N Am J Fish Manag **19**(2): 356–375. doi:10.1577/1548-8675(1999)019.

Ricker, W.E. 1975. Computation and interpretation of biological statistics of fish populations. Bulletin of the Fisheries Research Board of Canada **191**: 401. doi:10.1038/108070b0.

Robinson, J.M., Wilberg, M.J., Adams, J. V., and Jones, M.L. 2013. A spatial age-structured model for describing sea lamprey (*Petromyzon marinus*) population dynamics. Canadian Journal of Fisheries and Aquatic Sciences **70**(12): 1709–1722. doi:10.1139/cjfas-2012-0375.

Rothermel, E.R., Balazik, M.T., Best, J.E., Breece, M.W., Fox, D.A., Gahagan, B.I., Haulsee, D.E., Higgs, A.L., O'Brien, M.H.P., Oliver, M.J., Park, I.A., and Secor, D.H. 2020. Comparative migration ecology of striped bass and Atlantic sturgeon in the US Southern mid-Atlantic bight flyway. PLoS One **15**(6): 1–24. doi:10.1371/journal.pone.0234442.

Schonfeld, A.J. 2023. Climate Impacts on Spatiotemporal Habitat Usage of Mid-Atlantic Fishes. William & Mary Ph.D. Dissertation.

Secor, D.H. 2000. Longevity and resilience of Chesapeake Bay striped bass. ICES Journal of Marine Science **57**(4): 808–815. doi:10.1006/jmsc.2000.0560.

Secor, D.H., O'Brien, M.H.P., Gahagan, B.I., Carter Watterson, J., and Fox, D.A. 2020. Differential migration in Chesapeake Bay striped bass. PLoS One **15**(5): 1–19. doi:10.1371/journal.pone.0233103.

Secor, D.H., Trice, M., and Hornick, H.T. 1995. Validation of otolith-based ageing and a comparison of otolith and scale-based ageing in mark-recaptured Chesapeake Bay striped bass, *Morone saxatilis*. Fishery Bulletin **93**(1): 186–190.

Taylor, N.G., McAllister, M.K., Lawson, G.L., Carruthers, T., and Block, B.A. 2011. Atlantic bluefin tuna: A novel multistock spatial model for assessing population biomass. PLoS One **6**(12). doi:10.1371/journal.pone.0027693.

Thygesen, U.H., Albertsen, C.M., Berg, C.W., Kristensen, K., and Nielsen, A. 2017. Validation of ecological state space models using the Laplace approximation. Environ Ecol Stat **24**(2): 317–339. Springer US. doi:10.1007/s10651-017-0372-4.

Tierney, L., and Kadane, J.B. 1986. Accurate approximations for posterior moments and marginal densities. J Am Stat Assoc **81**(393): 82–86. doi:10.1080/01621459.1986.10478240.

Trijoulet, V., Albertsen, C.M., Kristensen, K., Legault, C.M., Miller, T.J., and Nielsen, A. 2023. Model validation for compositional data in stock assessment models: Calculating residuals with correct properties. Fish Res **257**(August 2022): 106487. Elsevier B.V. doi:10.1016/j.fishres.2022.106487.

Trijoulet, V., and Nielsen, A. 2022. compResidual: Residual calculation for compositional observations.

Tyszko, S.M., and Pritt, J.J. 2017. Comparing otoliths and scales as structures used to estimate ages of largemouth bass: Consequences of biased age estimates. N Am J Fish Manag **37**(5): 1075–1082. John Wiley and Sons Inc. doi:10.1080/02755947.2017.1350220.

Vincent, M.T., Brenden, T.O., and Bence, J.R. 2016. Simulation testing the robustness of a multiregion, tag-integrated assessment model that exhibits natal homing and estimates natural mortality and reporting rate. Canadian Journal of Fisheries and Aquatic Sciences **74**(11): 1930–1949. Canadian Science Publishing. doi:10.1139/cjfas-2016-0297.

Wirgin, I., Maceda, L., Waldman, J.R., and Crittenden, R.N. 1993. Use of mitochondrial DNA polymorphisms to estimate the relative contributions of the Hudson River and Chesapeake Bay striped bass stocks to the mixed fishery on the Atlantic coast. Trans Am Fish Soc **122**(5): 669–684. doi:https://doi.org/10.1577/1548-8659(1993)122<0669:UOMDPT>2.3.CO;2.

Chapter 3: Identifying data needs for spatially-explicit population models with implications for striped bass

3.1 Abstract

Simulation studies are useful for determining the implications of available data and mis-specified model structure on the accuracy of model estimates of abundance and fishing mortality. A multi-stock, spatially-explicit population model was developed to estimate abundance of striped bass *Morone saxatilis* in the Chesapeake Bay and along the Atlantic coast. However, this model has not been evaluated to understand how the accuracy of model estimates are affected by different assumptions of stock structure, age composition, and movement, compared to current methods used to inform management decisions. The goals of our study were to assess the performance of spatially-explicit models compared to spatially-implicit (i.e., fleets-as-areas) models in estimating abundance of striped bass in the Chesapeake Bay, determine how improved data quality (e.g., stock composition) affects spatially-explicit model performance, and characterize the effect of aging error on model accuracy. We conducted a simulation study to evaluate the accuracy of spatial assessment models under alternative scenarios of data availability and quality. Datasets with alternative amounts of information on stock structure and aging information were generated, and a range of estimation models with alternative assumptions about spatial dynamics and time-varying biological processes were fitted to the datasets. We found spatially-explicit estimates were approximately unbiased when they closely matched the assumptions of the data generating model. Data on stock composition or informative priors on occupancy probabilities were necessary for the spatially-explicit, multi-

stock assessment models. Models that ignored potential aging bias in datasets yielded biased and inaccurate estimates of abundance, biomass, and fishing mortality.

3.2 Introduction

In recent decades, significant advances have been made to incorporate spatial dynamics into fisheries population modeling (Berger et al., 2016; Cadrin, 2020; Cadrin and Secor, 2009; Goethel et al., 2023, 2011; Punt, 2019a). Spatially-explicit models improve model accuracy when populations exhibit movement among regions, spatially-varying recruitment, or other spatially-varying life history characteristics (Berger et al., 2016; Goethel et al., 2023; Goethel and Berger, 2016; Guan et al., 2013; Punt, 2019a; Punt et al., 2015). Many assessment models assume a single closed population, with homogenous fishing mortality and life history characteristics across its range (Goethel et al., 2011). However, many fish stocks have some degree of spatial complexities including in migration, spawning behavior, or fishery characteristics (Berger et al., 2016; Cadrin, 2020). Further, assessments commonly model stock structure based on management or geopolitical boundaries, which can improperly split populations into subpopulations (Cadrin, 2020; Goethel et al., 2011; Smedbol and Stephenson, 2001). Ignoring spatial complexities in assessments may cause bias in estimated abundance and fishing mortality rates and reduce the ability to estimate accurate reference points or biological indicators (Cope and Punt, 2011; Goethel et al., 2023; Guan et al., 2013), which may have negative effects on management performance (Berger et al., 2016). However, identifying spatial boundaries and biological considerations is challenging for many species (Cadrin, 2020; Cadrin and Secor, 2009; Goethel et al., 2023). Additionally, spatially-explicit

models often rely on increased data requirements (e.g., tagging studies) for accurate estimates (Goethel et al., 2011).

Management decisions for striped bass *Morone saxatilis* are informed by a spatially-implicit fleets-as-areas (FAA) stock assessment model that assumes striped bass are homogenously mixed in a single area from Maine to North Carolina (Northeast Fisheries Science Center, 2019). Additionally, the FAA model assumes a single stock, although the includes multiple distinct spawning stocks (Dorazio et al., 1994; Hasegawa et al., 2022; Kneebone et al., 2014; Northeast Fisheries Science Center, 2019). Management measures differ among and within states, which likely causes spatially variable fishing mortality. Striped bass are a highly migratory species with movement patterns that vary by sex and size (Schonfeld 2023; Kneebone et al. 2014; Secor et al. 2020). Their migration exposes them to spatially differing fishing mortality throughout the year. Ignoring spatial complexities in assessment models for striped bass may provide incorrect management advice.

Simulation studies are useful for determining the implications of available data and mis-specified stock structure on accuracy of spatial models (Kerr and Goethel, 2013). Simulation analyses develop operating models that represent "real world" conditions by simulating data based on initialized conditions, process dynamics, and observation error (Goethel et al., 2015; Kerr and Goethel, 2013). Operating models are then used to test assessment models by comparing assessment model estimates to the simulated truth generated by the operating models (Goethel et al., 2015; Kerr and Goethel, 2013). For example, simulation studies for Atlantic herring *Clupea harengus* showed that ignoring stock structure in population models

can lead to an underestimation of stock decline or an overestimation of the probability of recovery (Kell et al., 2009). Additionally, adding stock composition data for lake whitefish *Coregonus clupeaformis* was shown to reduce bias in estimates of SSB and recruitment (Li et al., 2018). Goethel et al. (2015) found that tagging data were necessary to accurately estimate stock dynamics of Yellowtail flounder *Limanda ferruginea,* even when tagging data had substantial uncertainty. When uncertainties exist in model specification, simulations can be utilized to understand how assumptions impact model estimates (Goethel et al., 2023; Kerr and Goethel, 2013).

A multi-stock, spatially-explicit assessment model was developed for striped bass to estimate abundance and fishing mortality in the Chesapeake Bay and along the Atlantic coast (Chapter 2). This spatially-explicit model, as well the assessment model currently used to inform management decisions, relies on data that has little information on the relative contribution of each spawning population to the fishery or each survey. Therefore, an important question is to determine the effect of alternative amounts and types of stock composition data on spatial assessment model performance. Furthermore, a compounding problem is that many fisheries-independent data sources used for the striped bass stock assessment rely on scale-aged fish to inform age composition. Scale ages commonly overestimate ages of striped bass under age-8 and underestimate fish that are above age-8 (Liao et al., 2013), providing statistically different underestimates for ages above 11 years old (Secor et al., 1995). Further, otoliths provide more accurate age estimates for striped bass than scales (Liao et al., 2013). Previous studies have demonstrated different perceived patterns in length- and weight-at-age of otolith-aged relative to scale-aged

striped bass (Schiano, 2022). Because the oldest age class in the spatially-explicit model and models used for management is 15+ and age composition primarily is determined by scale-aged fish, aging error could potentially create bias in model estimates.

Our goal was to evaluate the accuracy of spatially-explicit multi-stock and spatially-aggregated single stock assessment models for striped bass under alternative scenarios of data availability and quality. Additionally, we determined whether the performance of a multi-stock, spatially-explicit model was improved with increased stock composition data. We also investigated the effect of aging error on model accuracy.

3.3 Methods

We evaluated model performance of five estimation models under alternative scenarios of data quality and spatial complexity. A spatially-explicit operating model was developed to approximate striped bass dynamics in the Chesapeake Bay and along the Atlantic coast during 1990-2017. The operating model considered two spawning stocks and two regions. Datasets were generated with observation error from the operating model. The five estimation models were either spatially-explicit (SE) or spatially-implicit fleets-as-areas. Each estimation model differed in its assumed stock structure, assumptions of movement and recruitment, and whether aging error was accounted for in fishery age composition data. The simplest assessment model was built to match the current striped bass stock assessment (Northeast Fisheries Science Center, 2019), which is a spatially-implicit statistical catch-at-age model with FAA (FAA1). This FAA model assumed a single stock and a

single region. Thus, it does not account for movement or stock structure (Goethel et al., 2023; Punt et al., 2016). However, FAA models implicitly represent spatial structure through the use of fishery fleets for different regions by estimating region-specific fishery selectivity patterns. The SE models assumed two stocks and two regions. Estimates of abundance, fishing mortality, and reference points that describes the fishing mortality rate that achieves a specific spawning potential ratio from each estimation model were compared to the true simulated values to determine model accuracy. The simulated datasets represented a 30-year period. For each set of operating model assumptions, 500 simulations were run.

3.3.1 Operating Model

Striped bass data were simulated using an operating model to represent the true dynamics of the system and generate datasets of total catch, catch proportions-at-age, fisheries-independent survey catch, and survey age-proportions. The operating model included age-specific processes, such as natural mortality and selectivity, that were similar to those from the most recent stock assessment (Northeast Fisheries Science Center, 2019). Additionally, the operating model assumed two stocks, two regions, and assumed movement and biological processes occur in two sub-annual time-steps. The operating model was written in R (R Core Team, 2020).

Population dynamics in the operating model closely followed the multi-stock, spatially-explicit model described in Chapter 2 and used parameter estimates from Chapter 2 to generate datasets to test the performance of alternative assessment models. The operating model generated 30-year time series that were similar to the striped bass population dynamics estimated during 1990-2017 from Chapter 2.

Variable definitions are in Table 3.1, and model equations are in Table 3.2. Initial abundance-at-age by stock was calculated assuming each stock was in equilibrium in the first year (Eq. 3.2.1). Median recruitment for each stock was based on estimated recruitment for each stock (Chesapeake Bay and Atlantic coast) from Chapter 2 (Table 3.1). Annual recruitment was then calculated with log-normal deviations from the median recruitment (Eq. 3.2.2) with a standard deviation that was estimated for each stock from Chapter 2 (Table 1, Eq. 3.2.3). Fishing mortality (Feq) in the first year was assumed to be similar for each stock (Eq. 3.2.4) and the equilibrium fishing mortality for fully selected ages was set to 0.2 (Table 3.1). Equilibrium selectivity for each stock was assumed to be a logistic function (Eq. 3.2.5). Total abundance-at-age in the first subannual time step was calculated using an exponential mortality model summed over regions (Eq. 3.2.6-3.2.7), and the plus group included all fish age 15 and older (Eq. 3.2.8-3.2.9). Movement was calculated to occur after mortality at each 6-month time-step based on the estimates of occupancy probabilities for each stock during each time-step from Chapter 2 (Eq. 3.2.10).

Total instantaneous mortality for each region, year, and time-step was calculated by adding natural mortality for each age to the instantaneous fishing mortality-at-age for each region, year, and time-step (Eq. 3.2.11). Average fishing mortality for each region and time-step was set to the average mortality estimated from Chapter 2 during 1990-2017. Instantaneous fishing mortality rates for each region and time-step (Eq. 3.2.12) were the product of selectivity, the fishing intensity, and log-normal deviations for each region and time-step that were derived from the estimated fishing mortality rates in Chapter 2. Fishery selectivity was specified as

logistic (Eq. 3.2.13) in the Ocean region and double logistic (Eq. 3.2.14) in the Chesapeake Bay region, and the selectivity patterns were assumed to be constant over time and time-steps. The fishery selectivity parameters were based on estimates from Chapter 2 but were simplified to reduce operating model complexity. The operating model assumed that one multi-age (1-15+) fishery-independent survey was conducted in each region for each time-step, for a total of four surveys conducted each year. Logistic functions were specified for surveys in the Chesapeake Bay surveys and double logistic functions were used for surveys in the Ocean region. Constant catchability was assumed for each survey based on catchability estimated for a fishery-independent survey in the Chapter 2 (Table 3.1). Age-specific natural mortality was assumed to be the same for each time-step and region and was the same assumption made in Chapter 2 as well as the annual rate used in the current benchmark assessment (Table 3.1, Northeast Fisheries Science Center, 2019). Spawning stock biomass was calculated as the product of abundance for each stock in a time-step, the proportion female-at-age, the proportion mature-at-age, and the weight-at-age assumed for spawners (Eq. 3.2.15). We used the same values as the current benchmark assessment (Northeast Fisheries Science Center, 2019) for maturity-at-age and proportion female-at-age, that were constant for all years. Additionally, we used a 30-year time-series of mean weight-at-age for 1987-2017 from the benchmark assessment in our operating model (Table S3.1).

We calculated the true values of fishing mortality reference points from the operating model using the spawning potential ratio (SPR) based on a rescaled version of the methods used in the Woods Hole Assessment Model (Miller, 2023). SPR was

calculated as the weighted average SSB per recruit in the fished condition across stocks divided by weighted average SSB per recruit in the unfished conditions. Full descriptions of the equilibrium model to calculate reference points are found in the Supplemental Material 3.8.1.

3.3.2 Data Generation

Datasets were generated from the operating model by applying random observation errors to the true simulated values to match typical data sources used in statistical catch-at-age models. Simulated data for each of the five assessment models included catch per fleet in each region, proportions of catch-at-age for each fleet, age composition from each fleet, and indices of abundance and age composition for each of the fisheries-independent surveys. Datasets were initially created for two stocks, two spatial regions, and for 6-month time-steps. Next, datasets were then aggregated over time, stocks, and/or regions to match the data structure of each assessment model. Detailed calculations and descriptions for each dataset used in the five estimation models can be found in the Supplemental Material 3.8.2.

Fishery catch-at-age was calculated for each stock, time-step, and region using the Baranov catch equation (Eq. 3.2.16). To understand the effect of aging error on model estimates, catch-at-age for the fishery and multi-age surveys for all models were simulated with aging error to match scale-aged patterns (Eq. 3.2.17). Observed proportions-at-age were generated for the fishery by applying an aging error matrix (Table S3.2) based on assignment probabilities of scale-aged fish relative to otolith-aged fish (Chapter 2, Eq. 3.2.17). Total catch was calculated as the sum of catch-at-age across ages for each stock, region, and time-step (Eq. 3.2.18). Observed catch

proportions-at-age for the fishery were calculated as the number of fish caught in an age class, divided by the total number of fish caught that year for each stock, region, and time-step (Eq. 3.2.19).

The fishery-independent survey for each region and time-step were assumed to be conducted at the beginning of each time-step (i.e., January 1 or July 1). True survey catch-at-age was calculated based on the abundance of each stock in the corresponding time-step and region, catchability, and selectivity (Eq. 3.2.20). Observed survey catch-at-age with aging error was found by applying the aging error matrix to the true survey catch-at-age (Eq. 3.2.21). Stock specific indices of abundance for each survey were then found by summing the observed survey catch-at-age with aging error across ages (Eq. 3.2.22). Observed catch and the survey indices of abundance included a log-normal observation error (Table 3.3).

For each dataset, the log-scale standard deviations and effective sample sizes for observation error were based on the values assumed in Chapter 2 (Table 3.3). Log-normal observation error with a log-scale standard deviation of 0.2 was assumed to generate total catch for each stock, region, time-step, and year (Eq. 3.2.26). Log-normal observation error with a log-scale standard deviation of 0.4 was used to generate the indices of abundance for each fishery-independent survey (Eq. 3.2.27). Multinomially distributed samples were drawn to produce the observed fishery catch-at-age based on the true proportions-at-age and an ESS. The ESS was calculated based on the observed proportions of striped bass from a given stock in a region during a specific time-step such that the ESS summed to 100 for each region and year (Eq. 3.2.28). Multinomial observation error was assumed to calculate the catch-at-age

in the fishery-independent surveys and was controlled by a weighted ESS that summed to 100 for each region and year (Eq. 3.2.29). Log-normal observation error with a log-scale standard deviation of 0.5 was assumed to generate the indices of abundance for the age-1 and young-of-the-year surveys.

For the SE models, fishery and survey datasets were generated for each region, stock, and 6-month time-step. The FAA models represented the population as a single stock within one region with two "regional" fleets and four multi-age surveys on an annual time step. Therefore, for the FAA models, observed survey catch-at-age datasets were aggregated over subannual time-steps to match the annual time step of the FAA model. Similarly, observed fishery catch and proportions-at-age remained disaggregated by regions with each region representing a fleet. The same data from the surveys were used in the FAA and SE models. However, in the FAA models, data from the surveys were assumed to represent annual changes in abundance and recruitment of both stocks combined.

The effect of increased stock composition data (i.e., proportion of each stock in the fishery catch or survey) was evaluated by comparing spatially-explicit models with different types of stock information. Datasets for two SE estimation models (SE1 and SE2, Table 3.4) were generated without stock composition data in the fisheries or surveys. The stock-aggregated datasets were generated by summing stock-specific datasets over stocks. For example, the index of abundance for each survey was aggregated over the Chesapeake Bay stock and the Atlantic coast stocks to provide a single index of abundance for each spatial region and time-step. Datasets for a SE model with increased stock composition data (SE3, Table 3.4) included

disaggregated stock structure for the last 10 years of the time series for fishery catch, fishery catch proportions-at-age, the multi-age indices of abundance, and the proportions-at-age for the multi-age surveys, where the first 20 years had no stock composition data available.

3.3.3 Estimation Models

Five assessment models were evaluated under each data generating scenario (Table 3.4). The first model was an FAA model with two fleets that resembled the current assessment model used to inform management (FAA1). The two fleets for the FAA model were the Chesapeake Bay fleet and the Ocean fleet. FAA1 assumed a single region, a single unit stock, and annual time-steps. FAA1 did not correct for aging error. The second model was an FAA model that corrected for aging error (FAA2). The third model was a multi-stock, SE population model that assumed two spatial regions, two stocks, and two 6-month time-steps (SE1). However, the SE1 model did not correct for aging error. The fourth model was an SE model similar to SE1, but it corrected for aging error (SE2). SE1 and SE2 also included informative priors on the occupancy probabilities based on tagging data (Chapter 2). The fifth model was an SE model that incorporated additional data on stock composition for the last ten years and included aging error (SE3), but it did not include informative priors on the occupancy probabilities.

The five assessment models estimated abundance, spawning stock biomass, and fishing mortality. Each model was a statistical catch-at-age model that tracked cohorts through time, with spatially-implicit (FAA) or SE assumptions. Fishing mortality and selectivity were estimated for each fleet (Ocean and Chesapeake Bay).

All estimation models were coded in ADMB (Fournier et al., 2012). The two FAA models estimated abundance, fishing mortality rates, and spawning stock biomass assuming a single coastwide stock in a single area with an annual time step. The three SE models estimated abundance and spawning stock biomass for each region, stock, and 6-month time-step. Recruitment was estimated for each stock in the first time-step of each year. Fishing mortality was estimated for each region and time-step. Fishery selectivity was estimated for each region, time-step, and for two 15-year time-blocks. Finally, the SE models estimated occupancy probabilities for each stock in each region and time-step using informative priors from the results of Chapter 2 for SE1 and SE2. SE3 did not include a prior on the occupancy probabilities. For the three SE models, fishery catch, indices of abundance, and proportions-at-age were estimated with similar equations and dynamics defined in the operating model (Table 3.2). For the three models that corrected for aging error (FAA2, SE2, SE3), an aging error matrix was applied to catch-at-age for the fishery dependent and independent data sources (Eqs. 3.2.17, 3.2.21).

The dynamics equations for the FAA model (e.g., abundance-at-age) were the same as the equations defined in Table 3.2, but occurred in one region, over one annual time-step, and for one stock (Table 3.5). Abundance was calculated as the abundance in the previous year and age class multiplied by exponential total mortality (Eq. 3.5.1-3.5.2). Fishing mortality for the FAA models varied over time by fleet based on fleet-specific estimates of fishery selectivity. Fishery selectivity was estimated over time for two 15-year selectivity time-blocks, to reflect a simplified version of changes to fishery selectivity over time in Chapter 2. Fleet-specific fishing

mortality was estimated as the product of selectivity-at-age and for a given fleet and the fully recruited fishing mortality for a year. Total fishing mortality was then estimated as the instantaneous fishing mortality rates summed over fleets (Eq. 3.5.3) based on double logistic selectivity functions for both fleets (Eq. 3.5.4). Instantaneous total mortality rates were calculated as the sum of the age-specific instantaneous natural mortality and the total instantaneous fishing mortality rates (Eq. 3.5.5). Movement was not estimated in the FAA models. The remaining FAA functions can be found in Table 3.5.

Each estimation model estimated parameters by minimizing the sum of the negative log likelihood function for each data source (Eq. 3.6.1; e.g., total catch, catch proportions-at-age). The components of the negative log likelihood function for the estimation models are described in Table 3.6. The assumed distributions were the same as those used to generate the data. The prior for the estimated occupancy probabilities (Eq. 3.6.6) were only used in the SE1 and SE2 models. The log-scale standard deviations and ESSs were assumed the same as was used to generate the data for each estimation model. Datasets for each estimation model that were fit in the likelihood functions are described in Table 3.7.

Fishing mortality rate reference points were estimated for each model to determine how management advice may be affected by using different assessment models. The estimated fishing mortality rates expected to achieve 40% SPR ($F_{40\%}$) were estimated using an equilibrium model in each estimation model. For the SE models, SPR was calculated in a similar manner as in the operating model (Supplemental Material 3.8.1). For the FAA models, SPR was calculated for a single

stock and region. Full descriptions of the equilibrium model for the SE and FAA models are found in Supplemental Material 3.8.1.

3.3.4 Estimation Model Performance

We characterized estimation model bias and accuracy for important estimates for management (e.g., fishing mortality in the terminal year) from each assessment model to determine model performance. Bias and accuracy were calculated for each estimated time series of abundance, biomass, fishing mortality, and $F_{40\%}$, when applicable. Bias is defined as the difference between an estimated value and the expected value. Accuracy is defined by how close a set of estimated values are to the expected value. Abundance estimates were compared based on January 1 estimates. Therefore, for the SE models, abundance in the first time-step was used and summed across stocks to compare to FAA estimates. Fishing mortality rates were compared based on total annual estimates for each age. For the SE models, estimates of annual instantaneous fishing mortality at age experienced by the total population were the weighted average fishing mortality rate-at-age weighted by the proportion of fish from each stock in a given region. Weighted fishing mortality for each age was then summed across time-steps and regions to calculate an annual estimate of F for each age (Eq. 3.2.26) that was compared to annual estimates of fishing mortality in the FAA models that were summed over fleets (Eq. 3.5.3).

Relative error (RE) was used to describe the bias of estimation models and was calculated by dividing the difference between the estimated parameter and the true value by the true value,

$$RE = \frac{\hat{X} - X}{X} \tag{3.1}$$

where $\hat{X}$ was the estimated value and X was the true value for each metric. Model accuracy was characterized by the root mean square relative error (RMSRE),

$$RMSRE = \sqrt{\frac{\sum_1^n RE^2}{n}} \tag{3.2}$$

where n is the total number of simulations that converged. For all estimation models, a convergence criterion of 0.01 was set, where if final model estimates had a maximum gradient component greater than or equal to 0.01, they were removed from further analysis. Exploratory analyses were also conducted to further understand the performance of the FAA models under each scenario.

3.4 Results

Estimation models performed relatively well for all scenarios based on model convergence, but they differed in their ability to estimate abundance, fishing mortality, and $F_{40\%}$. All models had greater than 99% convergence based on the maximum gradient component threshold. FAA1, FAA2, and SE1 had all 500 models converge. Both SE2 and SE3 had 498 out of 500 models meet the gradient threshold.

The two FAA models produced biased estimates of abundance in the terminal year, but the bias was negative for FAA1 (median relative error (MRE)= -0.393) and positive for FAA2 (MRE=0.483; Figure 3.1; Table 3.8). SE1 produced negatively biased estimates of abundance that were similar to those of FAA1 (MRE=-0.515). The two SE models that corrected for aging error in data sources, SE2 and SE3, had approximately unbiased estimates of abundance ($|MRE| < 0.02$; Figure 3.1). For

stock-specific abundance, SE1 produced negatively biased estimates of abundance, particularly for the Atlantic coast stock for all years ($MRE > 0.75$). SE2 estimated abundance of the Chesapeake Bay stock with slight positive bias and was approximately unbiased for the Atlantic coast stock (Figure 3.1). SE3 estimated stock-specific abundance with little bias for both stocks, although it had slightly positively biased estimates of Chesapeake Bay stock abundance (MRE = 0.051) and negatively biased estimates of Atlantic coast abundance (MRE = -0.061). SE2 and SE3 produced slightly biased estimates of reference points in the terminal year (Figure 3.1).

Patterns of bias in estimates of fishing mortality at age-8 (F-8) were similar to those of abundance, but they generally had the opposite sign. FAA1 produced the most biased estimates of F-8 (MRE=1.408; Figure 3.1), and FAA2 estimated F-8 with a negative bias (MRE=-0.268). SE1 estimated F-8 with similar bias to FAA1 (Figure 1). SE2 and SE3 provided unbiased estimates of F-8 with SE2 provided the least biased estimates (MRE= -0.001), followed by SE3 (MRE= -0.012). Both FAA models, FAA1 and FAA2, produced positively biased estimates of $F40\%$ ($MRE >$ 0.088; Figure 3.1). The SE1 model that did not assume aging error (SE1), provided the least biased estimates of the $F_{40\%}$ reference point with an MRE of -0.12 (Figure 3.1, Table 3.8). However, the three spatially-explicit models, SE1, SE2, and SE3, provided similar estimates of reference points for both stocks combined (Figure 3.1). These models also estimated stock specific reference points for the Chesapeake Bay stock with more accuracy and less bias than the Atlantic coast stock (Figure 3.1), although estimates were similar for all three models. For SE1, the MRE of $F_{40\%}$ was

0.062 for the Chesapeake Bay stock and 0.135 for the Atlantic Coast stock. For SE2, MRE of $F_{40\%}$ was -0.124 for the Chesapeake Bay stock and -0.163 for the Atlantic coast stock. For SE3, MRE of $F_{40\%}$ was -0.109 for the Chesapeake Bay stock and -0.160 for the Atlantic coast stock. Estimates of stock specific reference points were not estimated for the FAA models.

Model estimates of accuracy followed similar patterns to that of bias (Figure 3.1). For abundance, the two models that ignored aging error, FAA1 and SE1 performed similarly with relatively inaccurate estimates ($RMSRE$ > 0.35). FAA2 produced the most inaccurate estimates of abundance ($RMSRE$ = 0.617). SE2 and SE3 had similar accuracy, with SE2 providing the most accurate estimates ($RMSRE$ = 0.1). FAA1 and SE1 produced the most inaccurate fishing mortality estimates in terminal year (Figure 3.1). FAA1 had a $RMSRE$ 1.346 and SE1 had a $RMSRE$ of 1.434 (Table 3.8). SE2 was the most accurate model for estimating fishing mortality at age-8, with a $RMSRE$ of 0.153, and SE3 had a slightly higher $RMSRE$ than SE2 (Table 3.8). Accuracy of $F_{40\%}$ was similar to those of bias. FAA1 produced the least accurate estimates of $F_{40\%}$ ($RMSRE$ >1.14) though estimates from FAA2 were also inaccurate reference points ($RMSRE$ =0.889, Table 3.8). SE1 provided the most accurate estimates of $F_{40\%}$ ($RMSRE$ = 0.12). SE2 and SE3 performed similarly to each other, with slightly less accuracy than SE1 (Table 3.8).

Estimates of relative error of abundance for all years were similar to those in the terminal year (Figure 3.2). Estimates of MRE were variable for each year for FAA1, though every year produced negatively biased estimates (Figure 3.2). For FAA2, estimates of MRE were similar year-to year, but were all positively biased.

SE1 produced similar estimates of MRE every year to FAA1. SE2 and SE3 provided the least biased estimates of abundance across all years compared to the other models (Figure 3.2). Estimates of SSB from each estimation model had similar patterns of relative error over time as abundance (Figure 3.3), with generally higher bias for all models. FAA1 and SE1 produced negatively biased estimates of SSB (MRE <-0.5). FAA2 produced positively biased estimates of SSB, that increased slightly over time (Figure 3.4). SE2 and SE3 performed similarly and were approximately unbiased (MRE >0.03 in the terminal year). Bias of F-8 was mostly similar over time for each model. FAA1 produced positively biased estimates of F-8 which decreased from year 7 to year 26 (Figure 3.4). FAA2 provided negatively biased estimates of fishing mortality at age-8 for all years. However, FAA2 estimated less biased fishing mortality rates compared to FAA1 (Figure 3.1, 3.4).

Accuracy and bias of estimated fishing mortality at age varied across estimation models (Figure 3.5). FAA1 and SE1 had positively biased estimates of fishing mortality at age that tended to increase with age. For FAA1, MRE increased from 0.173 at age-1 to 1.374 at age-15. For SE1, MRE of F increased from 1.081 at age-1 to 1.791 at age-15. FAA2 created negatively biases estimates of fishing mortality for all ages (Figure 3.5). SE2 and SE3 estimated unbiased fishing mortality for each age class (Figure 3.5). Estimated fishing mortality rates in SE2 and SE3 were relatively unbiased, but the bias increased with increasing age to a maximum MRE of -0.049 at age 15 for SE2 and -0.047 at age 15 for SE3.

3.5 Discussion

Our study demonstrated how multi-stock, spatially-explicit stock assessment models can improve accuracy of estimates of abundance, fishing mortality, and reference points for multi-population stocks with migration and spatially-varying fishing mortality rates like striped bass. Our results suggest that including spatial and stock structure in assessments to match spatial dynamics in fish populations may provide more accurate estimates in abundance and fishing mortality when potential aging bias in data is corrected, which is similar to other studies that found increasing spatial complexity in assessment models to match the complexity in fish populations can reduce bias in estimates of fishing mortality and spawning stock biomass (Goethel et al., 2015; Guan et al., 2013; Li et al., 2018; Taylor et al., 2011; Ying et al., 2011). Additionally, correctly accounting for aging error in data inputs was extremely important for obtaining unbiased estimates of abundance, SSB, and fishing mortality. Our results are similar to those that suggest incorporating aging error matrices to correct for potential aging bias can improve model outputs (Henríquez et al., 2016; Hulson and Williams, 2024).

Spatially-implicit FAA models produced highly biased estimates of abundance, fishing mortality rates, and $F_{40\%}$ reference points in our study. For example, the FAA2 model had the highest bias in estimated abundance and SSB. However, the FAA2 model estimated fishing mortality with less bias than the FAA1 and SE1 models that also did not include corrections for aging error. When fishing mortality in the operating model was the same across regions and time-steps, the FAA2 model provided unbiased estimates of abundance and fishing mortality.

Differences in fishing mortality rates between regions and time-steps resulted in increasingly biased estimates of abundance and SSB. Other studies have found FAA or spatially-aggregated approaches to be inappropriate when spatially-varying fishing mortality exists (Pincin and Wilberg, 2012; Punt et al., 2015). Punt et al. (2015) recommended that FAA models only be used with extreme caution, particularly in instances with varying age structure across regions. However, Lee et al. (2016) suggests FAA could be appropriate to estimate time-varying selectivity, particularly when other data to inform movement (e.g., tagging) are unavailable. While FAA models may be appropriate for fisheries with little spatial heterogeneity, our results suggest that they were quite sensitive to spatial and temporal patterns of fishing in the operating model.

Estimation of the occupancy probabilities for each of the spatially-explicit models required stock composition information. The SE3 model estimated the occupancy probability parameters using stock composition data in the last 10 years of the time series. It produced unbiased estimates of abundance, SSB, and fishing mortality, but had lower accuracy in the terminal year and over time compared to the SE2 model that had high-quality informative priors on the occupancy probability parameters. The SE3 model performed similarly to the SE2 models without increased stock data, suggesting including stock composition data in the fishery catch and surveys may not be necessary if accurate informative priors for these parameters are available. However, the SE2 model relied on tagging data for striped bass by using the output informed by a mark-recapture model as informative priors to inform movement rates, which were centered on the true values. In contrast, the SE3 model

did not require informative priors on occupancy probabilities to estimate accurate estimates of abundance and fishing mortality. Other studies have suggested that tagging information is required to estimate movement, particularly for species that exhibit natal homing (Berger et al., 2016; Goethel et al., 2011; Vincent et al., 2016). However, the performance of SE3 suggests tagging data may not be necessary to inform movement, if there is adequate information of stock composition in the fishery and fishery-independent surveys.

Ignoring stock structure in assessments can have negative consequences for management (Goethel and Berger, 2016; Kell et al., 2009; Kerr and Goethel, 2013; Ying et al., 2011). Kell et al., (2009) found that combining mixed-stock fisheries could lead to overexploitation of stocks. Ying et al., (2011) found that modeling yellow croaker *Larimichthys polyactis* with spatial population structure as a single unit may lead to local depletion. Our findings of biased estimates of abundance and reference points for FAA models also agree with these studies as the FAA models overestimated the reference points for striped bass which would imply a higher fishing mortality than the stock complex could sustain. However, we did not evaluate projections or forecasting of stock status and therefore the potential impacts of fishing mortality rates may not be fully described. Currently, data used for stock assessment of striped bass have limited stock composition information (Chapter 2; Northeast Fisheries Science Center, 2019). However, stock-specific movement rates (Schonfeld, 2023; Secor et al., 2020) and stock composition of fishery catch (Hasegawa et al., 2022; Kneebone et al., 2014) can be used to inform assessment estimates. For example, Chapter 2 incorporated stock composition estimates from literature with a

binomial prior that was used to inform the proportion of each stock of striped bass in the catch in the ocean region. When available, stock composition data should be collected and included in assessment modeling. When these data are unavailable, estimates from literature can be used as informative priors to estimate stock specific catch, movement, or abundance.

Aging error can cause substantial bias in estimates from age-structured stock assessment models (Henríquez et al., 2016; Liao et al., 2013). Patterns of error in models that ignored aging error (FAA1 and SE1) were similar in that they both had similar patterns of negative bias of abundance and positive bias of fishing mortality. Bias in fishing mortality tended to increase with age for these models, likely due to mis-representation of older ages of striped bass as younger (Liao et al., 2013; Secor et al., 1995). Correcting for aging error and bias in fisheries dependent and independent age compositions produced reduced bias and improved accuracy of spatial models, but our non-spatial model (FAA2) still showed substantial bias. The effect on estimation of $F_{40\%}$ was, however, less clear. The FAA1 model provided the most biased $F_{40\%}$ estimates, while the SE1 provided the least biased $F_{40\%}$ estimates. However, the performance of SE1 was largely driven by incorrect estimates of the proportion of recruitment for each stock and incorrect estimates of fishing mortality that coincidentally offset each other. While the stock specific estimates of $F_{40\%}$ were positively biased for the Chesapeake Bay and Atlantic coast stocks for SE1, when they were averaged by the incorrect average recruitment, they produced estimates of a total $F_{40\%}$ that were negatively biased. Aging error is present in age composition data sources and has been demonstrated to influence the striped bass stock assessment

(Liao et al., 2013). To improve data quality used for the striped bass stock assessment, age composition data from fisheries dependent and independent data should ideally be informed by otolith ages. When otolith-informed ages are not available, aging error matrices can be included to correct for aging error (Dorval et al., 2013; Henríquez et al., 2016; Methot and Wetzel, 2013). Additionally, if FAA models are to be used in stock assessment, it is important that any potential aging bias in the age composition data is addressed within the estimation model.

Estimates of SSB were the most inaccurate estimates for all models. While the spatially-explicit models that corrected for aging error (SE2 and SE3) estimated these with the least bias, they struggled to accurately estimate SSB for most simulations. One likely contributor of this inaccuracy in SSB is the estimation of the plus group as a result of dome-shaped selectivity parameters being poorly estimated. Estimates of selectivity parameters for the descending limb of dome shaped selectivity for the Chesapeake Bay fishery was consistently poorly estimated. For example, the inflection point of the descending limb was often estimated to be smaller than the inflection point of the ascending limb of the double logistic selectivity function. Complex selectivity curves with increased numbers of parameters have the potential to be highly correlated (Hulson and Hanselman, 2014). Additionally, the use of double logistic selectivity functions further suggest that older striped bass are not fully vulnerable to the fishery or surveys. Our operating model assumed a logistic selectivity function for the Ocean fishery for both time-steps, but double logistic selectivity in the Chesapeake Bay, based on the results and assumptions from Chapter 2. Incorrect assumptions about selectivity can have a large effect on output from

statistical catch-at-age models (Linton and Bence, 2011). Despite starting the parameters at reasonable estimates, these parameters were poorly estimated due to correlation. Complex selectivity curves may benefit from additional penalties (as done in Chapter 2) to prevent correlation and estimates from being unreasonable.

In this study, we made simplifying assumptions in the operating model to represent "true" striped bass population dynamics. For example, we assumed movement occurred only at the beginning of 6-month time-steps (Schonfeld, 2023). Striped bass have complex migration patterns that vary by stock, age, sex, and season (Grothues et al., 2009; Secor et al., 2020). The use of occupancy probabilities in the operating model allowed for a simplification of movement dynamics, where each stock is randomly distributed into different regions at each time-step that is constant over years (Punt, 2017). Typically, spatial fisheries models represent migration differently (e.g., box transfer method, Goethel et al., 2015). The operating model also assumed only two spawning stocks, although more stocks likely exist (Fabrizio, 1987; Hasegawa et al., 2022; Kneebone et al., 2014; Wirgin et al., 1993). Further, natural mortality for each age was assumed to remain constant over time and across regions, although studies suggest natural mortality has been increasing over time in the Chesapeake Bay (Schonfeld, 2023; Secor et al., 2020). Although the dynamics in the operating model exactly matched the spatial complexity of our three spatially-explicit estimation models (SE1, SE2, SE3), it is unlikely that these assumptions were the main drivers of the results we observed. However, by assuming similar structure in the operating and estimation models, we reduce the ability to accurately model the complexities of the true striped bass dynamics, so we could be overlooking possible

modeling concerns that are present when there is still a mis-match between reality and the estimation model assumptions. Model accuracy will likely be lower for real-world applications. Overall, the performance of multi-stock, spatially-explicit models in this study suggest these models are better suited to estimate abundance and fishing mortality for highly migratory species with spatially varying mortality.

Fishing mortality rates are distilled down to a single value for use in management decisions, requiring spatially-explicit models to summarize fishing mortality rates over space and time. However, many approaches that combine sub-annual and spatially-explicit fishing mortality rates, estimate biased fishing mortality for a single value (Langseth and Schueller, 2016), which can lead to misdiagnosis of stock status (Guan et al., 2013). Our results suggest similar issues when generating a singular fishing mortality reference point, as the spatially-explicit models estimated reference points with a negative bias. Our results indicate that stock-specific reference points were less biased for the Chesapeake Bay stock than the Atlantic coast stock. Based on the data used to develop the operating model (Chapter 2), striped bass from the Chesapeake Bay stock are abundant in both regions, comprising a significant portion of catch in each region and time-step. However, the Atlantic coast stock was not abundant in the Chesapeake Bay region for either time-step, resulting in limited age composition data for the fishery and surveys. Therefore, the bias in stock-specific reference points for both stocks may be a result of limited data availability for the Atlantic coast stock across all regions.

We tested multiple stock assessment models with two levels of spatial complexity, stock composition, and intra-annual time-steps that also had some

differences in data inputs. In our study, multi-stock, spatially-explicit models that accounted for aging error had substantially better accuracy than spatially-implicit models or those that did not account for aging error across most performance metrics. Other studies have found that spatially-explicit models reduce bias in model estimates (Punt et al., 2015). While our operating model was specified to represent striped bass, the conclusions likely apply to other highly migratory, moderately long-lived species. Prior to developing spatially-explicit assessment models, a review of all potential data available should be explored. Additionally, simulation analysis should be considered for new spatially-explicit models, to understand model performance (Kerr and Goethel, 2013). However, our study demonstrated that spatially-explicit models improved the accuracy of important stock assessment metrics, which has been documented in other studies (Goethel and Berger, 2016; Guan et al., 2013; Punt 2019; Punt et al., 2015; Ying et al., 2011). Multi-stock assessment models are still relatively rare (Punt, 2019b). Increasing collection of stock composition data for fisheries and surveys is likely necessary to allow for development of more multi-stock models for species with limited tagging studies.

3.6 Acknowledgements

I would like to thank A. Schueller and M.J. Wilberg for their collaboration on this chapter. Funding for this study was provided by NOAA and Sea Grant. We thank G. Nesslage, D. Secor, and R. Latour for their guidance on developing objectives and methods. We thank K. Drew and G. Nelson for their guidance on methods development for the spatially-explicit models.

3.7 Funding Statement

This research was supported by Sea Grant and the National Marine Fisheries Service Population and Ecosystem Dynamics Fellowship (grant number NA21OAR4170244) and the NOAA Chesapeake Bay Office (grant number NA19OAR4320074).

3.8 Supplemental Material

3.8.1 Biological Reference Points

Biological reference points were calculated as the fishing mortality rate ($F_{40\%}$) that achieves 40% spawning potential ratio (SPR) based on modified methods used in the Woods Hole Assessment Model (Miller, 2023). In the operating model used to develop datasets for striped bass, $F_{40\%}$ was calculated in an equilibrium model. Equilibrium recruitment was set to the relative contribution of recruits for each stock to the total population based on the average recruitment of the operating model ($R_{s=1} = 0.71, R_{s=2} = 0.29$). Equilibrium fishing mortality (eqF) for each region r, time-step ts, and age a, was set to the fishing mortality in the last year of the operating model (year 30). Total fishing mortality for each region, time-step and age, V, was calculated as

$$V_{r,ts,a} = \frac{eqF_{r,ts,a}}{\max\left(tF_{a}\right)}, \quad \text{(S3.1.1)}$$

where tF_a is the total fishing mortality at age,

$$tF_a = \sum_{r,ts} eqF_{r,ts,a}. \quad \text{(S3.1.2)}$$

The relative fishing mortality rate, F^* , was then found by

$$F^*_{r,ts,a} = G \times V_{r,ts,a}, \quad \text{(S3.1.3)}$$

where G is a scaler used to find the relative fishing mortality. Total equilibrium mortality was calculated as

$$Zeq_{r,ts,a} = F^*_{r,ts,a} + (0.5 \times M_a), \quad \text{(S3.1.4)}$$

where M is equal to the natural mortality-at-age used in the operating model (Table 3.1) divided by two to represent 6-month natural mortality. Equilibrium population

dynamics were simulated forward for 100 years and followed population dynamics observed in the operating model (Eq. 3.2.3-3.2.7). Occupancy probabilities were defined by the same dynamics used in the operating model. Recruitment was constant through time. Spawning stock biomass (SSB) was calculated using Equation 3.2.15. SPR for each stock was calculated as SSB in the fished condition during January-June divided by SSB in the unfished condition during January-June,

$$SPR_s = \frac{SSB_{s,y=100,ts=1}}{SSB_{U\,s,y=100,ts=1}}, \quad \text{(S3.1.5)}$$

where SSB_U is SSB in the unfished condition. SSB in the unfished conditions were represented by setting G equal to zero in equation S3.1.3.

To find the appropriate G values for each stock, a function was built to loop over all possible combinations of G from 0 to 1.5. SPR for each stock in the 100th year was calculated for each value of G. Stock specific G was then found using linear interpolation to estimate where SPR was equal to 0.40 for each stock. A single value of G was then found by weighting the stock specific G relative to recruitment,

$$G = \sum_s G_s \times R_s. \quad \text{(S3.1.6)}$$

With this G scaler, true fishing mortality $\bar{F}$ was then calculated by applying total fishing mortality,

$$\overline{F_{r,ts,a}} = G \times V_{r,ts,a}. \quad \text{(S3.1.7)}$$

Stock specific fishing mortality was calculated as by applying the occupancy probability and summing over regions and time-steps,

$$\overline{Fstock_{s,a}} = \sum_{r,ts} \overline{F_{r,ts,a}} \times occ_{s,r,ts,a}. \quad \text{(S3.1.8)}$$

Stock specific $F_{40\%}$ was then set equal to $\overline{Fstock}$, where age-8 was a reference age. Age-8 was set as the reference age because it reflects the age at which most fish are fully recruited in both fisheries, given the selectivity functions. A single $F_{40\%}$, combined across stocks, was found by weighting stock specific $F_{40\%}$ by stock specific recruitment as a proportion of total recruitment.

In the three spatially-explicit assessment models (SE1, SE2, SE3), estimation of biological reference points followed equations S3.1.1- S3.1.7 and were calculated after the final minimization of the objective function in ADMB. For each SE model, equilibrium fishing mortality was set equal to fishing mortality in the last year for each region, time-step, and age.

For the fleets-as-areas models, biological reference points were calculated in a similar way as the spatially-explicit models, but annually for fleets. For these fleets-as-areas models, equilibrium recruitment was set to 1. Equilibrium fishing mortality (eqF) for each fleet f and age a, was set to the fishing mortality in the terminal year of the estimation model. Total fishing mortality for each fleet and age was calculated as

$$V_{f,a} = \frac{eqF_{f,a}}{\max(tF_a)}, \tag{S3.1.9}$$

where tF_a is the total fishing mortality at age,

$$tF_a = \sum_f eqF_{f,a}. \tag{S3.1.10}$$

The relative fleet fishing mortality rate for each fleet and age, F^* , was then found by Eq. S3.1.3. Total equilibrium mortality for each age was calculated as the sum of F^* across fleets and added to annual mortality

$$Zeq_{f,a} = M_a + \sum_f F^*_{f,a}. \quad \text{(S.31.11)}$$

Population dynamics were simulated forward for 100 years and followed population dynamics observed in the estimation model (Eq. 3.2.23-3.2.24). SSB and SPR for the total population in the 100th year was calculated similarly to the spatially-explicit equilibrium model but for a single stock.

G for a single stock was found by looping through a function to test all values of G from 0 to 1.5, similar the spatially-explicit methods. Fishing mortality $\bar{F}$ for each fleet was then calculated by applying total fishing mortality to the G value,

$$\overline{F_{f,a}} = G \times V_{f,a}. \quad \text{(S3.1.12)}$$

$F_{40\%}$ for the terminal year was then found by adding $\bar{F}$ for each fleet for age-8. The relative error could then be calculated and compared across all estimation models.

3.8.2 Detailed Data Generation

Datasets were generated for five assessment models, sampled from the true population with observation error. Datasets for the two FAA models (FAA1 and FAA2) were the same, and datasets for the two SE models with tagging information (SE1 and SE2) were the same. Therefore, datasets are described for either a FAA or SE model. Data for the two FAA models are denoted with the FAA subscript (e.g., Cd_{FAA}) and data for the two SE models with tagging data are denoted with the SE subscript (e.g., Cd_{SE}). Data for the SE model with additional stock composition information (SE3) are specified.

True fishery catch-at-age CAA_T was generated for each stock s, region r, year y, time-step ts, and age a using the Baranov catch equation,

$$CAA_{T\,r,y,ts,a} = \frac{F_{r,y,ts,a}}{Z_{r,y,ts,a}} \times (1 - e^{-Z_{r,y,ts,a}}) \times N_{s,r,y,ts,a}, \quad \text{(S3.2.1)}$$

where F is the instantaneous fishing mortality, Z is the total instantaneous mortality, and N is the abundance. True fishery catch C_T was then calculated for each stock, region, year, and time-step by summing the true catch-at-age across ages

$$C_{T\,s,r,y,ts} = \sum_a CAA_{T\,r,y,ts,a}. \quad \text{(S3.2.2)}$$

Log-normal observation error ε_F with a log-scale standard deviation σ_F of 0.2 was applied to the true fishery catch to generate the total fishery catch datasets Cd_F for each stock, region, year, and time-step,

$$Cd_{F\,s,r,y,ts} = C_{T\,s,r,y,ts} * e^{\varepsilon_F \sim N(0,\sigma_F)}. \quad \text{(S3.2.3)}$$

For the SE models, fishery catch was summed over stocks to generate the appropriate datasets for all years,

$$Cd_{SE_{r,y,ts}} = \sum_s Cd_{F_{s,r,y,ts}}. \quad \text{(S3.2.4)}$$

For the SE3 model with added stock information, data for years 1-20 were set equal to $Cd_{SE_{r,y,ts}}$. However, for the SE3 model, datasets for years 21-30 were equal to $Cd_{F_{s,r,y,ts}}$. For the FAA1 and FAA2 models, fishery catch was summed over stocks and time-steps to generate annual catch for each fishery fleet f,

$$Cd_{FAA_{f,y}} = \sum_{s,ts} Cd_{F_{s,r,y,ts}}, \quad \text{(S3.2.5)}$$

where the two fleets were set equal to the two regions (i.e., f=1 represents the Chesapeake Bay region and f=2 represents the Ocean region).

True fishery proportions-at-age PAA_T were calculated for each stock, region, year, time-step and age by dividing the catch-at-age by the total catch,

$$PAA_{T_{s,r,y,ts,a}} = \frac{CAA_{T_{s,r,y,ts,a}}}{C_{T_{s,r,y,ts}}}. \quad \text{(S3.2.6)}$$

Datasets of fishery proportions-at-age were sampled with multinomial observation error that was controlled by the effective sample size (ESS_C). A weighted effective sample size was calculated so that the total effective sample size for the catch would sum to 100 annually for each region,

$$ESS_{C_{s,r,y,ts}} = 100 * \frac{C_{T_{s,r,y,ts}}}{\sum_{s,ts} C_{T_{s,r,y,ts}}}. \quad \text{(S3.2.7)}$$

Observed fishery catch-at-age, $CAAo$, was then found for each stock, region, year, time-step, and age by applying the weighted ESS to the true proportions-at-age,

$$CAAo_{s,r,y,ts,a} \sim Multi(PAA_{T_{s,r,y,ts,a}}, ESS_{C_{s,r,y,ts}}), \quad \text{(S3.2.8)}$$

where Multi represents observation errors sampled from the multinomial distribution. Observed fishery catch-at-age with aging bias ($CAAs$) were then calculated by applying an aging error matrix ($ageerr$) to redistribute observed striped bass ages to those that may have been observed under scale ages (i),

$$CAAs_{s,r,y,ts,a} = \sum_a ageerr_{a,i} \times CAAo_{s,r,y,ts,a}. \quad \text{(S3.2.9)}$$

Proportions-at-age datasets with scale ages $PAAs$ were generated by dividing the catch-at-age by the total sampled catch,

$$PAAs_{s,r,y,ts,a} = \frac{CAAs_{s,r,y,ts,a}}{\sum_a CAAs_{s,r,y,ts,a}}. \quad \text{(S3.2.10)}$$

For the SE models, proportions-at-age datasets (PAA_{SE}) were generated by summing $CAAs$ across stocks, and dividing the catch-at-age by the total sampled catch,

$$PAA_{SE\,r,y,ts,a} = \frac{\sum_s CAAs_{s,r,y,ts,a}}{\sum_{s,a} CAAs_{s,r,y,ts,a}}. \quad \text{(S3.2.11)}$$

For the SE3 model, proportion-at-age datasets were set equal to PAA_{SE} for years 1-20 and equal to $PAAs$ for years 21-30. If catch-at-age for a stock was observed to be 0 for all ages in a single year (potentially observed for the Atlantic coast stock in the Chesapeake Bay region), it was assumed no data was collected and $PAAs$ was set to -99 for all ages so that it would not be called in the likelihood function. For the FAA models, proportion-at-age datasets (PAA_{FAA}) were generating by summing the CAAs across stocks and time-steps, and dividing by the catch-at-age summed across ages,

$$PAA_{FAA\,f,y,a} = \frac{\sum_{s,ts} CAAs_{s,r,y,ts,a}}{\sum_{s,ts,a} CAAs_{s,r,y,ts,a}}. \quad \text{(S3.2.12)}$$

Datasets were generated for four fishery-independent surveys (n) and fed into FAA and SE models, with one survey occurring in each region for each time-step.

Fishery independent surveys were numbered one through four, such that the first survey ($n = 1$) was conducted in the Chesapeake Bay region ($r = 1$) during January-June ($ts = 1$), the second survey ($n = 2$) was conducted in the Chesapeake Bay region during July-December ($ts = 2$), the third survey ($n = 3$) was conducted in the Ocean region ($r = 2$) during January-June, and the fourth survey ($n = 4$) was conducted in the Ocean region during July-December. True survey catch-at-age for each survey $ICAA_T$ were generated for each stock based on the survey catchability q, survey selectivity $ssel$, and abundance,

$$ICAA_{T_{n,s,y,a}} = \begin{cases} q_{n=1} \times N_{s,r=1,y,ts=1,a} \times ssel_{n=1,a} \\ q_{n=2} \times N_{s,r=1,y,ts=2,a} \times ssel_{n=2,a} \\ q_{n=3} \times N_{s,r=2,y,ts=1,a} \times ssel_{n=3,a} \\ q_{n=4} \times N_{s,r=2,y,ts=2,a} \times ssel_{n=4,a} \end{cases}. \quad \text{(S3.2.13)}$$

The catchability was assumed to be the same for each survey but equal to the catchability estimated for the New Jersey Bottom Trawl survey (Chapter 2). Survey selectivity was assumed to be the same for each survey in the Chesapeake Bay (logistic, Eq. 3.2.13) and the same for the two surveys in the Ocean (double logistic, Eq. 3.2.14). A true index of abundance for each survey I_T was then found for each stock for each survey by summing $ICAA_T$ across ages,

$$I_{T_{n,s,y}} = \sum_a \ ICAA_{T_{n,s,y,a}}. \quad \text{(S3.2.14)}$$

Log-normal observation error ε_I with a log-scale standard deviation σ_I of 0.4 was applied to the true index of abundance for each survey to generate the index of abundance datasets Id_I for each survey, stock, and year,

$$Id_{I_{n,s,y}} = I_{T_{n,s,y}} * e^{\varepsilon_I \sim N(0,\sigma_I)}. \quad \text{(S3.2.15)}$$

For the SE1 and SE2 models, the index of abundance was summed over stocks to generate the index of abundance datasets Id_{SE} for all years,

$$Id_{SE_{n,y}} = \sum_s Id_{I_{n,s,y}}. \quad \text{(S3.2.16)}$$

For the SE3 model with added stock information, data for years 1-20 were set equal to $Id_{SE_{n,y}}$. However, for the SE3 models, data for years 21-30 were equal to $Id_{n,s,y}$. For the FAA models, the indices of abundance were the same as the SE models,

$$Id_{FAA_{n,y}} = Id_{SE_{n,y}}, \quad \text{(S3.2.17)}$$

but were assumed to reflect annual changes for a single stock, rather than temporal and spatial differences.

True survey proportions-at-age $IPAA_T$ were calculated for each survey, stock, year, and age by dividing the true survey catch-at-age by the true index of abundance,

$$IPAA_{T_{s,r,y,ts,a}} = \frac{ICAA_{T_{n,s,y,a}}}{I_{T_{n,s,y}}}. \quad \text{(S3.2.18)}$$

Datasets of survey proportions-at-age were calculated with multinomial observation error that was controlled by the effective sample size ESS_I. The weighted effective sample size was calculated so that the total effective sample size would sum to 100 annually for each region but was relative to the proportion of fish in each region for a stock,

$$ESS_{I_{n,s,y}} = \begin{cases} 100 * \frac{I_{n,s,y}}{\sum_{n,s} I_{n,s,y}}, & n = 1,2 \\ 100 * \frac{I_{n,s,y}}{\sum_{n,s} I_{n,s,y}}, & n = 3,4 \end{cases}. \quad \text{(S3.2.19)}$$

Observed survey catch-at-age $ICAA_O$ was then found for each stock, region, year, time-step, and age by applying the weighted effective sample size by the true proportions-at-age,

$$ICAA_{O\,n,s,y,a} \sim Multi(IPAA_{T\,n.s,y,a}, ESS_{I\,n,s,y}), \tag{S3.2.20}$$

where Multi represents observation errors sampled from the multinomial distribution. Observed survey catch-at-age with aging bias $ICAAs$ was then calculated by applying an aging error matrix to redistribute observed ages to those that may have been observed under scale ages,

$$ICAAs_{n,s,y,a} = \sum_a ageerr_{a,i} \times ICAA_{O\,n,s,y,a}. \tag{S3.2.21}$$

Survey proportions-at-age datasets with scale ages $IPAAs$ were generated by dividing the survey catch-at-age by the total index of abundance,

$$IPAAs_{n,s,y,a} = \frac{ICAAs_{n,s,y,a}}{\sum_a ICAAs_{n,s,y,a}}. \tag{S3.2.22}$$

For the SE models, proportions-at-age datasets ($IPAA_{SE}$) were generated by summing $CAAs$ across stocks, and dividing the catch-at-age by the total sampled catch,

$$IPAA_{SE\,n,y,a} = \frac{\sum_s ICAAs_{n,s,y,a}}{\sum_{s,a} ICAAs_{n,s,y,a}}. \tag{S3.2.23}$$

For the SE3 model, proportion-at-age datasets were set equal to $IPAA_{SE\,n,y,a}$ for years 1-20 and equal to $IPAAs_{n,s,y,a}$ for years 21-30. If survey catch-at-age for a stock was observed to be 0 for all ages in a single year, it was assumed no data were collected and $IPAAs$ was set to -99 for all ages. For the FAA models, the survey proportions-at-age of abundance were the same as the SE models,

$$IPAA_{FAA\,n,y,a} = IPAA_{SE\,n,y,a}, \tag{S3.2.24}$$

but were assumed to reflect annual changes for a single stock rather than represent temporal or spatial changes in abundance.

For the two age-1 surveys, a true index of abundance I_1 was generated by applying a catchability q_1 to the abundance of age-1 fish in each region and time-step,

$$I_{1_{n=1,y}} = q_{1_{n=1}} \times N_{s,r=1,y,ts=2,a=1}; \quad \text{(S3.2.25)}$$

$$I_{1_{n=2,y}} = q_{1_{n=2}} \times N_{s,r=2,y,ts=2,a=1}. \quad \text{(S3.2.26)}$$

The catchability was assumed the same for both surveys and was the estimated value from the New York Age 1 Survey (Chapter 2). Log-normal observation error ε_1 with a log-scale standard deviation σ_1 of 0.5 was applied to the true index of abundance for each age-1 survey to generate the index of abundance datasets Id_1 for each survey and year,

$$Id_{1_{n,y}} = I_{1_{n,y}} \times e^{\varepsilon_1 \sim N(0,\sigma_I)}. \quad \text{(S3.2.27)}$$

Because the operating model assumes all recruits remain in their natal regions, the index of abundance for each survey only comes from a single stock (i.e., the age-1 survey in the Chesapeake Bay is made up of only Chesapeake Bay stock 1 year old striped bass since there are no age-1 Atlantic coast striped bass in the Chesapeake Bay). Therefore, the same indices of abundance were used in all five estimation models but assumed to reflect trends for a single stock in the FAA models and two stocks in the SE models.

For the two young-of-the-year (YOY) surveys, a true index of abundance I_{YOY} was generated by the equations, applying a catchability q_{YOY} to the abundance of age-1 fish in each region and time-step,

$$I_{YOY_{n=1,y}} = q_{YOY_{n=1}} \times N_{s,r=1,y+1,ts=2,a=1} \quad \text{(S3.2.28)}$$

$$I_{YOY_{n=2,y}} = q_{YOY_{n=2}} \times N_{s,r=2,y+1,ts=2,a=1}, \quad \text{(S3.2.29)}$$

where the index is sampled from age-1 fish in the $y + 1$ year. The catchability was assumed the same for both surveys and was the estimated value from the Chesapeake Bay YOY Index (Chapter 2). Log-normal observation error ε_{YOY} with a log-scale standard deviation σ_{YOY} of 0.5 was applied to the true index of abundance for each YOY survey to generate the index of abundance datasets Id_{YOY} for each survey and year,

$$Id_{YOY_{n,y}} = I_{YOY_{n,y}} \times e^{\varepsilon_{YOY} \sim N(0,\sigma_{YOY})}. \quad \text{(S3.2.30)}$$

Similar to the age-1 surveys, because the operating model assumes all recruits remain in their natal regions, the index of abundance for each survey only comes from a single stock. Therefore, the same YOY indices of abundance were used in all five estimation models but were assumed to reflect different stocks based on the estimation model.

3.9 Tables

Table 3.1. Symbols and descriptions of variables for data-generating and estimation models. Values are for the Chesapeake Bay stock (CB) and Atlantic coast stock (AC), when applicable.

Variable	Description	Value
y	Year index	
a	Age index	
A	Plus group index	
ts	Sub-annual time-step index (1=Jan-Jun; 2=Jul-Dec)	
s	Stock index (1=Chesapeake Bay; 2=Atlantic Coast)	
r	Spatial region index (1=Chesapeake Bay; 2=Ocean)	
t	Fishery selectivity time block index (1=Years 1-15; 2=Years 16-20)	
n	Survey index	
$Nt_{s,y,\mathrm{ts},a}$	Total stock abundance for all spatial regions	
$N_{s,r,y,\mathrm{ts},a}$	Stock abundance for a specific spatial region	
R_s	Average recruitment	CB=145,982,893 AC=58,938,200
$Rdev_{s,y}$	Recruitment deviation	
$C_{r,y,ts}$	Total catch	
$CAA_{r,y,\mathrm{ts},a}$	Catch at age	
Feq_s	Equilibrium instantaneous fishing mortality for each stock	
$afeq_s$	Equilibrium fishing intensity for each stock	0.2 0.2
$F_{r,y,\mathrm{ts},a}$	Instantaneous fishing mortality in each region and time-step	
M_a	Annual instantaneous natural mortality	1.13 0.68 0.45 0.33 0.25 0.19 0.15 0.15 0.15 0.15 0.15 0.15 0.15 0.15 0.15
$Z_{r,y,\mathrm{ts},a}$	Instantaneous total mortality	
$ssel_{n,a}$	Survey selectivity	

Variable	Description	Value
$fsel_{r,t,ts,a}$	Fishery selectivity	
$occ_{s,ts}$	Occupancy probability	
$f_{r,ts}$	Fully recruited fishing intensity	0.1
$Fdev_{r,y,ts}$	Annual deviations for fishing mortality	
q_n	Catchability for 1+ surveys	1.42e-07
$q1_n$	Catchability for age 1 surveys	2.92e-08
$qyoy_n$	Catchability for young-of-the-year surveys	1.33e-06
sex_a	Proportion female at age	0.53 0.56 0.56 0.52 0.57 0.65 0.73 0.81 0.88 0.92 0.95 0.97 1 1 1
mat_a	Proportion of mature females at age	0 0 0 0.09 0.32 0.45 0.84 0.89 1 1 1 1 1 1 1
$ssbw_{y,a}$	Spawning stock biomass weight at age for each year	See Table S3.1
fp_1	Fishery selectivity slope parameter of logistic function; slope of ascending limb double logistic function	1
fp_2	Fishery selectivity age at 50% selectivity for logistic function; Inflection of ascending limb of double logistic function	4
fp_3	Fishery selectivity descending slope of double logistic	1
fp_4	Fishery selectivity inflection of descending limb of double logistic function	10
sp_1	Survey selectivity slope parameter of logistic function; slope of ascending limb double logistic function	1
sp_2	Survey selectivity age at 50% selectivity for logistic function; Inflection of ascending limb of double logistic function	4
sp_3	Survey selectivity descending slope of double logistic	1
sp_4	Survey selectivity inflection of descending limb of double logistic function	10
af_1	Slope parameter for equilibrium fishery selectivity	1
af_2	Age at 50% selectivity parameter for equilibrium fishery selectivity	4
ESS	Effective sample size	

Variable	Description	Value
$\sigma_{s=1}$	Standard deviation to estimate Chesapeake Bay annual recruitment deviations	0.43
$\sigma_{s=2}$	Standard deviation to estimate Atlantic Coast annual recruitment deviations	0.53
$\sigma_{F=1}$	Standard deviation of fishing mortality rate deviations in the Chesapeake Bay for both time-steps	0.70 0.38
$\sigma_{F=2}$	Standard deviation of fishing mortality rate deviations in the Ocean for both time-steps	0.50 0.24

Table 3.2. Equations for the operating model that assumes two stocks, two region, and two 6-month time-steps for striped bass dynamics.

Eq.		Description
3.2.1	$Nt_{s,y_{=1},ts_{=1},a} = Nt_{s,y_{=1},ts_{=1},a-1} \times e^{-M_{a-1}+Feq_s \times fsel_{a-1}}$	Total stock abundance in the first year
3.2.2	$Nt_{s,y_{=1},ts_{=1},a_{=1}} = R_s \times Rdev_{s,y}$	Recruitment in the first year
3.2.3	$Rdev_{s,y} = N(0,\sigma_s)$	Annual recruitment deviations for each stock
3.2.4	$Feq_s = afsel_s \times afeq_s$	Equilibrium fishing mortality
3.2.5	$afsel = \frac{1}{1+e^{-ap_1 \times (a-ap_2)}}$	Equilibrium fishery selectivity
3.2.6	$Nt_{s,y,ts=1,a} = \sum_r N_{s,r,y-1,ts=2,a-1} \times e^{-Z_{r,y-1,ts=2,a-1}}$	Total stock abundance for all spatial regions in Jan-Jun
3.2.7	$Nt_{s,y,ts=2,a} = \sum_r N_{s,r,y,ts=1,a} \times e^{-Z_{r,y,ts=1,a}}$	Total stock abundance for all spatial regions in Jul-Dec
3.2.8	$Nt_{s,y,ts=1,A} = \sum_r N_{s,r,y-1,ts=2,A-1} \times e^{-Z_{r,y-1,ts=2,A-1}} + \sum_r N_{s,r,y-1,ts=2,A} \times e^{-Z_{r,y-1,ts=2,A}}$	Total stock abundance for the plus group in Jan-Jun
3.2.9	$Nt_{s,y,ts=2,A} = \sum_r N_{s,r,y,ts=1,A} \times e^{-Z_{r,y,ts=1,A}}$	Total stock abundance for the plus group in Jul-Dec
3.2.10	$N_{s,r,y,ts,a} = Nt_{s,y,ts,a} \times occ_{s,r,ts,a}$	Stock abundance for each spatial region
3.2.11	$Z_{r,y,ts,a} = M_a + Z_{r,y,ts,a}$	Instantaneous total mortality
3.2.12	$F_{r,y,ts,a} = fsel_{r,t,ts,a} \times f_r \times Fdev_{r,y,ts}$	Instantaneous fishing mortality
3.2.13	$sel = \frac{1}{1+e^{-p_1 \times (a-p_2)}}$	Logistic selectivity
3.2.14	$sel = \frac{1}{1+e^{-p_1 \times (a-p_2)}} \times \frac{1}{1+e^{-p_3 \times (p_4-a)}}$	Double logistic selectivity

Eq.		Description
3.2.15	$SSB_{s,y,ts} = \sum_a Nt_{s,y,ts,a} \times sex_a \times mat_a \times ssbw_{y,a}$	Spawning stock biomass
3.2.16	$CAA_{r,y,ts,a} = \sum_s \frac{F_{r,y,ts}}{Z_{r,y,ts}} \times (1 - e^{-Z_{r,y,ts}}) \times N_{s,r,y,ts}$	True catch-at-age
3.2.17	$CAAerr_{r,y,ts,a} = \sum_a a\,geerr_a \times CAA_{r,y,ts,a}$	Observed catch-at-age with aging error
3.2.18	$C_{r,y,ts} = \sum_a CAAerr_{r,y,ts,a}$	Total catch
3.2.19	$PAA_{r,y,ts,a} = \frac{CAAerr_{r,y,ts,a}}{C_{r,y,ts}}$	Observed catch proportions-at-age
3.2.20	$ICAA_{n,s,r,y,ts,a} = q_n \times N_{s,r,y,ts,a} \times ssel_{n,ts,a}$	True survey catch-at-age
3.2.21	$ICAAerr_{n,r,y,a} = \sum_{s,a} a\,geerr_a \times ICAA_{n,s,r,y,a}$	Observed 1+ survey catch-at-age with aging error
3.2.22	$I_{n,r,y,ts} = \sum_a I\,CAAeer_{n,r,y,a}$	Index of abundance for 1+ surveys
3.2.23	$IPAA_{n,r,y,ts,a} = \frac{ICAAerr_{n,r,y,ts,a}}{I_{n,r,y,ts}}$	Observed 1+ survey proportions-at-age
3.2.24	$I_{n,r,y} = q1_n \times \sum_s N_{s,r,y,ts=2,a=1}$	Index of abundance for age1 surveys
3.2.25	$I_{n,r,y} = qyoy_n \times \sum_s N_{s,r,y+1,ts=2,a=1}$	Index of abundance for young-of-the-year surveys
3.2.26	$Cd_{r,y,ts} = N(C_{r,y,ts}, \sigma_F)$	Total catch datasets with observation error
3.2.27	$Id_{n,r,y} = N(I_{n,r,y}, \sigma_I)$	Indices of abundance with observation error
3.2.28	$PAAd_{r,y,ts,a} = Multi(PAAerr_{r,y,ts,a}, ESS)$	Proportions-at-age with observation error for the fishery
3.2.29	$IPAAd_{r,y,ts,a} = Multi(IPAAerr_{r,y,ts,a}, ESS)$	Proportions-at-age with observation error for the 1+ surveys
3.2.30	$Fw_{y,a} = \sum_{r,ts} \frac{F_{r,y,ts,a} \times \sum_s Nt_{s,r,y,ts,a}}{\sum_{s,r} N\,t_{s,r,y,ts,a}}$	Weighted annual fishing mortality for SE models

Table 3.3. Standard deviations (σ) and effective sample sizes (ESS) for generating each dataset. Effective sample size is weighted proportionally to the relative abundance of each stock in a region at a given time-step so that the total ESS sums to 100 in each region. Values are assumed the same for each time-step and/or region if only a single value is presented.

Parameter	Type	Value
Fishery Total Catch	σ	0.2
Fishery Age Composition Chesapeake Bay region	ESS	48, 52
Fishery Age Composition Ocean region	ESS	37, 63
Survey Indices of Abundance 1+	σ	0.4
Survey Age Composition 1+	ESS	57,43,54,46
Survey Age 1 Indices of Abundance	σ	0.5
Survey Young-of-the-Year Indices of Abundance	σ	0.5

Table 3.4. Description of the five estimation models for striped bass. Fleets-as-area models are denoted as 'FAA' models and spatially-explicit models are denoted as 'SE' models. Regions specify the number of spatial areas assumed in each model, Stocks refers to the number of stocks assumed in each model, Fleets refers to the number of fishery fleets assumed for each model, and Time-Step refers to either annual (12-months) or two sub-annual time-steps (6-months).

Model Number	Regions	Stocks	Fleets	Time-Step	Assumed aging error in data sources	Stock composition data?
FAA1	1	1	2	1 annual time-step	No	-
FAA2	1	1	2	1 annual time-steps	Yes	-
SE1	2	2	2	2 sub-annual time-steps	No	-
SE2	2	2	2	2 sub-annual time-steps	Yes	-
SE3	2	2	2	2 sub-annual time-steps	Yes	Last 10 years, stock data for fishery and surveys

Table 3.5. Equations for the fleets-as-areas (FAA) estimation models that assumes one stocks, two fleets, and 12-month time-steps for striped bass dynamics.

Eq.		Description
3.5.1	$Nt_{y,a} = N_{y-1,a-1} \times e^{-Z_{y-1,a-1}}$	Total annual abundance for FAA models
3.5.2	$Nt_{y,A} = N_{y-1,A-1} \times e^{-Z_{y-1,A-1}} + N_{y-1,A} \times e^{-Z_{y-1,A}}$	Abundance of plus group for FAA models
3.5.3	$F_{y,a} = \sum_{f} fsel_{f,t,a} \times f_f \times Fdev_{f,y}$	Instantaneous fishing mortality for FAA models
3.5.4	$fsel = \frac{1}{1+e^{-p_1\times(a-p_2)}} \times \frac{1}{1+e^{-p_3\times(p_4-a)}}$	Fishing selectivity for both fleets for the FAA models
3.5.5	$Z_{y,a} = F_{y,a} + M_a$	Instantaneous total mortality for FAA models
3.5.6	$CAA_{f,y,a} = \frac{F_{f,y,a}}{Z_{y,a}} \times (1 - e^{-Z_{y,a}}) \times Nt_{y,a}$	Estimated catch-at-age for the FAA models
3.5.7	$CAAerr_{f,y,a} = \sum_{a} a\,geerr_a \times CAA_{f,y,a}$	Estimated catch-at-age with scale aging error
3.5.8	$C_{f,y} = \sum_{a} CAAerr_{f,y,a}$	Estimated total catch with scale aging error
3.5.9	$PAA_{f,y,a} = \frac{CAAerr_{f,y,a}}{C_{f,y}}$	Estimated catch proportions-at-age with scale aging error
3.5.10	$ICAA_{n,y,a} = q_n \times Nt_{y,a} \times ssel_{n,a}$	Estimated fishery independent survey catch at-age for the FAA models
3.5.11	$ssel = \frac{1}{1+e^{-p_1\times(a-p_2)}} \times \frac{1}{1+e^{-p_3\times(p_4-a)}}$	Survey selectivity for each fishery independent survey
3.5.12	$ICAAerr_{n,y,a} = \sum_{a} a\,geerr_a \times ICAA_{n,y,a}$	Estimated survey catch-at-age with scale aging error
3.5.13	$I_{n,y} = \sum_{a} I\,CAAeer_{n,y,a}$	Estimated index of abundance of each fishery independent survey with scale aging error
3.5.14	$IPAA_{n,y,a} = \frac{ICAAerr_{n,y,a}}{I_{n,y}}$	Estimated survey proportions-at-age for each fishery independent survey with scale aging error
3.5.15	$I1_{n,y} = q1_n \times Nt_{y,a=1}$	Estimated index of abundance for age-1 fishery independent surveys

Eq.		Description
3.5.16	$Iy_{n,y} = qyoy_n \times Nt_{y+1,a=1}$	Estimated index of abundance for young-of-the-year fishery independent surveys
3.5.17	$SSB_y = \sum_a Nt_{y,a} \times sex_a \times mat_a \times ssbw_{y,a}$	Estimated spawning stock biomass

Table 3.6. Negative log likelihood components for the two-stock spatially-explicit striped bass models. Additive constants have been removed from the negative log likelihood functions. Parameter definitions are in Table 3.1.

Num.	Equation	Description
3.6.1	$nll_{tot} = -ln(L_{Catch}) - ln(L_{Index}) - ln(L_{CatchPAA}) - ln(L_{SurveyPAA}) - ln(L_{recruitment}) - ln(L_{Fdev}) - ln(L_{occ})$	Total negative log-likelihood
3.6.2	$-log_e(L_{Catch/Index}) = \sum_{y} \frac{\left(ln(X) - ln(\hat{X})\right)^2}{2\sigma^2}$	Log-normal negative log-likelihood
3.6.3	$-log_e(L_{Catch/SurveyPAA}) = \sum_{y,a} - ln\left(e^{\frac{0.5\times(-PAA-\widehat{PAA})^2}{\sigma^2}+0.01}\right)$	'Robust Multinomial' negative log-likelihood
3.6.4	$-log_e(L_{recruitment}) = \sum_{y} \left(ln(Rdev_{s=ac})\right) + \left(ln(Rdev_{s=cb})\right)$	Normal (on the log scale) negative log-likelihood for recruitment deviations with mean of 0 and standard deviation of 1
3.6.5	$-log_e(L_{Fdev}) = \sum_{r,y,ts} \frac{1}{0.5^2}\left(F_{dev_{r,y,ts}} - F_{dev_{r,y-1,ts}}\right)^2$	Log normal negative log-likelihood for year-to-year deviations in fishing mortality with standard deviation of 0.5
3.6.6	$-log_e(L_{occ}) = \sum_{s,r,a} \frac{0.5\left(prop_{s,r,ts,a} - \widehat{prop}_{s,r,ts,a}\right)^2}{\sigma^2_{s,r,ts,a}}$	Normal negative log-likelihood informative priors of occupancy probability

Table 3.7. Datasets used in the likelihood functions (Table 3.6) for each estimation model. Descriptions of the estimation models and their names are found in Table 3.4. Datasets and their assumptions are described for the fishery, fishery-independent surveys, age-1 surveys, young-of-the-year (YOY) surveys, and movement.

Data	FAA1	FAA2	SE1	SE2	SE3
Fishery Catch	Catch for each fleet	Catch for each fleet	Catch for each region and time-step	Catch for each region and time-step	Years 1-20: Catch for each region and timestep Years 21-30: Catch for each stock in each region and time-step
Fishery Age Composition	Proportions-at-age from scale age for each fleet	Proportions-at-age from scale age for each fleet	Proportions-at-age from scale age for each region and time-step	Proportions-at-age from scale age for each region and time-step	Years 1-20: Proportions-at-age from scale age for each region and time-step Years 21-30: Proportions-at-age from scale age for each stock in each region and time-step
Survey Index of Abundance	Indices of abundance for four 1-15+ surveys	Indices of abundance for four 1-15+ surveys	Indices of abundance for four 1-15+ surveys, one survey in each region and time-step	Indices of abundance for four 1-15+ surveys, one survey in each region and time-step	Years 1-20: Indices of abundance for four 1-15+ surveys, one survey in each region and time-step Years 21-30: Indices of abundance for four 1-15+ surveys for each stock, one survey in each region and time-step
Survey Age Composition	Proportions-at-age for four 1-15+ surveys from scale ages	Proportions-at-age for four 1-15+ surveys from scale ages	Proportions-at-age for four 1-15+ surveys from scale ages, one survey in each region and time-step	Proportions-at-age for four 1-15+ surveys from scale ages, one survey in each region and time-step	Years 1-20: Proportions-at-age for four 1-15+ surveys from scale ages, one survey in each region and time-step Years 21-30: Proportions-at-age for four 1-15+ surveys from scale ages for each stock, one survey in each region and time-step
Age 1 Survey	Indices of abundance for two age-1 surveys	Indices of abundance for two age-1 surveys	Indices of abundance for two age-1 surveys, one in each region	Indices of abundance for two age-1 surveys, one in each region	Indices of abundance for two age-1 surveys, one in each region
YOY Survey	Indices of abundance for two YOY surveys	Indices of abundance for two YOY surveys	Indices of abundance for two YOY surveys, one in each region	Indices of abundance for two YOY surveys, one in each region	Indices of abundance for two YOY surveys, one in each region

Data	FAA1	FAA2	SE1	SE2	SE3
Movement	-	-	Informative priors for occupancy probabilities for two stocks in each region and time-step	Informative priors for occupancy probabilities for two stocks in each region and time-step	-

Table 3.8. Median relative error (MRE) and root mean squared relative error (RMSRE) for estimated values for five estimation models. The values are presented for the terminal year estimated total annual abundance (N), spawning stock biomass (SSB), fishing mortality for age-8 (F-8), and the fishing mortality that yields 40% spawning potential ration (F40% SPR). Models are described in Table 3.4.

Metric	**FAA1**	**FAA2**	**SE1**	**SE2**	**SE3**
MRE N	-0.393	0.483	-0.515	-0.017	-0.002
RMSRE N	0.359	0.617	0.384	0.100	0.147
MRE SSB	-0.593	0.719	-0.614	0.032	0.040
RMSRE SSB	0.583	0.985	0.627	0.140	0.213
MRE F-8	1.408	-0.268	1.354	-0.001	-0.012
RMSRE F-8	1.346	0.361	1.434	0.153	0.192
MRE F40% SPR	1.145	0.887	-0.120	-0.134	-0.129
RMSRE F40% SPR	1.146	0.889	0.120	0.134	0.137

Supplemental Table S3.1. Spawning stock biomass weight-at-age for 30 years used to calculate spawning stock biomass. Values used are the same as those assumed for the benchmark assessment from years 1988-2017 (Northeast Fisheries Science Center 2019).

1	2	3	4	5	6	7	8	9	10	11	12	13	14	15+
0.24	0.62	1.01	1.82	2.83	3.57	3.95	4.40	5.11	5.59	8.00	9.67	10.35	11.43	13.07
0.10	0.65	1.13	1.87	2.74	4.13	5.00	5.70	5.67	7.65	7.96	9.44	10.97	11.85	13.46
0.04	0.58	1.05	1.80	2.32	3.62	4.81	5.81	5.83	5.99	7.73	9.04	9.62	10.70	11.51
0.16	0.50	1.18	1.85	2.46	2.94	4.54	5.45	6.33	6.10	8.43	8.08	9.85	10.75	12.23
0.06	0.51	1.20	1.75	2.63	3.37	4.39	5.53	6.60	7.69	8.73	11.62	11.95	13.82	17.23
0.04	0.46	1.12	1.79	2.53	3.37	4.49	5.78	6.70	7.73	9.16	10.50	12.27	13.65	15.20
0.18	0.53	1.38	1.94	2.61	3.30	4.56	5.82	6.62	7.40	9.27	10.39	11.62	13.02	14.69
0.20	0.54	1.27	2.05	2.62	3.43	4.83	5.83	6.99	8.29	7.56	9.73	10.89	12.04	13.20
0.10	0.75	1.22	2.03	2.93	4.00	5.56	6.63	7.36	8.67	9.20	9.40	11.30	12.48	14.17
0.08	0.43	1.15	2.16	2.68	3.53	4.51	5.37	6.82	8.81	9.75	10.00	11.70	13.30	15.35
0.32	0.49	1.02	1.50	2.30	2.91	4.40	5.35	6.33	6.95	8.09	9.89	10.67	12.15	13.41
0.64	0.73	1.01	1.38	1.83	2.44	3.25	4.94	6.32	7.58	8.24	9.22	11.19	12.65	15.04
0.37	0.57	1.05	1.36	1.81	2.54	3.49	4.59	6.52	7.16	9.20	10.16	11.88	13.77	16.51
0.14	0.38	0.94	1.56	1.99	2.86	3.74	4.71	6.02	7.61	8.31	8.62	10.49	11.89	12.87
0.08	0.26	0.82	1.40	2.06	2.90	3.93	5.10	5.76	7.24	8.75	9.46	10.62	12.34	14.62
0.07	0.40	0.75	1.31	2.00	2.91	3.84	4.93	5.94	6.89	8.25	9.32	10.63	12.13	13.76
0.19	0.24	0.77	1.29	2.12	2.85	3.88	4.88	5.84	6.85	7.92	8.89	10.25	11.62	13.18
0.10	0.41	0.84	1.39	1.98	3.01	3.88	5.22	6.05	6.91	8.14	9.51	10.68	12.15	14.21
0.14	0.29	0.72	1.29	1.87	2.64	3.68	5.03	6.42	7.14	8.21	9.17	10.96	12.42	14.37
0.07	0.36	0.75	1.15	1.88	2.74	3.87	4.90	6.47	7.54	8.85	9.71	11.40	13.14	15.54
0.16	0.31	0.85	1.29	1.89	3.06	4.46	5.18	6.32	7.89	8.83	9.71	11.34	12.96	14.74
0.20	0.47	0.84	1.31	1.78	2.95	4.21	5.56	6.50	7.46	8.67	9.40	10.95	12.51	14.20
0.12	0.55	0.96	1.30	1.83	2.91	4.00	5.02	6.13	7.45	8.64	9.06	10.66	12.19	13.91
0.16	0.39	0.94	1.43	1.83	2.76	3.90	4.90	6.09	7.20	8.06	9.72	10.75	12.39	14.40
0.05	0.39	0.86	1.48	2.08	2.88	4.05	5.37	6.18	7.79	8.65	9.81	11.54	13.06	15.31
0.15	0.31	0.81	1.28	2.10	3.07	3.90	5.07	6.48	7.29	9.01	10.07	11.67	13.34	15.49
0.56	0.42	0.77	1.18	1.93	2.85	4.03	4.98	6.52	7.96	8.74	11.18	12.66	14.61	17.69
0.12	0.33	0.81	1.38	2.11	3.26	4.13	5.30	6.51	7.51	8.82	10.18	11.95	13.48	15.03
0.13	0.33	0.61	1.16	2.01	3.15	4.48	5.64	6.69	8.39	9.39	10.61	12.64	14.39	17.26
0.18	0.37	0.85	1.33	2.10	2.96	4.17	5.16	6.29	8.16	9.56	10.61	12.58	14.48	16.07

Supplemental Table S3.2 Aging-error matrices used applied to the fisheries-independent and dependent data sources for striped bass ages 1-15+. Striped bass used for to develop this matrix were collected from Massachusetts, Rhode Island, and New Jersey that were aged with both scales and otoliths. Otolith (true) ages are along the columns and scale ages are along the rows.

	1	2	3	4	5	6	7	8	9	10	11	12	13	14	15+
1	0.667	0.051	0.000	0.000	0.000	0.000	0.000	0.000	0.000	0.000	0.000	0.000	0.000	0.000	0.000
2	0.333	0.949	0.481	0.000	0.000	0.000	0.000	0.000	0.000	0.000	0.000	0.000	0.000	0.000	0.000
3	0.000	0.000	0.444	0.047	0.000	0.000	0.000	0.000	0.000	0.000	0.000	0.000	0.000	0.000	0.000
4	0.000	0.000	0.074	0.748	0.096	0.014	0.003	0.000	0.000	0.000	0.000	0.000	0.000	0.000	0.000
5	0.000	0.000	0.000	0.168	0.426	0.150	0.036	0.000	0.000	0.000	0.000	0.000	0.000	0.000	0.000
6	0.000	0.000	0.000	0.037	0.415	0.652	0.270	0.046	0.009	0.000	0.000	0.000	0.000	0.000	0.000
7	0.000	0.000	0.000	0.000	0.043	0.171	0.593	0.282	0.101	0.047	0.041	0.000	0.000	0.009	0.005
8	0.000	0.000	0.000	0.000	0.011	0.014	0.075	0.541	0.332	0.215	0.091	0.066	0.014	0.009	0.005
9	0.000	0.000	0.000	0.000	0.011	0.000	0.022	0.120	0.447	0.366	0.231	0.077	0.041	0.009	0.010
10	0.000	0.000	0.000	0.000	0.000	0.000	0.000	0.012	0.097	0.331	0.248	0.165	0.068	0.094	0.010
11	0.000	0.000	0.000	0.000	0.000	0.000	0.000	0.000	0.014	0.041	0.331	0.319	0.205	0.142	0.062
12	0.000	0.000	0.000	0.000	0.000	0.000	0.000	0.000	0.000	0.000	0.050	0.352	0.370	0.179	0.120
13	0.000	0.000	0.000	0.000	0.000	0.000	0.000	0.000	0.000	0.000	0.008	0.022	0.247	0.340	0.193
14	0.000	0.000	0.000	0.000	0.000	0.000	0.000	0.000	0.000	0.000	0.000	0.000	0.055	0.179	0.245
15+	0.000	0.000	0.000	0.000	0.000	0.000	0.000	0.000	0.000	0.000	0.000	0.000	0.000	0.038	0.349

3.10 Figures

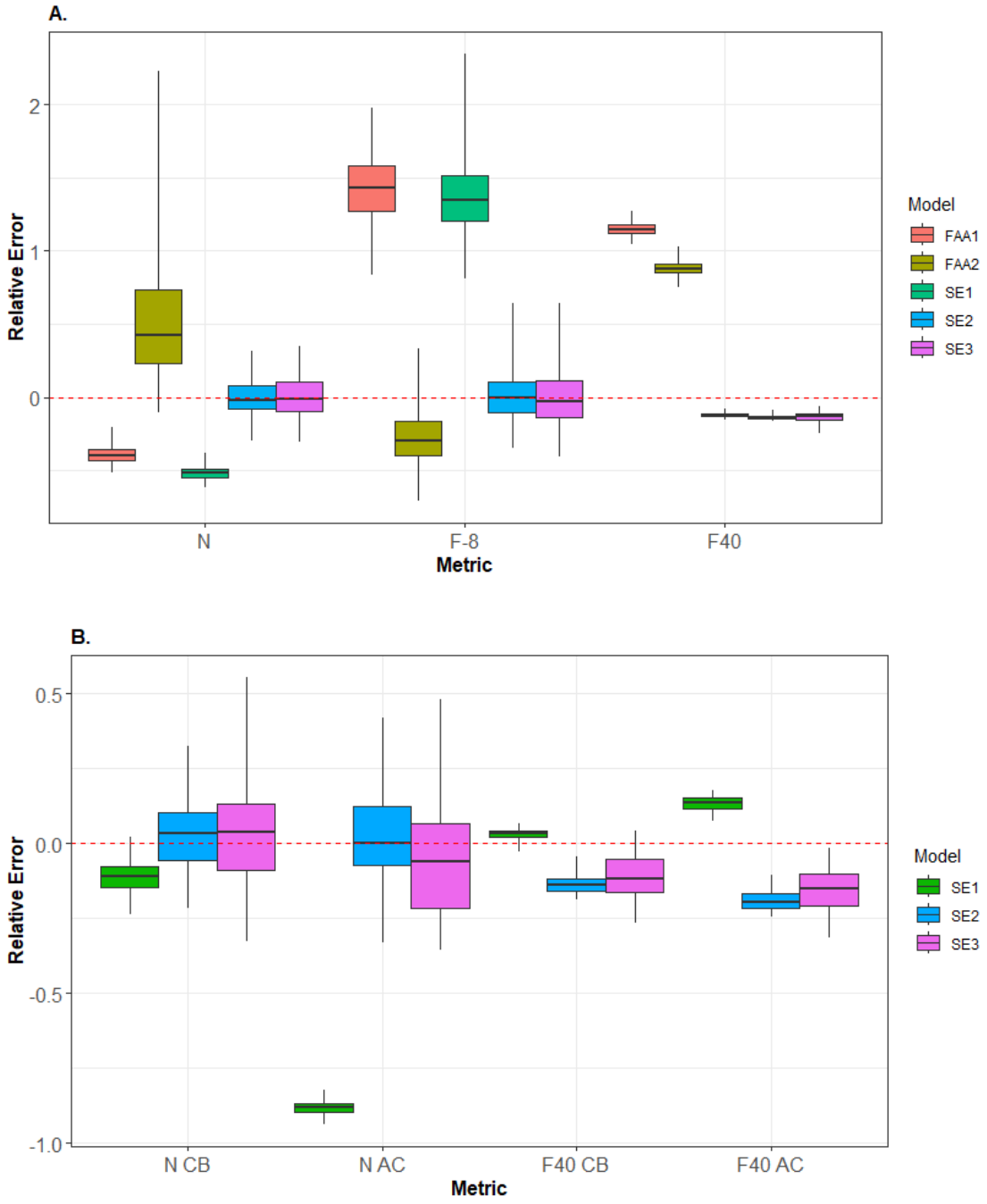

Figure 3.1. A) Boxplots of the distribution of relative errors of total abundance over stocks and regions (N), annual fishing mortality at age-8 (F-8), and fishing mortality that achieves a 40% spawning potential ratio (SPR) for the entire population (F40). B)

Boxplots of the distribution of relative errors of stock-specific abundance for the Chesapeake Bay stock (N CB) and Atlantic coast stock (N AC), fishing mortality that produces 40% SPR for the Chesapeake Bay stock (F40 CB), and fishing mortality that produces 40% SPR for the Atlantic coast stock (F40 AC). Estimation models are described in Table 3.4. For both figures, the dashed red line represents when relative error is equal to 0. The lower and upper hinge of the box represents the 25th and 75th percentiles. The middle line represents the median. The whiskers extend to the minimum and maximum values of relative error.

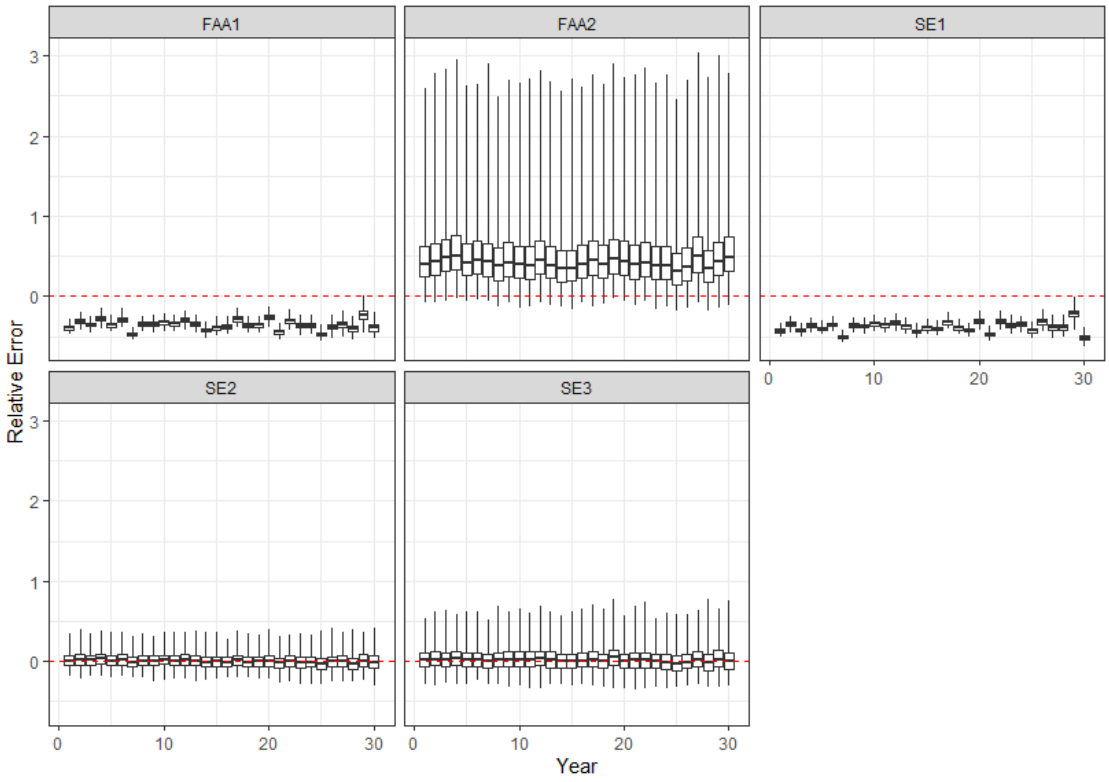

Figure 3.2. Relative error of total abundance (over stocks and regions) for each year and estimation model. Models are described in Table 3.4. The dashed red line represents when relative error is equal to 0. Boxplot definitions are found in Figure 3.1.

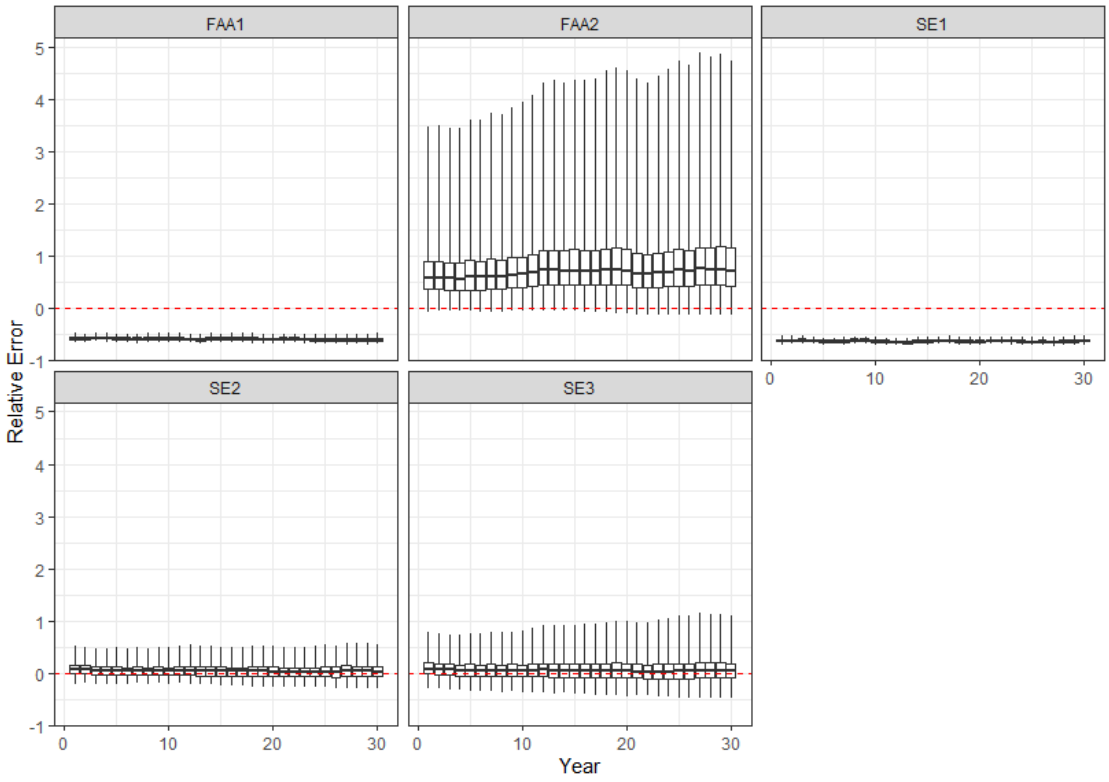

Figure 3.3. Relative error of total spawning stock biomass (SSB) (over stocks and regions) for each year and estimation model. Models are described in Table 3.4. The dashed red line represents when relative error is equal to 0. Boxplot definitions are found in Figure 3.1.

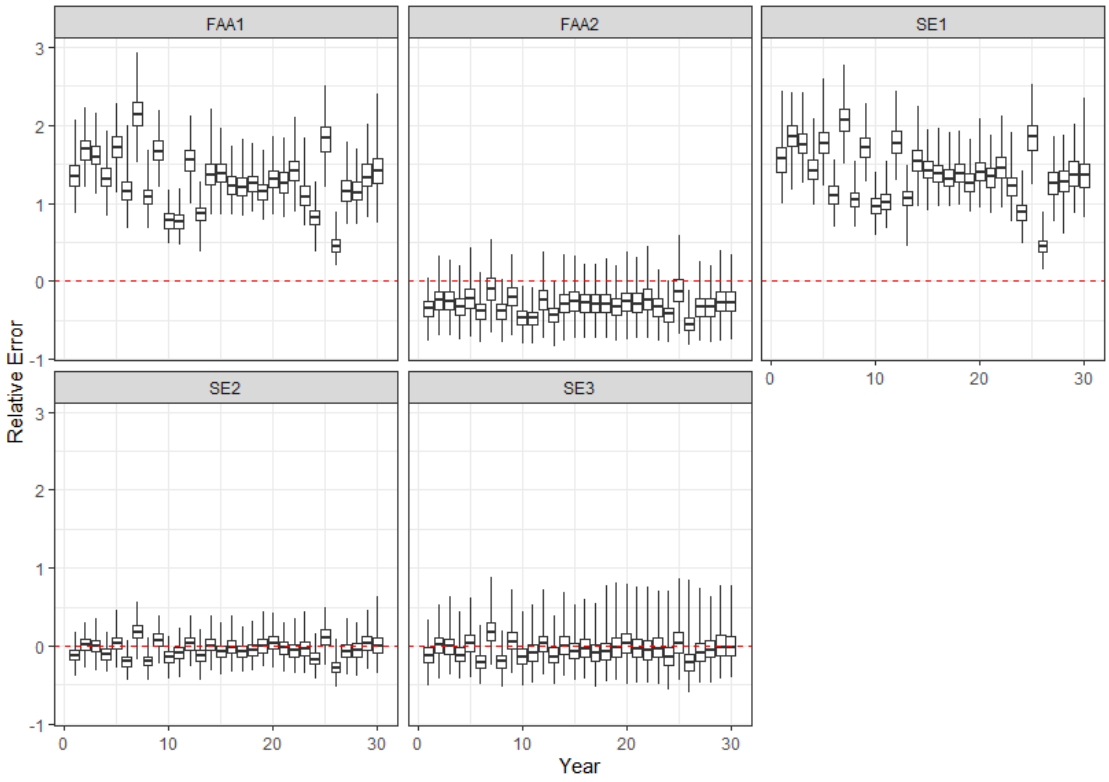

Figure 3.4. Relative error of total fishing mortality for age 8 (F-8) (over stocks and regions) for each year and estimation model. Models are described in Table 3.4. The dashed red line represents when relative error is equal to 0. Boxplot definitions are found in Figure 3.1.

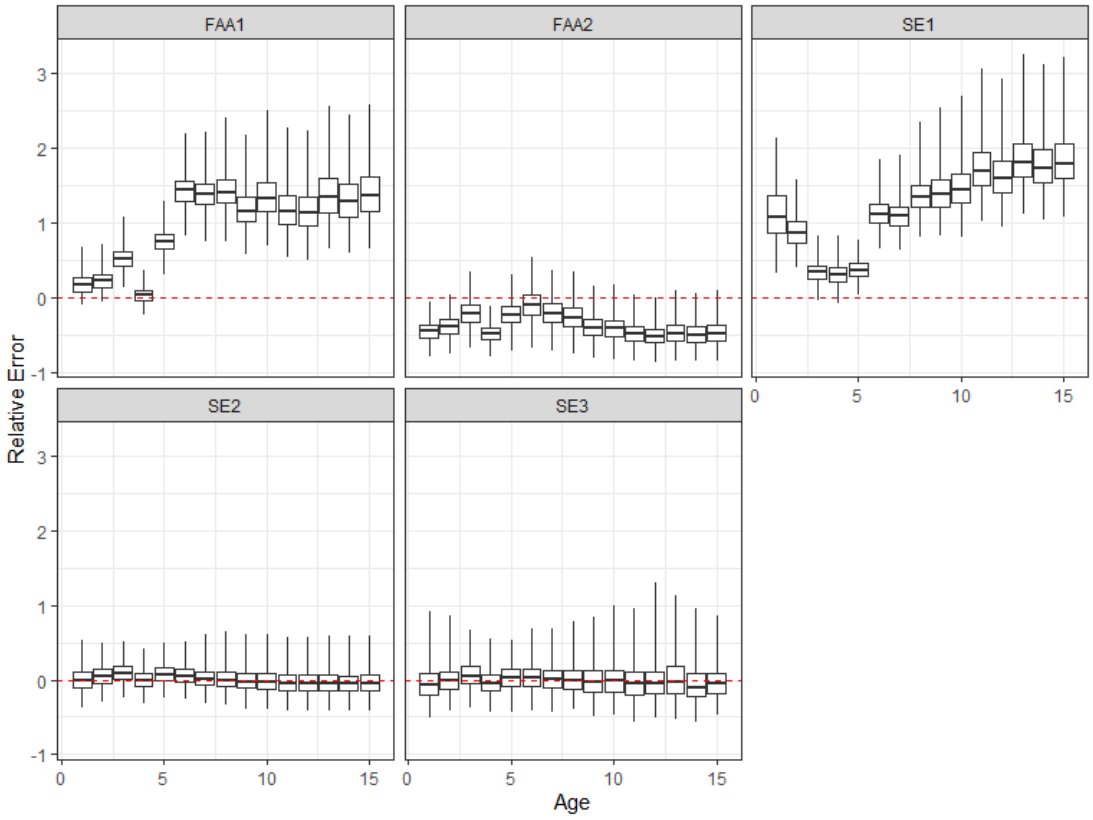

Figure 3.5. Relative error of fishing mortality for each age (over stocks and regions), aggregate for all years and each estimation model. Models are described in Table 3.4. The dashed red line represents when relative error is equal to 0. Boxplot definitions are found in Figure 3.1.

3.11 References

Berger, A.M., Goethel, D.R., Lynch, P.D., Quinn, T., Mormede, S., McKenzie, J., Dunn, A., 2016. Space oddity: The mission for spatial integration. Canadian Journal of Fisheries and Aquatic Sciences 74, 1698–1716. https://doi.org/10.1139/cjfas-2017-0150

Cadrin, S.X., 2020. Defining spatial structure for fishery stock assessment. Fish Res 221, 1–12. https://doi.org/10.1016/j.fishres.2019.105397

Cadrin, S.X., Secor, D.H., 2009. Accounting for spatial population structure in stock assessment: Past, present, and future. The Future of Fisheries Science in North America 405–426. https://doi.org/10.1007/978-1-4020-9210-7_22

Cope, J.M., Punt, A.E., 2011. Reconciling stock assessment and management scales under conditions of spatially varying catch histories. Fish Res 107, 22–38. https://doi.org/10.1016/j.fishres.2010.10.002

Dorazio, R.M., Hattala, K.A., McCollough, C.B., Skjeveland, J.E., 1994. Tag Recovery Estimates of Migration of Striped Bass from Spawning Areas of the Chesapeake Bay. Trans Am Fish Soc 123, 950–963.

Dorval, E., McDaniel, J.D., Porzio, D.L., Hodes, V., Felix-Uraga, R., Rosenfield, S., 2013. Computing and selecting ageing errors to include in stock assessment models of pacific sardine (*Sardinops sagax*). California Cooperative Oceanic Fisheries Investigations Reports 54, 192–204.

Fabrizio, M.C., 1987. Contribution of Chesapeake Bay and Hudson River Stocks of Striped Bass to Rhode Island Coastal Waters as Estimated by Isoelectric

Focusing of Eye Lens Proteins. Trans Am Fish Soc 116, 588–593. https://doi.org/10.1577/1548-8659(1987)116<588:cocbah>2.0.co;2

Fournier, D.A., Skaug, H.J., Ancheta, J., Ianelli, J., Magnusson, A., Maunder, M.N., Nielsen, A., Sibert, J., 2012. AD Model Builder: Using automatic differentiation for statistical inference of highly parameterized complex nonlinear models. Optim Methods Softw 27, 233–249. https://doi.org/10.1080/10556788.2011.597854

Goethel, D.R., Berger, A.M., 2016. Accounting for spatial complexities in the calculation of biological reference points: Effects of misdiagnosing population structure for stock status indicators. Canadian Journal of Fisheries and Aquatic Sciences 74, 1878–1894. https://doi.org/10.1139/cjfas-2016-0290

Goethel, D.R., Berger, A.M., Cadrin, S.X., 2023. Spatial awareness: Good practices and pragmatic recommendations for developing spatially structured stock assessments. Fish Res 264. https://doi.org/10.1016/j.fishres.2023.106703

Goethel, D.R., Legault, C.M., Cadrin, S.X., 2015. Testing the performance of a spatially explicit tag-integrated stock assessment model of yellowtail flounder (*Limanda ferruginea*) through simulation analysis. Canadian Journal of Fisheries and Aquatic Sciences 72, 582–601. https://doi.org/10.1139/cjfas-2014-0244

Goethel, D.R., Quinn, T.J., Cadrin, S.X., 2011. Incorporating spatial structure in stock assessment: Movement modeling in marine fish population dynamics. Reviews in Fisheries Science 19, 119–136. https://doi.org/10.1080/10641262.2011.557451

Grothues, T.M., Able, K.W., Carter, J., Arienti, T.W., 2009. Migration patterns of striped bass through nonnatal estuaries of the U.S. Atlantic coast. American Fisheries Society Symposium 69, 135–150.

Guan, W., Cao, J., Chen, Y., Cieri, M., 2013. Impacts of population and fishery spatial structures on fishery stock assessment. Canadian Journal of Fisheries and Aquatic Sciences 70, 1178–1189. https://doi.org/10.1139/cjfas-2012-0364

Hasegawa, E.H., Waldman, J., Wirgin, I., 2022. Stock composition of Atlantic coastal migratory striped bass using microsatellite DNA analysis. Fish Res 254, 1–10. https://doi.org/10.1016/j.fishres.2022.106384

Henríquez, V., Licandeo, R., Cubillos, L.A., Cox, S.P., 2016. Interactions between ageing error and selectivity in statistical catch-at-age models: Simulations and implications for assessment of the Chilean Patagonian toothfish fishery. ICES Journal of Marine Science 73, 1074–1090. https://doi.org/10.1093/icesjms/fsv270

Hulson, P.J.F., Hanselman, D.H., 2014. Tradeoffs between bias, robustness, and common sense when choosing selectivity forms. Fish Res 158, 63–73. https://doi.org/10.1016/j.fishres.2013.12.016

Hulson, P.J.F., Williams, B.C., 2024. Inclusion of ageing error and growth variability using a bootstrap estimation of age composition and conditional age-at-length input sample size for fisheries stock assessment models. Fish Res 270. https://doi.org/10.1016/j.fishres.2023.106894

Kell, L.T., Dickey-Collas, M., Hintzen, N.T., Nash, R.D.M., Pilling, G.M., Roel, B.A., 2009. Lumpers or splitters? Evaluating recovery and management plans for

metapopulations of herring. ICES Journal of Marine Science 66, 1776–1783. https://doi.org/10.1093/icesjms/fsp181

Kerr, L.A., Goethel, D.R., 2013. Simulation modeling as a tool for synthesis of stock identification information, in: Stock Identification Methods: Applications in Fishery Science: Second Edition. pp. 501–533. https://doi.org/10.1016/B978-0-12-397003-9.00021-7

Kneebone, J., Hoffman, W.S., Dean, M.J., Fox, D.A., Armstrong, M.P., 2014. Movement patterns and stock composition of adult striped bass tagged in Massachusetts coastal waters. Trans Am Fish Soc 143, 1115–1129. https://doi.org/10.1080/00028487.2014.889752

Langseth, B.J., Schueller, A.M., 2016. Calculation of population-level fishing mortality for single- versus multi-area models: Application to models with spatial structure. Canadian Journal of Fisheries and Aquatic Sciences 74, 1821–1831. https://doi.org/10.1139/cjfas-2016-0295

Lee, H.H., Piner, K.R., Maunder, M.N., Taylor, I.G., Methot, R.D., 2016. Evaluation of alternative modelling approaches to account for spatial effects due to age-based movement. Canadian Journal of Fisheries and Aquatic Sciences 74, 1832–1844. https://doi.org/10.1139/cjfas-2016-0294

Li, Y., Bence, J.R., Brenden, T.O., 2018. Can spawning origin information of catch or a recruitment penalty improve assessment and fishery management performance for a spatially structured stock assessment model? Canadian Journal of Fisheries and Aquatic Sciences 75, 2136–2148. https://doi.org/10.1139/cjfas-2017-0523

Liao, H., Sharov, A.F., Nelson, G.A., 2013. Quantifying the effects of aging bias in Atlantic striped bass stock assessment. Trans Am Fish Soc 142, 193–207. https://doi.org/10.1080/00028487.2012.705255

Linton, B.C., Bence, J.R., 2011. Catch-at-age assessment in the face of time-varying selectivity. ICES Journal of Marine Science 68, 611–625. https://doi.org/10.1093/icesjms/fsq173

Methot, R.D., Wetzel, C.R., 2013. Stock synthesis: A biological and statistical framework for fish stock assessment and fishery management. Fish Res 142, 86–99. https://doi.org/10.1016/j.fishres.2012.10.012

Miller, T.J., 2023. A mullti-stock, multi-region extension of the Woods Hole Assessment Model.

Northeast Fisheries Science Center, 2019. 66th Northeast Regional Stock Assessment Workshop (66th SAW) Assessment Report. Northeast Fisheries Science Center Reference Document 457–1170.

Pincin, J.S., Wilberg, M.J., 2012. Surplus Production Model Accuracy in Populations Affected by a No-Take Marine Protected Area. Marine and Coastal Fisheries 4, 511–525. https://doi.org/10.1080/19425120.2012.685145

Punt, A.E., 2019a. Spatial stock assessment methods: A viewpoint on current issues and assumptions. Fish Res 213, 132–143. https://doi.org/10.1016/j.fishres.2019.01.014

Punt, A.E., 2019b. Modelling recruitment in a spatial context: A review of current approaches, simulation evaluation of options, and suggestions for best practices. Fish Res 217, 140–155. https://doi.org/10.1016/j.fishres.2017.08.021

Punt, A.E., 2017. Review of contemporary cetacean stock assessment models. Journal of Cetacean Research Management 17, 35–56.

Punt, A.E., Haddon, M., Little, L.R., Tuck, G.N., 2016. The effect of marine closures on a feedback control management strategy used in a spatially aggregated stock assessment: A case study based on pink ling in Australia. Canadian Journal of Fisheries and Aquatic Sciences 74, 1960–1973. https://doi.org/10.1139/cjfas-2016-0017

Punt, A.E., Haddon, M., Tuck, G.N., 2015. Which assessment configurations perform best in the face of spatial heterogeneity in fishing mortality, growth and recruitment? A case study based on pink ling in Australia. Fish Res 168, 85–99. https://doi.org/10.1016/j.fishres.2015.04.002

R Core Team, 2020. R: A language and environment for statistical computing.

Schiano, S.E., 2022. Evaluating the consequences of alternative Atlantic striped bass harvest control rules on their prey, Atlantic menhaden. University of Maryland College Park M.S. Thesis.

Schonfeld, A.J., 2023. Climate Impacts on Spatiotemporal Habitat Usage of Mid-Atlantic Fishes. William & Mary Ph.D. Dissertation.

Secor, D.H., O'Brien, M.H.P., Gahagan, B.I., Carter Watterson, J., Fox, D.A., 2020. Differential migration in Chesapeake Bay striped bass. PLoS One 15, 1–19. https://doi.org/10.1371/journal.pone.0233103

Secor, D.H., Trice, M., Hornick, H.T., 1995. Validation of otolith-based ageing and a comparison of otolith and scale-based ageing in mark-recaptured Chesapeake Bay striped bass, *Morone saxatilis*. Fishery Bulletin 93, 186–190.

Smedbol, R.K., Stephenson, R., 2001. The importance of managing within-species diversity in cod and herring fisheries of the north-western Atlantic. J Fish Biol 59, 109–128. https://doi.org/10.1006/jfbi.2001.1765

Taylor, N.G., McAllister, M.K., Lawson, G.L., Carruthers, T., Block, B.A., 2011. Atlantic bluefin tuna: A novel multistock spatial model for assessing population biomass. PLoS One 6. https://doi.org/10.1371/journal.pone.0027693

Vincent, M.T., Brenden, T.O., Bence, J.R., 2016. Simulation testing the robustness of a multiregion, tag-integrated assessment model that exhibits natal homing and estimates natural mortality and reporting rate. Canadian Journal of Fisheries and Aquatic Sciences 74, 1930–1949. https://doi.org/10.1139/cjfas-2016-0297

Wirgin, I., Maceda, L., Waldman, J.R., Crittenden, R.N., 1993. Use of mitochondrial DNA polymorphisms to estimate the relative contributions of the Hudson River and Chesapeake Bay striped bass stocks to the mixed fishery on the Atlantic coast. Trans Am Fish Soc 122, 669–684. https://doi.org/https://doi.org/10.1577/1548-8659(1993)122<0669:UOMDPT>2.3.CO;2

Ying, Y., Chen, Y., Lin, L., Gao, T., 2011. Risks of ignoring fish population spatial structure in fisheries management. Canadian Journal of Fisheries and Aquatic Sciences 68, 2101–2120. https://doi.org/10.1139/F2011-116

Chapter 4: Testing the performance of a spatially-explicit population model for striped bass under different climate change scenarios

4.1 Abstract

Climate change is expected to alter the dynamics of many ecologically and economically important fish species, but few stock assessments consider climatic effects. Striped bass *Morone saxatilis* have undergone many dynamic changes as a result of changing environmental conditions, particularly in the Chesapeake Bay. For example, water temperature has been shown to affect striped bass spawning behavior, recruitment, movement, and natural mortality. We developed a simulation framework to evaluate how potential climate-change induced variability in the Chesapeake Bay striped bass stock may affect the performance of a spatially-explicit stock assessment model. We simulated five scenarios with alternative assumptions of potential climate effects on striped bass. Datasets generated under each scenario were introduced into three stock assessment models with varying degrees of spatial complexity and stock structure. The spatially-explicit models were better able to account for changes in recruitment and movement over time with relatively little bias in estimates of abundance and fishing mortality. However, when natural mortality changed over time, all models yielded substantially biased estimates of abundance, spawning stock biomass, and fishing mortality. Ignoring time-varying natural mortality and migration can lead to the overestimation of striped bass abundance, potentially providing incorrect management advice.

4.2 Introduction

Sustainable management depends on reliable stock assessments and the ability to accurately estimate population dynamics in response to climate change (Hare et al., 2016). However, few stock assessments used to inform management decisions include ecosystem or climatic effects (Pepin et al., 2022). If population models cannot account for shifts in distribution or productivity, abundance and fishing mortality estimates may be biased. Management decisions, like catch limits, that are based on population estimates that do not consider population responses to climate change may lead to an over or underutilized resource (Goethel et al., 2021; Mazur et al., 2023; Wayte, 2013).

Stock assessment models can produce biased estimates if their assumptions are violated. Spatially-explicit population models have the potential to reduce the bias for estimates of abundance when spatial complexity exists in life history and fishery characteristics, whereas spatially-implicit (e.g., fleets-as-areas) approaches may result in bias in estimates of mortality over time (Bosley et al., 2022). Also, stock assessment models commonly assume many life history parameters such as natural mortality are constant over time (Maunder et al., 2023; Punt et al., 2021). Incorrectly specifying natural mortality and movement dynamics in assessment models can lead to biased assessment estimates (Deroba and Schueller, 2013; Goethel et al., 2021).

Striped bass *Morone saxatilis* is an ecologically important species in the Chesapeake Bay and supports an important recreational and commercial fishery on the U.S. Atlantic coast and in the Chesapeake Bay (Hartman and Margraf, 2003). Striped bass undergo seasonal migrations that vary by sex, size, and age between

Maine and North Carolina (Secor et al., 2020a). This coastal population is supported by four major spawning stocks that are biologically distinct, including the Hudson River stock, Delaware Bay stock, Chesapeake Bay stock, and Roanoke River stock (Northeast Fisheries Science Center, 2019). However, the Chesapeake Bay contributes disproportionately to the migratory contingent (Fabrizio, 1987; Hasegawa et al., 2022; Kneebone et al., 2014; Wirgin et al., 1993). A spatially-explicit model was developed to estimate abundance of striped bass in the Chesapeake Bay (Chapter 2) and was shown to improve the accuracy of abundance estimates compared to spatially-implicit models (Chapter 3). However, this model does not consider potential environmental and climatic changes in the Chesapeake Bay. For example, the Chesapeake Bay has experienced increased frequency of hypoxia events (Du et al., 2018; Hagy et al., 2004), varying nutrient loads due to land use practices (Goetz et al., 2004), and declines in ecologically significant species (Wilberg et al., 2011) in the last few decades, which can have negative consequences on fish species and habitat quality. Additionally, habitat quality in the Chesapeake Bay is expected to worsen overtime with climate change (Du et al., 2018) impacting habitat use within the Chesapeake Bay (Schonfeld et al., 2022). Understanding how these environmental changes to the Chesapeake Bay affect ecologically and economically valuable species like striped bass could potentially improve assessments and fisheries management.

The Chesapeake Bay is expected to experience increased water temperature, increased variability of salinity (Najjar et al., 2010), and a higher prevalence of disease (Jesse et al., 2021) due to climate change. Increased water temperature is expected to be a major driver of striped bass declines in the Chesapeake Bay (Allen et

al., 2023). However, changes to nutrient loads and sea level rise could partially offset negative consequences from increased water temperature (Irby et al., 2018; Ni et al., 2020). Increased temperatures as a result of climate change are suggested as a mechanism for increased mortality and disease prevalence (Jesse et al., 2021). For example, mortality of striped bass from mycobacteriosis increases as water temperature increases (Groner et al., 2018), and mycobacteriosis prevalence in striped bass was 90% for certain ages between 2003-2007 (Latour et al., 2012). Mycobacteriosis may also affect recruitment, as diseased fish have slower growth, implying that egg production may be reduced for affected populations (Gervasi et al., 2019; Latour et al., 2012). Mycobacteria appear to have upper temperature thresholds (Gauthier et al., 2021), which may reduce effects of mycobacteriosis at high temperature. Because the Chesapeake Bay has a higher prevalence of mycobacteriosis than other spawning areas along the Atlantic coast, recruitment in the Chesapeake Bay could be reduced over time as a result. Furthermore, natural mortality of striped bass is likely increasing over time and is higher for Chesapeake Bay fish than other stocks along the Atlantic coast (Schonfeld, 2023; Secor et al., 2020a). As a result of climate change, the severity of mycobacteriosis is increasing overtime within the Chesapeake Bay (Groner et al., 2018), driving increases in natural mortality of striped bass over time as well. However, population models often assume constant mortality over time.

Climate change may also affect striped bass spawning behavior, movement, and recruitment trends. Striped bass spawning is directly related to water temperature and environmental conditions, because water temperature determines when striped

bass spawn (Peer and Miller, 2014; Secor and Houde, 1995) and when striped bass move off spawning grounds (Rothermel et al., 2020; Secor et al., 2020b). Additionally, recruitment disproportionately comes from a narrow window of spawning that changes annually based on water temperature. As a result, striped bass may benefit from numerous spawning days in order to hedge against inconsistent or variable environmental conditions (Secor, 2007; Secor and Houde, 1995). However, the striped bass spawning window may shorten in the future due to projected changes in water temperature (Nack et al., 2019). Water temperature also affects early life-stage survival, as warm and cool temperatures can increase mortality for striped bass (Secor and Houde, 1995). Finally, winter water temperature and river discharge drive spring abundance of larval striped bass prey, implying warming waters could cause a mis-match in the timing of prey availability for young-of-the-year striped bass (Millette et al., 2020). In the Hudson River, river discharge was positively correlated to the abundance of post-yolk-sac larval striped bass (O'Connor et al., 2012).

Data limitations and violations of assumptions of the spatially-explicit population model described in Chapter 2 may cause estimates to be biased. First, the spatially-explicit model has relatively little data on stock composition of the coastal fishery. Though recruitment can vary over time for each stock in the spatially-explicit model, changes in productivity due to climate change induced variability may not be able to be captured in this model as it lacks data to track specific changes in stock composition in the fishery and fishery-independent surveys. Further, stock composition was also driven by movement of each stock. Striped bass migration is assumed to be driven by temperature, as striped bass move off spawning grounds as

waters warm (Rothermel et al., 2020). Therefore, warming waters due to climate change may cause spatially driven migration changes (Rothermel et al., 2020; Secor et al., 2020b). Finally, natural mortality is an important parameter in assessment models due to its effects on estimating recruitment (Maunder et al., 2023). Thus, understanding how the assumption of constant natural mortality used in Chapter 2 impacts estimates of abundance and fishing mortality under stochastic environments is of importance. Ignoring these population dynamics may reduce accuracy of the Chapter 2 model in a changing climate.

In this study, we developed a simulation framework to evaluate how potential climate effects on the Chesapeake Bay striped bass stock may affect the performance of the spatially-explicit stock assessment model developed in Chapter 2 and two other models from Chapter 3. Additionally, we tested whether current assessment methods used to inform management decisions for striped bass can provide accurate estimates of abundance under climate induced population shifts. Our specific objectives were to determine how increases in natural mortality in the Chesapeake Bay over time may affect the performance of stock assessment models that assume constant mortality over time and space. Further, we tested how changes in productivity and increases to movement out of the Chesapeake Bay affected performance of stock assessment models that assumed stationary recruitment and migration.

4.3 Methods

We evaluated the performance of three stock assessment models for estimating abundance, recruitment, and fishing mortality under multiple scenarios that assumed changes to striped bass dynamics over time. These scenarios included

increases to natural mortality in the Chesapeake Bay, increases to movement out of the Chesapeake Bay, and declines in average recruitment for the Chesapeake Bay stock. Datasets were generated based on a simulated populations that represented striped bass population dynamics scenarios and fitted with three stock assessment models that differed in their assumptions of spatial complexity and data inputs. The estimation models were a fleets-as-areas (FAA) model, a multi-stock, spatially-explicit model (SE), or a multi-stock, spatially-explicit model that included additional stock composition data in the fishery and surveys (SE-S). Model estimates of interest (i.e., abundance, fishing mortality) from each estimation model were summarized and compared to the true simulated values to determine model performance. The operating models simulated data sets that represented a 30-year period. For each set of operating model assumptions (i.e., scenario), 300 simulations were run.

4.3.1 Operating Models

Five operating models were developed to represent potential "true" population dynamics for striped bass. Each operating model included similar age-specific processes (e.g., maturity at age, sex proportions at age) to those in the most recent stock benchmark assessment (Northeast Fisheries Science Center, 2019) and the model described in Chapter 2. All operating models assumed two stocks, two regions, and assumed that biological processes occurred during 6 sub-annual, two-month time-steps (e.g., Jan.-Feb., Mar.-Apr., etc.). Variable definitions can be found in Table 4.1 and model equations are found in Table 4.2.

The first operating model (OM-B) was the base scenario. In the base scenario, population dynamics for natural mortality and movement were constant over time and

recruitment followed a stationary stochastic process. OM-B followed the same dynamics described for Chapter 3 and used parameter estimates from Chapter 2. The operating model generated 30-year time series of observed catches, indices of abundance, and proportions-at-age that were similar to striped bass dynamics estimated in Chapter 2. Abundance of striped bass in January-February in the first year was calculated by assuming each stock was in equilibrium in the first year (Eq. 4.2.1). Recruitment was assumed to be lognormally distributed for each stock (Eq. 4.2.2) with different means based on output from Chapter 2 for the Chesapeake Bay and Atlantic coast stocks (Table 4.1). Equilibrium fishing mortality in January-February in the first year for each stock was calculated as the equilibrium fishing selectivity multiplied by the average fully selected fishing mortality (Eq. 4.2.3). Equilibrium fishing selectivity was defined as a logistic selectivity function for each stock (Eq. 4.2.4). Total abundance-at-age for the remaining years was calculated using an exponential mortality model summed over regions (Eq. 4.2.5-4.2.6). The plus group in the first subannual time-step included all fish age 15 and older (Eq. 4.2.7). Movement was calculated to occur after mortality at each 2-month time-step (Eq. 4.2.8). Total instantaneous mortality for each age was calculated as the sum of natural mortality and fishing mortality for each region and time-step (Eq. 4.2.9). Average fishing mortality was set to the output of fishing mortality from Chapter 2, between 1990-2017. However, Chapter 2 estimated fishing mortality across two 6-month time-steps. Therefore, in the operating model, fishing mortality for a 6-month time-step was lognormally distributed with standard deviation estimates from Chapter 2. To calculate age-specific fishing mortality for each 2-month time-step, the fishing

mortality was multiplied by the fishery selectivity (Eq. 4.2.10) and then divided by three. Fishery selectivity followed a logistic function for the Ocean region (Eq. 4.2.11) and a double logistic function in the Chesapeake Bay (Eq. 4.2.12), with patterns constant overtime. Parameters that defined fishery selectivity functions were based on estimates from Chapter 2 but were simplified to reduce complexity (Table 4.1). Four multi-age fishery-independent surveys were assumed to occur each year, one in January-February in each region and one in July-August in each region. Logistic selectivity functions were used for the Chesapeake Bay surveys and double logistic selectivity functions were used in the Ocean region. Constant catchability was assumed for each survey based on catchability estimated in Chapter 2. One age-1 and one young-of-the-year survey were assumed to occur in each region during July-August. Occupancy probabilities were based on the output of a Brownie mark-recapture model that estimated movement into and out of the Chesapeake Bay for two 6-month time-steps (Schonfeld, 2023). In OM-B, movement was assumed to occur in January-February and July-August to match assumptions in Schonfeld (2023); however, movement for the remaining time-steps was based on the percent of striped bass from each stock remaining in each region during each time-step (Eq. 4.2.13). For OM-B, the percent remaining was assumed to be 100%, to prohibit movement outside of 6-month periods defined in Schonfeld (2023). All other operating models followed similar assumptions to OM-B unless otherwise stated.

The second operating model (OM-M) assumed that natural mortality changed over time based on the results of the Brownie mark-recapture model that estimated natural mortality from 1990-2020 (Schonfeld, 2023). Schonfeld (2023) estimated

natural mortality for fish ages 2 through 11+ in the Ocean region as a single rate from 1990-2020 but estimated natural mortality in the Chesapeake Bay as changing over three decades:1990-1999, 2000-2009, and 2010-2020 (Table 4.3). The average annual natural mortality for each decade was set as the mid-point for each decade the operating model (i.e., the average for 1990-1999 was the natural mortality in year 5 of the operating model). Natural mortality for age-1 was set to the value used in the benchmark assessment (Northeast Fisheries Science Center, 2019). Natural mortality for ages 12-15+ were set as the natural mortality rate for age 11+ from Schonfeld (2023). Linear interpolation was then used to calculate annual natural mortality-at-age for each year such that the average mortality of each decade in the operating model was equal to the estimates from the brownie mark recapture model. Natural mortality rate at age were constrained so that the start and end of each decade could not be more than 50% below or above the average mortality for that decade (Figure 4.1).

The third operating model (OM-P) assumed migration of striped bass changed over time. OM-P assumed migration into and out of the Chesapeake Bay occurred more gradually throughout the year than at 6-month intervals to better match the observed movement of Chesapeake Bay striped bass (Secor et al., 2020a). Additionally, OM-P assumed time-varying migration by allowing the occupancy probabilities for the Chesapeake Bay stock to change each year. To calculate year-specific occupancy probabilities for the Chesapeake Bay stock in January-February, occupancy probabilities estimated from Schonfeld (2023) in January-June were used as the average for the time-series (years 1-30). To keep this series average, the average occupancy probability in OM-P for years 1-10 was equal to 25% less than the

probabilities estimated in Schonfeld (2023), the average for years 11-20 was equal to the probability estimates from Schonfeld (2023), and the average from years 21-30 were set equal to 25% higher than the probability estimates from Schonfeld (2023). The percent difference for each decade (e.g., 25%) was selected somewhat arbitrarily, as there are few quantifiable estimates of movement changes over time. However, this percent difference represents gradual changes in movement that are still realistic and centered around an estimated average based on tagging information (Schonfeld, 2023). Linear interpolation was then used to estimate annual occupancy probabilities during January-February for each year. Occupancy probabilities in March-April and May-June were set equal to occupancy probabilities assumed in January-February. In July-August, occupancy probabilities were assumed to be similar to those from Schonfeld (2023) but deviated slightly in the later years. In this time-step, occupancy probabilities assumed striped bass increasingly leave the Chesapeake Bay region over time and the rate increases with each age. For this time-step, the occupancy probabilities for striped bass ages 8+ deviated from those estimated in Schonfeld (2023) during July-December for some years. Studies suggest the age at 50% migration out of the Chesapeake Bay is approximately age-10 (Secor et al., 2020a; Secor and Piccoli, 2007). Further, acoustic tagging data suggests striped bass 12-15+ have a higher probability of occurring the Ocean in July-December than the occupancy probabilities from conventional tagging data suggest (Secor et al., 2020a), and older striped bass may be less likely to remain in the Chesapeake Bay during the summer months (Nack et al., 2019). Therefore, average occupancy probabilities for each decade used linear interpolation to increase occupancy between age-7 (0.15) to

an occupancy in the Ocean of 100% for age 15+ in the second decade, and 100% occupancy in the Ocean by age 13+ in the last decade. However, similar to January-February, the average of the occupancy probabilities during July-August for fish ages 1-8 were assumed to be 25% lower in the first decade and 25% higher in the third decade. The percent of each stock remaining in each region also contributed to the observed migration rate of Chesapeake Bay striped bass. As water temperature increases in the Chesapeake Bay, striped bass spawning is expected to start earlier and the spawning season is expected to shorten (Giuliano, 2023; Nack et al., 2019; Pan et al., 2023; Peer and Miller, 2014). Therefore, striped bass were simulated to begin their migrations out of the Chesapeake Bay earlier than July with time. Gradual changes of the percent of striped bass remaining in the Chesapeake Bay decreased from 100% in year 1, to 90% during March-April and 80% in May-June in year 30. Additionally, striped bass were simulated to commence their migration back into the Chesapeake Bay before January-February to represent an earlier start to spawning (Nack et al., 2019) and to reflect observed movement rates for migratory striped bass in 2018 (Secor et al., 2020a). Therefore, the percent remaining in the Ocean was assumed to change in November-December from 100% in year 1 to 75% in year 30 (Figure 4.2). For the Atlantic coast stock, the percent remaining was set at 100% for all time-steps, regions, and years. Linear interpolation was then used to gradually change the percent remaining every year based on values in year 1 to year 30 for all time-steps. An additional OM-P scenario was run (OM-P-50) that considered occupancy was 50% lower in the first decade and 50% higher in the last decade (Figure S4.2). The OM-P-50 scenario was considered to evaluate movement on the

same time-varying scale as natural mortality. Further, there are few quantifiable estimates of time-varying movement (as are for mortality) for striped bass, thus the OM-P-50 scenario provides an alternative hypothesis of the rate of change of striped bass entering and leaving the Chesapeake Bay over time.

The fourth operating model (OM-R) represented changes to recruitment and productivity over time. Spawning and recruitment dynamics of striped bass are influenced by water temperature (Nack et al., 2019; Pan et al., 2023; Peer and Miller, 2014; Secor, 2000; Secor and Houde, 1995), salinity or river discharge (Allen et al., 2023; O'Connor et al., 2012), and larval and juvenile mortality (e.g., from disease, prey availability) (Gervasi et al., 2019; Groner et al., 2018). While little evidence of striped bass undergoing a range shift exists (Nack et al., 2019), climate change may have a negative impact on recruitment in the Chesapeake Bay due to changes to salinity (O'Connor et al., 2012), decrease in prey availability (Millette et al., 2020), and a potential mismatch of optimal conditions due to a change in spawning season (Allen et al., 2023; Millette et al., 2020; Pan et al., 2023; Peer and Miller, 2014). Therefore, we assumed that climate change has the potential to reduce recruitment of the Chesapeake Bay stock, making it less of a contributor to the overall striped bass migratory population. Average recruitment was simulated to decline over time for the Chesapeake Bay stock. The year-1 average recruitment was set to the overall average recruitment in OM-B (log_R=18.801) and the last year recruitment was set equal to the Atlantic coast stock average recruitment. Linear interpolation was used to simulate a time-series of average recruitment for the Chesapeake Bay stock, after

which lognormal recruitment deviations with the same standard deviations as OM-B were applied (Table 4.1; Table 4.4).

The fifth operating model (OM-MPR) included changes to natural mortality, recruitment, and movement over time. In OM-MPR, assumptions match those made in OM-M for natural mortality, those in OM-P for occupancy probabilities, and those made in OM-R for recruitment. The five operating models and their assumptions are described in Table 4.5.

4.3.2. Estimation Models

Three estimation models were evaluated for each data generating scenario based on the estimation models that were described in Chapter 3. All estimation models and their assumptions are described in Table 4.2. Each model was a statistical catch-at-age model that tracked cohorts over time. All assessment models estimated abundance, recruitment, spawning stock biomass (Eq. 4.2.14), and fishing mortality. Natural mortality was age-specific but was assumed to be constant over time and constant across regions, following assumptions made in the benchmark assessment (Table 4.1, Northeast Fisheries Science Center, 2019). All assessment models were coded in AD Model Builder (Fournier et al., 2012).

The first estimation model (FAA) was a similar structure to the current stock assessment model used to inform management of striped bass (Northeast Fisheries Science Center, 2019). This model was a spatially-implicit statical catch-at-age model that assumes fleets-as-areas. The FAA model considered a single stock and region with an annual time step. The FAA model assumed two fishery fleets for the Chesapeake Bay and Ocean regions. The FAA model estimated abundance and

spawning stock biomass for a single coastwide stock in one region with an annual time-step. Fishing mortality and selectivity were estimated for each fleet (Ocean and Chesapeake Bay).

The second model was a multi-stock, spatially-explicit population model that assumed two regions, two stocks, and had two 6-month time-steps defined in Chapter 2 (SE). The third assessment model was a multi-stock, spatially-explicit model that included data with additional stock composition for the last ten years (SE-S). The SE-S model had the same structure as the SE model except for stock-specific likelihood functions for the fishery and survey data sources for the last ten years. The two spatially-explicit models estimated abundance and spawning stock biomass for two spatial regions and two-stocks with a 6-month time-step. There was one fleet per region and time step, and fishing mortality and selectivity were estimated for each region, time-step, and 15-year time-block. Recruitment was estimated for each stock in January-June and varied annually with lognormal deviations. Further, the spatially-explicit models estimated occupancy probabilities for each stock in each region and time-step. Occupancy probabilities were estimated and were constant over time. For the SE model, occupancy probabilities were estimated with informative priors from Schonfeld (2023) (Eq. 4.7.5). The SE-S did not include an informative prior on occupancy probability. Dynamics for the FAA model and both spatially-explicit models are similar to the operating model that can be found in Table 4.2. However, in the assessment models, dynamics were assumed to occur over 12-months for the FAA model or 6-months for the SE models.

Each estimation model estimated parameters by minimizing the sum of the negative log likelihood function for each source of data (e.g., total catch, proportions-at-age). All components of the negative log likelihood function for the estimation models are described in Table 4.7. The log-scale standard deviations and ESSs were the same for each estimation model. All ESS and log-scale standard deviations were set equal to the values used to generate each dataset.

4.3.3. Data Generation

Datasets were generated from each of the five operating models by incorporating random observation errors to the true simulated values to match the typical datasets used in a statistical catch-at-age model. Data inputs needed for each of the three estimations models include catch, proportions of catch-at-age, and indices of abundance and age composition for each of the four fisheries-independent surveys for each region and time step. Datasets were at first generated for two-stocks, two regions, and for 2-month intra-annual time-steps. Then datasets were aggregated over time, stocks, and/or regions in order to match the data structure for each assessment model. Fishery catch-at-age was calculated using the Baranov catch equation (Eq. 4.2.15). Total catch for each year, times-step, and region was then found by summing fishery catch-at-age across ages (Eq. 4.2.16). The fishery-independent surveys were assumed to be conducted in January-February or July-August (Eq. 4.2.17-4.2.20). Log-normal observation error was assumed to generate total catch (Eq. 4.2.21) and the indices of abundance (Eq. 4.2.22). Multinomial error distributions were used to generate proportions-at-age based on the true proportions at age and the effective

sample size (Eq. 4.2.23). Log-scale standard deviations and effective sample sizes used to generate datasets can be found in Table 4.6.

The FAA model assumed a single stock within one region, two regional fleets, and four fishery-independent surveys with an annual time-step. The same four fishery-independent surveys and their respective indices of abundance and survey catch-at-age were assumed in the FAA as the SE models, but assumed to represent annual trends for a single region. The FAA model also included data for two age-1 surveys and two young-of-the-year surveys that were assumed to represent annual trends for age-1 and young-of-the-year striped bass. Additionally, observed fishery catch and proportions-at-age remained disaggregated by region with each region representing a fleet. Fishery-independent surveys represented both stocks within a region.

For the two spatially-explicit models, survey catch-at-age, fishery catch, and fishery catch proportions at age datasets were aggregated across 2-month time-steps in the operating model to represent two 6-month time-steps (January-June and July-December). For the SE model, datasets were aggregated across stocks within a region to match data inputs from Chapter 2. To understand the effects of additional stock composition data (i.e., fishery catch) on model estimates, datasets for one spatially-explicit model (SE-S) were generated to include stock data for the last 10 years, similar to methods described in Chapter 3. For this model, survey catch-at-age, indices of abundance, fishery catch, and fishery catch-proportions-at-age data were generated for two regions, two 6-month time-steps, and aggregated over stocks for

years 1-20. However, during years 21-30 survey catch-at-age, indices of abundance, fishery catch, and catch proportions-at-age were by stock within a region.

4.3.3. Estimation Model Performance

The performance of each estimation model under each data generating scenario was compared based on the number of models that converged and the accuracy of estimated parameters. Because there were too many models and simulated data sets to individually check the diagnostics for every scenario, we used the absolute value of the maximum gradient component as an indicator of likely convergence. For all estimation models, if the absolute value of the maximum gradient component was greater than 0.01, they were removed from analysis as they likely did not converge. Each model that had a maximum gradient component less than 0.01, was assumed to converge and was included in analysis. We determined model bias and accuracy for estimates of abundance, spawning stock biomass, and fishing mortality. Relative error (RE) was used to describe the bias of model estimates and was calculated by dividing the difference between the estimated and the true values by the true value,

$$RE = \frac{\hat{X} - X}{X} \tag{4.1}$$

where $\hat{X}$ was the estimated parameter and X was the true parameter for each metric. Model accuracy was characterized by the root mean square relative error (RMSRE),

$$RMSRE = \sqrt{\frac{\sum_1^n RE^2}{n}} \tag{4.2}$$

where n was the total number of observations.

4.4 Results

All simulations and estimations had a near total convergence rate (>98%; Table 4.8), but they varied in their ability to estimate abundance, fishing mortality, and spawning stock biomass (Tables 4.9-4.10). Estimates of abundance, spawning stock biomass, and fishing mortality in the base scenario (OM-B) were the least biased and most accurate for most models (Table 4.9). Under this scenario, the FAA model produced positively biased estimates of abundance (median relative error (MRE)=0.032), spawning stock biomass (MRE=0.34), and negatively biased estimates of fishing mortality (MRE= -0.217) in the terminal year (Figure 4.3). The SE model estimated abundance, spawning stock biomass, and fishing mortality for age-8 with the least amount of bias compared to the FAA and SE-S models (Table 4.9). The SE-S model was approximately unbiased for all metrics (Table 4.9). In OM-B, the FAA produced relatively accurate estimates of abundance ($RMSRE$=0.198), but produced the least accurate estimates of spawning stock biomass ($RMSRE$=0.495), and fishing mortality at age-8 ($RMSRE$=0.253) in the terminal year (Table 4.10). The SE model had the lowest $RMSRE$ for estimated abundance, spawning stock biomass, and fishing mortality for age-8 in the terminal year across estimation models. Abundance had the lowest $RMSRE$ across all metrics in the SE model ($RMSRE$ =0.115; Table 4.10). Estimates of abundance, spawning stock biomass, and fishing mortality from the SE-S model were slightly less accurate than those from the SE model (Figure 4.3).

Under the OM-M scenario with time-varying natural mortality, all models produced highly biased estimates of abundance, spawning stock biomass, and fishing

mortality for age-8 that were also the least accurate across all scenarios for all models (Figure 4.3). In this scenario, estimates of abundance were positively biased for all estimation models (MRE >2.5), though the FAA provided the most biased estimates of abundance (MRE=6.688). Estimates from the SE model were less biased than those from the FAA model (Table 4.9). Estimated spawning stock biomass performed similarly to abundance but generally had more bias for all models (MRE > 3.6). Fishing mortality for age-8 was negatively biased, with the FAA being most biased (MRE= -0.904) and the SE-S model being least biased (MRE < -0.824; Figure 4.3). Bias generally was reduced during years 10-20 for all assessment models (Figure 4.6). For the OM-M scenario, estimates of abundance, spawning stock biomass, and fishing mortality at age-8 also had the highest $RMSRE$s of any scenario (Figure 4.3; Table 4.10). $RMSRE$ of abundance was $RMSRE$= 6.693, 3.022, and 2.715 for the FAA, SE, and SE-S models respectively. Spawning stock biomass had the highest $RMSRE$ across metrics for all estimation models, with the FAA being the least accurate ($RMSRE$=9.597). $RMSREs$ for fishing mortality at age-8 (Figure 4.7) were similar across estimation models (Table 4.10).

Under the OM-P scenario with time-varying movement, estimates of abundance, spawning stock biomass, and fishing mortality for age-8 were estimated with less bias than the OM-B scenario in most cases. The FAA had the least biased estimates of abundance (MRE=0.001) and spawning stock biomass (MRE=-0.009) in the terminal year (Figure 4.3). Fishing mortality for age-8 was estimated with little bias (MRE=0.081) for the FAA model. The SE had relatively unbiased estimates of abundance (MRE=0.024) and spawning stock biomass (MRE= -0.079) and provided

the least biased estimates for fishing mortality at age-8 (MRE=-0.017) of the estimation models (Table 4.9). The SE-S model provided unbiased estimates of abundance (MRE=-0.022), but estimated spawning stock biomass with negative bias (MRE=-0.143). SE-S estimates of fishing mortality for age-8 were positively biased (MRE=0.115; Figure 4.3). For the FAA model, estimates of abundance, spawning stock biomass, and fishing mortality produced similar bias over time. The MRE of abundance for the SE and SE-S models increased over the last 5 years (Figure 4.4). The MRE of spawning stock biomass for the SE and SE-S models became increasingly negatively over time (Figure 4.5). Estimates of fishing mortality were similar over time for all models (Figure 4.6). For the OM-P scenario, the FAA was least accurate for most metrics across the estimation models, though produced estimates of spawning stock biomass and fishing mortality for age-8 with more accuracy than the OM-B scenario (Table 4.10). The SE model was the most accurate for abundance, spawning stock biomass, and fishing mortality for age-8 with $RMSRE$s of 0.118 for abundance and 0.128 for spawning stock biomass. The SE model estimated fishing mortality for age-8 with a $RMSRE$ of 0.113, which was more accurate than the OM-B scenario. The SE-S model estimated abundance and spawning stock biomass with less accuracy than the SE model, but performed better than the OM-B scenario in all metrics. Estimates of fishing-mortality for age-8 from the SE-S model were not as accurately estimated ($RMSRE$=0.212) relative to the performance of the SE model.

Under the OM-R scenario that assumed average Chesapeake Bay recruitment was decreasing overtime, estimates of abundance, spawning stock biomass, and

fishing mortality for age-8 in the terminal year were generally less biased than in the OM-P scenario. The FAA model provided the most biased estimates of abundance (MRE=0.21), spawning stock biomass (MRE=0.487) and fishing mortality for age-8 (MRE=-0.143). The SE model provided unbiased estimates of abundance (MRE=-0.015), spawning stock biomass (MRE=0.033), and provided the least biased estimates for fishing mortality for age-8 (MRE=0.028) in the terminal year. The SE-S model provided the least biased estimates of abundance (MRE=-0.005), spawning stock biomass (MRE=-0.02) but also estimated fishing mortality with little bias. Trends of abundance and spawning stock biomass were similar over years for all models, though bias tended to increase in years 20-30. The estimation models in the OM-R scenario were more accurate than estimates under the OM-B scenario for many metrics (Table 4.10). The FAA model had the least accurate estimates of abundance ($RMSRE$=0.369), spawning stock biomass ($RMSRE$=0.693), and fishing mortality for age-8 ($RMSRE$=0.253). The SE model had the most accurate estimates of abundance, spawning stock biomass, and fishing mortality for age-8, and the SE-S model had similar, but worse performance than the SE model (Table 4.10).

Under the OM-MPR scenario that included time-varying natural mortality, migration, and recruitment for the Chesapeake Bay stock, all models provided biased estimates of abundance, spawning stock biomass, and fishing mortality, but the median REs were lower than the OM-M scenario (Table 4.9). Estimates of abundance in the terminal year and spawning stock biomass were heavily positively biased (MRE >1.4) for all estimation models, and fishing mortality was negatively biased for all models (MRE < -0.7). However, the FAA provide the most biased estimates of

abundance (MRE=6.472), spawning stock biomass (MRE=8.937), and fishing mortality for age-8 (MRE=-0.886). The SE-S model had the least amount of bias across for all years for abundance, spawning stock biomass, and fishing mortality. The FAA model provided the least accurate estimates for all metrics with $RMSRE$s = 6.297 for abundance, 8.472 for spawning stock biomass, and 0.874 for fishing mortality at age-8 in the terminal year. The SE model also had relatively high $RMSRE$s for abundance, spawning stock biomass, and fishing mortality, but it was more accurate than the FAA model. The SE-S model estimated parameters with the most accuracy, although estimates were still inaccurate relative to the OM-P and OM-R.

4.5 Discussion

Climate change is expected to alter aspects of population dynamics for many fish species. For striped bass, warming temperatures are expected to change spawning behavior, juvenile survival, natural mortality, and movement, particularly in the Chesapeake Bay (Allen et al., 2023; Giuliano, 2023; Groner et al., 2018; Millette et al., 2020; Nack et al., 2019; Pan et al., 2023). This study demonstrated that, in almost all cases, accuracy of abundance, spawning stock biomass, and fishing mortality estimates worsened under climate change scenarios for all estimation models. Notably, the spatially-implicit model always performed worse under time-varying conditions and provided more biased and less accurate estimates of abundance, spawning stock biomass, and fishing mortality compared to the two spatially-explicit models. The multi-stock, spatially-explicit model with tagging information may be able to provide relatively accurate and unbiased estimates of fishing mortality when

there are small changes in recruitment and movement dynamics. However, not accounting for changes in natural mortality resulted in substantially biased estimates of abundance, regardless of estimation method. When recruitment, movement, and natural mortality were changing simultaneously, all estimation models provided inaccurate estimates of abundance, spawning stock biomass, and fishing mortality, though the multi-stock, spatially-explicit model with stock composition information in the fishery and fishery independent surveys performed the best relative to the other two models. Therefore, ignoring time-varying dynamics for a moderately long-lived species like striped bass may provide incorrect management advice.

Mis-specifying natural mortality is known to cause bias in estimates of spawning stock biomass and fishing mortality in age-structured stock assessments (Deroba and Schueller, 2013; Johnson et al., 2014; Mazur et al., 2023). Deroba and Schueller (2013) found that stock assessments that assume natural mortality is constant over time, when natural mortality changes over time, had substantially biased estimates of spawning stock bias in the terminal year. However, this bias was reduced when assessments considered time varying natural mortality (Deroba and Schueller, 2013). Mazur et al. (2023) demonstrated that when natural mortality increases, assessments that did not consider time-varying natural mortality can increase the duration stocks spend in an overfished state. Our results, while similar in trend, demonstrated larger biases in estimates of spawning stock biomass than those reported in the literature due primarily to the simulated increase in natural mortality used in this analysis was greater than those assumed in previous studies. For instance, Mazur et al. (2023) assumed an increase in annual natural mortality from 0.2 to 0.4

over 15 years for Gulf of Maine cod *Gadus morhua*. Though our simulated change in natural mortality varies for each age, certain age groups saw substantial increases based on the estimated natural mortality estimated in Schonfeld (2023). Specifically, age-2 increased in natural mortality for each 2-month time-step from 0.037 in year 1, to 0.245 in year 15, to 0.172 in year 30. Calculated as an annual rate, instantaneous natural mortality changed by over 1.2 in 15 years. Natural mortality is a significant parameter in stock assessments, as it affects other model estimates such as fishing mortality and recruitment (Maunder et al., 2023; Punt et al., 2021). Our results demonstrated that time-varying changes in natural mortality can greatly bias model estimates from spatially-implicit and -explicit assessments when stationary mortality is assumed in the assessment model. Therefore, assumptions of natural mortality in stock assessments should be carefully considered and evaluated for species that may be experiencing time-varying mortality, especially for single stock, single area models.

Most stock assessment models allow stochastic variation in recruitment through the use of annual recruitment deviations about a constant mean or stationary stock-recruitment relationship, which allows for trends in estimated recruitment over time (Maunder and Thorson, 2019). The FAA, SE, and SE-S models estimated recruitment each year based on a log-scale average and annual normally distributed deviations (on the log scale); for the SE models, recruitment was stock-specific. When declining trends in Chesapeake Bay recruitment were simulated, spatially-explicit models were able to provide relatively unbiased estimates of abundance, spawning stock biomass, and fishing mortality, although accuracy was slightly

reduced for some metrics than when average recruitment was constant. The SE model performed better under the OM-R scenario than the OM-B scenario, though under both conditions the SE model produced relatively unbiased estimates of fishing mortality with high accuracy. Additionally, the SE-S produced less biased estimates of fishing mortality in the OM-R scenario than the OM-B scenario. In contrast, the FAA model produced more biased and less accurate estimates of abundance and spawning stock biomass compared to the OM-B scenario and other spatially-explicit models in the OM-R scenario. This may be a result of the FAA model being unable to capture changes in recruitment observed for one stock (Chesapeake Bay) when the model assumes recruitment is aggregate across stocks. Though estimates of abundance and spawning stock biomass were slightly worsened for the SE model under the OM-R scenario, multi-stock, spatially-explicit models appear better suited to capture time-vary trends observed in recruitment when trends are not similar across stocks.

Ignoring climate-induced movement in spatially-explicit integrated population models can increase bias in estimates of fishing mortality and spawning stock biomass (Goethel et al. 2021). However, there have been few studies of how ignoring time-varying movement in population models impacts model estimates for long-lived species with complex migration patterns, such as those observed in striped bass. Our study demonstrated that spatially-explicit population models that assume constant migration rates over time may be able to estimate abundance and fishing mortality with relatively little bias when movement is changing moderately over time. However, the rate at which movement changed drove differences in model

performance. Additionally, spatially-explicit models with tagging information performed better than those without tagging information. When movement changed by about 25% per decade, the SE model was able to provide relatively unbiased estimates of abundance and spawning stock biomass, but the SE-S model provided less accurate estimates of fishing mortality. The slightly degraded performance of the SE-S model may be a result of limited information on stock composition for most years. Specifically, the SE-S model only includes stock composition for the last 10 years, thus the first 20 years of the time-series has no information to inform changes in movement through stock composition in the fishery and surveys. An additional scenario was conducted in which occupancy probabilities changed by 50% per decade (OM-P-50; Figure S4.2). The OM-P-50 scenario performed differently than the OM-P-25 scenario. Interestingly, the FAA model provided unbiased estimates of abundance (MRE= 0.082), spawning stock biomass (MRE=0.071) and fishing mortality at age-8 (MRE=0.051; Figure S4.3), although it is unclear why this occurred. The SE model performed similarly to the FAA model, but estimates were more accurate; although the FAA performed well, spatially-explicit models with tagging information are still able produce the most accurate estimates of population dynamics under time-varying movement with high rates of change. The SE-S model performed poorly compared to the FAA and SE models, and estimated biased estimates of fishing-mortality and spawning stock biomass (Figure S4.3). Although these results differ from those under OM-P, when movement out of the Chesapeake Bay is increased so dramatically, few fish remain for sampling, particularly of older ages. Additionally, under the OM-P-50 scenario, the last 10 years of the observed

population are very different than the first 20 years (e.g., age composition in the Chesapeake Bay). Therefore, it is likely that the SE-S does not have enough information throughout the time series to accurately estimate abundance trends for two stocks and two regions. Incorporating time-varying movement rates is important for future stock assessments, but methods for including time-varying movement in stock assessments require additional research (Punt et al., 2020).

Modeling population changes as a result of climatic variability can be challenging. For many species, regime shifts are still being explored and specific mechanisms are not well documented (Mazur et al., 2023). For striped bass, water temperature has been shown to affect migration (Peer and Miller, 2014; Secor et al., 2020a), adult spawning timing (Peer and Miller, 2014; Rothermel et al., 2020), recruitment success (Millette et al., 2020; Secor and Houde, 1995), and natural mortality from diseases (Gervasi et al., 2019; Groner et al., 2018; Jesse et al., 2021). Increased water temperature is responsible for species range shifts along the Atlantic coast (Kleisner et al., 2017; Pinsky and Fogarty, 2012; Slesinger et al., 2019). For striped bass, range shifts have been suggested, but there is limited evidence to date (Nack et al., 2019). For example, (Limburg et al., 2016) stated overwintering striped bass have moved northward from North Carolina to the mouth of the Chesapeake Bay, though this was not part of a formal analysis and has not been further studied. Furthermore, responses to environmental and climatic events can vary within estuarine systems (Pan et al., 2023), which further complicate understanding specific responses for species within natal estuaries. As a result, this study greatly simplified

striped bass responses to climate change, particularly in the movement and recruitment scenarios.

Natural mortality appears to have increased for striped bass in the Chesapeake Bay (Schonfeld 2023), and the spatially-explicit model from Chapter 2 may overestimate abundance and underestimate fishing mortality rates. The estimates of natural mortality used in OM-M based on Schonfeld (2023) show an approximate doubling of natural mortality during 1990-2020 in the Chesapeake Bay. These estimated trends over time follow those observed in previous studies for striped bass (Jiang et al., 2007). Further, other studies have found the current estimates of natural mortality for striped bass utilized in the assessment that inform management decisions are much lower than recent observations of mortality (Hoenig et al., 2017). Secor et al. (2020a) estimated that mortality for resident striped bass in the Chesapeake Bay was approximately twice that of striped bass that emigrated from the Chesapeake Bay. The presence of mycobacteriosis in the Chesapeake Bay has increased since the 1990s and may cause the increased natural mortality for striped bass (Gauthier et al., 2008; Hoenig et al., 2017; Jiang et al., 2007). Additionally, warming water temperature increases the rate of mortality from mycobacteriosis (Groner et al., 2018). Although the values of natural mortality we assumed in this climate change scenario (OM-M and OM-MPR) are much higher for certain age classes than is accepted in the stock assessment used for management purposes, it is likely that the mortality of striped bass in the Chesapeake Bay has increased significantly due to climate change and increased disease prevalence. Additionally, the values of natural mortality used in this scenario reflect observed estimates that

have already occurred. It is plausible that natural mortality will increase in the future, potentially worsening these trends in bias that we observed in the estimation models. However, studies suggest there may be a limit to the spread of mycobacteria based on thermal limits evaluated in a laboratory setting (Gauthier et al., 2021).

For striped bass, future changes to migration as a results of increased water temperatures and worsened environmental conditions have been speculated but have not been quantified. For instance, (Nack et al., 2019) hypothesized that climate change could promote straying into more northward and non-natal estuaries. Changes to movement over time used in the movement scenario were based on these speculations and could be overstated. Additionally, we assumed a continuous increase in movement out of the Chesapeake Bay over 30 years. In reality, these changes may be variable from year-to-year depending on specific temperature cues. Future research should attempt to quantify the rate of change in movement for striped bass in the Chesapeake Bay.

Many species have experienced shifts in recruitment as a result of environmental changes (Ma et al., 2024; Szuwalski and Punt, 2013; Wayte, 2013). However, ignoring potential trends or shifts in recruitment could potentially provide incorrect management advice when advice is based on projections or forecasting (Maunder and Thorson, 2019). When climate-induced trends in recruitment are ignored, stock assessments have the potential to incorrectly project higher total allowable catch, which could confound conservation strategies (Wayte, 2013). Our models do not project into the future. However, if these models were used to develop projected future catch, they would likely be informed by mis-specified population

dynamics with incorrect population estimates in the last few years of the time-series, possibly leading to incorrect management advice. While our spatially-explicit models performed well when recruitment is changing over time, caution is warranted when using these estimates to forecast for management advice, as trends may be masked in these estimation models. For instance, the FAA model had much higher bias and inaccuracy in estimates of abundance than the two spatially-explicit models or compared to the OM-B scenario. For striped bass, management decisions are based on FAA models; thus, recommended regulation changes may be based on incorrect information on stock status and future fishery conditions.

Climate change is expected to cause changes in population dynamics of many fish species. The Chesapeake Bay is predicted to experience increases in water temperature, hypoxic events, disease prevalence, and sea level as a result of climate change (Najjar et al., 2010) which may affect habitat suitability of many significant fish species. Thus, the ability to accurately estimate population dynamics in response to climate change is of importance for this region (Hare et al., 2016). Though FAA models are still commonly used in management, they generally perform worse compared to spatially-explicit models for species with complex spatial structure such as movement (Bosley et al., 2022; Punt, 2019; Punt et al., 2015). We found that the FAA model was the most sensitive to time-varying patterns of natural mortality, movement, and recruitment than SE models. Other studies have demonstrated that FAA model may provide biased estimates of abundance and mortality for species with complex migrations like Alaskan sablefish *Anoplopoma fimbria* (Bosley et al., 2022). Failure to consider the spatial complexity of mixed fisheries may create biased

estimates and ignore a particular spawning stock's response to environmental changes (Kell et al., 2009). For anadromous species, management informed by models that consider environmental factors may be beneficial, as these species typically have life stages that are greatly influenced by local environmental conditions in nursery areas (Haltuch et al., 2019). Therefore, for species with highly complex migration patterns and multi-stock structure like striped bass, management may be improved by incorporating climatic and ecosystem drivers into assessment modeling.

4.6 Acknowledgements

I would like to thank A.M. Schueller, R.J. Latour, A.J. Schonfeld, and M.J. Wilberg for their collaboration on this chapter. Funding for the research was provided by NOAA and Sea Grant. We thank D. Secor and G. Nesslage for their guidance on developing research methods. We thank K. Drew and G. Nelson for providing their assistance forming testable questions.

4.7 Funding Statement

This research was supported by Sea Grant and the National Marine Fisheries Service's Population and Ecosystem Dynamics Fellowship (grant number NA21OAR4170244) and the NOAA Chesapeake Bay Office (grant number NA19OAR4320074).

4.8 Tables

Table 4.1. Symbols and descriptions of variables for data-generating and estimation models. Values are for the Chesapeake Bay stock (CB) and Atlantic coast stock (AC), when applicable. When variables differ for a 6-month time-step, they are denoted with the number 1 (January-June) or 2 (July-December).

Variable	Description	Value
y	Year index	
a	Age index	
A	Plus group index	
ts	Sub-annual time-step index (1=Jan-Feb; 2=Mar-Apr; 3=May-Jun; 4=Jul-Aug; 5=Sept-Oct; 6=Nov-Dec)	
s	Stock index (1=Chesapeake Bay; 2=Atlantic Coast)	
r	Spatial region index (1=Chesapeake Bay; 2=Ocean)	
t	Fishery selectivity time block index (1=Years 1-15; 2=Years 16-20)	
n	Survey index	
$Nt_{s,y,ts,a}$	Total stock abundance for all spatial regions	
$N_{s,r,y,ts,a}$	Stock abundance for a specific spatial region	
R_s	Median recruitment	CB=146,275,151 AC=60,369,828
$Rdev_{s,y}$	Recruitment deviation	
$C_{r,ts,y}$	Total catch	
$Cd_{r,y,ts}$	Total catch data with observation error	
$I_{n,r,y}$	Index of abundance for fishery-independent survey	
$Id_{n,r,y}$	Index of abundance data with observation error	
$CAA_{r,y,ts,a}$	Catch at age	
$PAA_{r,y,ts,a}$	Proportions-at-age	

Variable	Description	Value
$PAAd_{r,y,ts,a}$	Proportions-at-age data with observation error	
Feq_s	Equilibrium instantaneous fishing mortality for each stock	
$afeq_s$	Equilibrium fishing intensity for each stock	0.2 0.2
$F_{r,y,ts,a}$	Instantaneous fishing mortality in each region and time-step	
M_a	Annual instantaneous natural mortality-at-age	1.13 0.68 0.45 0.33 0.25 0.19 0.15 0.15 0.15 0.15 0.15 0.15 0.15 0.15 0.15
$Z_{r,y,ts,a}$	Instantaneous total mortality	
$ssel_{n,a}$	Survey selectivity	
$fsel_{r,t,ts,a}$	Fishery selectivity	
$prop_{s,ts,a}$	Occupancy probability of each stock in the Atlantic Coast	
$pr_{s,r,y,ts,a}$	Percent remaining in each region	
$occ_{s,r,y,ts,a}$	Total Occupancy probability	
$f_{r,ts}$	Fully recruited fishing intensity	CB1=0.012 CB2=0.018 AC1=0.0297 AC2=0.058
$Fdev_{r,y,ts}$	Annual deviations for fishing mortality	
q_n	Catchability for 1+ surveys	1.39e-07
$q1_n$	Catchability for age 1 surveys	2.85e-08
$qyoy_n$	Catchability for young-of-the-year surveys	1.34e-06
sex_a	Proportion female at age	0.53 0.56 0.56 0.52 0.57 0.65 0.73 0.81 0.88 0.92 0.95 0.97 1 1 1
mat_a	Proportion of mature females at age	0 0 0 0.09 0.32 0.45 0.84 0.89 1 1 1 1 1 1 1
fp_1	Fishery selectivity slope parameter of logistic function; slope of ascending limb double logistic function	1
fp_2	Fishery selectivity age at 50% selectivity for logistic function; Inflection of ascending limb of double logistic function	4
fp_3	Fishery selectivity descending slope of double logistic	1
fp_4	Fishery selectivity inflection of descending limb of double logistic function	10

Variable	Description	Value
sp_1	Survey selectivity slope parameter of logistic function; slope of ascending limb double logistic function	1
sp_2	Survey selectivity age at 50% selectivity for logistic function; Inflection of ascending limb of double logistic function	4
sp_3	Survey selectivity descending slope of double logistic	1
sp_4	Survey selectivity inflection of descending limb of double logistic function	10
af_1	Slope parameter for equilibrium fishery selectivity	1
af_2	Age at 50% selectivity parameter for equilibrium fishery selectivity	4
ESS	Effective sample size	
$\sigma_{r=1}$	Standard deviation to estimate Chesapeake Bay annual recruitment deviations	0.43
$\sigma_{r=2}$	Standard deviation to estimate Atlantic Coast annual recruitment deviations	0.53
$\sigma_{F=1}$	Standard deviation of fishing mortality rate deviations in the Chesapeake Bay for both time-steps	1=0.69 2=0.23
$\sigma_{F=2}$	Standard deviation of fishing mortality rate deviations in the Ocean for both time-steps	1=0.51 2=0.25

Table 4.2. Equations for the operating model that assumes two stocks, two regions, and six 2-month time-steps for striped bass dynamics. Normally distributed errors are denoted with N(mean, error) and multinomial errors are denoted by Multi(Mean, effective sample size).

Eq.		Description
4.2.1	$Nt_{s,y_{=1},ts_{=1},a} = Nt_{s,y_{=1},ts_{=1},a-1} \times e^{-M_{a-1}+Feq_{s,a}}$	Total stock abundance in the first year
4.2.2	$Nt_{s,y_{=1},ts_{=1},a_{=1}} = R_s \times Rdev_{s,y}$	Recruitment in the first year
4.2.3	$Feq_{s,a} = afsel_{s,a} \times afeq_s$	Equilibrium fishing mortality
4.2.4	$afsel = \frac{1}{1+e^{-ap_1\times(a-ap_2)}}$	Equilibrium fishery selectivity
4.2.5	$Nt_{s,y,ts=1,a} = \sum_r N_{s,r,y-1,ts=6,a-1} \times e^{-Z_{r,y-1,ts=6,a-1}}$	Total stock abundance for all regions in Jan-Feb
4.2.6	$Nt_{s,y,ts,a} = \sum_r N_{s,r,y,ts-1,a} \times e^{-Z_{r,y,ts-1,a}}$	Total stock abundance for all regions during timesteps 2-6
4.2.7	$Nt_{s,y,ts=1,A} = \sum_r N_{s,r,y-1,ts=6,A-1} \times e^{-Z_{r,y-1,ts=6,A-1}} + \sum_r N_{s,r,y-1,ts=6,A} \times e^{-Z_{r,y-1,ts=6,A}}$	Total stock abundance for the plus group in Jan-Feb
4.2.8	$N_{s,r,y,ts,a} = Nt_{s,y,ts,a} \times occ_{s,r,ts,y,a}$	Stock abundance for each region
4.2.9	$Z_{r,y,ts,a} = M_a + Z_{r,y,ts,a}$	Instantaneous total mortality
4.2.10	$F_{r,y,ts,a} = fsel_{r,t,ts,a} \times f_r \times Fdev_{r,y,ts}$	Instantaneous fishing mortality
4.2.11	$sel = \frac{1}{1+e^{-p_1\times(a-p_2)}}$	Logistic selectivity
4.2.12	$sel = \frac{1}{1+e^{-p_1\times(a-p_2)}} \times \frac{1}{1+e^{-p_3\times(p_4-a)}}$	Double logistic selectivity
4.2.13	$occ_{s,cb,ts,y,a} = prop_{s,cb,ts,y,a} \times pr_{s,cb,ts,y,a} + prop_{s,ac,ts,y,a} \times \left(1 - pr_{s,ac,ts,y,a}\right)$	Total occupancy probability described for the Chesapeake Bay stock

Eq.		Description
4.2.14	$SSB_{s,y,ts} = \sum_{a} Nt_{s,y,ts,a} \times sex_a \times mat_a \times ssbw_{age}$	Spawning stock biomass
4.2.15	$CAA_{r,y,ts,a} = \frac{F_{r,y,ts}}{Z_{r,y,ts}} \times (1 - e^{-Z_{r,y,ts}}) \times N_{s,r,y,ts}$	True catch-at-age
4.2.16	$C_{y,ts,r} = \sum_{a} CAA_{r,y,ts,a}$	Total catch
4.2.17	$PAA_{y,ts,r,a} = \frac{CAA_{r,y,ts,a}}{C_{y,ts,r}}$	Observed catch proportions-at-age
4.2.18	$I_{n,r,y,ts} = q_n \times \sum_{s,a} N_{s,r,y,ts,a} \times ssel_{n,a}$	Index of abundance for 1+ surveys
4.2.19	$I_{n,r,y,ts} = q1_n \times \sum_{s} N_{s,r,y,ts,a=1}$	Index of abundance for age1 surveys
4.2.20	$I_{n,y} = qyoy_n \times \sum_{s} N_{s,r,y+1,ts,a=1}$	Index of abundance for young-of-the-year surveys
4.2.21	$Cd_{y,ts,r} = N(C_{y,ts,r}, \sigma_F)$	Total catch datasets with observation error
4.2.22	$Id_{n,y,r} = N(I_{n,y,r}, \sigma_I)$	Indices of abundance with observation error
4.2.23	$PAAd_{y,ts,r,a} = Multi(PAAerr_{r,y,ts,a}, ESS)$	Proportions-at-age with observation for the fishery and survey
4.2.24	$Nt_{y,a} = N_{y-1,a-1} \times e^{-Z_{y-1,a-1}}$	Total annual abundance for FAA models
4.2.25	$Nt_{y,A} = N_{y-1,A-1} \times e^{-Z_{y-1,A-1}} + N_{y-1,A} \times e^{-Z_{y-1,A}}$	Abundance of plus group for FAA models
4.2.26	$F_{y,a} = \sum_{f,t} fsel_{f,t,a} \times f_f \times Fdev_{f,y}$	Instantaneous fishing mortality for FAA models
4.2.27	$Fw_{y,a} = \sum_{r,ts} \frac{F_{r,y,ts,a} \times \sum_s Nt_{s,r,ts,y,a}}{\sum_{s,r} N\,t_{s,r,y,ts,a}}$	Weighted annual fishing mortality for SE models to compared to FAA models

Table 4.3. Instantaneous natural mortality rates (yr^{-1}) for striped bass in the Chesapeake Bay (CB) and Ocean (Oc) region from the Brownie mark-recapture model described in Schonfeld (2023). Age-1 estimates of natural mortality are from the benchmark assessment for striped bass (Northeast Fisheries Science Center 2019). Natural mortality for ages 12-15+ were the same as natural mortality for age 11.

Region	Years	1	2	3	4	5	6	7	8	9	10	11	12	13	14	15+
CB	1990-1999	1.13	0.440	0.282	0.259	0.210	0.159	0.246	0.085	0.301	0.129	0.099	0.099	0.099	0.099	0.099
CB	2000-2009	1.13	1.430	0.391	0.336	0.422	0.388	0.301	0.372	0.404	0.403	0.011	0.011	0.011	0.011	0.011
CB	2010-2020	1.13	1.164	0.606	0.361	0.531	0.244	0.573	0.544	0.694	0.693	0.229	0.229	0.229	0.229	0.229
Oc	1990-2020	1.13	0.545	0.285	0.330	0.148	0.160	0.073	0.092	0.007	0.056	0.067	0.067	0.067	0.067	0.067

Table 4.4. Average log recruitment (log R) for the Chesapeake Bay region for each year used in the OM-R scenario.

Year	Log_R	Year	Log_R	Year	Log_R
1	18.801	11	18.496	21	18.191
2	18.770	12	18.465	22	18.160
3	18.740	13	18.435	23	18.130
4	18.709	14	18.404	24	18.099
5	18.679	15	18.374	25	18.069
6	18.648	16	18.343	26	18.038
7	18.618	17	18.313	27	18.008
8	18.587	18	18.282	28	17.977
9	18.557	19	18.252	29	17.947
10	18.526	20	18.221	30	17.916

Table 4.5. A) Description and assumptions of each operating model (OM) scenario for striped bass; B) Description of the fleets-as-areas (FAA) and spatially-explicit (SE) estimations models for striped bass.

A)

Model Number	Name	Description
OM-B	Base	Constant natural mortality-at-age for each year, time-step, and region; average recruitment is constant over time but varies for each stock; Movement-at-age varies for each stock and 6-month period but is constant over years
OM-M	Mortality	Natural mortality-at-age for each year varies for each region, increases over-time for the Chesapeake Bay stock
OM-P	Migration	Occupancy probabilities-at-age increases over-time for the Chesapeake Bay stock
OM-R	Recruitment	Recruitment of the Chesapeake Bay stock decreases over time
OM-MPR	Combo	Occupancy probabilities-at-age increases over-time for the Chesapeake Bay stock, Recruitment of the Chesapeake Bay stock decreases over time

B)

Model Number	Model Type	Stocks	Time-Step	Stock composition Used
FAA	fleets-as-areas	1	1 annual time-step	-
SE	spatially-explicit	2	2 sub-annual time-steps	Occupancy probabilities informative priors
SE-S	spatially-explicit	2	2 sub-annual time-steps	Last 10 years, stock composition data for fishery and surveys

Table 4.6. Standard deviations (σ) and effective sample sizes (ESS) used to generate each data set for a 6-month period. When multiple values are provided, it represents approximately the weighted ESS for the Base scenario (OM-B) for each region and time-step.

Parameter	Type	Value
Fishery Total Catch	σ	0.2
Fishery Age Composition	ESS	47, 53, 35, 65
Survey Indices of Abundance 1+	σ	0.4
Survey Age Composition 1+	ESS	57, 43, 54, 46
Survey Age 1 Indices of Abundance	σ	0.5
Survey Young-of-the-Year Indices of Abundance	σ	0.5

Table 4.7. Negative log-likelihood components for the estimation models for striped bass. Equations are written for the two-stock, spatially-explicit models but were similar for the fleets-as-areas model. Additive constants have been removed from the negative log-likelihood functions. Parameter definitions are in Table 4.1.

Num.	Equation	Description
4.7.1	$nll_{tot} = -ln(L_{Catch}) - ln(L_{Index}) - ln(L_{CatchPAA}) - ln(L_{SurveyPAA}) - ln(L_{recruitment}) - ln(L_{Fdev}) - ln(L_{occ})$	Total negative log-likelihood
4.7.2	$-log_e(L_{Catch/Index}) = \sum_{y} \frac{\left(ln(X) - ln(\hat{X})\right)^2}{2\sigma^2}$	Log-normal negative log-likelihood
4.7.3	$-log_e(L_{Catch/SurveyPAA}) = \sum_{y,a} -ln\left(e^{\frac{0.5\times(-PAA-\widehat{PAA})^2}{\sigma^2}+0.01}\right)$	Robust multinomial negative log-likelihood with added constant of 0.01
4.7.4	$-log_e(L_{recruitment}) = \sum_{y} \left(ln(Rdev_{s=ac})\right)^2 + \left(ln(Rdev_{s=cb})\right)^2$	Normal (on the log scale) negative log-likelihood for recruitment deviations with mean of 0 and standard deviation of approximately 0.7
4.7.5	$-log_e(L_{Fdev}) = \sum_{r,y,ts} \frac{1}{2 * \sigma^2}\left(F_{dev_{r,y,ts}} - F_{dev_{r,y-1,ts}}\right)^2$	Normal (on the log scale) negative log-likelihood for year-to-year deviations in fishing mortality with standard deviation of 0.5
4.7.6	$-log_e(L_{occ}) = \sum_{s,r,a} \frac{0.5\left(prop_{s,r,ts,a} - \widehat{prop}_{s,r,ts,a}\right)^2}{\sigma^2_{s,r,ts,a}}$	Normal negative log-likelihood informative priors of occupancy probability, used only in the SE model

Table 4.8. Total number of model convergence for each estimation model under the five operating model scenarios.

Operating Model	FAA	SE	SE-S
OM-B	300	300	297
OM-M	299	300	300
OM-P	300	300	295
OM-R	299	300	300
OM-MPR	299	299	299

Table 4.9. Median relative error (MRE) for estimated values for three estimation models and five operating model scenarios. The values are presented for total annual abundance (N), spawning stock biomass (SSB), and the fishing mortality for age-8 (F). Operating models and estimation models are described in Table 4.5.

Parameter	Operating Model	FAA	SE	SE-S
N	OM-B	0.032	-0.026	0.030
N	OM-M	6.688	3.024	2.595
N	OM-P	0.001	0.024	-0.022
N	OM-R	0.210	-0.015	-0.005
N	OM-MPR	6.472	2.586	1.770
SSB	OM-B	0.340	0.022	0.104
SSB	OM-M	9.641	4.023	3.633
SSB	OM-P	-0.009	-0.079	-0.143
SSB	OM-R	0.487	0.033	-0.020
SSB	OM-MPR	8.937	2.689	1.465
F	OM-B	-0.217	-0.121	-0.168
F	OM-M	-0.904	-0.833	-0.824
F	OM-P	0.081	-0.017	0.115
F	OM-R	-0.143	0.028	0.062
F	OM-MPR	-0.886	-0.782	-0.703

Table 4.10. Root mean squared relative error (RMSRE) for estimated values for three estimation models and five operating model scenarios. The values are presented for total annual abundance (N), spawning stock biomass (SSB), and the fishing mortality for age-8 (F). Operating models and estimation models are described in Table 4.5.

Parameter	Operating Model	FAA	SE	SE-S
N	OM-B	0.198	0.115	0.203
N	OM-M	6.693	3.022	2.715
N	OM-P	0.209	0.118	0.202
N	OM-R	0.369	0.120	0.180
N	OM-MPR	6.297	2.796	2.006
SSB	OM-B	0.495	0.117	0.288
SSB	OM-M	9.597	3.969	3.710
SSB	OM-P	0.323	0.128	0.291
SSB	OM-R	0.693	0.131	0.239
SSB	OM-MPR	8.472	2.968	1.861
F	OM-B	0.253	0.153	0.222
F	OM-M	0.902	0.830	0.813
F	OM-P	0.222	0.113	0.273
F	OM-R	0.253	0.133	0.212
F	OM-MPR	0.874	0.775	0.698

4.9 Figures

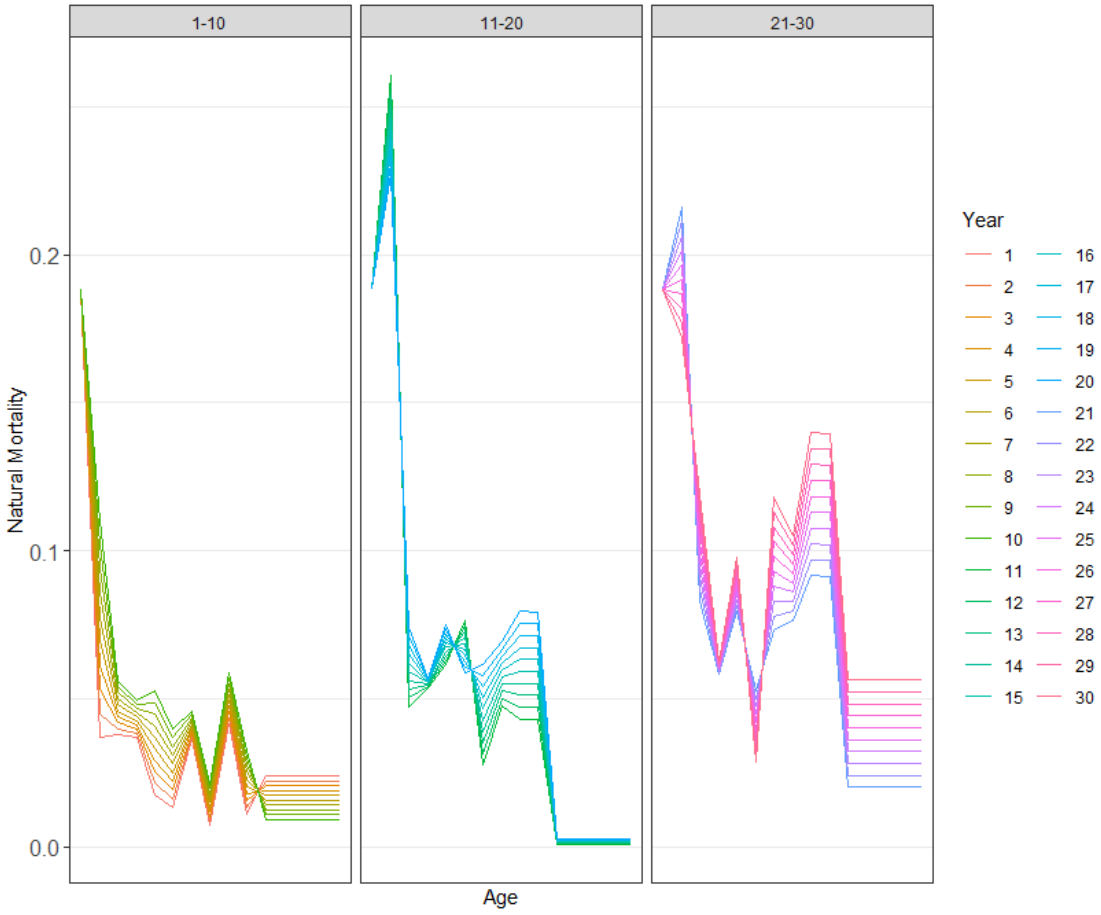

Figure 4.1. Natural mortality for each region of each 2-month time-step and year used in the OM-M scenario. Each panel represents a different decade of the operating model.

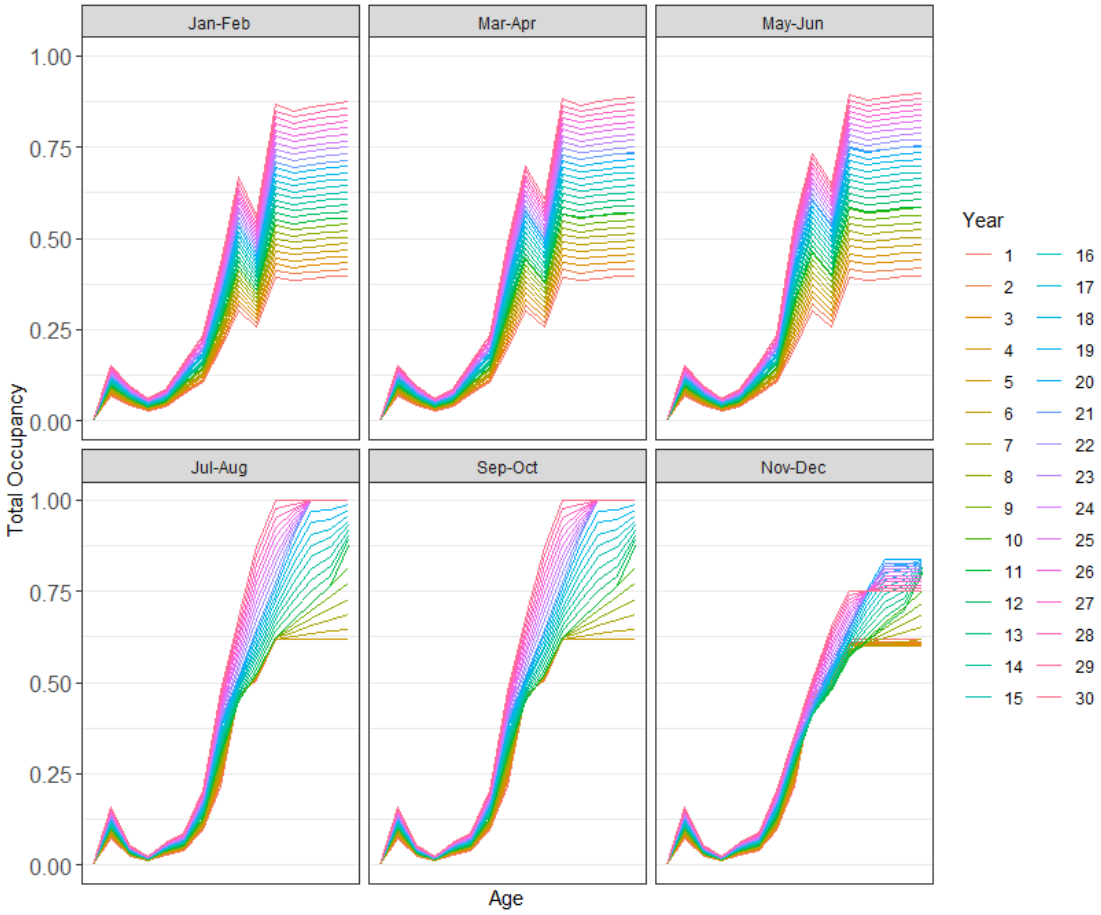

Figure 4.2. Occupancy probabilities of the Chesapeake Bay stock in the Ocean region over-time, including average occupancy and the percent remaining for each time-step, for each 2-month time-step used in the OM-P scenario.

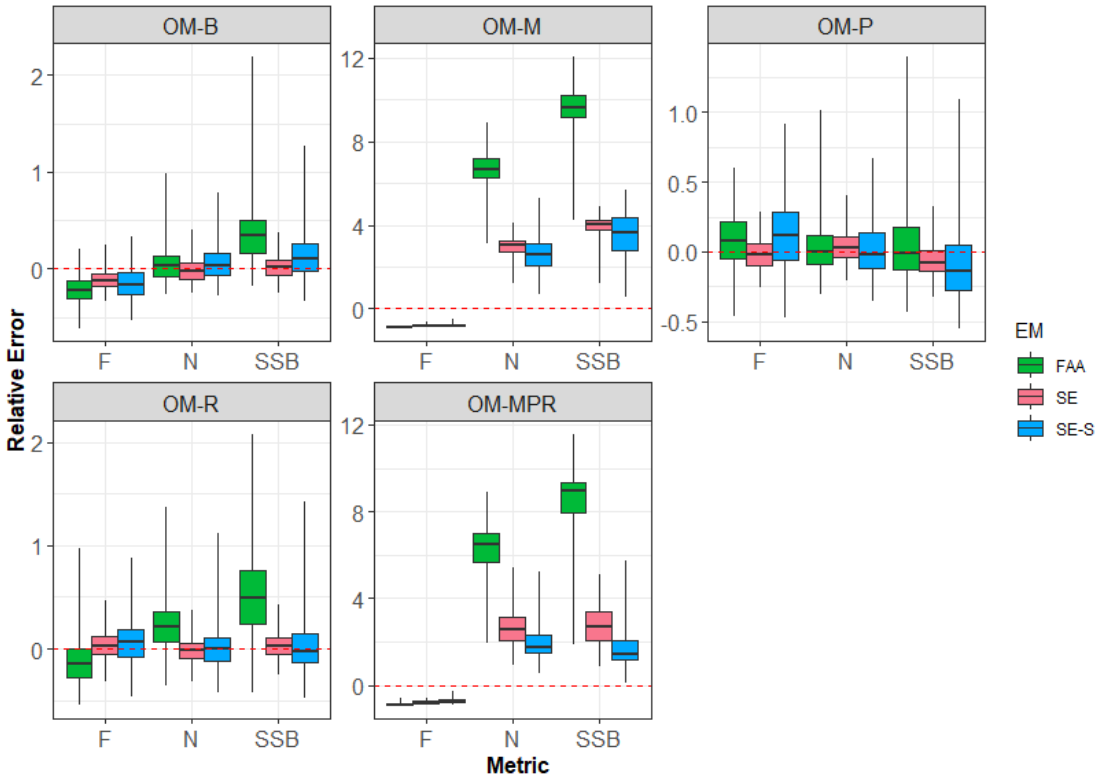

Figure 4.3. Boxplots of the distribution of relative errors of annual abundance over stocks and regions (N), spawning stock biomass in January 1 (SSB), and fishing mortality at age 8 in the terminal year of all operating model simulations for three estimation models. The estimation models are a fleets-as-areas model (FAA), the multi-stock spatially-explicit model (SE), and the multi-stock spatially-explicit model with additional stock composition data (SE-S). The dashed red line represents when relative error is equal to 0. The box represents the 25th and 75th percentiles. The middle line represents the median. The whiskers extend to the minimum and maximum relative error for each metric.

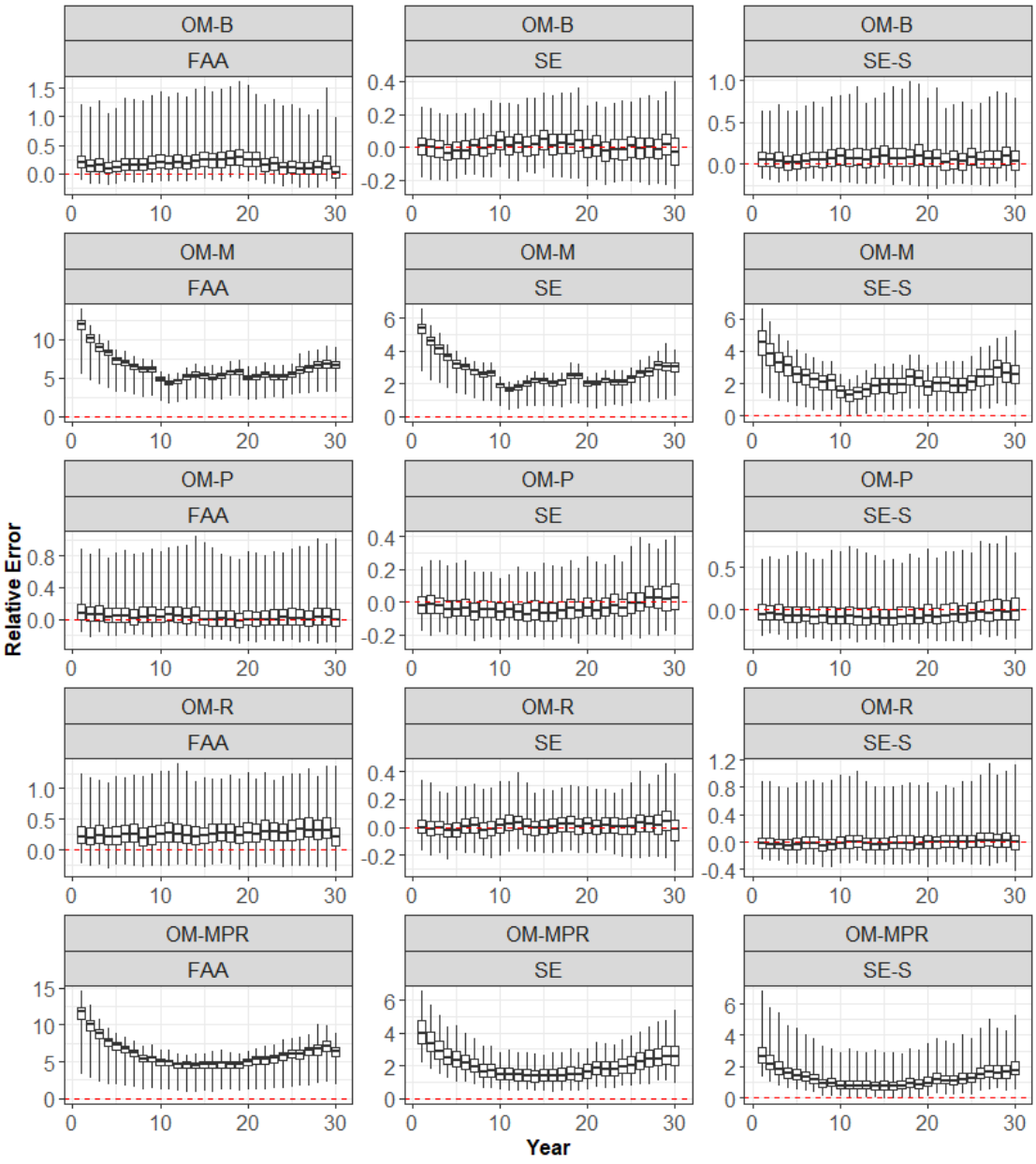

Figure 4.4. Relative error of striped bass abundance (1-15+) for all model years for each operating model and estimation model scenario. Estimates for RE of abundance are provided for the base model (OM-B, top row), natural mortality (OM-M, second row), time-varying movement (OM-P, 3rd row), time-varying average recruitment (OM-R, 4th row), and the mortality, movement and recruitment model (OM-MPR, last row) for the fleets-as-areas model (FAA), spatially-explicit model without stock

data (SE), and the spatially-explicit model with additional stock data in the last 10 years (SE-S). Boxplot definitions are the same as Figure 4.3.

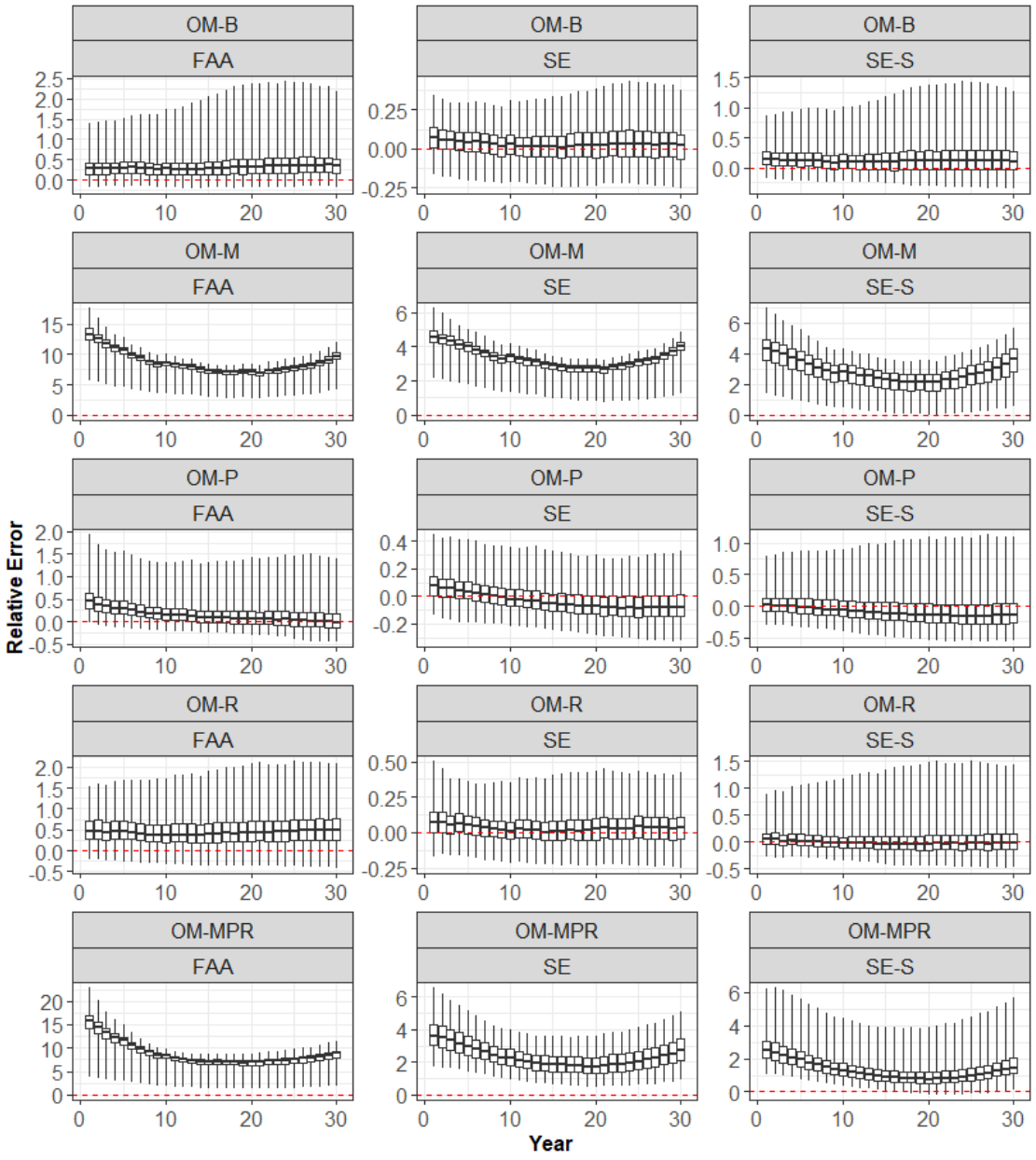

Figure 4.5. Relative error for each year of striped bass spawning stock biomass (SSB) for each operating model and estimation model scenario. Estimates for RE of abundance are provided for the base model (OM-B, top row), natural mortality (OM-M, second row), time-varying movement (OM-P, 3rd row), time-varying average recruitment (OM-R, 4th row), and the mortality, movement and recruitment model (OM-MPR, last row) for the fleets-as-areas model (FAA), spatially-explicit model

without stock data (SE), and the spatially-explicit model with additional stock data in the last 10 years (SE-S). Boxplot definitions are the same as Figure 4.3.

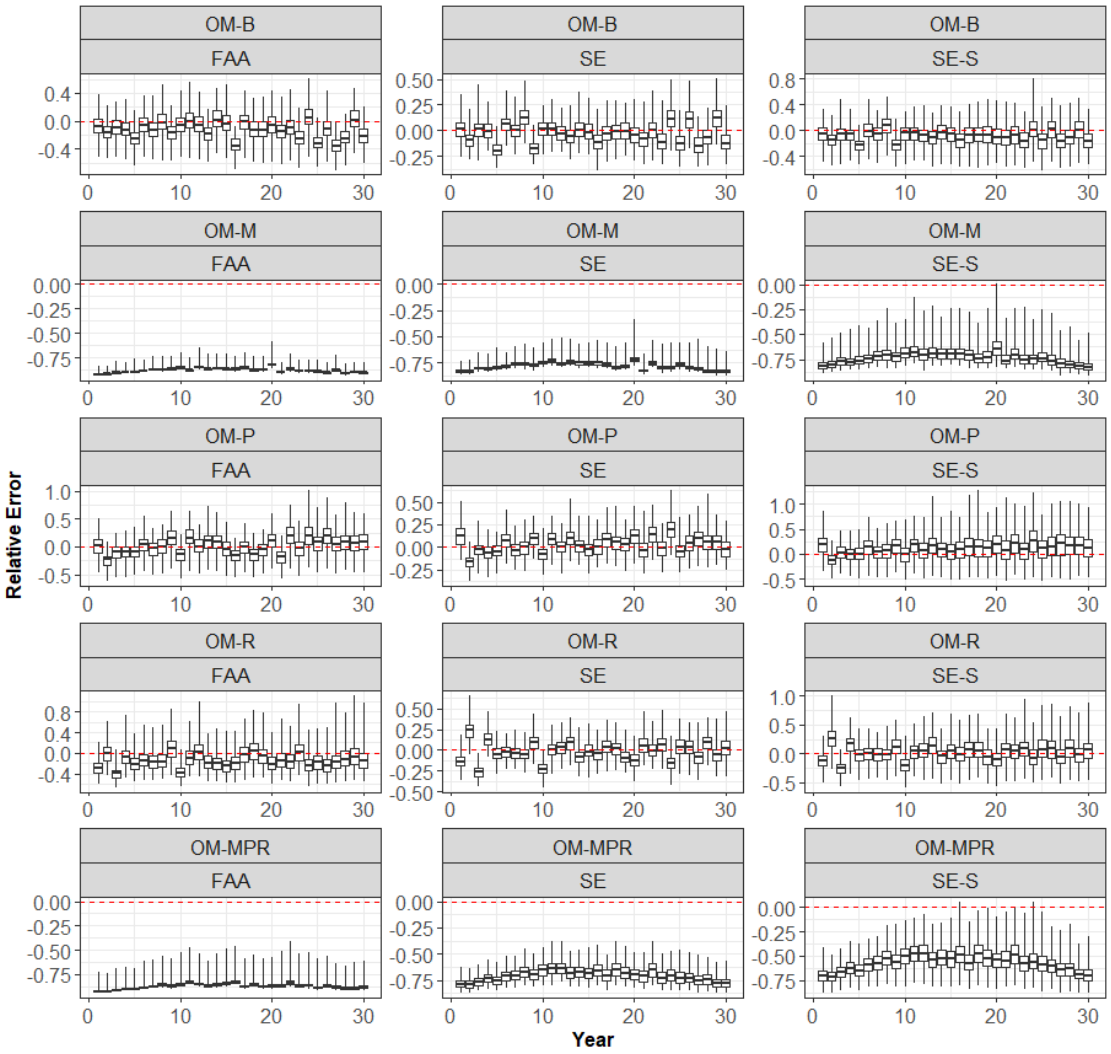

Figure 4.6. Relative error of fishing mortality for age-8 for each year, operating model, and estimation model. Estimates for RE of abundance are provided for the base model (OM-B, top row), natural mortality (OM-M, second row), time-varying movement (OM-P, 3rd row), time-varying average recruitment (OM-R, 4th row), and the mortality, movement and recruitment model (OM-MPR, last row) for the fleets-as-areas model (FAA), spatially-explicit model without stock data (SE), and the spatially-explicit model with additional stock data in the last 10 years (SE-S). Boxplot definitions are the same as Figure 4.3.

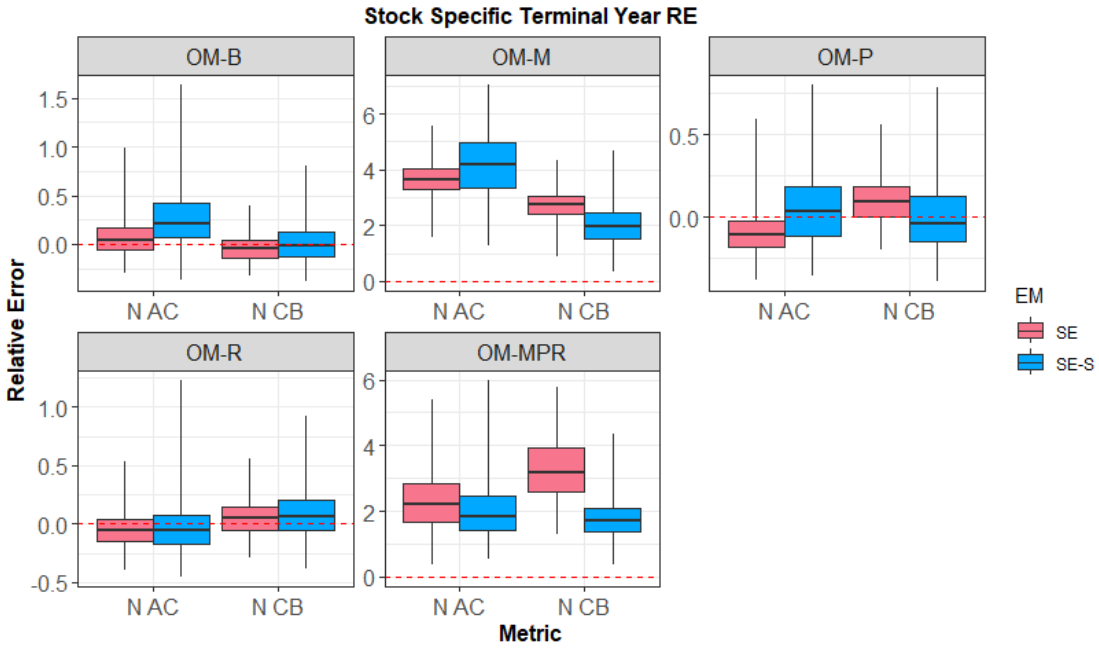

Figure S4.1. Stock specific estimates of relative error in the terminal year of all operating model simulations and the spatially-explicit estimation model without additional stock composition data (SE) and the spatially-explicit model with additional stock composition data (SE-S). Error is provided for the terminal relative error for stock specific abundance when applicable for the Chesapeake Bay (N CB) and Atlantic coast (N AC). Boxplot definitions are the same as Figure 4.3.

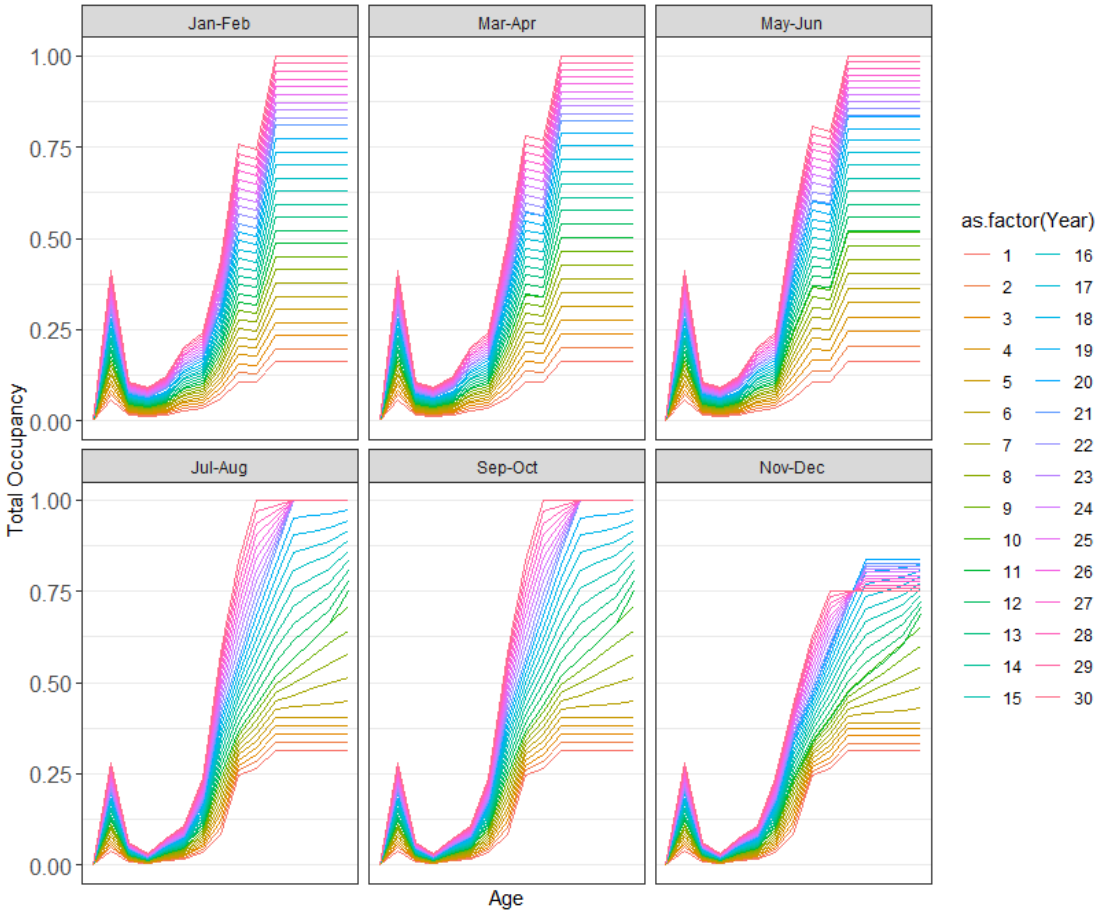

Figure S4.2. Occupancy probabilities-at-age for the Chesapeake Bay stock in the Ocean region over-time, including average occupancy and the percent remaining for each time-step, for each 2-month time-step used in the OM-P 50% scenario.

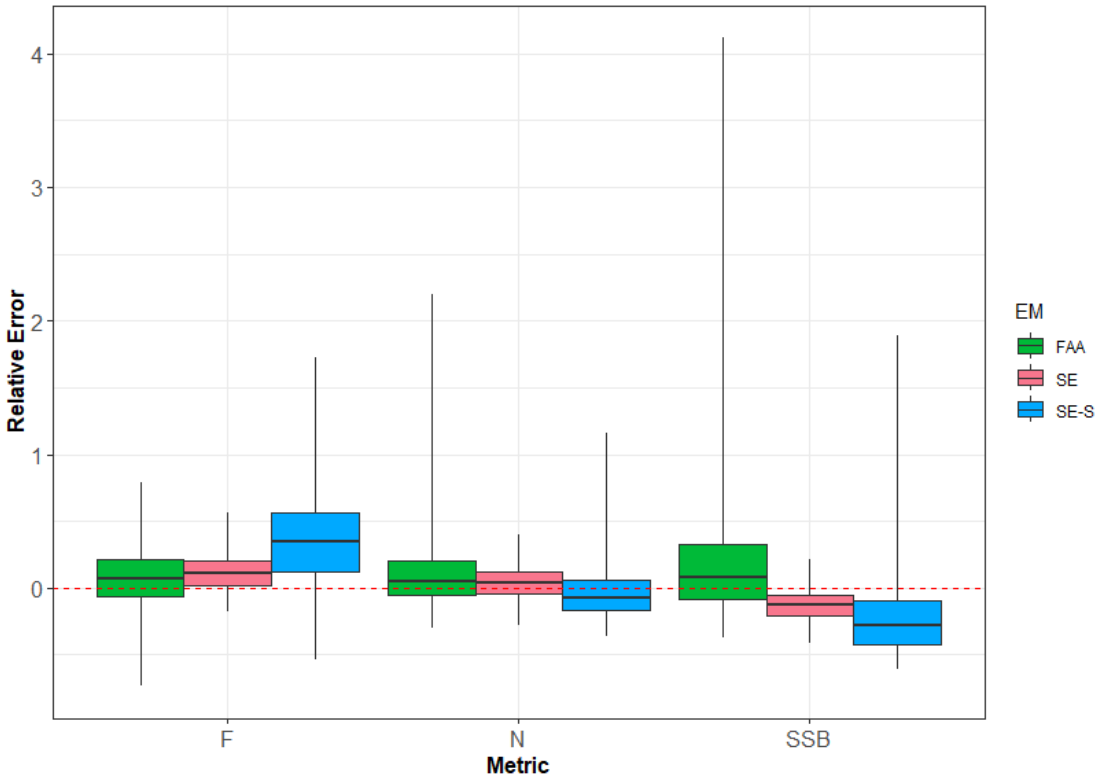

Figure S4.3. Relative error in the terminal year for the estimation models under the OM-P model that assumes changes of 50% migration each decade. Relative error is provided for total annual abundance (N), spawning stock biomass (SSB), and fishing mortality at age-8 (F). Boxplot definitions are the same as Figure 4.3.

4.10 References

Allen, K.L., Ihde, T., Knoche, S., Townsend, H., Lewis, K.A., 2023. Simulated climate change impacts on striped bass, blue crab and Eastern oyster in oyster sanctuary habitats of Chesapeake Bay. Estuar Coast Shelf Sci 292. https://doi.org/10.1016/j.ecss.2023.108465

Bosley, K.M., Schueller, A.M., Goethel, D.R., Hanselman, D.H., Fenske, K.H., Berger, A.M., Deroba, J.J., Langseth, B.J., 2022. Finding the perfect mismatch: Evaluating misspecification of population structure within spatially explicit integrated population models. Fish and Fisheries 23, 294–315. https://doi.org/10.1111/faf.12616

Deroba, J.J., Schueller, A.M., 2013. Performance of stock assessments with misspecified age- and time-varying natural mortality. Fish Res 146, 27–40. https://doi.org/10.1016/j.fishres.2013.03.015

Du, J., Shen, J., Park, K., Wang, Y.P., Yu, X., 2018. Worsened physical condition due to climate change contributes to the increasing hypoxia in Chesapeake Bay. Science of the Total Environment 630, 707–717. https://doi.org/10.1016/j.scitotenv.2018.02.265

Fabrizio, M.C., 1987. Contribution of Chesapeake Bay and Hudson River Stocks of Striped Bass to Rhode Island Coastal Waters as Estimated by Isoelectric Focusing of Eye Lens Proteins. Trans Am Fish Soc 116, 588–593. https://doi.org/10.1577/1548-8659(1987)116<588:cocbah>2.0.co;2

Fournier, D.A., Skaug, H.J., Ancheta, J., Ianelli, J., Magnusson, A., Maunder, M.N., Nielsen, A., Sibert, J., 2012. AD Model Builder: Using automatic differentiation

for statistical inference of highly parameterized complex nonlinear models. Optim Methods Softw 27, 233–249. https://doi.org/10.1080/10556788.2011.597854

Gauthier, D.T., Haines, A.N., Vogelbein, W.K., 2021. Elevated temperature inhibits Mycobacterium shottsii infection and Mycobacterium pseudoshottsii disease in striped bass Morone saxatilis. Dis Aquat Organ 144, 159–174. https://doi.org/10.3354/dao03584

Gauthier, D.T., Latour, R.J., Heisey, D.M., Bonzek, C.F., Gartland, J., Burge, E.J., Vogelbein, W.K., 2008. Mycobacteriosis-associated mortality in wild striped bass (*Morone saxatilis*) from Chesapeake Bay, USA. Ecological Applications 18, 1718–1727. https://doi.org/10.1890/07-2083.1

Gervasi, C.L., Lowerre-Barbieri, S.K., Vogelbein, W.K., Gartland, J., Latour, R.J., 2019. The reproductive biology of Chesapeake Bay striped bass with consideration of the effects of mycobacteriosis. Bull Mar Sci 95, 117–137. https://doi.org/10.5343/bms.2018.0017

Giuliano, A., 2023. Climate effects on the timing of Maryland Striped Bass spawning runs. Marine and Coastal Fisheries 15. https://doi.org/10.1002/mcf2.10274

Goethel, D.R., Bosley, K.M., Langseth, B.J., Deroba, J.J., Berger, A.M., Hanselman, D.H., Schueller, A.M., 2021. Where do you think you're going? Accounting for ontogenetic and climate-induced movement in spatially stratified integrated population assessment models. Fish and Fisheries 22, 141–160. https://doi.org/10.1111/faf.12510

Goetz, S.J., Jantz, C.A., Prince, S.D., Smith, A.J., Varlyguin, D., Wright, R.K., 2004. Integrated analysis of ecosystem interactions with land use change: The Chesapeake bay watershed. Geophysical Monograph Series 153, 263–275. https://doi.org/10.1029/153GM20

Groner, M.L., Hoenig, J.M., Pradel, R., Choquet, R., Vogelbein, W.K., Gauthier, D.T., Friedrichs, M.A.M., 2018. Dermal mycobacteriosis and warming sea surface temperatures are associated with elevated mortality of striped bass in Chesapeake Bay. Ecol Evol 8, 9384–9397. https://doi.org/10.1002/ece3.4462

Hagy, J.D., Boynton, W.R., Keefe, C.W., Wood, K. V., 2004. Hypoxia in Chesapeake Bay, 1950-2001: Long-term change in relation to nutrient loading and river flow. Estuaries 27, 634–658. https://doi.org/10.1007/BF02907650

Haltuch, M.A., Brooks, E.N., Brodziak, J., Devine, J.A., Johnson, K.F., Klibansky, N., Nash, R.D.M., Payne, M.R., Shertzer, K.W., Subbey, S., Wells, B.K., 2019. Unraveling the recruitment problem: A review of environmentally-informed forecasting and management strategy evaluation. Fish Res 217, 198–216. https://doi.org/10.1016/j.fishres.2018.12.016

Hare, J.A., Morrison, W.E., Nelson, M.W., Stachura, M.M., Teeters, E.J., Griffis, R.B., Alexander, M.A., Scott, J.D., Alade, L., Bell, R.J., Chute, A.S., Curti, K.L., Curtis, T.H., Kircheis, D., Kocik, J.F., Lucey, S.M., McCandless, C.T., Milke, L.M., Richardson, D.E., Robillard, E., Walsh, H.J., McManus, M.C., Marancik, K.E., Griswold, C.A., 2016. A vulnerability assessment of fish and invertebrates to climate change on the northeast U.S. continental shelf. PLoS One 11, 1–30. https://doi.org/10.1371/journal.pone.0146756

Hartman, K.J., Margraf, F.J., 2003. US Atlantic coast striped bass: Issues with a recovered population. Fish Manag Ecol 10, 309–312. https://doi.org/10.1046/j.1365-2400.2003.00361.x

Hasegawa, E.H., Waldman, J., Wirgin, I., 2022. Stock composition of Atlantic coastal migratory striped bass using microsatellite DNA analysis. Fish Res 254, 1–10. https://doi.org/10.1016/j.fishres.2022.106384

Hoenig, J.M., Groner, M.L., Smith, M.W., Vogelbein, W.K., Taylor, D.M., Landers, D.F., Swenarton, J.T., Gauthier, D.T., Sadler, P., Matsche, M.A., Haines, A.N., Small, H.J., Pradel, R., Choquet, R., Shields, J.D., 2017. Impact of disease on the survival of three commercially fished species: Ecological Applications 27, 2116–2127. https://doi.org/10.1002/eap.1595

Irby, I.D., Friedrichs, M.A.M., Da, F., Hinson, K.E., 2018. The competing impacts of climate change and nutrient reductions on dissolved oxygen in Chesapeake Bay. Biogeosciences 15, 2649–2668. https://doi.org/10.5194/bg-15-2649-2018

Jesse, J.A., Agnew, M.V., Arai, K., Armstrong, C.T., Hood, S.M., Kachmar, M.L., Long, J.T., McCarty, A.J., Ross, M.O., Rubalcava, K.D., Shaner, J., Tanaka, S., Wood, L., Schott, E.J., Wilberg, M.J., 2021. Effects of Infectious Diseases on Population Dynamics of Marine Organisms in Chesapeake Bay. Estuaries and Coasts 44, 2334–2349. https://doi.org/10.1007/s12237-021-00915-4

Jiang, H., Pollock, K.H., Brownie, C., Hoenig, J.M., Latour, R.J., Wells, B.K., Hightower, J.E., 2007. Tag Return Models Allowing for Harvest and Catch and Release: Evidence of Environmental and Management Impacts on Striped Bass

Fishing and Natural Mortality Rates. N Am J Fish Manag 27, 387–396. https://doi.org/10.1577/m06-089.1

Johnson, K.F., Monnahan, C.C., McGilliard, C.R., Vert-Pre, K.A., Anderson, S.C., Cunningham, C.J., Hurtado-Ferro, F., Licandeo, R.R., Muradian, M.L., Ono, K., Szuwalski, C.S., Valero, J.L., Whitten, A.R., Punt, A.E., 2014. Time-varying natural mortality in fisheries stock assessment models: Identifying a default approach, in: ICES Journal of Marine Science. Oxford University Press, pp. 137–150. https://doi.org/10.1093/icesjms/fsu055

Kell, L.T., Dickey-Collas, M., Hintzen, N.T., Nash, R.D.M., Pilling, G.M., Roel, B.A., 2009. Lumpers or splitters? Evaluating recovery and management plans for metapopulations of herring. ICES Journal of Marine Science 66, 1776–1783. https://doi.org/10.1093/icesjms/fsp181

Kleisner, K.M., Fogarty, M.J., McGee, S., Hare, J.A., Moret, S., Perretti, C.T., Saba, V.S., 2017. Marine species distribution shifts on the U.S. Northeast Continental Shelf under continued ocean warming. Prog Oceanogr 153, 24–36. https://doi.org/10.1016/j.pocean.2017.04.001

Kneebone, J., Hoffman, W.S., Dean, M.J., Fox, D.A., Armstrong, M.P., 2014. Movement patterns and stock composition of adult striped bass tagged in Massachusetts coastal waters. Trans Am Fish Soc 143, 1115–1129. https://doi.org/10.1080/00028487.2014.889752

Latour, R.J., Gauthier, D.T., Gartland, J., Bonzek, C.F., Mcnamee, K.A., Vogelbein, W.K., 2012. Impacts of mycobacteriosis on the growth of striped bass (*Morone*

saxatilis) in Chesapeake Bay. Canadian Journal of Fisheries and Aquatic Sciences 69, 247–258. https://doi.org/10.1139/F2011-158

Limburg, K., Brown, R., Johnson, R., Pine, B., Rulifson, R., Secor, D., Timchak, K., Walther, B., Wilson, K., 2016. Round-the-Coast: Snapshots of Estuarine Climate Change Effects. Fisheries (Bethesda) 41, 392–394. https://doi.org/10.1080/03632415.2016.1182506

Ma, S., Huse, G., Ono, K., Nash, R.D.M., Sandø, A.B., Nedreaas, K., Sætre Hjøllo, S., Sundby, S., Clegg, T., Vølstad, J.H., Kjesbu, O.S., 2024. Recruitment regime shifts and nonstationarity are widespread phenomena in harvestable stocks experiencing pronounced climate fluctuations. Fish and Fisheries 25, 320–348. https://doi.org/10.1111/faf.12810

Maunder, M.N., Hamel, O.S., Lee, H.H., Piner, K.R., Cope, J.M., Punt, A.E., Ianelli, J.N., Castillo-Jordán, C., Kapur, M.S., Methot, R.D., 2023. A review of estimation methods for natural mortality and their performance in the context of fishery stock assessment. Fish Res 257. https://doi.org/10.1016/j.fishres.2022.106489

Maunder, M.N., Thorson, J.T., 2019. Modeling temporal variation in recruitment in fisheries stock assessment: A review of theory and practice. Fish Res 217, 71–86. https://doi.org/10.1016/j.fishres.2018.12.014

Mazur, M.D., Jesse, J., Cadrin, S.X., Truesdell, S., Kerr, L., 2023. Consequences of ignoring climate impacts on New England groundfish stock assessment and management. Fish Res 262. https://doi.org/10.1016/j.fishres.2023.106652

Millette, N.C., Pierson, J.J., North, E.W., 2020. Water temperature during winter may control striped bass recruitment during spring by affecting the development time of copepod nauplii. ICES Journal of Marine Science 77, 300–314. https://doi.org/10.1093/icesjms/fsz203

Nack, C.C., Swaney, D.P., Limburg, K.E., 2019. Historical and Projected Changes in Spawning Phenologies of American Shad and Striped Bass in the Hudson River Estuary. Marine and Coastal Fisheries 11, 271–284. https://doi.org/10.1002/mcf2.10076

Najjar, R.G., Pyke, C.R., Adams, M.B., Breitburg, D., Hershner, C., Kemp, M., Howarth, R., Mulholland, M.R., Paolisso, M., Secor, D., Sellner, K., Wardrop, D., Wood, R., 2010. Potential climate-change impacts on the Chesapeake Bay. Estuar Coast Shelf Sci 86, 1–20. https://doi.org/10.1016/j.ecss.2009.09.026

Ni, W., Li, M., Testa, J.M., 2020. Discerning effects of warming, sea level rise and nutrient management on long-term hypoxia trends in Chesapeake Bay. Science of the Total Environment 737. https://doi.org/10.1016/j.scitotenv.2020.139717

Northeast Fisheries Science Center, 2019. 66th Northeast Regional Stock Assessment Workshop (66th SAW) Assessment Report. Northeast Fisheries Science Center Reference Document 457–1170.

O'Connor, M.P., Juanes, F., McGarigal, K., Gaurin, S., 2012. Findings on American shad and striped bass in the Hudson River estuary: A fish community study of the long-term effects of local hydrology and regional climate change. Marine and Coastal Fisheries 4, 327–336. https://doi.org/10.1080/19425120.2012.675970

Pan, X., Arsenault, S., Rokosz, K., Chen, Y., 2023. Spatial variability of striped bass spawning responses to climate change. Glob Ecol Conserv 42. https://doi.org/10.1016/j.gecco.2023.e02405

Peer, A.C., Miller, T.J., 2014. Climate Change, Migration Phenology, and Fisheries Management Interact with Unanticipated Consequences. N Am J Fish Manag 34, 94–110. https://doi.org/10.1080/02755947.2013.847877

Pepin, P., King, J., Holt, C., Smith, H.G., Shackell, N., Hedges, K., Bundy, A., 2022. Incorporating knowledge of changes in climatic, oceanographic and ecological conditions in Canadian stock assessments. Fish and Fisheries 23, 1332–1346. https://doi.org/10.1111/faf.12692

Pinsky, M.L., Fogarty, M., 2012. Lagged social-ecological responses to climate and range shifts in fisheries. Clim Change 115, 883–891. https://doi.org/10.1007/s10584-012-0599-x

Punt, A.E., 2019. Spatial stock assessment methods: A viewpoint on current issues and assumptions. Fish Res 213, 132–143. https://doi.org/10.1016/j.fishres.2019.01.014

Punt, A.E., Castillo-Jordán, C., Hamel, O.S., Cope, J.M., Maunder, M.N., Ianelli, J.N., 2021. Consequences of error in natural mortality and its estimation in stock assessment models. Fish Res 233. https://doi.org/10.1016/j.fishres.2020.105759

Punt, A.E., Dunn, A., Elvarsson, B.Þ., Hampton, J., Hoyle, S.D., Maunder, M.N., Methot, R.D., Nielsen, A., 2020. Essential features of the next-generation

integrated fisheries stock assessment package: A perspective. Fish Res 229. https://doi.org/10.1016/j.fishres.2020.105617

Punt, A.E., Haddon, M., Tuck, G.N., 2015. Which assessment configurations perform best in the face of spatial heterogeneity in fishing mortality, growth and recruitment? A case study based on pink ling in Australia. Fish Res 168, 85–99. https://doi.org/10.1016/j.fishres.2015.04.002

Rothermel, E.R., Balazik, M.T., Best, J.E., Breece, M.W., Fox, D.A., Gahagan, B.I., Haulsee, D.E., Higgs, A.L., O'Brien, M.H.P., Oliver, M.J., Park, I.A., Secor, D.H., 2020. Comparative migration ecology of striped bass and Atlantic sturgeon in the US Southern mid-Atlantic bight flyway. PLoS One 15, 1–24. https://doi.org/10.1371/journal.pone.0234442

Schonfeld, A.J., 2023. Climate Impacts on Spatiotemporal Habitat Usage of Mid-Atlantic Fishes. William & Mary Ph.D. Dissertation.

Schonfeld, A.J., Gartland, J., Latour, R.J., 2022. Spatial differences in estuarine utilization by seasonally resident species in Mid-Atlantic Bight, USA. Fish Oceanogr 31, 615–628. https://doi.org/10.1111/fog.12611

Secor, D.H., 2007. The year-class phenomenon and the storage effect in marine fishes. J Sea Res 57, 91–103. https://doi.org/10.1016/j.seares.2006.09.004

Secor, D.H., 2000. Spawning in the nick of time? Effect of adult demographics on spawning behaviour and recruitment in Chesapeake Bay striped bass. ICES Journal of Marine Science 57, 403–411. https://doi.org/10.1006/jmsc.1999.0520

Secor, D.H., Houde, E.D., 1995. Temperature effects on the timing of striped bass egg production, larval viability, and recruitment potential in the Patuxent River (Chesapeake Bay). Estuaries 18, 527–544. https://doi.org/10.2307/1352370

Secor, D.H., O'Brien, M.H.P., Gahagan, B.I., Carter Watterson, J., Fox, D.A., 2020a. Differential migration in Chesapeake Bay striped bass. PLoS One 15, 1–19. https://doi.org/10.1371/journal.pone.0233103

Secor, D.H., O'Brien, M.H.P., Gahagan, B.I., Fox, D.A., Higgs, A.L., Best, J.E., 2020b. Multiple spawning run contingents and population consequences in migratory striped bass *Morone saxatilis*. PLoS One 15. https://doi.org/10.1371/journal.pone.0242797

Secor, D.H.;, Piccoli, P.M., 2007. Oceanic migration rates of Upper Chesapeake Bay striped bass (*Morone saxatilis*), determined by otolith microchemical analysis. Fisheries Bulletin 105, 62–73.

Slesinger, E., Andres, A., Young, R., Seibel, B., Saba, V., Phelan, B., Rosendale, J., Wieczorek, D., Saba, G., 2019. The effect of ocean warming on black sea bass (*Centropristis striata*) aerobic scope and hypoxia tolerance. PLoS One 14, 1–22. https://doi.org/10.1371/journal.pone.0218390

Szuwalski, C., Punt, A.E., 2013. Regime shifts and recruitment dynamics of snow crab, Chionoecetes opilio, in the eastern Bering Sea. Fish Oceanogr 22, 345–354. https://doi.org/10.1111/fog.12026

Wayte, S.E., 2013. Management implications of including a climate-induced recruitment shift in the stock assessment for jackass morwong (*Nemadactylus*

macropterus) in south-eastern Australia. Fish Res 142, 47–55. https://doi.org/10.1016/j.fishres.2012.07.009

Wilberg, M.J., Livings, M.E., Barkman, J.S., Morris, B.T., Robinson, J.M., 2011. Overfishing, disease, habitat loss, and potential extirpation of oysters in upper Chesapeake Bay. Mar Ecol Prog Ser 436, 131–144. https://doi.org/10.3354/meps09161

Wirgin, I., Maceda, L., Waldman, J.R., Crittenden, R.N., 1993. Use of mitochondrial DNA polymorphisms to estimate the relative contributions of the Hudson River and Chesapeake Bay striped bass stocks to the mixed fishery on the Atlantic coast. Trans Am Fish Soc 122, 669–684. https://doi.org/https://doi.org/10.1577/1548-8659(1993)122<0669:UOMDPT>2.3.CO;2

Chapter 5: Conclusions

Sustainable fisheries management depends upon readily available and reliable stock assessments. Estimates of abundance, fishing mortality, spawning biomass, and stock status are important for management advice (Goethel et al. 2023). In practice, spatially-explicit stock assessments are often not used for management because it takes time to develop a complex spatially-explicit model that is robust enough to provide management advice in a timely manner. Furthermore, spatially-explicit models have higher data requirements that spatially-implicit models, including tagging data or sampling data across spatial ranges (Goethel et al. 2011, 2023; Berger et al. 2016). However, almost all stocks have some degree of spatial patterns in mortality rates, and spatial assessments have the potential to reduce bias in abundance estimates (Punt et al. 2015). When spatial dynamics are ignored, the potential for overexploitation is increased (Goethel and Berger 2016). Similarly, the ability of a population to recover from collapse is diminished when assessment models fail to consider spatial dynamics (Bosley et al. 2022; Goethel et al. 2023). Therefore, spatially-explicit models are useful for species that exhibit great biological spatial complexity and to inform management decisions.

A multi-stock, spatially-explicit model was developed for Striped Bass (Chapter 2). This model assumed two stocks, two regions, and estimated abundance, fishing mortality, and other parameters for two 6-month time-steps between 1982-2017. Incorporating stock and spatial structure into population models for Striped Bass greatly changed estimates of abundance and fishing mortality. My results suggest that fishing mortality is higher in the Ocean region than the Chesapeake Bay

for most years. Additionally, estimated abundance increased until 2004 and then declined slightly through 2017, although my model estimates were much higher than abundance estimates the current model used to inform management decisions (Northeast Fisheries Science Center 2019). Methods developed for this spatially-explicit model can be applied to other ecologically and economically important fish species in the Chesapeake Bay, and can improve our understanding of how fisheries populations are responding to management decisions (Mahévas and Pelletier 2004). Further, as protecting marine resources is a major objective of NOAA and other governmental agencies, spatially-explicit models have the potential to increase our understanding of the consequences of increasingly used spatial management approaches like marine protected areas (MPAs) (Pelletier and Mahévas 2005). Spatially-explicit models have been able to improve bias and accuracy of biomass estimates for species that have an MPAs within a part of its range (Pincin and Wilberg 2012), suggesting that these models may be used to identify how species are responding to new area designations. In addition, offshore wind farms are increasingly being developed as a way to transition to clean energy, including new development in the Mid-Atlantic region (Secor et al. 2020, 2024). Development of wind farms may have negative consequences on fish populations as species could have adverse responses to increases in sound from pile driving (Popper and Hastings 2009). However, wind farms can also increase fish abundance, particularly in areas that lack hard structure or hard bottom (Methratta and Dardick 2019). As this development will likely increase in the future, spatial population estimates could be

useful to understand how populations are responding to new, localized development from wind farms.

This dissertation also explored how data enhancements and alternative model structures may affect bias and accuracy of population estimates (Chapter 3). My results suggest that incorporating spatial dynamics into assessments for species with stock structure, high rates of migration, and spatially-varying fishing mortality can improve bias and increase accuracy of abundance and fishing mortality estimates when time-varying population dynamics are occurring as a result of climate change. However, bias and accuracy are only improved when spatial models properly correct for potential aging bias in data sources. Therefore, accurate age composition information is necessary for any age-structured assessment (Dorval et al. 2013; Liao et al. 2013; Hulson and Williams 2024). Additionally, tagging data may not always be necessary for spatial assessments if stock composition information is also available. Methods evaluated in this dissertation can also be useful to better inform management decisions for exploited species or to develop new tools management (e.g., ecosystem-based fisheries management) in the Chesapeake Bay. However, spatially-implicit models like fleets-as-areas models remain common practice to inform management decisions (Berger et al. 2016; Cadrin 2020; Goethel et al. 2023), despite their poor performance relative to spatially-explicit models (Punt et al. 2015; Langseth and Schueller 2016; Bosley et al. 2022). My results also suggest that fleets-as-areas models do not accurately estimate abundance and fishing mortality compared to spatially-explicit models. I recommend that when data sources are available across spatial gradients, population models for species with spatially-varying fishing

mortality incorporate spatially-explicit structure to estimate abundance and fishing mortality.

Climate change is a pressing issue, as many species along the Atlantic coast will be affected and undergo range shifts or other changes to their population dynamics (Hare et al. 2016). The Chesapeake Bay is predicted to experience increases in water temperature, hypoxic events, disease prevalence, and sea level as a result of climate change (Najjar et al. 2010), which may affect habitat suitability and use for many important fish species (Schonfeld et al. 2022). Thus, the ability to accurately estimate population dynamics in response to climate change is of importance for the Chesapeake Bay (Hare et al. 2016). Many studies have highlighted how an increase in mycobacteriosis may negatively affect the Chesapeake Bay Striped Bass spawning stock (Gauthier et al. 2008; Latour et al. 2012; Groner et al. 2018; Gervasi et al. 2019; Jesse et al. 2021; Schonfeld 2023). However, these changes in natural mortality from mycobacteriosis and other factors have not yet been incorporated into stock assessment models for this species. My results suggest that ignoring time-varying dynamics of natural mortality, movement, and recruitment reduces accuracy of assessment models (Chapter 4). Specifically, spatially-implicit fleets-as-areas models almost always showed worsened bias in estimates of abundance, spawning stock biomass, and fishing mortality compared to spatially-explicit models. Additionally, spatially-explicit models have the potential to capture time-vary changes in movement and recruitment, even when the assessment assumed stationary conditions, particularly when the assessment includes tagging or stock composition information.

However, ignoring temporal and spatial differences in natural mortality in population models has negative consequences for abundance and fishing mortality estimates. Failure to consider the spatial complexity of mixed-stock fisheries may create biased estimates and ignore a particular spawning stock's response to environmental changes (Kell et al. 2009). My research explored how incorrect assumptions that do not account for climate induced population changes may impact model estimates of abundance. However, the development of spatially-explicit models may not be feasible, particularly for data limited species. When spatially-implicit models are the best-case scenario, caution is warranted and care should be taken to ensure any bias in data sources are appropriately addressed and that assumptions of biological processes in the assessment model accurate reflect the dynamics of the modeled species as much as possible. The methods and models described in this dissertation can be applied to other ecologically and economically significant species in the Chesapeake Bay to understand the potential impacts of climate change on stock assessments.

5.1 References

Berger, A. M., D. R. Goethel, P. D. Lynch, T. Quinn, S. Mormede, J. McKenzie, and A. Dunn. 2016. Space oddity: The mission for spatial integration. Canadian Journal of Fisheries and Aquatic Sciences 74(11):1698–1716.

Bosley, K. M., A. M. Schueller, D. R. Goethel, D. H. Hanselman, K. H. Fenske, A. M. Berger, J. J. Deroba, and B. J. Langseth. 2022. Finding the perfect mismatch: Evaluating misspecification of population structure within spatially explicit integrated population models. Fish and Fisheries 23(2):294–315.

Cadrin, S. X. 2020. Defining spatial structure for fishery stock assessment. Fisheries Research 221(105397):1–12.

Dorval, E., J. D. ; McDaniel, D. L. Porzio, V. Hodes, R. Felix-Uraga, and S. Rosenfield. 2013. Computing and selecting ageing errors to include in stock assessment models of pacific sardine (*Sardinops sagax*). California Cooperative Oceanic Fisheries Investigations Reports 54:192–204.

Gauthier, D. T., R. J. Latour, D. M. Heisey, C. F. Bonzek, J. Gartland, E. J. Burge, and W. K. Vogelbein. 2008. Mycobacteriosis-associated mortality in wild striped bass (*Morone saxatilis*) from Chesapeake Bay, USA. Ecological Applications 18(7):1718–1727.

Gervasi, C. L., S. K. Lowerre-Barbieri, W. K. Vogelbein, J. Gartland, and R. J. Latour. 2019. The reproductive biology of Chesapeake Bay striped bass with consideration of the effects of mycobacteriosis. Bulletin of Marine Science 95(2):117–137.

Goethel, D. R., and A. M. Berger. 2016. Accounting for spatial complexities in the calculation of biological reference points: Effects of misdiagnosing population structure for stock status indicators. Canadian Journal of Fisheries and Aquatic Sciences 74(11):1878–1894.

Goethel, D. R., A. M. Berger, and S. X. Cadrin. 2023. Spatial awareness: Good practices and pragmatic recommendations for developing spatially structured stock assessments. Fisheries Research 264(106703).

Goethel, D. R., T. J. Quinn, and S. X. Cadrin. 2011. Incorporating spatial structure in stock assessment: Movement modeling in marine fish population dynamics. Reviews in Fisheries Science 19(2):119–136.

Groner, M. L., J. M. Hoenig, R. Pradel, R. Choquet, W. K. Vogelbein, D. T. Gauthier, and M. A. M. Friedrichs. 2018. Dermal mycobacteriosis and warming sea surface temperatures are associated with elevated mortality of striped bass in Chesapeake Bay. Ecology and Evolution 8(18):9384–9397.

Hare, J. A., W. E. Morrison, M. W. Nelson, M. M. Stachura, E. J. Teeters, R. B. Griffis, M. A. Alexander, J. D. Scott, L. Alade, R. J. Bell, A. S. Chute, K. L. Curti, T. H. Curtis, D. Kircheis, J. F. Kocik, S. M. Lucey, C. T. McCandless, L. M. Milke, D. E. Richardson, E. Robillard, H. J. Walsh, M. C. McManus, K. E. Marancik, and C. A. Griswold. 2016. A vulnerability assessment of fish and invertebrates to climate change on the northeast U.S. continental shelf. PLoS ONE 11(2):1–30.

Hulson, P. J. F., and B. C. Williams. 2024. Inclusion of ageing error and growth variability using a bootstrap estimation of age composition and conditional age-

at-length input sample size for fisheries stock assessment models. Fisheries Research 270.

Jesse, J. A., M. V. Agnew, K. Arai, C. T. Armstrong, S. M. Hood, M. L. Kachmar, J. T. Long, A. J. McCarty, M. O. Ross, K. D. Rubalcava, J. Shaner, S. Tanaka, L. Wood, E. J. Schott, and M. J. Wilberg. 2021. Effects of Infectious Diseases on Population Dynamics of Marine Organisms in Chesapeake Bay. Estuaries and Coasts 44(8):2334–2349.

Kell, L. T., M. Dickey-Collas, N. T. Hintzen, R. D. M. Nash, G. M. Pilling, and B. A. Roel. 2009. Lumpers or splitters? Evaluating recovery and management plans for metapopulations of herring. ICES Journal of Marine Science 66(8):1776–1783.

Langseth, B. J., and A. M. Schueller. 2016. Calculation of population-level fishing mortality for single- versus multi-area models: Application to models with spatial structure. Canadian Journal of Fisheries and Aquatic Sciences 74(11):1821–1831.

Latour, R. J., D. T. Gauthier, J. Gartland, C. F. Bonzek, K. A. Mcnamee, and W. K. Vogelbein. 2012. Impacts of mycobacteriosis on the growth of striped bass (*Morone saxatilis*) in Chesapeake Bay. Canadian Journal of Fisheries and Aquatic Sciences 69(2):247–258.

Liao, H., A. F. Sharov, and G. A. Nelson. 2013. Quantifying the effects of aging bias in Atlantic striped bass stock assessment. Transactions of the American Fisheries Society 142:193–207.

Mahévas, S., and D. Pelletier. 2004. ISIS-Fish, a generic and spatially explicit simulation tool for evaluating the impact of management measures on fisheries dynamics. Ecological Modelling 171(1–2):65–84.

Methratta, E. T., and W. R. Dardick. 2019. Meta-Analysis of Finfish Abundance at Offshore Wind Farms. Reviews in Fisheries Science and Aquaculture 27(2):242–260.

Najjar, R. G., C. R. Pyke, M. B. Adams, D. Breitburg, C. Hershner, M. Kemp, R. Howarth, M. R. Mulholland, M. Paolisso, D. Secor, K. Sellner, D. Wardrop, and R. Wood. 2010. Potential climate-change impacts on the Chesapeake Bay. Estuarine, Coastal and Shelf Science 86(1):1–20.

Northeast Fisheries Science Center. 2019. 66th Northeast Regional Stock Assessment Workshop (66th SAW) Assessment Report. Northeast Fisheries Science Center Reference Document (19–08):457–1170.

Pelletier, D., and S. Mahévas. 2005. Spatially explicit fisheries simulation models for policy evaluation. Fish and Fisheries 6:307–349.

Pincin, J. S., and M. J. Wilberg. 2012. Surplus Production Model Accuracy in Populations Affected by a No-Take Marine Protected Area. Marine and Coastal Fisheries 4(1):511–525.

Popper, A. N., and M. C. Hastings. 2009. The effects of anthropogenic sources of sound on fishes. Journal of Fish Biology 75(3):455–489.

Punt, A. E., M. Haddon, and G. N. Tuck. 2015. Which assessment configurations perform best in the face of spatial heterogeneity in fishing mortality, growth and

recruitment? A case study based on pink ling in Australia. Fisheries Research 168:85–99.

Schonfeld, A. J. 2023. Climate Impacts on Spatiotemporal Habitat Usage of Mid-Atlantic Fishes. William & Mary Ph.D. Dissertation.

Schonfeld, A. J., J. Gartland, and R. J. Latour. 2022. Spatial differences in estuarine utilization by seasonally resident species in Mid-Atlantic Bight, USA. Fisheries Oceanography 31(6):615–628.

Secor, D. H., M. H. P. O'Brien, and H. Bailey. 2024. The flyway construct and assessment of offshore wind farm impacts on migratory marine fauna. ICES Journal of Marine Science.

Secor, D., M. O'Brien, E. Rothermel, C. Wiernicki, and H. Bailey. 2020. Movement and habitat selection by migratory fishes within the Maryland wind energy area and adjacent reference sites.